



National Library  
of Canada

Bibliothèque nationale  
du Canada

Canadian Theses Service

Service des thèses canadiennes

Ottawa, Canada  
K1A 0N4

## NOTICE

The quality of this microform is heavily dependent upon the quality of the original thesis submitted for microfilming. Every effort has been made to ensure the highest quality of reproduction possible.

If pages are missing, contact the university which granted the degree.

Some pages may have indistinct print especially if the original pages were typed with a poor typewriter ribbon or if the university sent us an inferior photocopy.

Previously copyrighted materials (journal articles, published tests, etc.) are not filmed.

Reproduction in full or in part of this microform is governed by the Canadian Copyright Act, R.S.C. 1970, c. C-30.

## AVIS

La qualité de cette microforme dépend grandement de la qualité de la thèse soumise au microfilmage. Nous avons tout fait pour assurer une qualité supérieure de reproduction.

Si il manque des pages, veuillez communiquer avec l'université qui a conféré le grade.

La qualité d'impression de certaines pages peut laisser à désirer, surtout si les pages originales ont été dactylographiées à l'aide d'un ruban usé ou si l'université nous a fait parvenir une photocopie de qualité inférieure.

Les documents qui font déjà l'objet d'un droit d'auteur (articles de revue, tests publiés, etc.) ne sont pas microfilmés.

La reproduction, même partielle, de cette microforme est soumise à la Loi canadienne sur le droit d'auteur, S.R.C. 1970, c. C-30.

THE UNIVERSITY OF ALBERTA

PIPE DRIVEABILITY PREDICTION

by



M. VASAVITHASAN

A THESIS

SUBMITTED TO THE FACULTY OF GRADUATE STUDIES AND RESEARCH  
IN PARTIAL FULFILMENT OF THE REQUIREMENTS FOR THE DEGREE  
OF MASTER OF SCIENCE

DEPARTMENT OF CIVIL ENGINEERING

EDMONTON, ALBERTA

SPRING 1988

Permission has been granted to the National Library of Canada to microfilm this thesis and to lend or sell copies of the film.

The author (copyright owner) has reserved other publication rights, and neither the thesis nor extensive extracts from it may be printed or otherwise reproduced without his/her written permission.

L'autorisation a été accordée à la Bibliothèque nationale du Canada de microfilmer cette thèse et de prêter ou de vendre des exemplaires du film.

L'auteur (titulaire du droit d'auteur) se réserve les autres droits de publication; ni la thèse ni de longs extraits de celle-ci ne doivent être imprimés ou autrement reproduits sans son autorisation écrite.

ISBN 0-315-42877-5

THE UNIVERSITY OF ALBERTA

RELEASE FORM

NAME OF AUTHOR M.VASAVITHASAN  
TITLE OF THESIS PILE DRIVEABILITY PREDICTION  
DEGREE FOR WHICH THESIS WAS PRESENTED MASTER OF SCIENCE  
YEAR THIS DEGREE GRANTED SPRING 1988

Permission is hereby granted to THE UNIVERSITY OF ALBERTA LIBRARY to reproduce single copies of this thesis and to lend or sell such copies for private, scholarly or scientific research purposes only.

The author reserves other publication rights, and neither the thesis nor extensive extracts from it may be printed or otherwise reproduced without the author's written permission.

(SIGNED) *M. Vasavithasan*

PERMANENT ADDRESS:

#115635 105 STREET.  
EDMONTON, ALBERTA  
T6H 2N2

DATED 3rd December 1987

THE UNIVERSITY OF ALBERTA  
FACULTY OF GRADUATE STUDIES AND RESEARCH

The undersigned certify that they have read, and  
recommend to the Faculty of Graduate Studies and Research,  
for acceptance, a thesis entitled **PILE DRIVEABILITY**  
**PREDICTION** submitted by M.VASAVITHASAN in partial fulfilment  
of the requirements for the degree of MASTER OF SCIENCE.

.....*Visser*.....

Supervisor

.....*CC*.....

.....*W. J. J. J.*.....

Date. *12th November 1987*.....

## ABSTRACT

A number of wave equation computer programs have been developed since Smith (1960) first proposed the mathematical method to handle pile driving problems. During the past twenty five years these programs have experienced a gradual and continuous increase in use for the analysis of pile driving. Also, the wave equation method for predicting the driveability of foundation piles for offshore as well as onshore structures is well established in geotechnical practice.

Some of the soil parameters such as damping or quake and the behaviour of soil during pile driving were not well understood at the time the solution was first proposed, with values for quake and damping parameters recommended based on empiricism. Subsequent studies made by various investigators suggest that the assumptions made in the original formulation regarding the soil parameters were incorrect and new concepts have been recommended for the behaviour of soil during pile driving.

However, most of the wave equation computer programs widely known and used in pile driving practice use Smith's original formulation. This thesis presents the details of the development of a wave equation computer program with facility to adapt for new soil parameters derived from recent studies on soil behaviour during pile driving, and also modification to Smith's formulation to include the gravity effect which is not taken into account in his

formulation. This report also includes the studies made on the influence of some of the input parameters on the predicted bearing capacity and stress in the pile.

The program discussed herein incorporates the facility of using the damping parameters derived from three different methods. One of these methods allows the user to select the damping parameters based on basic soil properties such as liquidity index or angle of internal friction. Performance of the program is tested using five case histories by comparing the predicted bearing capacities with the load test results. Bearing capacities predicted by the program are in very close agreement with those estimated from the load tests.

### ACKNOWLEDGEMENT

Sincere gratitude is due to my supervisor Dr. Z. Eisenstein for his help and guidance during this project.

The author expresses his sincere thanks to Mr. John Mekechuk, Geotechnical Engineer of CN Rail for releasing the test results and providing valuable materials to prepare this report.

The author is considerably indebted to Mr. Lal Samarasekara for his continuous encouragement and help throughout this project. Also, the author is considerably indebted to Mr. Richard Wan for his help and his painstaking scrutiny of the manuscript.

The author is thankful to the Department of Civil Engineering for providing partial financial assistance. Finally, the author thanks his wife Gowrie for her silent sacrifices throughout this task.



## Table of Contents

Chapter	Page
1. INTRODUCTION .....	1
2. BASIC STRESS WAVE THEORY .....	8
2.1 Longitudinal Elastic Waves in a Bar .....	8
2.2 Wave Propagation Analysis .....	11
2.2.1 Basic Axial Wave Propagation Equation .....	11
2.2.2 Consideration of Boundary Conditions .....	14
2.2.3 Discontinuity in Bar Properties .....	18
2.3 Wave Theory Applied to Piles .....	23
2.3.1 Stress Waves Developed During Pile Driving .....	24
2.3.2 Particle and Wave Velocity .....	28
2.3.3 Influence of Impedance on Stresses .....	30
2.4 Summary .....	32
3. PILE DRIVING HAMMERS .....	33
3.1 Working Principle of Various Impact Type of Hammers .....	34
3.1.1 Drop and Single-Acting Air/Steam Hammers ..	34
3.1.2 Double-Acting or Differential-Acting Hammers .....	37
3.1.3 Diesel Hammers .....	41
3.1.3.1 Open Ended Diesel Hammer .....	42
3.1.3.2 Closed Ended Diesel Hammer .....	43
3.1.3.3 Vacuum Chamber Diesel Hammer .....	43
3.1.4 Generalised Diesel Hammer Operation .....	47
3.1.4.1 Force in Compression, Combustion and Expansion Phases .....	47
3.1.4.2 Velocity at Impact .....	52
3.1.4.3 Ram Stiffness .....	53

3.2	Function of Accessories .....	54
3.2.1	Anvil .....	54
3.2.2	Pile Cap (Helmet) .....	55
3.2.3	Cap Block and Cushion .....	56
3.3	Summary .....	57
4.	MATERIAL RESPONSE TO DYNAMIC LOADING .....	59
4.1	Soil Response During Pile Driving .....	59
4.1.1	Soil Response Under Dynamic Loads .....	60
4.1.1.1	Smith's Idealization .....	61
4.1.1.2	Coyle and Gibson's Proposal .....	64
4.1.1.3	Proposal by Case Western Reserve University .....	67
4.1.2	Time Effects .....	69
4.1.2.1	Soil Set-Up Factor .....	71
4.2	Internal Damping in Pile and Accessories .....	73
4.2.1	Pile .....	73
4.2.2	Hammer Accessories .....	75
4.3	Summary .....	79
5.	MATHEMATICAL MODELS AND DEVELOPMENT OF PROGRAM "ALWAP" .....	81
5.1	Mathematical Models .....	82
5.1.1	Hammer .....	82
5.1.2	Pile and Soil .....	85
5.2	Numerical Treatment .....	87
5.2.1	Development of Basic Formulae .....	87
5.2.1.1	Gravity Effect .....	92
5.2.2	Computer Solution .....	94
5.2.2.1	Selection of Time Interval and Segment Length .....	97

5.3 Summary .....	99
6. CHARACTERISTICS OF ALWAP AND INPUT INFORMATIONS ....	100
6.1 Program Flow .....	100
6.2 Input Informations .....	103
6.2.1 Input Data .....	103
6.2.1.1 Pile Properties and Time Interval	104
6.2.1.2 Soil Properties .....	106
6.2.1.3 Hammer Details .....	107
6.3 Program Limitations .....	110
6.4 Gravity Effect .....	111
6.5 Influence of Input Parameters .....	113
6.5.1 Hammer Selection .....	113
6.5.2 Cap Block Properties .....	117
6.5.3 Soil Properties .....	120
6.6 Summary .....	128
7. PROGRAM PERFORMANCE .....	138
7.1 Introduction .....	138
7.1.1 Interpretation of Load Test Results .....	141
7.1.2 Damping Models .....	145
7.1.3 Representaion of Results .....	146
7.2 Edmonton Rapid Transit 112-Avenue Station .....	148
7.2.1 Pile Capacity From Static Formula .....	148
7.2.2 Wave Equation Analysis and Hiley's Formula .....	150
7.2.3 Summary .....	151
7.3 Test Pile At Beaumont, Texas .....	155
7.3.1 Damping Parameters and Soil Set-Up Factor	155
7.3.2 Pile Capacity From Static Formula .....	156

7.3.3 Pile Capacity From Load Test .....	157
7.3.4 Wave Equation Analysis and Hiley's Formula .....	158
7.3.5 Summary .....	160
7.4 Test Pile No V11-9-22C Thornton Yard .....	165
7.4.1 Damping Parameters .....	165
7.4.2 Pile Capacity From Static Formula .....	166
7.4.3 Pile Capacity From Load Test .....	167
7.4.4 Wave Equation Analysis and Hiley's Formula .....	167
7.4.5 Summary .....	169
7.5 Test Pile at M.6.6, Fraser Subdivision .....	177
7.5.1 Damping Parameters and Set-Up Factor ....	178
7.5.2 Pile Capacity From Static Formula .....	179
7.5.3 Pile Capacity From Load Test .....	180
7.5.4 Wave Equation Analysis and Hiley's Formula .....	180
7.5.5 Summary .....	182
7.6 Test Pile No 'U, Research Project Report .....	189
7.6.1 Damping Parameters .....	189
7.6.2 Pile Capacity From Static formula .....	190
7.6.3 Pile Capacity From load Test .....	191
7.6.4 Wave Equation Analysis and Hiley's Formula .....	191
7.6.5 Summary .....	194
7.7 Discussion of Results .....	202
8. CONCLUSIONS AND RECOMMENDATIONS .....	212
BIBLIOGRAPHY .....	215
APPENDIX A-1 .....	226

APPENDIX A-2 .....	228
APPENDIX A-3 .....	237
APPENDIX A-4 .....	260
APPENDIX B-1 .....	264
APPENDIX B-2 .....	266
APPENDIX B-3 .....	268
APPENDIX C-1-A .....	269
APPENDIX C-1-B .....	270
APPENDIX C-2-A .....	271
APPENDIX C-3-A .....	273
APPENDIX C-3-B .....	275
APPENDIX C-4-A .....	276
APPENDIX C-4-B .....	278
APPENDIX C-5-A .....	279
APPENDIX D .....	281

## List of Tables

Table	Page
6.1 Gravity Effect on Maximum Forces and Permanent Set .....	112
6.2 Change in Compressive Stress .....	126
7.1 Summary of Test Piles Analysed by the Program .....	208

## List of Figures

Figure		Page
2.1	Longitudinal Elastic Waves in a Uniform Bar .....	9
2.2	Axial Displacement Waves Propagating Along Bar .....	9
2.3	Propagation of Wave During Time Interval $\Delta t$ .....	11
2.4	Reflection of Displacement and Stress Waves at Free End .....	11
2.5	Reflection of Displacement and Stress Waves at Fixed End .....	11
2.6	Wave Reflection and Refraction at Discontinuity .....	19
2.7	Analysis of Pile Driving Contact Force .....	25
2.8	Stress Condition in a Pile During Driving .....	25
3.1	Drop Hammer .....	35
3.2	Single-Acting Air/Steam Hammer .....	38
3.3	Double-Acting Hammer .....	39
3.4	Components of Typical Open Ended Diesel Hammer .....	44
3.5	Simulation of Gas Force After Rempe and Davisson (1977) .....	44
3.6	Operational Cycle of Diesel Hammer .....	45
3.7	Closed Ended Diesel Hammer .....	46
3.8	Vacuum Chamber Diesel Hammer .....	48
3.9	Simulation of Combustion and Expansion Phases .....	51
3.10	Vertical Section of Diesel Hammer Ram .....	51
4.1	Load - Deformation Relationship for Soil .....	62
4.2	Relationship between Dynamic Resistance and Velocity .....	66
4.3	Load Deformation Relationship for Soil .....	66

Figure	Page
4.4 Effective Angle of Internal Shearing Resistance Versus Damping Constant for Sand (After Coyle & Gibson 1970) .....	68
4.5 Liquidity Index Versus Damping Constant for Clays (After Coyle & Gibson 1970) .....	68
4.6 Gain in Carrying Capacity with Time of Piles Driven into Soft to Stiff Clays (After Vesic 1970) .....	70
4.7 Effect of Pile Characteristics (McClelland et al., 1969) .....	70
4.8 Load Deformation Relationships .....	74
4.9 Stress Strain Relationships of Accessories .....	77
5.1 Schematic Representation of Hammer and its Model .....	84
5.2 Smith's Mathematical Model of Pile and Soil .....	86
5.3 Representation of Soil Model .....	88
5.4 Element Displacements .....	90
5.5 Element Forces .....	90
6.1 Details of Pile and Soil Resistance .....	114
6.2 Effect of Gravity on Blow Count and Compressive Stress .....	115
6.3 Effect of Gravity on Blow Count and Tensile Stress .....	116
6.4 Effect of Driving Energy on Blow Count and Compressive Stress .....	118
6.5 Effect of Driving Energy on Blow Count and Tensile Stress .....	119
6.6 Effect of Cap Block Stiffness on Blow Count and Compressive Stress .....	121
6.7 Effect of Cap Block Stiffness on Blow Count and Tensile Stress .....	122
6.8 Effect of Coefficient of Restitution on Blow Count and Compressive Stress .....	123



Figure	Page
6.9 Effect of Coefficient of Restitution on Blow Count and Tensile Stress .....	124
6.10 Effect of Quake on Blow Count and Compressive Stress .....	129
6.11 Effect of Quake on Blow Count and Tensile Stress .....	130
6.12 Effect of Percent of Point Load on Blow Count and Compressive Stress .....	131
6.13 Effect of Percent of Point Load on Blow Count and Tensile Stress .....	132
6.14 Effect of Varying Smith Damping Value .....	133
6.15 Effect of Varying Gibson & Coyle Damping Value .....	134
6.16 Effect of Varying Case Damping Value .....	135
6.17 Effect of Damping Factors on Blow Count .....	136
7.1 Bearing Graphs for Blow Count and Maximum Stress .....	152
7.2 Maximum Stress in Pile Segments .....	153
7.3 Variation of Force, Velocity and Displacements with Time Interval .....	154
7.4 Bearing Graphs for Blow Count and Maximum Stress .....	161
7.5 Bearing Graphs for Blow Count and Maximum Stress .....	162
7.6 Maximum Stress in Pile Segments .....	163
7.7 Variation of Force, Velocity and Displacements with Time Interval .....	164
7.8 Construction of Davisson Limit Load .....	171
7.9 Failure Loads According to Butler & Hoy and Fuller & Hoy .....	171
7.10 Construction of Failure Load According to Van de Veen .....	172
7.11 Construction of Failure Load According to Chin .....	172

Figure	Page
7.12 Bearing Graphs for Blow Count and Maximum Stress .....	173
7.13 Bearing Graphs for Blow Count and Maximum Tensile Stress .....	174
7.14 Maximum Stress in Pile Segments .....	175
7.15 Variation of Force, Velocity and Displacements with Time Interval .....	176
7.16 Construction of Davisson Limit Load .....	183
7.17 Failure Loads According to Butler & Hoy and Fuller & Hoy .....	183
7.18 Construction of Failure Load According to Van de Veen .....	184
7.19 Construction of Failure Load According to Chin .....	184
7.20 Bearing Graphs for Blow Count and Maximum Stress .....	185
7.21 Bearing Graphs for Blow Count and Maximum Stress .....	186
7.22 Maximum Stress in Pile Segments .....	187
7.23 Variation of Force, Velocity and Displacements with Time Interval .....	188
7.24 Construction of Davisson Limit Load .....	195
7.25 Failure Loads According to Butler & Hoy and Fuller & Hoy .....	195
7.26 Construction of Failure Load According to Van de Veen .....	196
7.27 Construction of Failure Load According to Chin .....	196
7.28 Bearing Graphs for Blow Count and Maximum Stress .....	197
7.29 Maximum Stress in Pile Segments .....	198
7.30 Bearing Graphs for Blow Count and Maximum Stress .....	199
7.31 Maximum Stress in Pile Segments .....	200

Figure	Page
7.32 Variation of Force, Velocity and Displacements with Time Interval .....	201
7.33 Davisson Limit Load Versus Predicted Pile Capacity .....	209
7.34 Butler & Hoy's Failure Load Versus Predicted Pile Capacity .....	209
7.35 Van de Veen's Failure Load Versus Predicted Pile Capacity .....	210
7.36 Fuller & Hoy's Failure Load Versus Predicted Pile Capacity .....	210
7.37 Davisson Limit Load Versus Hiley's Ultimate Soil Resistance .....	211
7.38 Comparison between Wave Equation and Hiley's Formula .....	211

## 1. INTRODUCTION

Engineers have used pile driving formulae for many years to estimate the pile bearing capacity. Some of these formulae are also used to determine the stresses in the pile during driving. The rapidly increasing use of pile foundations and the appearance of new pile driving techniques have led the engineers to find more reliable methods of dynamic pile analysis and design. The diversity and variability of piles, types of driving hammers, and soil encountered have always been major problems in building construction and offshore structures.

A number of pile driving formulae are in use and engineers have never been able to agree as to which one is best. This is because, the mathematics of pile-driving action could not be solved in any particular manner and as a result all pile-driving formulae are partly empirical and, consequently, apply only to certain types or lengths of piles.

All the pile driving formulae were established on the assumption that the energy delivered by the hammer after losing portion of this energy on nonuseful work such as compressing the capblock, pile cushion and pile would be immediately transmitted to the tip of the pile at impact. Pile driving is not a simple problem of impact that may be solved directly by Newton's law. Isaacs (1931) was the first to point out that the energy transmission from the hammer to the pile tip is not instantaneous at impact and it is a

problem in longitudinal wave transmission. The elasto-plastic response of the ground, freezing and relaxation of soils, remoulding of soils and generation of pore pressure are the major problems encountered in pile driving. Also, pile driving involves many complications such as the use of cap block, helmet, cushion block, composite piles and tapered piles.

The dynamic formulae do not represent the driving system properly. All effects of pile flexibility are neglected in dynamic formula and it assumes a rigid pile in its derivation. The soil resistance is assumed to be constant and this type of soil model is far too simple to even approximately represent a real soil. However, the rated energy is the most important parameter of hammer included in these formulae and some dynamic formulae include weight of ram.

Stress wave or an elastic strain is generated at the pile head when the hammer strikes a pile. With time, this wave progresses longitudinally through the pile down to its tip where the soil is displaced to produce the pile penetration or set. The propagation of the stress or strain wave is governed by the one dimensional wave equation. Following the study of pile driving impact by Smith (1955), the use of the theory of wave propagation for the analysis of pile driving has gradually developed to result in the formal proposition of the so called Wave Equation method of analyzing the driving behaviour of piles and for predicting

their bearing capacity. Smith (1960) presented a comprehensive treatment of the application of the wave equation method of analysis of pile driving.

If the dynamic parameters are available and the hammer performs properly, the driving system can be represented by wave equation analysis of piles with considerable realism. In wave equation analysis, the pile is represented by a series of springs and masses. The pile is well represented in this method to account for its flexibility. Also, the soil model is substantially improved over that is used in the dynamic formula.

There are few commercially available computer programs for the wave equation analysis of pile driving. The programs most widely known and used in North America are the TTI program and the WEAP program. The TTI program originates from Smith's (1960) approach but it is modified to accommodate a large variation of field problems. It was developed primarily for analysis of piles driven with air/steam hammers or drop hammers. Diesel hammers are simply modelled as drop hammers with an explosive force acting in conjunction with the impact. The TTI program uses Smith damping approach which results in a zero damping force in unloading when the static resistance is zero.

The WEAP program was developed in response to some shortcomings of the TTI program with regard to piles driven by diesel hammers. The WEAP program models the actual combustion sequence of the diesel hammer considering the

volume of the combustion chamber and the fuel injection. The program also calculates the ram rebound of the hammer. If the rebound distance does not agree with the original downward travel of the ram, the analysis is repeated with a new initial ram travel until agreement is achieved. WEAP program allows the alternative use of both Smith and Case damping.

In CAPWAP computer analysis, the advantages of the wave equation analysis and the field measurements by means of the Pile Driving Analyser have been combined. The CAPWAP analysis is very much superior to conventional wave equation analysis, because input of actually measured data independent of both natural variations of input data and of subperforming hammers are used. Values of quake and damping constants are assumed in the analysis. From the recorded acceleration the force at the top of the pile is calculated and compared with that derived from the strain gauge readings.

Several programs other than those mentioned above are available to determine the bearing capacity and to check the integrity of piles. A few of the programs and their purposes are summarized below.

Program

Purpose

CAPWAP

Wave equation and pile driving  
analysis is combined

PEBWAP	Similar to CAPWAP (Used for point bearing piles)
DIESEL-1	Special program for diesel hammers
TTI Program	Smilar to Smith's original program
The Raymond International Program	Similar to the TTI
DUKFOR	Similar to the TTI program Considers residual stresses in the pile and soil
WEAP	Special program for diesel and include Case and Smith damping

Smith damping as well as Case damping assume that the damping resistance is linearly proportional to the pile velocity. However, studies of Gibson & Coyle (1970), Heerema (1979) and Likouhi & Poskitt (1980) show that this is incorrect. Studies of Heerema (1979 & 1981) indicate that for clay soils, skin friction is very strongly velocity dependent at low velocities and relatively insensitive at high velocities. However, for sands, wall friction is not velocity dependent and point bearing is strongly velocity



dependent.

Based on their studies, they concluded that the damping resistance varies non-linearly with velocity and also recommended a power law for use in wave equation analysis. Gibson & Coyle (1970) recommended damping parameters for highly compressible clay and sand to be used in conjunction with this power law as well. These parameters are related to the basic soil properties such as liquidity index and angle of internal friction. Most of these programs do not include the gravity effect (ie, weight of the pile) which may be substantial in the case of large diameter piles.

In contrast to Case and Smith damping factors, Gibson & Coyle's damping factors are related to soil properties and are easy to use. The purpose of this study is to develop a computer program, for analyzing piles driven by impact type hammers, to examine the possibility of using the power law and the damping parameters recommended by Gibson and Coyle, and to produce a program that includes gravity effect as well as options of using the damping parameters recommended by Smith, Case and Gibson & Coyle. Also, the performance of the program is tested by comparing the predicted pile capacity with the load test results evaluated by various methods.

In Chapter 2 of this report the basic development and use of the wave equation are discussed. Construction and operation of impact type hammers used in pile driving practice are discussed in Chapter 3. Dynamic properties of

materials involved in pile driving, details of soil damping models and behaviour of soils during and after driving are discussed in Chapter 4. Chapters 5 & 6 deal with the mathematical modelling, development and general description of the program. Finally testing of the program for its performance are reported in Chapter 7.

## 2. BASIC STRESS WAVE THEORY

### 2.1 Longitudinal Elastic Waves in a Bar

If a load is suddenly applied to a body, the part of the body closest to the source of disturbance will be affected first. The deformation of the body due to the load will gradually spread throughout the body via stress waves. The dynamic response of a uniform bar to a suddenly applied axial loading as well as the nature of propagation of stress waves in a uniform bar are discussed in this section.

Figure (2.1) shows a uniform bar with cross-sectional area equal to  $A$  and the unit weight of the material which constitutes the bar equal to  $\gamma$ . Let the Young's modulus of the bar be  $E$ . Assume the stress along the section a-a of the bar to increase by  $\sigma$ . The stress increase along the section b-b can be given by  $\sigma + (\partial\sigma/\partial x)\Delta x$ . Newton's second law states that;

$$\sum \text{Force} = (\text{mass})(\text{acceleration})$$

Summation of the forces in the x direction;

$$\sigma A - \left(\sigma + \frac{\partial\sigma}{\partial x}\Delta x\right)A = - \frac{A\Delta x\gamma}{g} \frac{\partial^2 u}{\partial t^2} \quad (2.1)$$

where  $A\Delta x\gamma$  = weight of the bar of length  $\Delta x$

$g$  = acceleration due to gravity

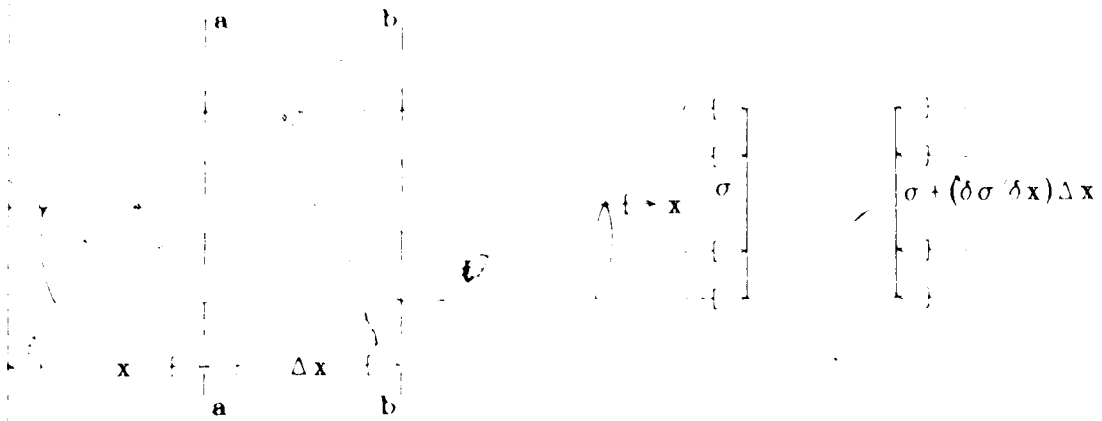


Figure 2.1 Longitudinal Elastic Waves in a Uniform Bar

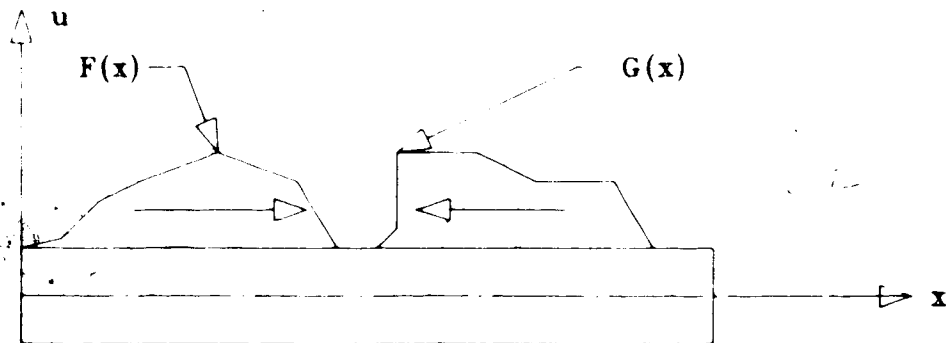


Figure 2.2 Axial Displacement Waves Propagating Along Bar

$u$  = displacement in the  $x$  direction

$t$  = time

Equation (2.1) is based on the following assumptions.

- 1) The stress is uniform over the entire cross sectional area.
- 2) The cross-section remains plane during the motion.

Simplification of Equation (2.1) gives

$$\frac{\partial \sigma}{\partial x} = \rho \left( \frac{\partial^2 u}{\partial t^2} \right) \quad (2.2)$$

where  $\rho = \frac{\gamma}{g}$  is the density of the material of the bar.

However, stress = (strain)(Young's modulus)

$$\sigma = E \left( \frac{\partial u}{\partial x} \right) \quad (2.3)$$

$$\frac{\partial \sigma}{\partial x} = E \frac{\partial^2 u}{\partial x^2} \quad (2.4)$$

Combining Equations (2.2) and (2.4) leads to

$$\begin{aligned} \frac{\partial^2 u}{\partial t^2} &= \left( \frac{E}{\rho} \right) \frac{\partial^2 u}{\partial x^2} \\ \frac{\partial^2 u}{\partial t^2} &= c^2 \frac{\partial^2 u}{\partial x^2} \end{aligned} \quad (2.5)$$

$$\text{where } c = \sqrt{\frac{E}{\rho}} \quad (2.6)$$

The term  $c$  is the velocity of the longitudinal stress wave propagation.

## 2.2 Wave Propagation Analysis

### 2.2.1 Basic Axial Wave Propagation Equation

The dynamic response of a uniform bar to a suddenly applied axial loading is of very simple form, which can be interpreted as the propagation of a stress and deformation wave along its length. These facts can be demonstrated by referring to the solution of Equation (2.5) written in the form

$$u_{(x,t)} = F(x - ct) + G(x + ct) \quad (2.7)$$

where  $F$  and  $G$  are arbitrary functional relationships of the parameters  $(x - ct)$  and  $(x + ct)$ . This expression represents a pair of displacement waves propagating in the positive and negative directions along the axis of the bar as shown in Figure (2.2).

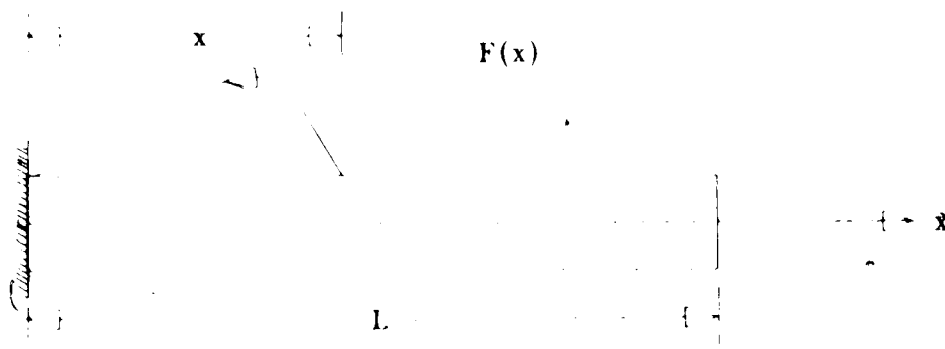
Consider the forward propagating wave at two instants of time,  $t = t$  and  $t = t + \Delta t$ , as shown in Figure (2.3).

At a given time  $t$ , let the function  $F(x - ct)$  be represented by Figure (2.3a) and

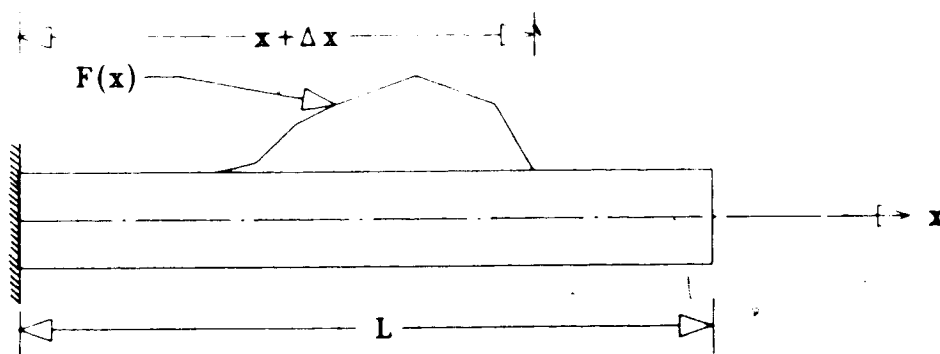
$$u_{(x,t)} = F(x - ct) \quad (2.8)$$

At time  $t = t + \Delta t$ , the function will be represented by Figure (2.3b)

$$u_{(x,t+\Delta t)} = F[(x + \Delta x) - c(t + \Delta t)] \quad (2.9)$$



(a) At time  $t=t$



(b) At time  $t=t+\Delta t$

Figure 2.3 Propagation of Wave During Time Interval  $\Delta t$

If the wave moves unchanged in shape from its position at time  $t$  to  $t + \Delta t$ .

$$u_{(x,t)} = u_{(x,t+\Delta t)}$$

$$F(x - ct) = F((x - ct) + (\Delta x - c\Delta t))$$

$$\text{or } c\Delta t = \Delta x \quad (2.10)$$

Thus the velocity of the longitudinal stress wave propagation is equal to  $c = \Delta x / \Delta t$ . By similar reasoning it can be shown that the second term in Equation (2.7) represents a wave form  $G$  moving in the negative  $x$  direction.

The dynamic behaviour of the bar can also be expressed in terms of its stress distribution rather than with respect to its displacements.

$$\sigma_{(x,t)} = E \frac{\partial u}{\partial x}$$

$$\sigma_{(x,t)} = E \frac{\partial F}{\partial x}(x - ct) + E \frac{\partial G}{\partial x}(x + ct) \quad (2.11)$$

If the stress wave functions  $E \frac{\partial F}{\partial x}$  and  $E \frac{\partial G}{\partial x}$  are designated by  $f$  and  $g$ , Equation (2.11) may be written as

$$\sigma_{(x,t)} = f(x - ct) + g(x + ct) \quad (2.12)$$



### 2.2.2 Consideration of Boundary Conditions

The function defining the shape of any wave propagating through a uniform bar is controlled by the conditions imposed at the ends of the bar. The wave form within the bar is generated by the requirements of equilibrium and compatibility at the boundaries.

If the end of the bar ( $x=l$ ) is free as shown in Figure (2.3a), the condition of zero stress must be maintained at all times at that end. This condition may be satisfied by a second stress wave propagating toward the origin ( $x=0$ ), which, when superposed on the incident wave. Both waves cancel each other, resulting in zero stress at the free end section. This concept may be expressed mathematically by means of Equation (2.11) which leads to

$$\sigma_{(x=l)} = 0 = E \frac{\partial F}{\partial x}(L-ct) + E \frac{\partial G}{\partial x}(L+ct)$$

ie

$$\frac{\partial F}{\partial x}(L-ct) = - \frac{\partial G}{\partial x}(L+ct) \quad (2.13)$$

It is evident from Equation (2.13) that the slope ( $\partial u/\partial x$ ) of the wave propagating towards the origin must be the negative of the slope of the wave propagating towards the end as each part of the waves passes the free end of the bar. The displacement waves shown in Figure (2.4a) demonstrate this condition; and the corresponding stress waves in Figure (2.4b) show clearly how the stresses at the tip are cancelled.

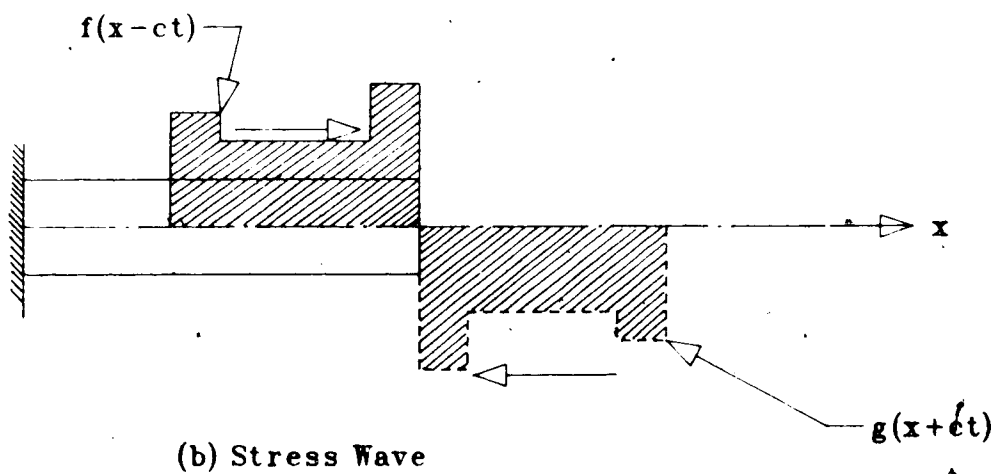
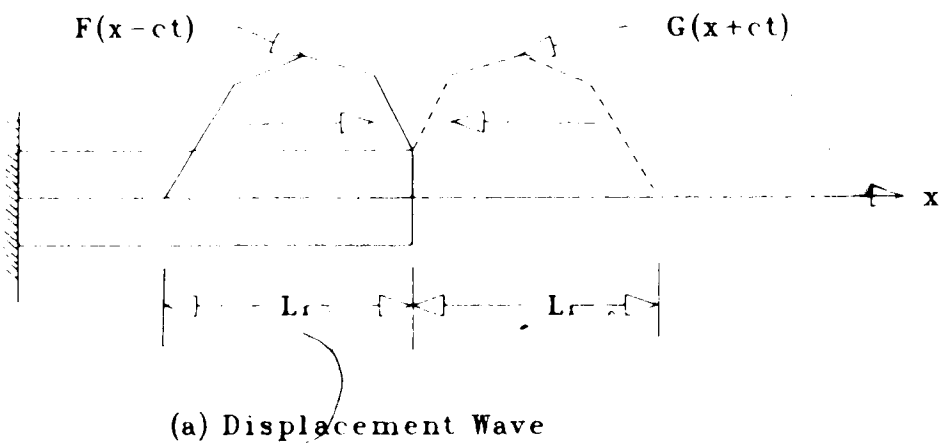


Figure 2.4 Reflection of Displacement and Stress Waves at Free End

This indicates that the reflected wave at the free end also has the same deflection as the incident wave, but the stresses are reversed because the direction of travel is reversed. It may be noted that the total deflection at the free end is doubled by the superposition of the incident and reflected waves, while the two stress components cancel each other.

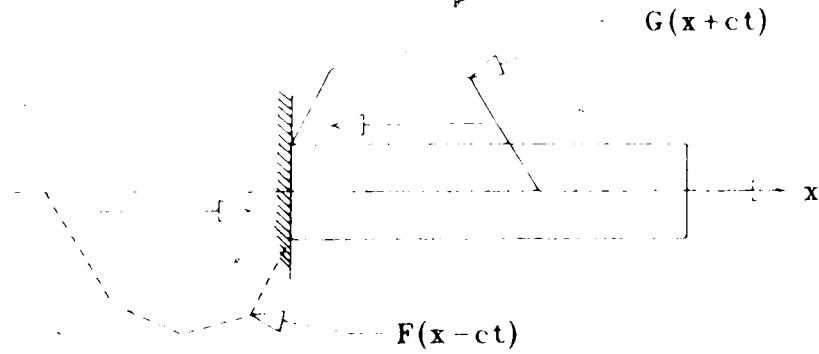
To analyse the fixed end of a bar, consider the Equation (2.7)

$$\begin{aligned} u_{(x=1)} &= 0 = F(L-ct) + G(L+ct) \\ G(L+ct) &= -F(L-ct) \end{aligned} \quad (2.14)$$

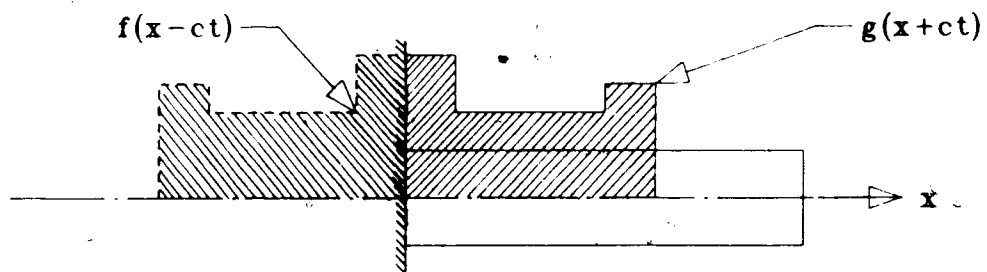
The displacement waves in this case are having opposite signs, and by analogy with the preceeding discussion it can be inferred that the incident and reflected stress waves have the same sign as shown in Figure (2.5).

Hence in satisfying the required zero displacement condition, the reflected wave produces a doubling of stress at the fixed end of the bar.

Thus it can be concluded that, at the free end of a bar, a compression wave is reflected back as a tension wave having the same magnitude and shape. In similar manner, a tension wave is reflected back as a compression wave at the free end of a bar. Also, at the fixed end a compression wave is reflected back as a compression wave of the same magnitude and shape. In similar manner, a tension wave is



(a) Displacement Wave



(b) Stress Wave

Figure 2.5 Reflection of Displacement and Stress Waves at Fixed End

reflected back as a tension wave at the fixed end of a bar.

### 2.2.3 Discontinuity in Bar Properties

The wave reflections which take place at the fixed or free end of a uniform bar may be considered as special cases of the general reflection and refraction phenomena occurring at any discontinuity in the bar properties. The conditions of equilibrium and compatibility which must be satisfied at all points along the bar require that additional reflected and refracted waves be generated at the juncture between bars of different properties in response to the action of any given incident wave.

Consider the juncture between bars 1 & 2 shown in Figure (2.6). The mass per unit length of the bar is  $m = \rho A$ .

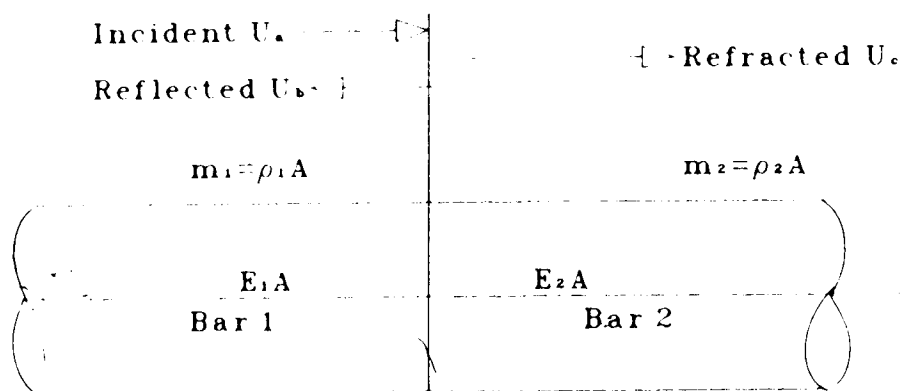
The forward propagating wave  $u_a$  which arrives at the juncture in bar 1 generates a reflection wave  $u_b$  which travels in the opposite direction of  $u_a$  in bar 1 and at the same time creates a refracted wave  $u_c$  which propagates in the direction of  $u_a$  in bar 2.

Continuity conditions that are imposed at the juncture are displacement and force.

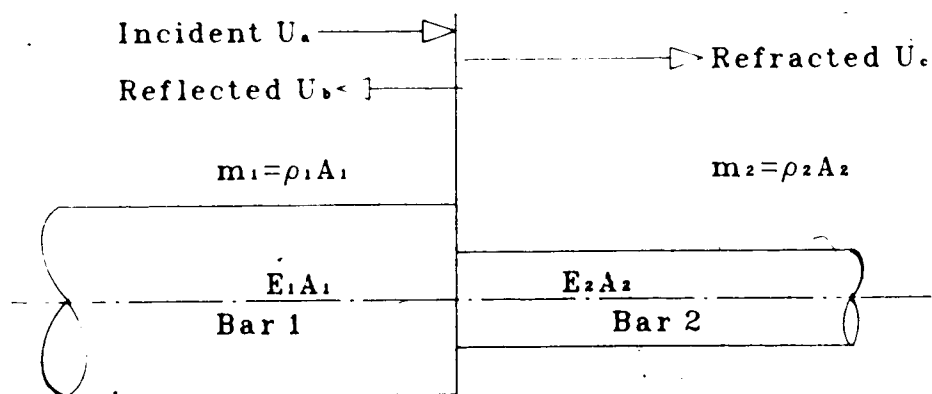
$$\begin{aligned} u_1 &= u_2 \\ u_a + u_b &= u_c \end{aligned} \quad (2.15)$$

$$\begin{aligned} F_1 &= F_2 \\ F_a + F_b &= F_c \end{aligned} \quad (2.16)$$

The time derivative of the displacement condition must be satisfied to satisfy the continuity condition at the



(a) Pile with uniform x-section



(a) Pile with varying x-section

Figure 2.6 Wave Reflection and Refraction at Discontinuity

junction.

$$\frac{\partial u_a}{\partial t} + \frac{\partial u_b}{\partial t} = \frac{\partial u_c}{\partial t} \quad (2.17)$$

The incident wave  $u_a$  can be expressed in the form

$$u_a = f_a(x-ct) = f_a(\xi)$$

$$\frac{\partial u_a}{\partial x} = \frac{\partial f_a}{\partial \xi} \frac{\partial \xi}{\partial x} = \frac{\partial f_a}{\partial \xi} \quad (2.18)$$

$$\frac{\partial u_a}{\partial t} = \frac{\partial f_a}{\partial \xi} \frac{\partial \xi}{\partial t} = -c \frac{\partial f_a}{\partial \xi} \quad (2.19)$$

where the variable  $\xi$  is introduced for convenience.

Combining Equations (2.18) & (2.19) gives

$$\frac{\partial u_a}{\partial t} = -c_1 \frac{\partial u_a}{\partial x} \quad (2.20a)$$

Similar analysis can be carried out for reflected and refracted waves which will result in

$$\frac{\partial u_b}{\partial t} = c_1 \frac{\partial u_b}{\partial x} \quad (2.20b)$$

$$\frac{\partial u_c}{\partial t} = -c_2 \frac{\partial u_c}{\partial x} \quad (2.20c)$$

By substituting Equation (2.20) in to Equation (2.17) leads to

$$-c_1 \frac{\partial u_a}{\partial x} + c_1 \frac{\partial u_b}{\partial x} = -c_2 \frac{\partial u_c}{\partial x} \quad (2.21)$$

where  $\frac{\partial u_a}{\partial x}$  can be expressed in the form

$$\frac{\partial u_a}{\partial x} = \frac{\sigma_a}{E} = \frac{F_a}{A \cdot E}$$

Hence the compatibility condition of Equation (2.21) can be expressed in terms of the force waves.

$$-c_1 \frac{F_a}{A \cdot E} + c_1 \frac{F_b}{A \cdot E_1} = -c_2 \frac{F_c}{A_2 \cdot E_2}$$

$$F_c = \frac{c_1 A_2 E_2}{c_2 A_1 E_1} (F_a - F_b)$$

$$\text{where } c_1 = \sqrt{\frac{E_1 A_1}{m_1}} \text{ and } c_2 = \sqrt{\frac{E_2 A_2}{m_2}}$$

$$a = \frac{c_1 A_2 E_2}{c_2 A_1 E_1} = \sqrt{\frac{m_2 E_2 A_2}{m_1 E_1 A_1}} \quad (2.22)$$

$$F_c = a(F_a - F_b) \quad (2.23)$$

Combining Equations (2.16) & (2.23) leads to

$$F_a + F_b = a(F_a - F_b)$$

$$F_b = F_a \left[ \frac{a-1}{a+1} \right] \quad (2.24)$$

$$F_c = F_a \frac{2a}{(a+1)} \quad (2.25)$$



Equations (2.24) and (2.25) express the relationships between the incident, reflected and refracted force waves at the bar discontinuity. Corresponding relationships can be obtained for the displacement waves by noting that

$$F = AE \frac{\partial u}{\partial x} = AE \frac{\partial u}{\partial t} \frac{\partial t}{\partial x}$$

$$F = \frac{+AE \partial u}{c \partial t}$$

Substituting the above in to Equation(2.24) and integrating gives

$$\begin{aligned} \frac{A_1 E_1}{C_1} u_b &= \frac{A_1 E_1}{C_1} u_a \left[ \frac{a-1}{a+1} \right] \\ u_b &= u_a \left[ \frac{a-1}{a+1} \right] \end{aligned} \quad (2.26)$$

Similarly by substituting in Equation(2.25) and integrating gives

$$u_c = u_a \frac{2a}{(a+1)} \quad (2.27)$$

It is evident that the factor  $a$  defines the character of the discontinuity at the juncture between two bars and controls the relative amplitudes of the reflected and refracted waves. In this context, the fixed and free end conditions discussed in Section 2.2.2 can be considered as limiting cases of bar discontinuity and are defined by infinite and zero values of  $a$ , respectively.

### 2.3 Wave Theory Applied to Piles

It is evident from the preceeding sections that, if a pile rests on a rigid support no displacement can take place at this point. The reflected stress wave produced by the incident wave that was created by the hammer impact must be compressive. The total stress at subsequent times is then given by the sum of the incident and reflected components.

The other limiting case occurs if the end of the pile is resting on very soft clay so that there is essentially no resistance to its displacement and the tip stress is required to be zero. Hence the reflected stress wave must be tensile, and the total stress in the pile is given by the difference between the tensile and compressive components.

The other practical aspect is that, when a stress wave reaches a gap or a joint, part of the stress wave is reflected while the remainder will be transmitted unaltered through the joint. The ratio between the transmitted and the reflected waves depends on the dynamic properties of the pile segments above and below the jointed sections as well as on the properties of the joint itself.

The nature of wave propagation and development of the stress wave during pile driving are examined in this section. Also, the influence of pile impedance and particle velocity are analysed.

### 2.3.1 Stress Waves Developed During Pile Driving

In practical situations where impact type hammers are used, the hammer is heavier than the pile. This generates a displacement response of the pile. For the purposes of analysing the nature of the driving impulse the driving hammer is assumed rigid and the cushion between the pile and hammer is represented by a weightless spring.

The displacement of the hammer from its point of contact with the driving cushion is denoted by  $Z$  and the displacement of pile top by  $u_o$ . Consider the equilibrium of the hammer during impact

$$F_c = W + F_1$$

where  $W = mg$ ,  $F_1 = m\left(\frac{\partial^2 Z}{\partial t^2}\right)$

$$F_c = m\left(g + \frac{\partial^2 Z}{\partial t^2}\right) \quad (2.28)$$

Continuity of displacement requires that the movement of the hammer be equal to the displacement of the end of the pile plus the compression of the cushion. Spring constant of cushion is denoted by  $k$ .

$$Z = u_o + \frac{F_c}{k} \quad (2.29a)$$

$$\frac{\partial^2 Z}{\partial t^2} = \frac{\partial^2 u_o}{\partial t^2} + \frac{1}{k} \frac{\partial^2 F_c}{\partial t^2} \quad (2.29b)$$

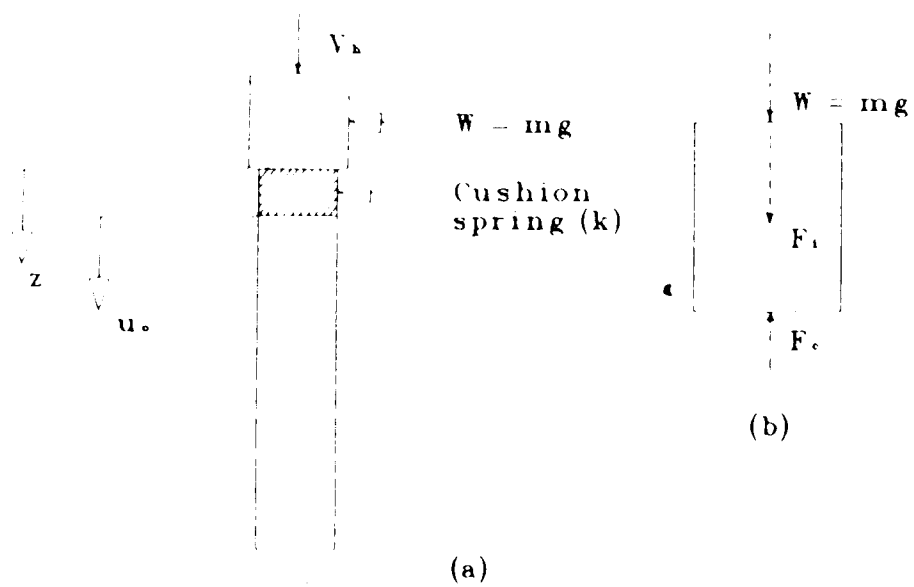


Figure 2.7 Analysis of Pile Driving Contact Force

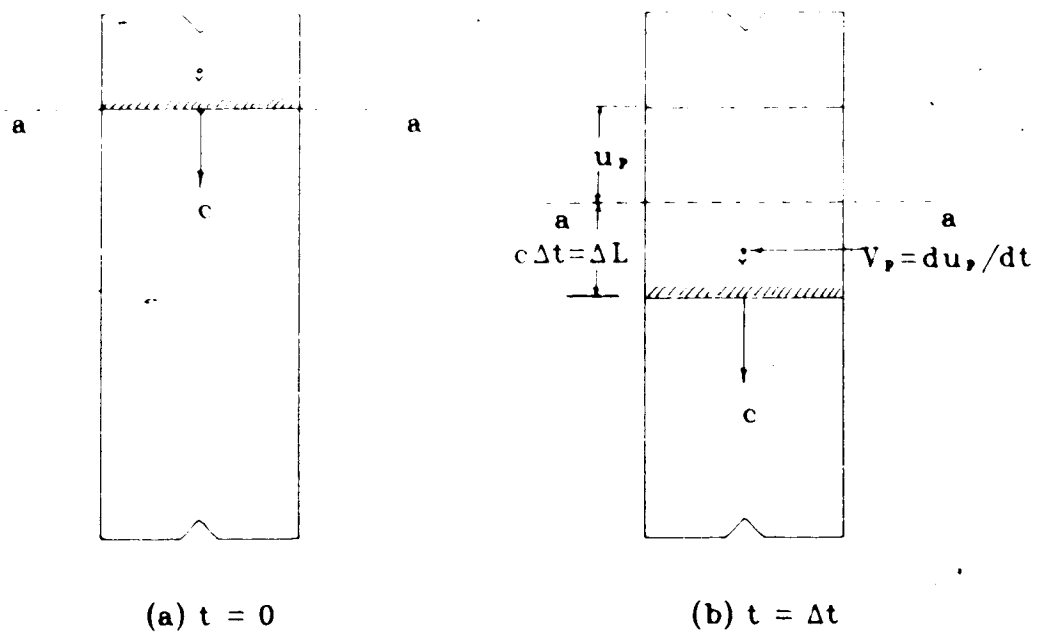


Figure 2.8 Stress Condition in a Pile During Driving

Substituting Equation(2.29b) in Equation(2.28) yields

$$F_c = m \left[ g - \frac{\partial^2 u_c}{\partial t^2} - \frac{1}{k} \frac{\partial^2 F_c}{\partial t^2} \right] \quad (2.30)$$

$$F_c = \sigma_c A$$

where  $\sigma_c$  is the stress in the pile and A is the area of cross-section.

$$F_c = AE \frac{\partial u_c}{\partial x} \text{ and } \sigma = E \frac{\partial u_c}{\partial x}$$

$$F_c = AE \frac{\partial u_c}{\partial t} \frac{\partial t}{\partial x}$$

$$F_c = \frac{AE}{c} \frac{\partial u_c}{\partial t} \quad (2.31)$$

$$\text{where } c = \frac{\partial x}{\partial t}$$

Combining Equations (2.30) & (2.31) and rearranging leads to

$$\frac{m}{k} \frac{AE}{c} \frac{\partial^3 u_c}{\partial t^3} + m \frac{\partial^2 u_c}{\partial t^2} + \frac{AE}{c} \frac{\partial u_c}{\partial t} = mg$$

If the velocity of the end of the pile is denoted by  $V_p$  and noting that  $\frac{\partial u_c}{\partial t} = V_p$ , the equation above becomes

$$\frac{\partial^2 V_p}{\partial t^2} + \frac{kC}{AE} \frac{\partial V_p}{\partial t} + \frac{k}{m} V_p = \frac{kC}{AE} g \quad (2.32)$$

This equation may be recognized as the equation of motion of a single degree of freedom system subjected to

static loading. In Equation(2.32)  $\frac{kC}{AE}g$  represents the part of the contact force applied to the hammer weight, which is a small fraction of the inertial effect and it may be neglected. Therefore the Equation(2.32) becomes

$$\frac{\partial^2 V_p}{\partial t^2} + 2\omega\xi \frac{\partial V_p}{\partial t} + \omega^2 V_p = 0$$

Where  $\omega^2 = \frac{k}{m}$  and  $2\omega\xi = \frac{kC}{AE}$

The solution of this single degree of freedom damped free vibration equation is

$$V_p = e^{-\xi\omega t} \left[ A \sin\omega_n t + B \cos\omega_n t \right] \quad (2.33)$$

where  $\omega_n = \omega(1 - \xi^2)^{1/2}$ ; by differentiating the Equation (2.29) with respect to  $t$ ,

$$\frac{\partial Z}{\partial t} = \frac{\partial u_o}{\partial t} + \frac{1}{k} \frac{\partial F_c}{\partial t}$$

$$\text{at } t = 0, \quad \frac{\partial u_o}{\partial t} = 0; \quad \frac{\partial Z}{\partial t} = \frac{1}{k} \frac{\partial F_c}{\partial t} = V_h$$

where  $V_h$  is the hammer velocity at impact

$$\frac{\partial F_c}{\partial t} = kV_h \quad (2.34)$$

By differentiating Equation(2.31)

$$\frac{\partial F_c}{\partial t} = \frac{AE}{C} \frac{\partial^2 u_o}{\partial t^2} \quad (2.35)$$

Combining Equations (2.34) & (2.35) gives

$$\frac{\partial^2 u_o}{\partial t^2} = \frac{kC}{AE} V_h = 2\omega\xi V_h$$

Using the initial condition at  $t = 0$

$$\frac{\partial u_o}{\partial t} = 0 = \left[ A(0) + B(1) \right]; \text{ ie, } B = 0$$

$$\frac{\partial^2 u_o}{\partial t^2} = 2\omega\xi V_h = \left[ A \omega_n(1) \right]$$

$$\text{Therefore } A = 2\xi \frac{\omega}{\omega_n} V_h$$

$$\text{Hence the tip velocity } V_p = \frac{\partial u_o}{\partial t} = e^{-\xi\omega_n t} \cdot 2\xi \frac{\omega}{\omega_n} V_h \sin\omega_n t$$

The variation of contact force is given by

$$F_c = \frac{k}{\omega_n} V_h \cdot e^{-\xi\omega_n t} \sin\omega_n t$$

This solution demonstrates the nature of stress wave during pile driving. However, this solution is valid only while the hammer is in contact with the cushion and before the stress wave is reflected from the other end of the pile and returns to the pile head.

### 2.3.2 Particle and Wave Velocity

There exist a simple relationship between the particle velocity and the stress level in the pile. The particle velocity of pile during driving depends on the striking velocity of the hammer which is normally about 2 to 8 m/sec

while the wave velocity in pile is about 4000 to 5000 m/sec

Figure (2.8) shows the stress condition in a pile during driving. Figure (2.8a) shows stress wave which propagates in a pile with velocity  $c$  and reaches the section a-a at time  $t=0$ .

The velocity of the particles ahead the wave front is equal to zero while behind the front, the velocity will be  $V_p = \frac{du_p}{dt}$ , where  $u_p$  is the particle displacement.

Figure (2.8b) shows the situation at time  $t=\Delta t$ . As mentioned in Section 2.1, the cross-section of the pile at section a-a which has been displaced by distance  $u_p$  is assumed to be plane. Also, the velocity  $V_p$  is considered to be constant during this time increment  $\Delta t$ . Displacement of the particle in time  $\Delta t$  is given by

$$u_p = \int_0^{\Delta t} \frac{du_p}{dt} \cdot dt = \frac{du_p}{dt} \cdot \Delta t \quad (2.36)$$

During this time interval  $\Delta t$ , the wave front would have travelled the distance  $\Delta L = c\Delta t$

The ratio between the particle displacement and distance of wave travel  $\epsilon = u_p/\Delta L$ .

$$\epsilon = \frac{u_p}{\Delta L} = \frac{u_p}{c\Delta t} = \frac{V_p}{c}, \text{ where } V_p = \frac{du_p}{dt}$$

$$\epsilon = \frac{V_p}{c} \quad (2.37)$$

Thus the axial strain corresponds to the ratio of the particle and wave velocities. The relationship between the



axial force in the pile and particle velocity  $V_p$  can be obtained from Equation (2.37).

$$\epsilon = \frac{V_p}{c} = \frac{\sigma}{E}, \quad \sigma = \frac{E}{c} V_p$$

$$F = \sigma A = \frac{AE}{c} V_p$$

$$F = Z V_p$$

The factor  $\frac{AE}{c} = Z$  is called the impedance.

This simple relationship is frequently used to calculate the axial force in a pile from the particle velocity by measuring the acceleration during the driving. The impedance  $Z$  is also called dynamic stiffness due to its similarity with the expression for the axial stiffness of a rod  $\frac{AE}{L}$ .

### 2.3.3 Influence of Impedance on Stresses

When the hammer with velocity  $V_0$  strikes the pile, the particle velocity in the pile is  $V_p = \frac{du_p}{dt}$ . The corresponding particle velocity in the hammer which is directed upwards is  $V_h = \frac{du_h}{dt}$ . A compression wave is generated which simultaneously moves upwards through the hammer and downwards through the pile with the velocity  $c$ .

During the impact, the pile and hammer will remain in contact only for a short time. At the time of impact, the force between the hammer and the pile must be equal.

$$Z_h \cdot V_h = Z_p \cdot V_p \quad (2.38)$$

Where  $Z_h$  and  $Z_p$  are the impedance of the hammer and pile, respectively. The particle velocities in the pile and in the hammer at the contact surface must be same.

$$V_o - V_h = V_p \quad (2.39)$$

If  $Z_h = Z_p$ , by combining Equations (2.38) & (2.39)

$$V_p = \frac{1}{2}V_o$$

If  $Z_h \neq Z_p$

$$V_p = \left(1 + \frac{Z_p}{Z_h}\right)V_o$$

The force  $F$  during the impact depends on the striking velocity of the hammer  $V_o$  and the impedance of the pile  $Z$ . This force can be calculated from  $F = \frac{1}{2}V_o \cdot Z$

It is evident from the above discussion that the ratio of the transmitted and reflected stress waves depends on the impedance of the different pile segments. Also, pile integrity can be checked by measuring force and acceleration at the pile head using strain gauge and accelerometer.

## 2.4 Summary

The solution of one dimensional wave equation has been used to investigate the wave-propagation mechanism in a pile during driving. This solution has also been made use to show that the energy delivered by the hammer is transferred to the pile toe via stress or an elastic strain wave. These analyses indicate that when the pile being driven into a hard material such as rock or very dense sand, the incident wave created by the hammer impact is reflected at the pile toe as compressive wave. On the other hand, when the soil at the tip is soft and driving is easy, the compressive wave is reflected at the pile point as tensile wave. Further, the total stress in the pile at subsequent times depends on the incident and reflected waves.

The factor  $\alpha$  has been derived from the continuity condition imposed at the pile joint. This factor defines the character of the discontinuity or joint in a pile and controls the relative amplitude of the reflected and refracted waves.

It has been shown that the pile velocity and the stress level in the pile can be related using stress-strain relationship. The existence of this simple relationship is frequently used to calculate the axial force in a pile. The factor relating the force and the velocity is called the impedance.

### 3. PILE DRIVING HAMMERS

The development of piling equipment proceeded on different lines in various parts of the world, depending mainly on the influence of the local ground conditions. Typical pile driving hammers include drop hammers, single-acting hammers, double-acting hammers, differential hammers, compound hammers, diesel hammers and vibratory drivers. In addition there are special types of hammers, such as air-gun, vibratory-impact and electrohydraulic hammers. Powered pile-driving hammers can be classified as air or steam hammers, diesel hammers and vibratory drivers.

The growth of the offshore oil industry in many parts of the world necessitated the development of an entirely new range of very heavy single acting steam hammers designed for driving large diameter steel piles guided by tubular-jacket structures. However, diesel hammers have gained acceptance throughout most of the world, principally because they are economical to operate, do not require a remote energy source, are easily mobilized, and lighter than comparable steam/air hammers. In this chapter, the discussion is confined to the impact type of hammers and their working principle and also to the hammer accessories and its functions. Detail informations about various types of pile driving hammers can be found in Fuller (1983) and Tomlinson (1977).

## 3.1 Working Principle of Various Impact Type of Hammers

### 3.1.1 Drop and Single-Acting Air/Steam Hammers

The drop hammer is the oldest type and simplest form of pile driving hammer in use and is simply a heavy weight that is allowed to drop freely on the head of the pile. The drop weight is ~~usually~~ guided by lugs or jaws sliding in the leaders and actuated by the lifting rope. Today, because of their slow rate of operation and inconsistent delivered energy, drop hammers are seldom used to drive foundation piles. They are sometimes used to drive piles for small projects and in remote areas. Details of the hammer and accessories are shown in Figure (3.1).

The drop hammer consists of a solid mass or assemblies of forged steel. The striking speed is slower than in the case of single or double acting hammers, and when drop hammers are used to drive concrete piles, there is a risk of damage to the pile if an excessively high drop of the hammer is adopted when the driving becomes difficult.

The velocity of the ram which is the heavy weight that strikes the pile can be computed from the kinetic-energy equation.

$$\frac{1}{2}W_r \cdot V_h^2 = (E_f)(\text{ram energy})$$

where ram energy =  $W_r g h_f$

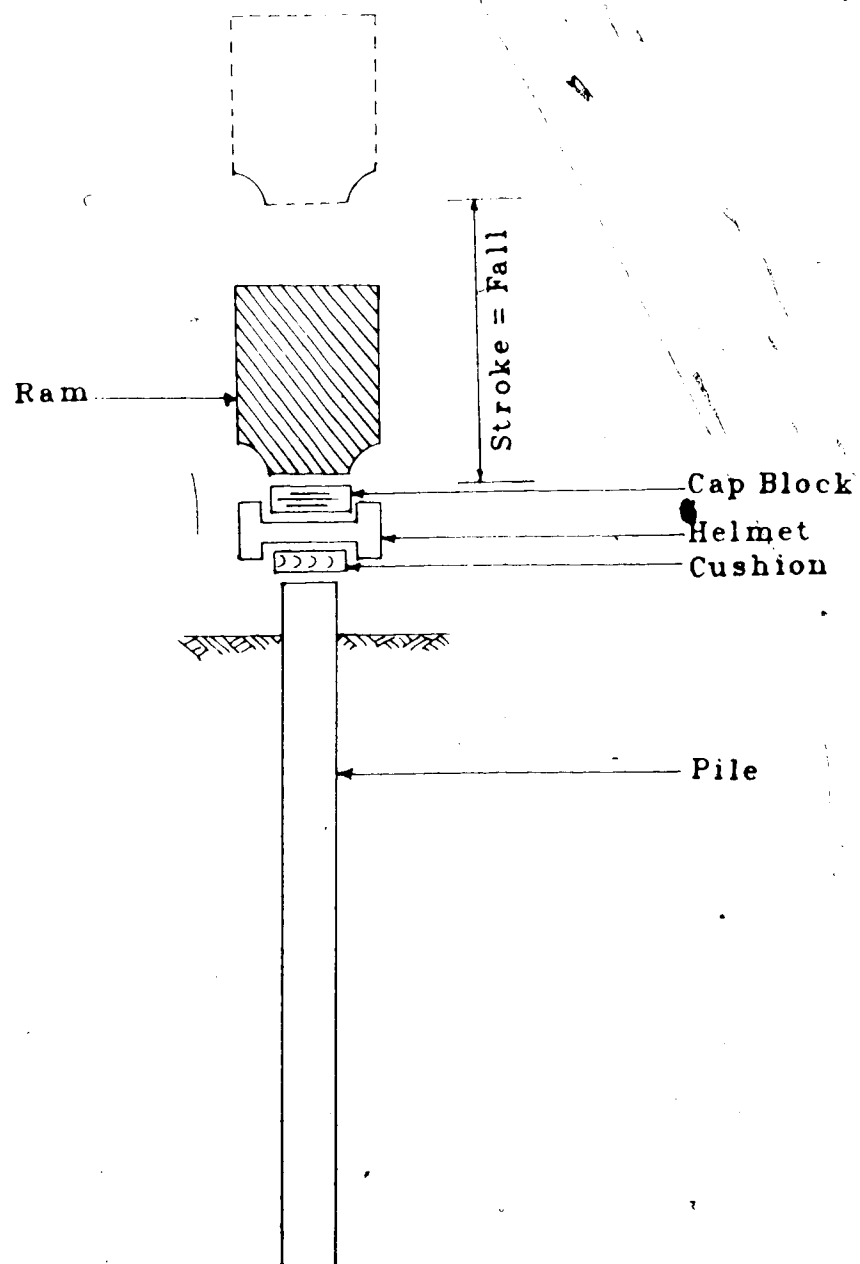


Figure 3.1 Drop Hammer

$W_r$  is the weight of ram and  $h_r$  is the height of its fall;  $E_r$  is the hammer efficiency to accommodate energy losses during hammer operation.

$$V_h^2 = 2gh_r E_r$$

$$V_h = \sqrt{2gh_r E_r} \quad (3.1)$$

The single acting hammers are powered by compressed air or steam pressure, which is used to raise the hammer ram for each stroke. The steam or air is exhausted on the down stroke. The delivered energy results from the kinetic energy developed by the gravity fall of the ram.

Figure (3.2) shows schematically the operation of a single acting hammer. At the start of the cycle, the ram has impacted, and air or steam pressure is being admitted into the cylinder below the piston. The upward force resulting from this pressure is about twice the weight of the ram. This pressure raises and accelerates the ram until the lower wedge on the slide bar trips the valves to shut off the air or steam supply and open the exhaust. Because of upward acceleration, the ram continues to move up until its kinetic energy is zero, at which time it starts its gravity fall. Just prior to impact, the upper wedge on the slide bar trips the valves to close off the exhaust and admit air or steam. The complete valve action is not immediate, and the ram

continues its downward movement to impact on the cap block. By this time the intake valve is completely open. The air or steam pressure builds up rapidly to raise the ram, and the cycle is repeated.

The velocity of the hammer at impact can be computed from the kinetic equation as explained above. Also, Equation (3.1) is applicable for single acting air-steam hammers.

### 3.1.2 Double Acting or Differential-Acting Hammers

Double acting hammers are steam or air operated both on the upstroke and down stroke, and are designed to impart a rapid succession of small stroke blows to the pile. The double acting hammer exhaust the air or steam on both up and down strokes. In the case of differential-acting hammer, however, the cylinder is under equal pressure above and below the piston and is exhausted only on the upward stroke. The downward force is a combination of the weight of the ram and the difference in total force above and below the piston. The force below the piston is less because of the area occupied by the piston rod. Double acting hammers have light rams and operate at relatively high speed. Differential hammers have shorter strokes than comparable single acting hammers and combine the advantages of the heavy ram of the single acting hammers with higher operating speed of the double-acting hammers.

The working principle of one type of double acting hammer is illustrated in Figure (3.3). The pressure applied



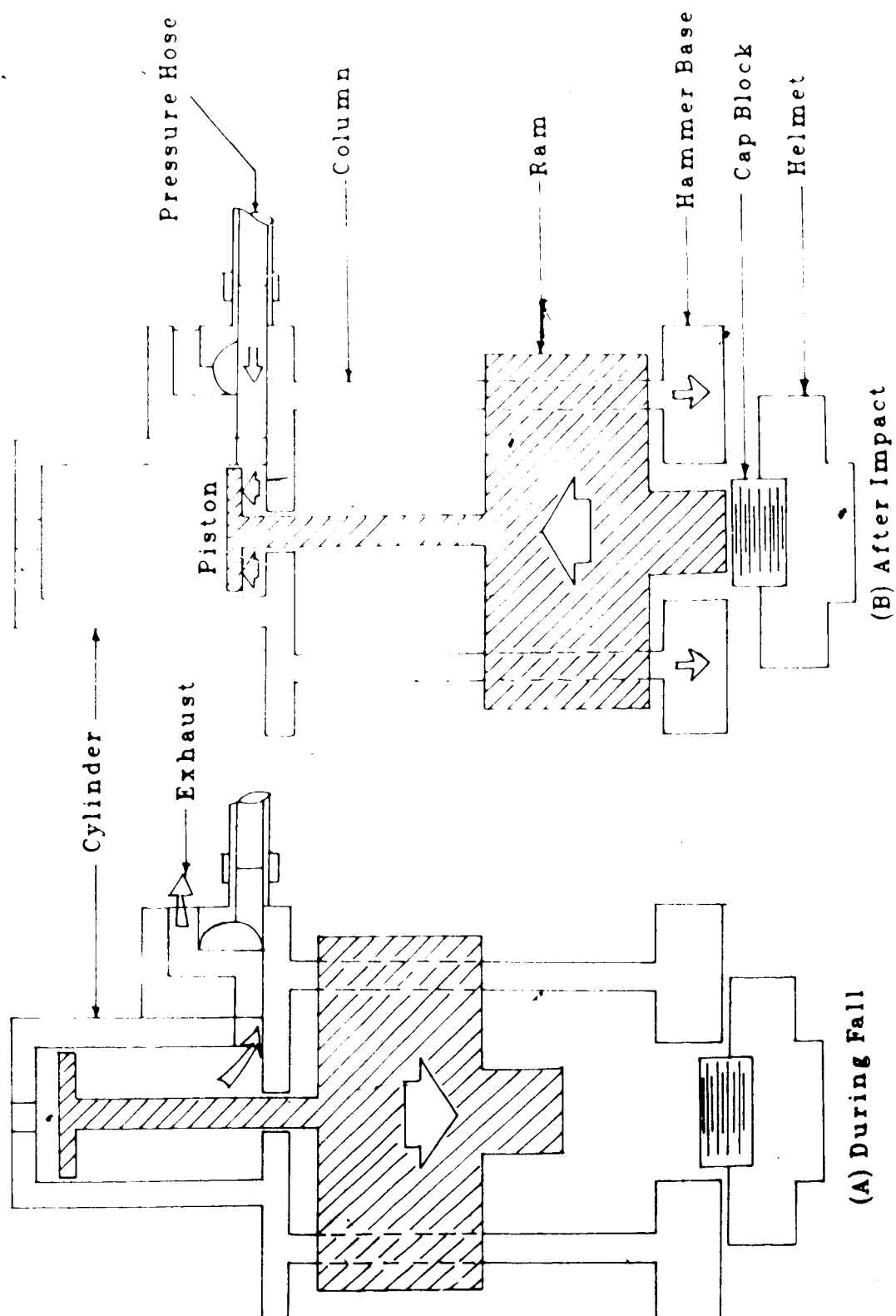


Figure 3.2 Single-Acting Air/Steam Hammer

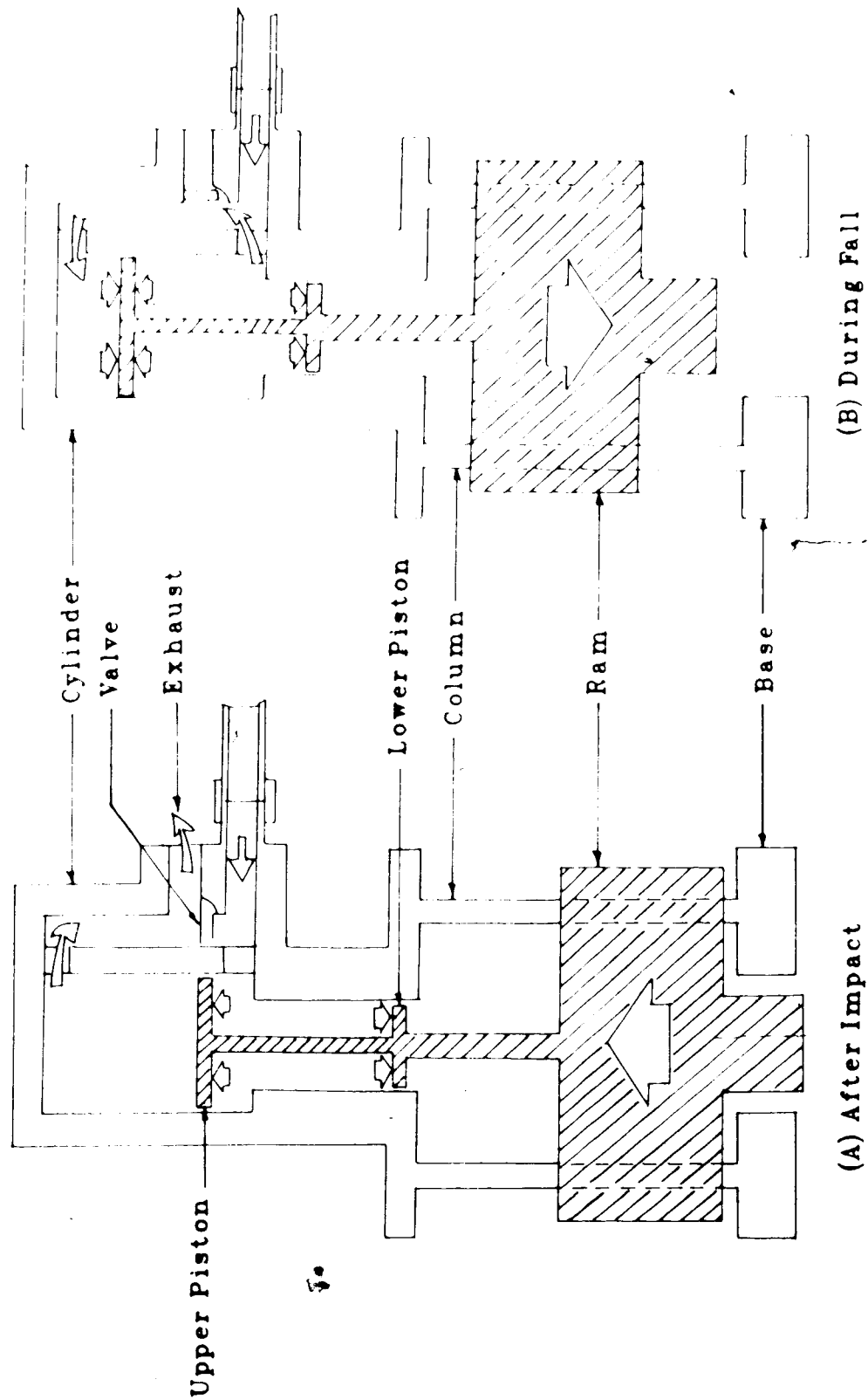


Figure 3.3 Double-Acting Hammer

at the top of the piston acts against the top of the cylinder. The pressure could lift the hammer assembly of weight  $W_h$  to which the cylinder is connected. Maximum hammer output will be achieved when the pressure is kept at its upper limit  $P_1$  (ie, gauge pressure) at which assembly lift off is incipient. The maximum energy of a differential acting hammer is  $E_{max}$

$$E_{max} = (W_r + P_1 A_c) h_f$$

Where  $A_c$  is the effective area of the cylinder,  $W_r$  is the weight of ram and  $h_f$  is the maximum stroke of the hammer.

$$P_1 A_c = W_h$$

$$A_c = \frac{W_h}{P_1}$$

The potential energy of a hammer driven by an actual pressure  $P_a$  is  $E_a$

$$E_a = (W_r + P_a \cdot \frac{W_h}{P_1}) h_f$$

From this relation, an effective stroke  $H_e$  is derived that a weight  $W_r$  should fall in order to provide a kinetic energy equal to  $E_a$ .

$$H_e \cdot W_r = (W_r + \frac{P_a}{P_1} \cdot W_h) h_f$$

$$H_e = (1 + \frac{P_a}{P_1} \cdot \frac{W_h}{W_r}) h_f \quad (3.2)$$

Pressure and other losses might occur during the fall of the ram and also, the ram might not rise high enough. For these reasons it is common to multiply the effective stroke by an efficiency  $E_e$ .

The ram velocity at impact is calculated same as in Section 3.1.1.

$$V_i = \sqrt{2gh_e E_e} \quad (3.3)$$

### 3.1.3 Diesel Hammers

Diesel hammers are self contained power units. The principle of the diesel hammer is that as the falling ram compresses air in the cylinder, diesel fuel is injected into the cylinder and this is atomized by the impact of the ram on the concave base. The impact ignites the fuel and the resulting explosion imparts an additional 'kick' to the pile, which is already moving downwards under the blow of the ram. Thus the blow is sustained and imparts energy over a longer period than the simple blow of a drop or single-acting hammer.

The hammer is started by raising the ram or piston with a crane line to the top of its stroke and releasing it, permitting it to fall inside the cylinder. As the ram descends, it closes off the air intake port. Some hammers are of the impact-atomization type, whereas others have a spray-atomization fuel injection system. The ram continues to compress and heat up the air in the cylinder, and at impact, the air-fuel mixture ignites under pressure and

heat. The resulting explosion raises the ram for its next stroke. At the start of the upstroke, the exhaust intake port is opened, and the products of combustion are exhausted. As the ram moves upward, fresh air is drawn into the cylinder. The ram continues its ascent to the top of its stroke, and the cycle repeats.

A difficulty arises in using the diesel hammer in soft clays or weak fills, since the pile yields to the blow of the ram and the impact is insufficient to atomize the fuel. When the hammer is used to penetrate such soils to reach more resistant soil below, the fuel is cut off and the hammer is operated from the winch rope as a simple drop hammer, performing what are known as 'cold blows'. The diesel hammer operates automatically and continuously at a given height of drop unless the lever is adjusted. Whereas with the single-acting hammer every blow is controlled in height. There are three basic types of diesel hammers in practice and these are discussed below.

#### 3.1.3.1 Open Ended Diesel Hammer

Figure (3.6) shows schematically the operational cycle of an open ended diesel hammer and components of the hammer are shown in Figure(3.4). Basically this hammer differ from other type of diesel hammers by having an open end at the cylinder top. The open end diesel hammer operates on a two stroke diesel cycle.

As mentioned in Section 3.1.3, the hammer is started by raising the ram with lifting mechanism. At

the upper end of travel the lifting mechanism is tripped, the ram is released and descends by gravity. At the time the ram bottom passes the exhaust ports a certain volume of air at atmospheric pressure is trapped and is compressed. When the ram impacts against the anvil the air is compressed to a final volume.

#### 3.1.3.2 Closed Ended Diesel Hammer

The closed end diesel hammer works very much like the open ended one. In principle the main change consists of a closed cylinder top. Figure (3.7) shows two of these hammer types. When the ram moves upward, air is being compressed at the top of the ram which causes shorter stroke and, therefore higher blow rate.

The bounce chamber has ports such that atmospheric pressure exists as long as the ram top is below these ports. As the ram moves towards the cylinder top it creates a pressure which increases until it is just in balance with the weight of the cylinder itself. Further compression is not possible and if the ram still has an upward velocity, uplift of the cylinder will result.

#### 3.1.3.3 Vacuum Chamber Diesel Hammer

This hammer type employs a vacuum chamber below its ram to increase its operating speed. Two phases of this hammer's operation are shown in Figure (3.8). As can be seen, the hammer is not really closed at the top although a protective cover is usually present.

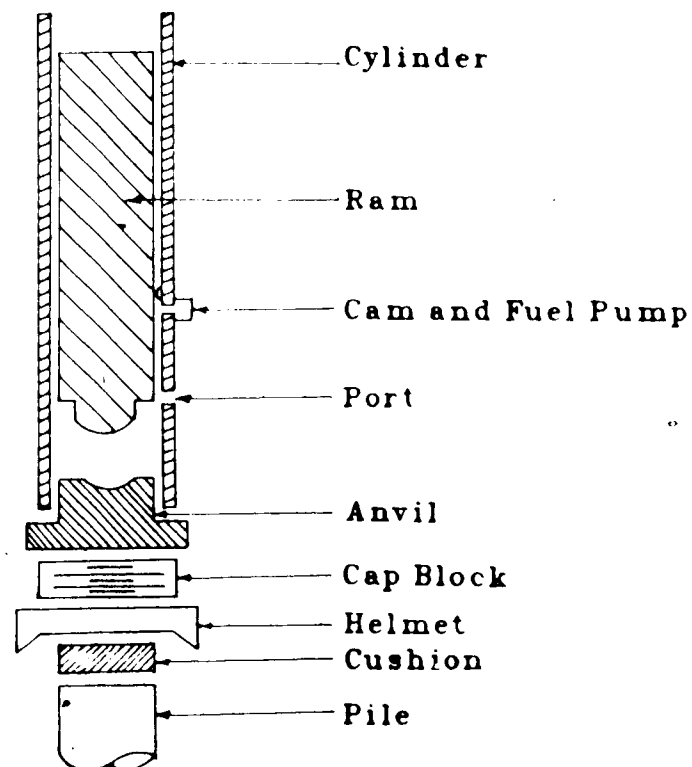


Figure 3.4 Components of Typical Open Ended Diesel Hammer

The material involved has been removed because of the unavailability of copyright permission.

This portion of the page contains the recommendation of Rempe and Davisson (1977) on gas force development during diesel hammer operation. Refer proceedings of the International Conference on Soil Mechanics and Foundation Engineering, 9th, Tokyo, pp.350, July, 1977.

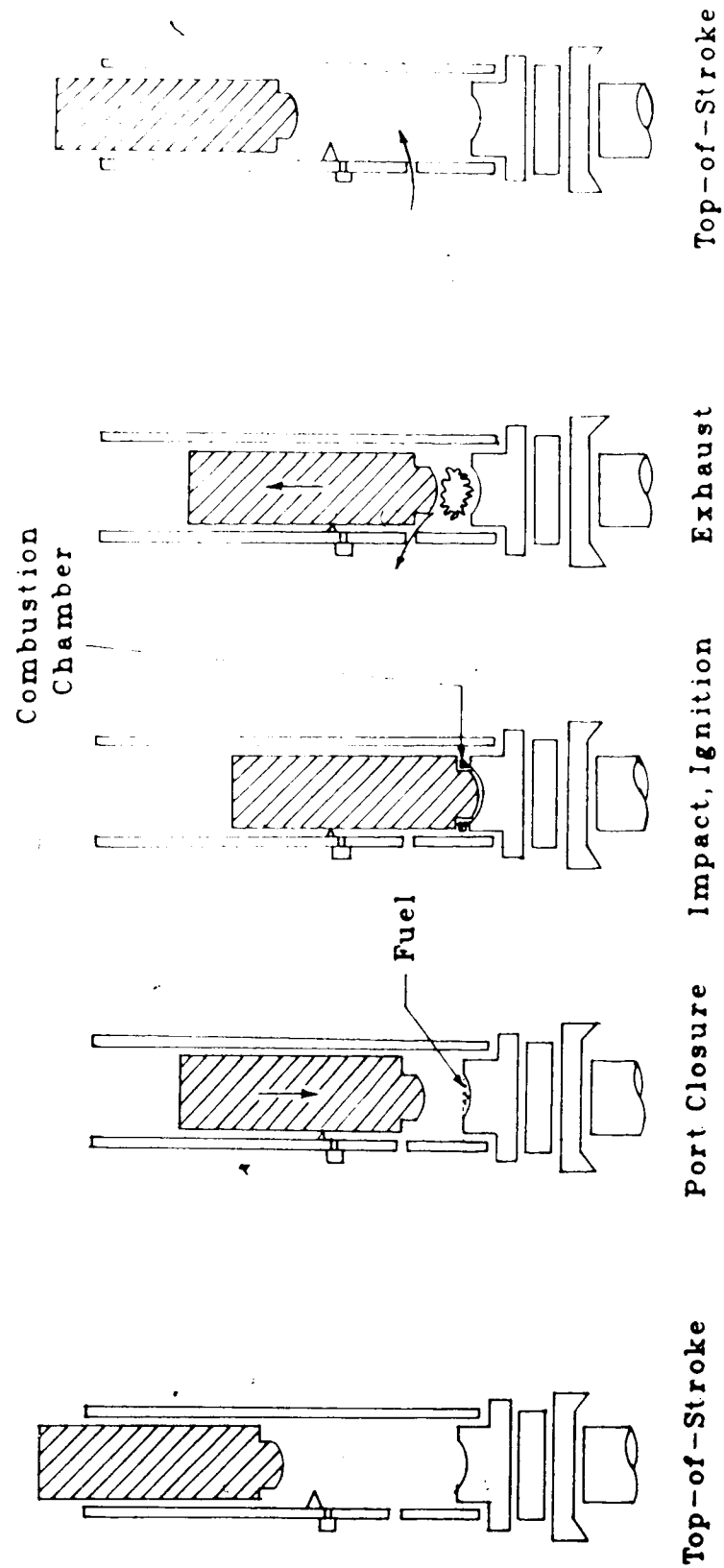


Figure 3.6 Operational Cycle of Diesel Hammer



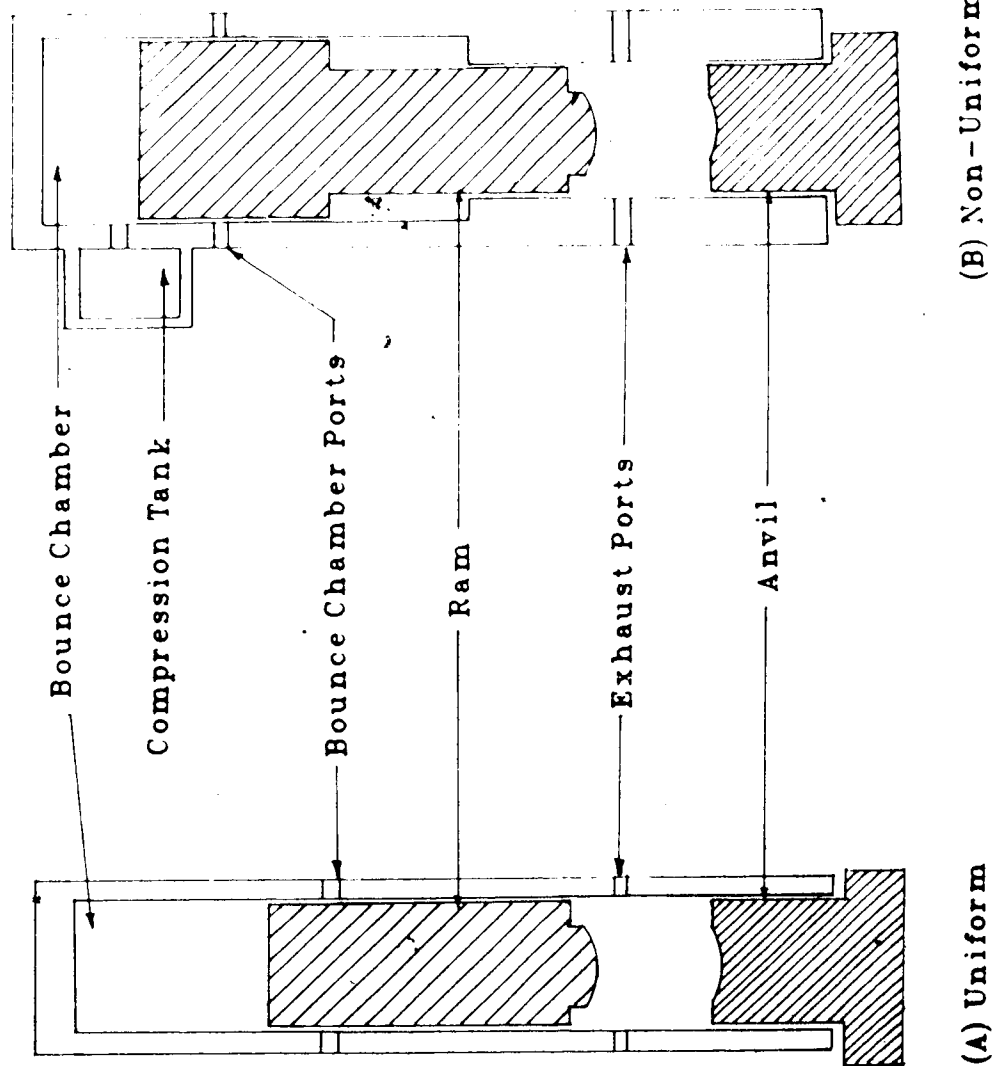


Figure 3.7 Closed Ended Diesel Hammer

However, the stroke is limited by the vacuum action under the upper portion of the ram such that it does not become visible during operation. In addition to being faster than an open end hammer, this hammer type has the advantage of not lifting off during operation since the vacuum force is always less than the cylinder weight.

### 3.1.4 Generalised Diesel Hammer Operation

#### 3.1.4.1 Force in Compression, Combustion and Expansion Phases

As discussed above, the falling ram when passes the exhaust ports prevent further escape of air. Continued downward motion compresses the remaining air into a progressively decreasing volume. The lower ram and upper anvil surfaces are mated, such that when impact occurs the fuel pooled on the top of the anvil is displaced laterally into the annular combustion chamber where it mixes with the compressed air. The result is spontaneous ignition of the fuel-air mixture and a rapid increase of gas pressure. The ram is in contact with the anvil for several milliseconds, during which time the impact and gas force continue to decelerate the ram to zero. The gas forces may be approximated in three phases; compression, combustion and expansion (Rempe & Davisson (1977)). All three phases are shown in Figure (3.5).

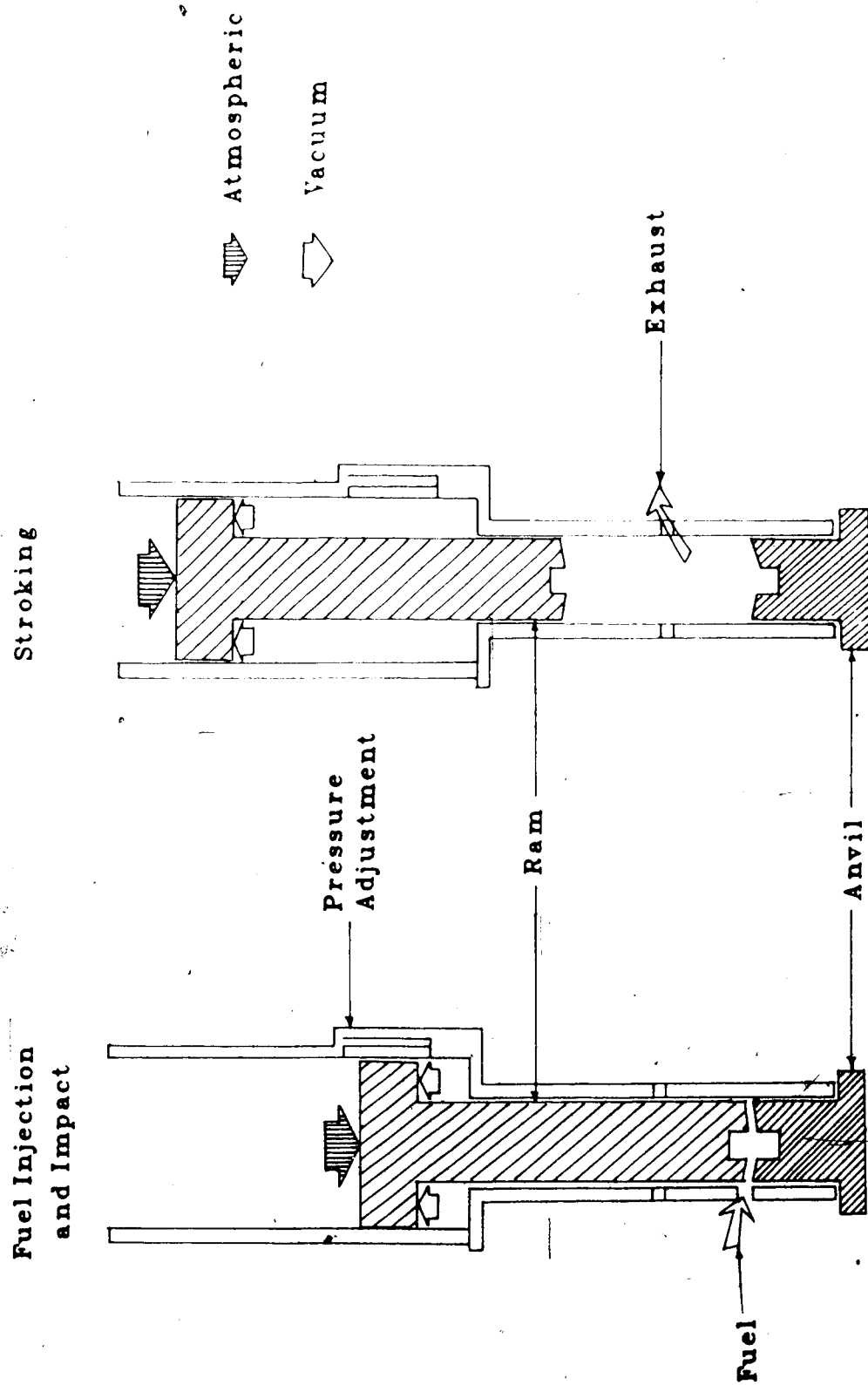


Figure 3.8 Vacuum Chamber Diesel Hammer

It is evident from Figure (3.5) that the maximum gas pressure in compression phase is developed at the time of impact. Force on the pile during compression phase is estimated from the gas pressure at the time of impact. This phase is approximated according to the gas law which is given by the equation below.

$$P_i = P_{at} \left[ \frac{V_o}{V_t} \right]^n$$

where

$P_i$  - Gas pressure at the time of impact

$P_{at}$  - Atmospheric pressure (14.7psi)

$V_o$  - Initial volume of gas

$V_o = V_i + V_t$

$V_i = A_i h_{ex}$

$A_i$  - Area of cross-section of the ram

$h_{ex}$  - Distance between anvil and exhaust port

$V_t$  - Volume of combustion chamber

$n$  - Gas constant

The constant  $n$  is a parameter dependent on the specific heats of the gas in the cylinder. For adiabatic compression of air  $n$  is taken as 1.4. Since the process is not completely adiabatic,  $n$  should be chosen less than 1.4 and greater than 1.2 (Goble et al. (1976)). Hence a value of 1.3 is assigned for  $n$ .

$$P_t = P_{at} \left[ \frac{A_t h_{ex}}{V_t} + 1 \right]^{1.3}$$

Therefore the force  $F_p$  exerted on the pile is given by

$$F_p = A_t P_{at} \left[ \frac{A_t h_{ex}}{V_t} + 1 \right]^{1.3} \quad (3.4)$$

As indicated in Figure (3.5), the delay, rise and hold time depend on hammer design, injection timing, hammer temperature, fuel volume and other factors (Rempe & Davisson (1977)). However, the additional force after impact at any time interval  $t$  is estimated by approximating the combustion and expansion phases as indicated in Figure (3.9).

The cycle is simulated from impact by considering the gas force in combustion and expansion phases. The combustion phase is approximated by three straight lines (Figure (3.9)), described by the delay, rise, and minimum hold time. Expansion phase is approximated by considering the time taken for the gas force to become ineffective. The pile force is calculated throughout the period from impact to exhaust. Figure (3.9) is used to correlate a relationship between the gas force  $F_g$  and lapse time  $t$  in each phase after the hammer impact. Details of these correlations are given below.

- 1) Delay time is the time lag between the ram impact and development of gas force after ignition. Figure (3.5) indicates that the gas force on the pile during

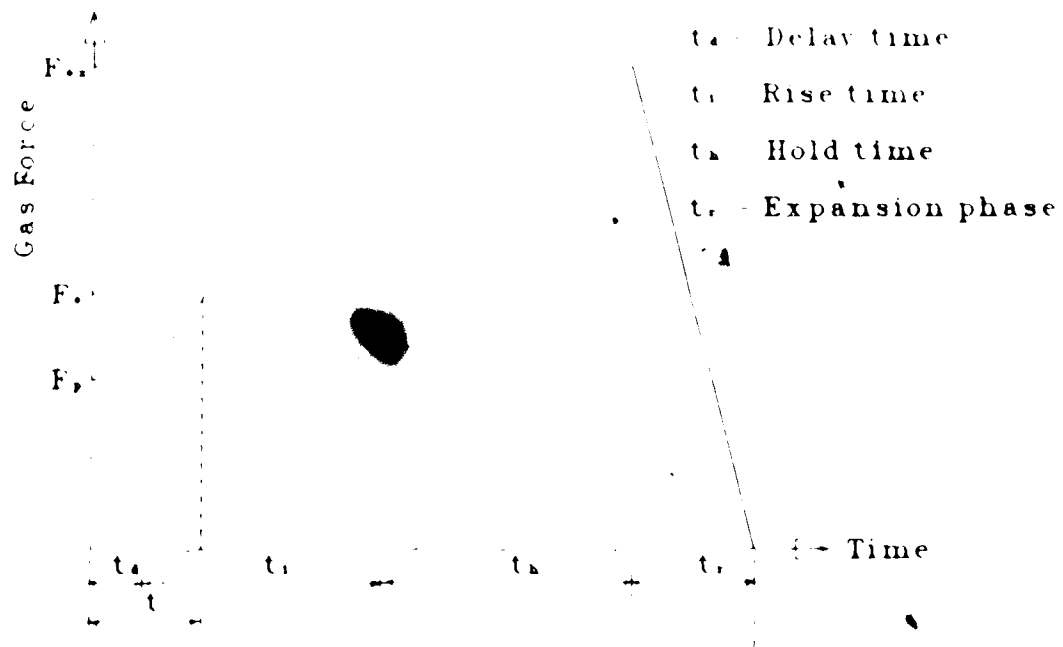


Figure 3.9 Simulation of Combustion and Expansion Phases

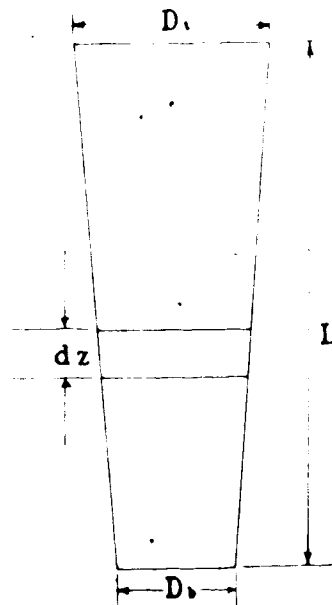


Figure 3.10 Vertical Section of Diesel Hammer Ram

this period  $(t \cdot t_d)$  is equal to the gas force  $(F_p)$  prior to the impact

$$F_e = F_p \quad (3.5)$$

2) Rise time  $t_r$  is the time taken to increase the gas force to its peak value  $F_{ex}$  after impact. Gas force on the pile during this period  $(t \cdot t_d + t_r)$  is given by the equation.

$$F_e = (F_{ex} - F_p) \frac{(t - t_d)}{t_r} + F_p \quad (3.6)$$

3) Hold time is the period during which the peak force is maintained  $(t_d + t_r) < t < (t_d + t_r + t_h)$ . Gas force in this period is equal to the peak value.

$$F_e = F_{ex} \quad (3.7)$$

4) The expansion phase is when  $(t_d + t_r + t_h) < t < (t_d + t_r + t_h + t_r)$  and the gas force is given by

$$F_e = F_{ex} \frac{(t_d + t_r + t_h + t_r - t)}{t_r} \quad (3.8)$$

#### 3.1.4.2 Velocity at Impact

The velocity at impact is calculated assuming that the ram velocity remains constant after the ram passes the exhaust ports on the impact stroke.

The potential energy of the ram at impact

$$E = W_1 g H_1 E_1$$

where  $H_1 = H_1 - H_2$

The kinetic energy equation is  $E = \frac{1}{2} W_1 V_1^2$

$$V_1^2 = 2g(h_1 - h_2) E_1$$

$$V_1 = \sqrt{2gE_1(h_1 - h_2)} \quad (3.9)$$

where  $V_1$  is the velocity of ram at impact,  $h_1$  is the ram stroke during impact and  $E_1$  is the hammer efficiency.

#### 3.1.4.3 Ram Stiffness

As shown in Figure (3.10), consider an element of thickness  $d_z$  and diameter  $D_z$ ,

where

$$D_z = \frac{Z}{L}(D_t - D_b) + D_b$$

$L$  - Length of the ram

$D_t$  - Top diameter of the ram

$D_b$  - Bottom diameter of the ram

$$A_z = \frac{\pi D_z^2}{4} = \frac{\pi}{4} \left[ (D_t - D_b) \frac{Z}{L} + D_b \right]^2$$

$$\sigma = E\epsilon, \quad \frac{F}{A} = E\epsilon$$

$$d\sigma = E d\epsilon, \quad \epsilon_z = \frac{\delta z}{dz}$$



$$\frac{F}{A} = E \frac{\delta z}{dz}$$

$$\int_0^L \frac{F}{AE} dz = \int_0^L \delta z = \frac{4F}{\pi E} \int_0^L \left[ (D_t - D_b) \frac{z}{L} + D_b \right] dz$$

$$\delta = F \cdot \frac{4L}{\pi E D_t D_b}$$

$$F = \frac{\pi D_t D_b E}{4L} \cdot \delta$$

Therefore the stiffness  $k_b$  of the diesel hammer ram is given by

$$k_b = \frac{\pi}{4L} D_t D_b E \quad (3.10)$$

### 3.2 Function of Accessories

#### 3.2.1 Anvil

The anvil is one of the basic components of diesel hammer and it acts as a impact block for the ram. The lower ram and upper anvil surfaces are mated such that when impact occurs the fuel pooled on the top of the anvil is displaced laterally in to the annular combustion chamber. The stiffness of the anvil  $k_a$  is given by

$$K_a = \frac{A_a E_a}{L_a} \quad (3.11)$$

where

$L_a$  - Length of the anvil

$A_a$  - Cross-sectional area of the anvil

$E_a$  Modulus of elasticity of the material constitute the anvil

### 3.2.2 Pile Cap (Helmet)

Generally some type of cast or forged steel helmet is used to fit the hammer base to the top of the pile and to uniformly distribute the hammer blows to the pile top. The hammer energy must be transmitted through the helmet, and energy losses within the helmet are usually quite small.

The helmet is short heavy rigid object and it should be of the correct size and provide full bearing over the entire cross section of the pile. For precast concrete piles, the helmet should be sufficiently loose so as not to restrain the piles from their tendency to rotate during driving. When sectional precast concrete piles are driven, a special pile cap may be required to accommodate any protrusions above the surface of the joint fitting such as rods, bolts, pins or raised portions.

Pile caps for H-piles are often of the H-shape to fit the size and configuration of the piles. Pipe-pile helmets are called adapters. This can be of the inside or outside type constructed to accommodate a variety of pile sizes. The pipe pile helmet must fit the pile diameter accurately and have a mechanical surface to fully engage the end of the pipe.

### 3.2.3 Cap Block and Cushion

The hammer cushion, or cap block, is inserted between the striking part of the hammer (ram) and the helmet to condition the blow by reducing peak forces. Thus both the pile and the hammer are protected from damage. However, the cap block must effectively transmit the hammer energy to the pile, and the ability to transmit such energy depends upon the elastic properties of the cap block material.

In the past, most cap blocks consisted of a hard wood block. This type of cap block becomes crushed and burned during pile driving, and the result is variations in elastic properties and the need for frequent changing. Now most cap blocks are of laminated construction, with alternating layers of aluminium and micarta disks or similar material. Others are made of material such as asbestos or woven steel wire. These cap blocks are generally stiffer than the wooden cap blocks and more efficiently transmit hammer energy to the pile. Also, some of these hammer cushions retain constant elastic properties and have relatively long life.

Mechanical cap blocks have been developed. They consist of a cylinder, a piston and disk springs or other types of springs. The hammer ram strikes the piston and compresses the springs. This reduces the forces and prolongs the duration of the hammer blow. Cap blocks having consistent elastic properties must be used if piles are being driven to a penetration resistance determined by a wave equation analysis.

A pile cushion is necessary between the helmet and the top of a precast concrete pile. The primary purpose of the pile cushion is to protect the pile from damaging under compression and tension stresses. The cushion also serves to distribute the hammer blows uniformly over the pile head and to compensate for any irregularities on the top surface of the pile.

The pile cushion generally consists of layers of hardwood or softwood boards or plywood. The pile cushion must protect the pile while at the same time transmitting sufficient hammer energy to the top of the pile. Stiffness of the cushion and cap block  $k_c$  is given by

$$k_c = \frac{A_c E_c}{L_c} \quad (3.12)$$

where  $L_c$  - Thickness of the cap block or cushion

$A_c$  - Area of cross-section

$E_c$  - Modulus of elasticity of cushion or cap block material

### 3.3 Summary

The operation and construction of various impact type hammers have been discussed. These information indicate that the energy delivered by the drop hammer or air/steam hammer results from the kinetic energy developed by the gravity fall of the ram. Also, the operation of these hammers are

not complicated. As such the kinetic-energy equation has been used to compute the velocity of ram at impact. The information about the diesel hammers reveal that the operation and construction of these hammers are complicated and also, the explosion resulting from the ram impact imparts additional kick to the pile. Gas law has been used to calculate the force exerted by the gas at the time of impact. The velocity of the diesel hammer at impact is computed assuming that the ram velocity remains constant after the ram passes the exhaust ports on the impact stroke.

Information presented above indicate that the hammer accessories such as helmet, cap block and cushion are used to uniformly distribute the force resulting from the hammer blows. Also, in the case of concrete piles a cushion is provided to protect the pile from damaging under compressive and tensile stresses. Further, if wave equation analysis is used to determine the resistance to penetration, cap block having consistent elastic properties must be used to drive the pile.

#### 4. MATERIAL RESPONSE TO DYNAMIC LOADING

##### 4.1 Soil Response During Pile Driving

There are two types of driven piles used in practice to support the superstructures. These are the displacement and non displacement types. The displacement type piles such as timber piles, prestressed precast concrete piles, and closed end steel pipe piles displace a significant volume of soil from the bottom of the pile during driving. Piles such as open ended pipe piles, steel H piles, sheet piles and cylindrical precast concrete piles do not displace a significant volume of soil mass during driving. These piles are called non displacement piles.

During pile driving the soil underneath the tip of the pile is subjected to shear stress in excess of the shear strength of the soil. Excessive stress cause deformation of the soil mass and its ultimate failure. The failure of the soil mass during driving is in the form of plastic flow which is different from the failure during static loading.

During flow and deformation, clayey soil is disturbed and remoulded, and excess pore water pressures are generated. As a result of remoulding and generation of excess pore water pressure, the shear strength of the soil around the pile during driving is significantly lower than the shear strength of the undisturbed soil. However, when a pile is driven into sands and cohesionless soils, the soil is usually compacted by displacement and vibration,

resulting in permanent rearrangement and some crushing of the particles.

#### 4.1.1 Soil Response Under Dynamic Loads

Dynamic soil response is of particular importance in fine grained soils and is associated with the layers of water which are bound to the soil particles by molecular forces. These layers surround the particles and prevent mineral to mineral contact. Relative movement between particles take place within the layers and due to the molecular forces gives rise to a strong viscous resistance. For clay soils, the resistance at fast rates of loading may be several times greater than when the soil is loaded slowly.

It is known from the dynamic tests on soil samples that the compressive strength of a soil sample is greater under a short term impulse loading than under static condition. The magnitude of excess pore water pressure generated during driving is several times greater than the excess pore water pressure generated during static pile load test.

In wave equation work the word damping is used to indicate the gain in strength which soils show under fast rate of loading. This dynamic behaviour is characterised by the damping constant which is a viscous parameter. Various methods proposed by different authors to handle the damping constant in wave equation analysis are discussed in this section.

#### 4.1.1.1 Smith's Idealization

In 1960, Smith suggested a numerical solution to the pile driving problem. He presented the concept for static loading at the point of a pile such that the ground compresses elastically for a certain distance and then fails plastically with a constant resistance. This concept is illustrated in Figure (4.1a). The maximum static elastic ground deformation or quake is represented by  $Q$  in Figure (4.1a) and the total ultimate plastic ground resistance to the pile is represented by  $R_u$ .

Under static loading, the pile deforms the ground elastically through OA and then plastically through a distance S. The soil then rebounds from B to C leaving a permanent set of S.

Smith (1960) developed a mathematical equation which accounts for both static and dynamic soil behaviour. Figure (4.1c) shows the rheological model which simulates the mathematical equation proposed by Smith. The model consists of a spring and a friction block in series connected in parallel to a dashpot. If the model is suddenly compressed a distance,  $x$ , the following equation will describe the soil resistance in the elastic region (Figure (4.1b))

$$R = K_s x + S_d V_p \quad (4.1)$$

where,



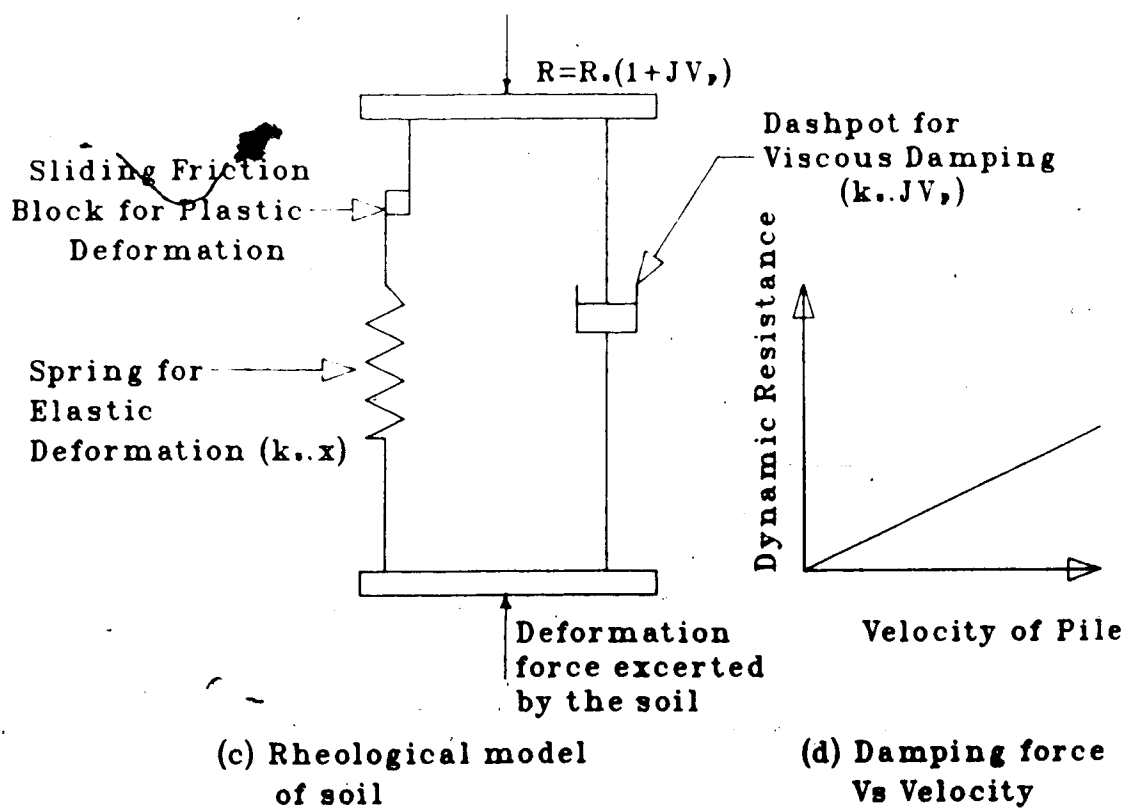
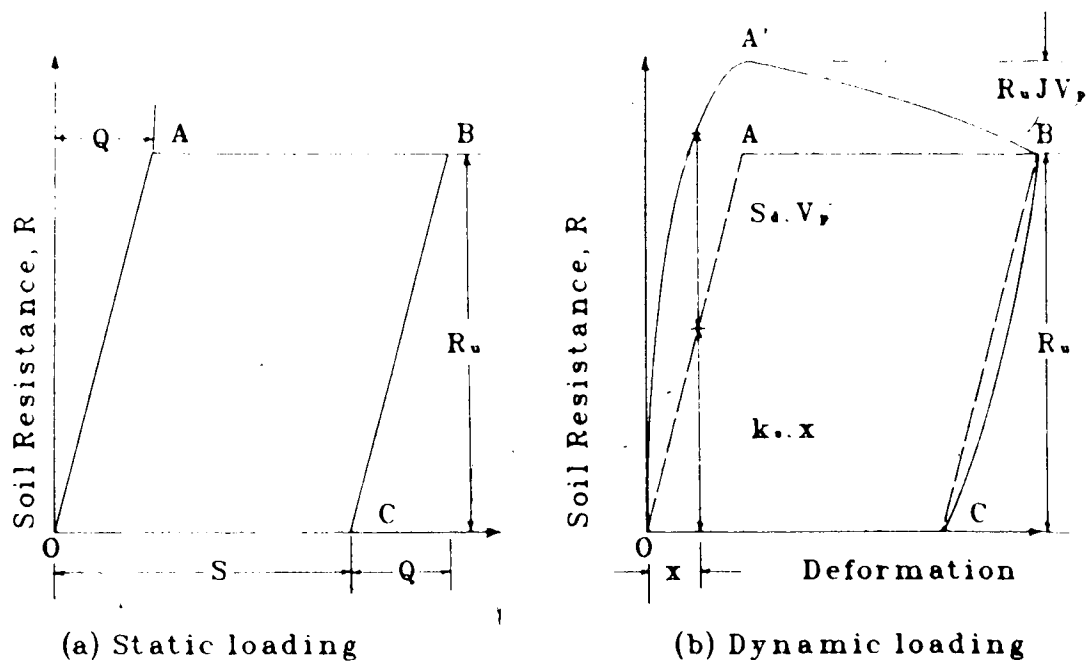


Figure 4.1 Load - Deformation Relationship for Soil

$R$  = Soil resistance

$K_s$  = Soil Spring constant

$S_d$  = Viscous damping of soil

$x$  = Elastic deformation of the soil

$V_p$  = The instantaneous velocity of the pile point in any time interval

The friction block accounts for the constant soil resistance in the plastic region during static loading. Smith (1960) assumed that the damping resistance is linearly proportional to the instantaneous velocity of the pile (Figure (4.1d)). The ratio between the velocity and the damping resistance is called the damping constant. It is usually denoted by  $J$ . In Smith's model, the dimension of the damping factor is inverse velocity, time/length (sec/m or sec/ft), and the damping force generated is equal to the damping factor times the velocity of the pile point times the activated static soil resistance.

$$R_d = S_d V_p = R_s J V_p$$

where,  $R_s = K_s x$  and the Equation (4.1) can be rewritten as

$$R = K_s x (1 + J V_p) \quad (4.2)$$

The concept of the dynamic loading is represented by line OA'BC in Figure (4.1b). If  $R_u$  is the peak static soil resistance, then  $R_u J V_p$  is the dynamic component of the peak

total soil resistance  $R_p$ .

$$R_p = R_u(1 + JV_p)$$

$$R_p = K_s Q(1 + JV_p) \quad (4.3)$$

$$K_s = \frac{R_u}{Q} \quad (4.4)$$

It is evident from Equation (4.3) that the concept for the resistance at the point of the pile takes into account:

- 1) Elastic ground deformation
- 2) Ultimate ground resistance
- 3) Viscous damping based on damping constant  $J$

Smith assigned a value of  $J = 0.15 \text{ sec/ft}$  for use by investigators until such time that new facts are developed. For practical purposes, it was suggested that  $J_p = 3J_s$ , where  $J_p$  and  $J_s$  are the damping constant for pile toe and shaft, respectively.

#### 4.1.1.2 Coyle and Gibson's Proposal

Various attempts have been made to measure  $J$  from static and dynamic tests on triaxial specimens (Coyle & Gibson, 1970). It has been found however, that  $J$  is dependent on the velocity of deformation for both sands and clays, decreasing as velocity increases. The linear proportionality of the damping resistance with the pile

velocity assumed by Smith(1969) has been shown to be incorrect. The relationship between the dynamic resistance and velocity of pile assumed in all three proposals which are being discussed is shown in Figure (4.2). However, the assumption of linearity is considered as an acceptable simplification in most practical cases and this approach is used in commercially available computer programs to handle pile driving using wave equation. Coyle and Gibson suggested that this problem can be overcome by rewriting Smith's original Equation (4.2).

$$R = K_d x (1 + J_m V_p^N) \quad (4.5)$$

where,  $J_m$  is the modified damping constant and the exponent  $N$  is less than 1. The most suitable values were found to be

$$N = 0.20 \text{ for sands}$$

$$N = 0.18 \text{ for clays}$$

On the basis of modified Equation (4.5), Coyle and Gibson found  $J_m$  to be almost independent of velocity, and reasonable correlation between  $J_m$  and soil properties could be obtained. The relationship between  $J_m$  and  $\phi'$  for sands is shown in Figure (4.4), while the relationship between  $J_m$  and liquidity index (LI) for clays is shown in Figure (4.5).

Subsequently this view was supported by several authors, Litkouhi and Poskitt (1980), Heerema (1981). In papers published by Heerema (1979 & 1981), it is shown that

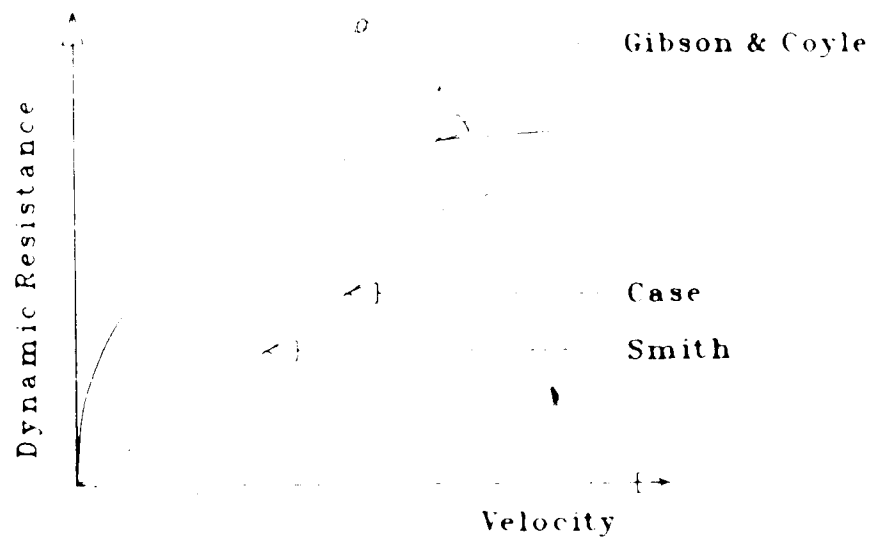
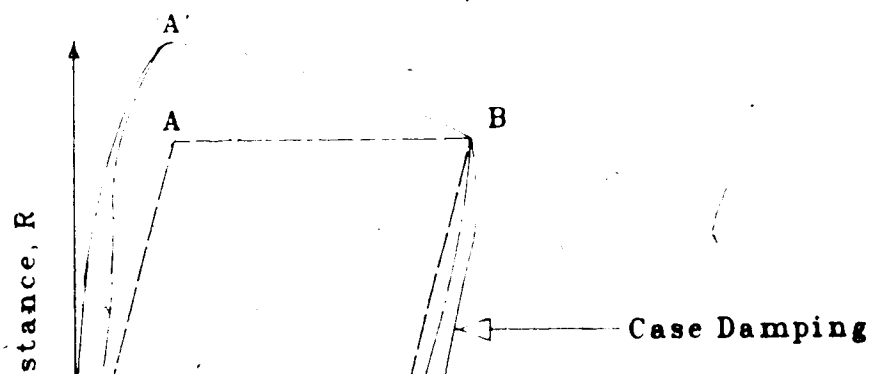


Figure 4.2 Relationship between Dynamic Resistance and Velocity



for clays, skin friction is very strongly velocity dependent at low velocities and relatively insensitive at high velocity, whereas wall friction in sand is not velocity dependent ( $J_w = 0$ )

#### 4.1.1.3 Proposal by Case Western Reserve University

In an approach by Goble and Rausche(1976), the damping factors are dimensionless and damping force is obtained by multiplying the velocity with the damping factor and the pile material impedance,  $\frac{AE}{C}$ , which is defined in Section 2.3.2. Total soil resistance in this approach is given by

$$R = K_s x + J_c \frac{(AE)}{C} \cdot V_p \quad (4.6)$$

where,  $J_c$  is called the case damping factor.

This approach also assumes that the damping resistance is linearly proportional to the velocity of the pile (Figure (4.2)). In Smith's approach the dynamic resistance is zero, when the static resistance is zero (Figure (4.1b), point C) even though the pile has a velocity at this point. But in this approach, irrespective of static resistance, the dynamic resistance is zero only when the pile velocity becomes zero. This is shown in Figure (4.3) (point C'). However, with case damping, the soil damping force becomes dependent on the particular pile material and cross-sectional area.

The material involved has been removed because of the unavailability of copyright permission.

This page contains the damping parameters for soils recommended by Coyle and Gibson (1970).

Refer proceedings of ASCE, Vol.96, SM3, pp. 956 & 962, 1970.

#### 4.1.2 Time Effects

There are number of foundation reports, Yang(1970), George et al. (1976) and Thompson and Thompson (1985) suggest that piles exhibit a drop-off in resistance after a period of rest in the ground. Such a drop-off is usually observed at the re-entry of pile driving and this phenomena is called "relaxation". Increase in pile capacity after driving in fine grained soils due to the adjustment of soil structure together with the pore water fluctuation after the driving is called "freezing".

Several cases are reported in the literature and text books. Figure (4.6) shows the increase in bearing capacity with time of piles driven in soft clays. It indicates that in most cases 75 percent of the ultimate carrying capacity is achieved in 30 days of driving. From several case records, Yang (1970) reviews the effect on pile capacity of time lag between initial driving and restriking or test loading. He concludes that pile relaxation could be encountered for piles driven in dense fine sand and inorganic silts. It is clear from the above mentioned reports and case records that the calculated capacity of pile represents only the resistance during the time interval of driving and it is necessary to introduce a factor to estimate the static pile resistance from the soil resistance during driving. The ratio of soil strength a considerable time after driving to that immediately after driving is called the soil set-up factor.



The material involved has been removed because of the unavailability of copyright permission. This page contains the following.

- 1) The observation and recommendation made by Vesic (1970) on gain in carrying capacity with time of piles driven in soft to stiff clays. Refer proceedings of ASCE, Vol.96, SM2, pp.561-584, 1970.
- 2) Effect of pile characteristics observed by McClelland et al. (1969). Refer proceedings of ASCE, Vol.95, SM6, pp.1503, 1969.

#### 4.1.2.1 Soil Set-Up Factor

The pile load test is always carried out many days after the pile has been installed. The time lag between these two events will permit the general relaxation or freezing of the pile and its surrounding soils after the pile driving.

Cases have been reported where the capacity of shaft bearing piles in clay has kept increasing over a period of time longer than the duration of the clay reconsolidation resulting from the equalization of pore pressure (Flaate 1972; Cooke et al. 1979; Bergdahl & Hult 1981). Based on the tests carried out on jacked piles in London clay, Cooke et al. (1979) found a considerable increase in pile capacity with time. The increase in capacity over a long period of time varies between 20 and 50 percent. Also, the results published by Bergdahl and Hult (1981), based on a series of loading tests on half-scale shaft bearing wood piles in clay indicate an average increase in capacity of about 22% during the period from 1 to 2 months after pile installation, and also the increase extended over several months.

A prediction of the pile capacity on the basis of the wave equation, however, will only give the pile capacity immediately after driving; thus, if pile capacity some time after driving is required, some knowledge of the amount of "set-up" is needed. When the

pile is acted on by combination of soils having different set-up factors the following general equation suggested by Lowery et al (1969) can be used to transform the after set up resistance into the static resistance immediately after driving by

$$R_{dr} = (R_{uf})(S_t) \quad (4.7)$$

where,

$$S_t = \left[ 1.0 - \frac{(\Delta R_t)}{R_{uf}} \frac{(S_{ti} - 1.0)}{S_{ti}} \right] \quad (4.8)$$

$R_{dr}$  = Resistance immediately after driving

$R_{uf}$  = Total soil resistance determined by load test after all set-up has ceased

$\Delta R_t$  = The ratio of the amount of resistance of each type of soil "i" to the total soil resistance, both determined after set-up has ceased

$S_{ti}$  = The set-up factor, corresponding to the soil type "i"

Lowery et al. (1969) tentatively suggested that a set up factor of 3 might be appropriate for soft clays, 2 for firm and stiff clays, and 1 for other soils. McClelland et al. (1969) (Figure (4.7)), on the other hand, consider that for piles driven into hard clay or sand, a decrease of soil strength and adhesion with time could occur. The final static resistance of the pile would then be less than the

resistance during driving. However, for purposes of estimating the soil set up factor, local geology and soil response to pile driving and its behaviour with time should be considered.

## 4.2 Internal Damping in Pile and Accessories

### 4.2.1 Pile

When the pile is subjected to driving force, the force in the pile is given by

$$F_m = K_m C_t \quad (4.9)$$

$$K_m = \frac{AE}{L}$$

where,

$F_m$  = Force in the pile

$K_m$  = Pile stiffness or spring constant

$C_t$  = Compression of pile at time interval  $t$

Equation (4.9) is valid only, if there is no internal damping present in pile (Figure (4.8a)). Figure (4.8) suggests different possibilities for representing the load deformation characteristics of the pile material. In Figures (4.8b) and (4.8d), the material is assumed to have internal damping according to the linear relationships. In Figure (4.8c), loading and unloading are considered to occur along a hysteresis loop. The assumption that should be made for a given problem depends on the material and its load deformation behaviour under dynamic loading.

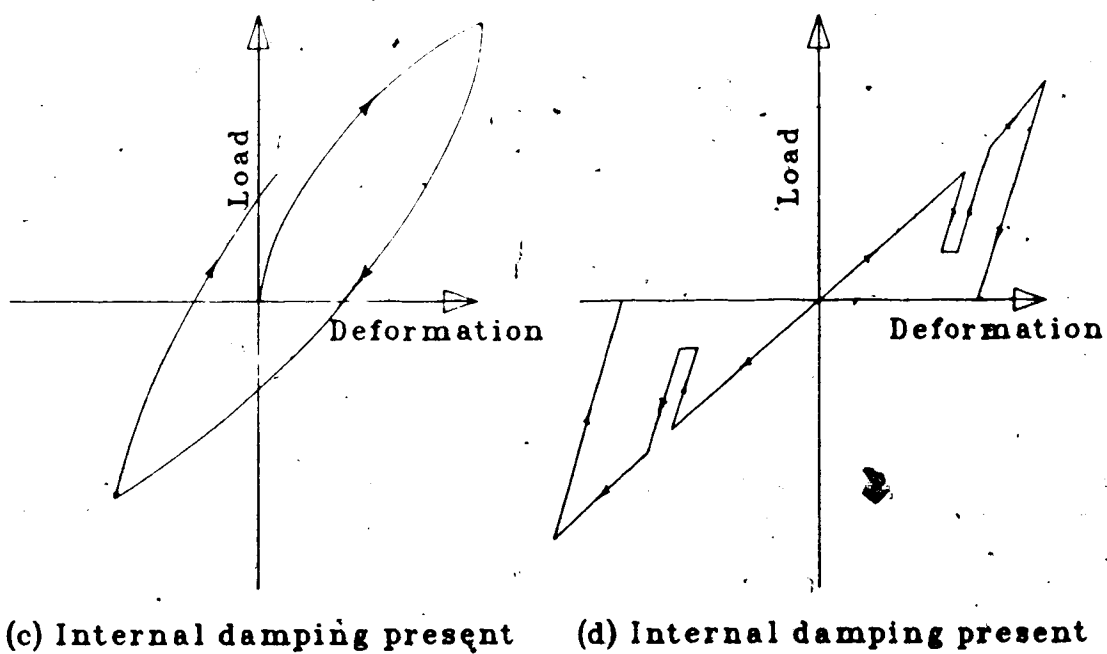
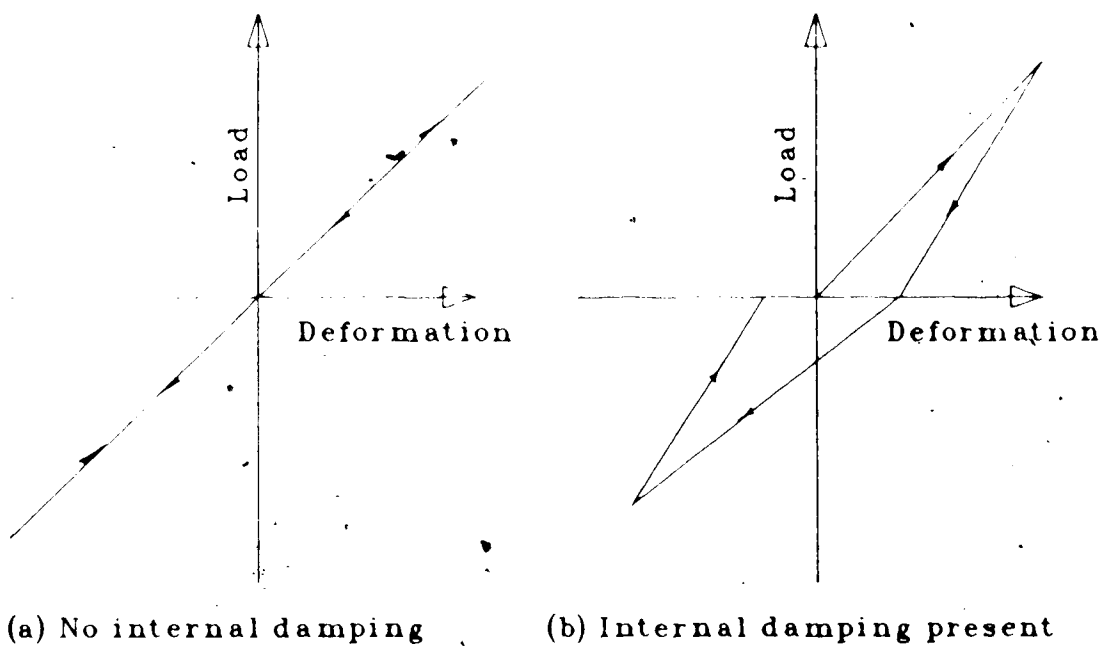


Figure 4.8 Load Deformation Relationships

Smith (1960) suggested that the Equation (4.9) may be modified as follows to accommodate the internal damping in pile.

$$F_m = C_t K_m + BK_m \frac{(C_t - C_{t-1})}{\Delta t} \quad (4.10)$$

where,

$\Delta t$  = Time interval

B = Internal damping constant of pile material

Smith further suggested that a small value such as 0.0002 should be assumed for B so as to produce a narrow hysteresis loop. Since little is known about the correct structural damping behaviour and also this type of damping produces relatively small forces compared to soil damping, a detail analysis may not be justified.

#### 4.2.2 Hammer Accessories

The elastic modulus for most engineering materials in practice is never truly constant, nor is the average slope of loading and unloading curve. It varies with the stress level and depends on whether the load causing the elastic deformation is increasing or decreasing. This variation is usually considered insignificant in practice for common pile materials, such as concrete and steel. However, for wood and other materials used in cap blocks and cushions, and when energy transfer takes place from hammer to anvil, the difference in stiffness in loading and unloading causes a loss of energy that is far from insignificant.

The form of the force-displacement diagram that is produced as the cap block or cushion is suddenly compressed and then allowed to expand is shown in Figure (4.9a). Compression occurs along AB whose slope is determined by the elastic constant  $k_c$  of the cap block. Restitution occurs first along the line BD and then, it is completed along DA, because the cap block cannot transmit tension. From Newton's law

$$e(M_r V_{ir} + M_c V_{ic}) = (M_r V_{fr} + M_c V_{fc}) \quad (4.11)$$

The relative energy loss is given as coefficient of restitution  $e$  of the cap block or cushion material.

where

$M_r$  - Mass of ram

$M_c$  - Mass of cap block or cushion (approximately zero)

$V_{ir}, V_{ic}$  - Initial velocities of ram and cap block, respectively ( $V_{ic}=0$ )

$V_{fr}, V_{fc}$  - Final velocities

Substituting  $V_{ic}=0$  and  $M_c=0$  in Equation (4.11) leads to

$$e = \frac{V_{fr}}{V_{ir}}$$

The kinetic energy equation is  $\frac{1}{2} MV^2$

From Figure (4.9a)

$$\frac{\text{Energy output}}{\text{Energy input}} = \frac{\text{Area BCD}}{\text{Area ABC}} = \frac{V_{fr}^2}{V_{ir}^2}$$

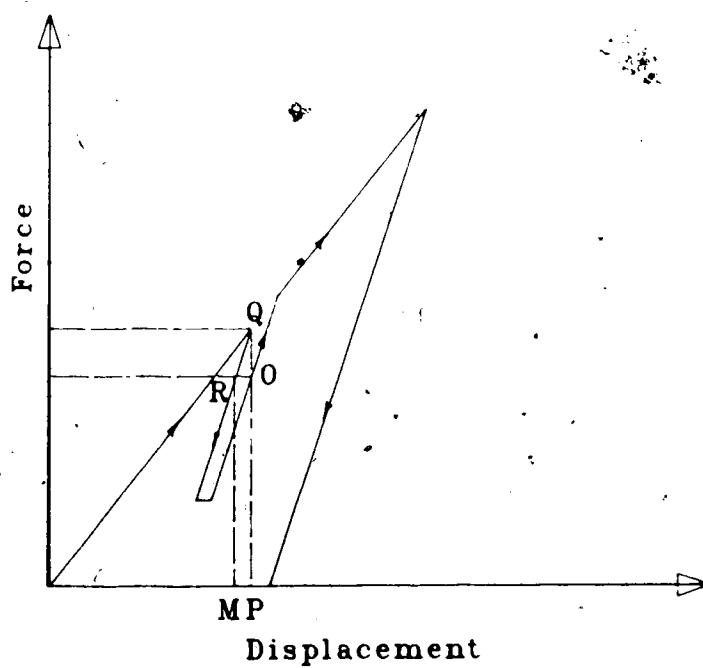
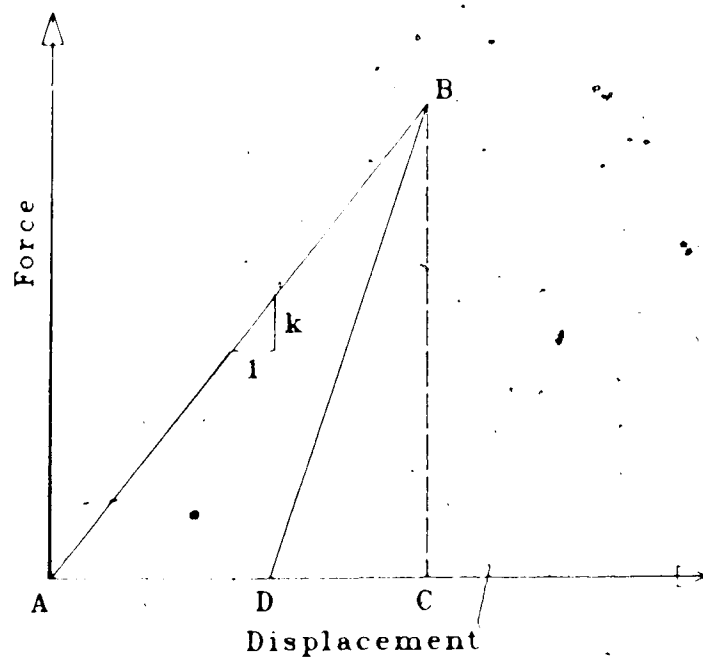


Figure 4.9 Stress-Strain Relationships of Accessories



$$\frac{\text{Area BCD}}{\text{Area ABC}} = e^2 = \frac{DC}{AC}$$

$$BC = k_c \cdot AC = k'_c \cdot DC = k'_c \cdot AC \cdot e$$

$$k'_c = \frac{k_c}{e^2} \quad (4.12)$$

where  $k'_c$  is the unloading stiffness of the cap block or cushion.

From Section 2.3.1, it is clear that a stiffer cushion transmits higher peak stress with shorter impact duration. The magnitude of energy transmitted to the pile is greatly dependent on the coefficient of restitution of the cushion material. The cushion properties directly affect the shape of the impact force pulse imparted to the pile.

Based on the test performed on cushion materials at Texas A & M University (Holloway (1975)), the dynamic static stress-strain behaviour of most cushion materials are very similar. Holloway (1975) suggested that the secant modulus from static stress-strain behaviour corresponding to the peak stress condition must be used to calculate the loading and unloading stiffness of the cushion materials.

Instantaneous load transfer through cushion material is shown in Figure (4.9b). The cushion material is assumed to exhibit internal damping according to the linear relationships. Force in the cushion at time  $t$  is given by MR and the force corresponding to temporary maximum compression ( $C_{\max}$ ) of cushion is given by PQ. Equation (4.9) may be modified as follows to accommodate the internal damping in

anvil, cap block and cushion. In Figure (4.9b), force  $F_m$  is given by

$$F_m = PQ - QQ$$

$$F_m = k_c \cdot C_{max} + \frac{k_c}{e^{\lambda}} (C_t - C_{max}) \quad (4.13)$$

Equation (4.13) takes into account of the energy loss in the accessories due to internal damping. However, other forms of energy losses during hammer impact are not considered in the analysis.

#### 4.3 Summary

The damping parameters derived from various methods, behaviour of soil during and after pile driving and material response to dynamic loading have been discussed. These information reveal that in wave equation analysis the word damping is used to indicate the gain in strength which soils exhibit under fast rate of loading. Also, the damping constant is a viscous parameter which characterise the dynamic behaviour of soils. The following have been revealed from the examination of the three methods which suggested damping parameters.

- 1) In Smith's method the damping constant is the ratio between the velocity and the damping resistance. This is based on the assumption that the damping resistance is linearly proportional to the instantaneous velocity of the pile.

- 2) The damping constants recommended by Coyle and

Gibson are independent of pile velocity. These damping parameters are related to the basic soil properties such as liquidity index or effective angle of internal shearing resistance. The power law as well as the damping parameters were recommended based on triaxial tests.

3) In the case method the damping factors are dimensionless. These factors depend more on the pile properties rather than on soil.

Information presented in the reports of various studies on soil response to pile driving indicate that after a period of rest in the ground the driven piles exhibit a drop-off or gain in resistance depending on the type of soil in which pile was driven. Also, knowledge of the soil set-up is very important to predict the pile capacity on the basis of the wave equation analysis.

Various possibilities for representing the load deformation characteristics of the pile and cap block materials have been discussed. These details reveal that the presence of internal damping in any material depends on its load deformation behaviour under dynamic loading. Also, internal damping is insignificant in common pile materials such as concrete and steel. However, this is very significant for wood and other materials used in cap blocks and cushions.

## 5. MATHEMATICAL MODELS AND DEVELOPMENT OF PROGRAM "ALWAP"

The operation and working principle of various types of pile driving hammers were discussed in chapter 3, and also, in chapter 4 the dynamic response of material and the method of handling damping constant in wave equation analysis were examined in detail. In this chapter mathematical modelling of hammer, pile and soil, and also the use of the wave equation to develop the computer program "ALWAP" will be discussed.

The analysis is based on the numerical equivalent proposed by Smith (1955) to replace the differential Equation (2.5) describing transmission of a shock wave along the pile. Smith's finite difference solution is extended to include gravity effect and subsequent research works by various authors to handle soil damping properties in wave equation analysis. The gravity effect is included by giving the initial values to produce equilibrium of the system. Considering the diesel hammer operation and its construction, modelling of diesel hammer is separated from other type of hammers.

The hammer, pile and other parts involved are represented by a series of weights and springs. The time during which action occurs is divided into small time intervals. The velocities, forces and displacements for each time interval are computed so as to differ from those existing in the preceeding interval by just enough to represent the change occurring during the time interval.

The foregoing materials outline the problem and discuss the physical conditions that must be taken into account. The following gives the mathematics used for the numerical solution of the wave equation as applied to pile driving. The equations and routines required to generate a computer program are developed in following sections.

## 5.1 Mathematical Models

### 5.1.1 Hammer

The idealization of the ram of a pile driver depends upon its construction. Drop hammers and steam hammers are usually constructed so that the ram impacts directly on a cap block which cushion the impact of the ram. Also, the ram of drop hammers and steam hammers is ordinarily a short, heavy, rigid object. For these reasons the flexibility of the ram is ignored and represented by a single rigid mass.

In the case of diesel hammers, the ram is fairly slender compared to other type of hammers under discussion and also the ram strikes against the anvil. The ram of diesel hammer is represented by a concentrated weight and a weightless spring. Even though the anvil is a short rigid body, it is represented by a concentrated mass and a spring to take into account of the energy loss at the interface of the ram and anvil. The springs which represent the ram and anvil are connected in series, the force is the same in both springs and the total deformation is the sum of the

individual spring deformation. Therefore, the combined stiffness of the ram and anvil is given by the equation

$$\frac{1}{SP_{(1)}} = \frac{1}{k_h} + \frac{1}{k_a} \quad (5.1)$$

Where,  $SP_{(1)}$  is the combined stiffness of ram and anvil,  $k_h$  and  $k_a$  are given by the Equations (3.10) and (3.11), respectively.

The idealization of the cap block and cushion consist of specifying weightless spring with coefficient of restitution. Dynamic response and coefficient of restitution of hammer accessories were discussed in detail in Section 4.2.2. Stiffness of the cap block and cushion springs are represented by  $SP_{(2)}$  and  $SC$ , respectively. These parameters are calculated by Equation (3.12). When the coefficient of restitution is equal to one, the load transfer property of these hammer components is characterised by Equation (4.9) and if the coefficient of restitution is less than one it is characterised by Equation (4.13). Hammer accessories such as anvil, cap block and cushion are separate pieces which cannot transmit tension and expected to transmit compressive forces only. The helmet is a short rigid body and it is represented by a concentrated weight  $W_{(3)}$  without elasticity. Figure (5.1) shows the schematic representation of pile driving hammer and its model.

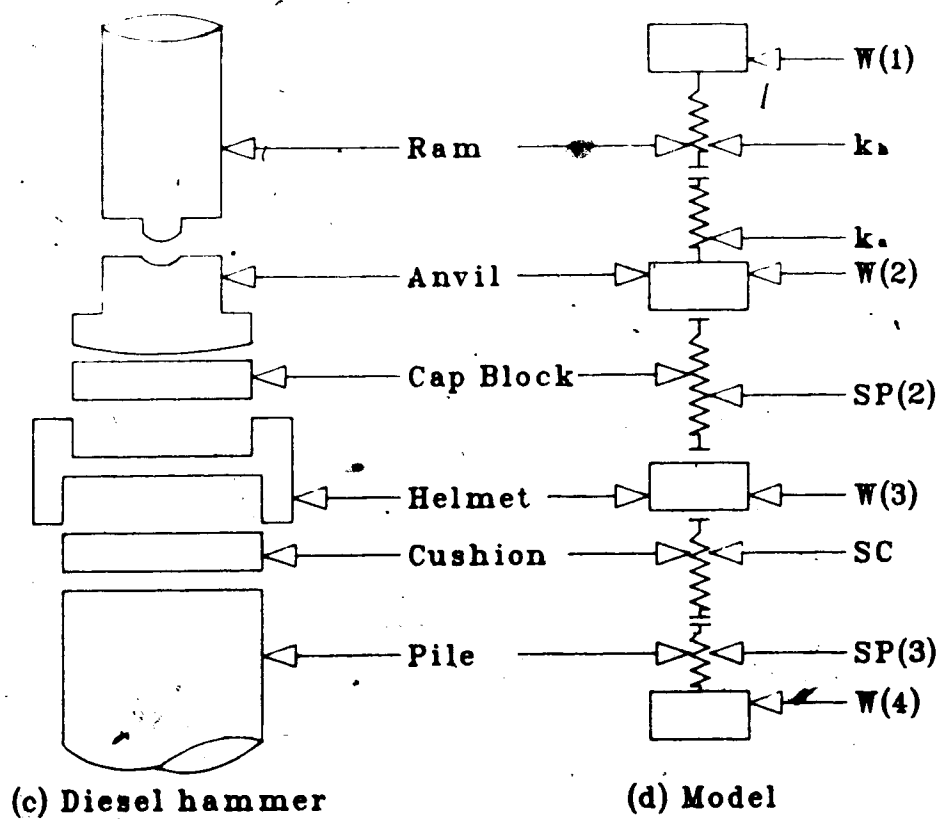
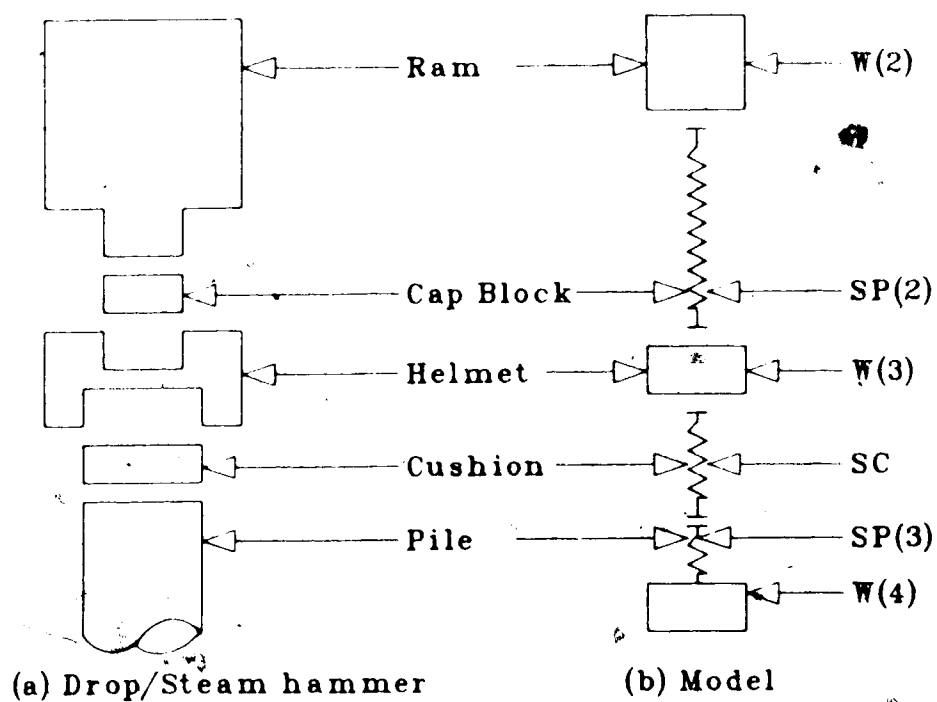


Figure 5.1 Schematic Representation of Hammer and its Model

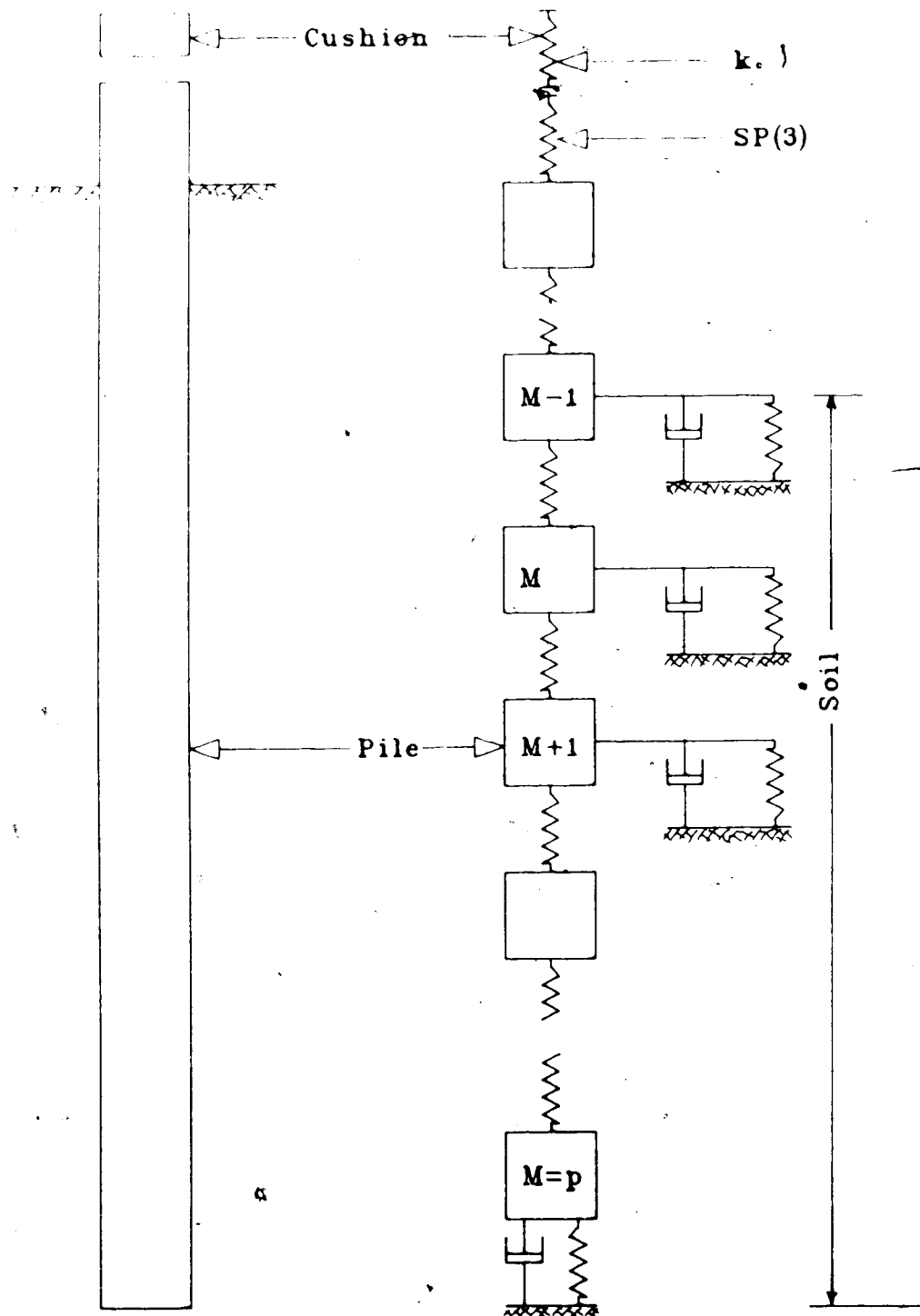
### 5.1.2 Pile and Soil

The pile and the corresponding model are shown in Figure (5.2). The model consists of a series of mass elements connected by weightless springs and subjected to outside soil forces. The mass elements are infinitely stiff. Their actual stiffness is represented by the weightless spring, which has stiffness  $K_{(m)}$  equal to  $\frac{AE}{L}$ , where  $E$  is the modulus of elasticity of the material,  $A$  is the cross-sectional area,  $L$  is the length of the mass element. The weight of the element is concentrated at the bottom of the spring. The last pile segment weight includes weight of drive point if used. As explained in Section 4.2.1, internal damping of the pile material is not simulated in the model. If cushion is provided, the combined stiffness  $SP_{(3)}$  of the cushion and first pile segment is given by

$$\frac{1}{SP_{(3)}} = \frac{1}{K_{(m)}} + \frac{1}{k_c} \quad (5.2)$$

As explained in Section 4.1.1.1, the soil forces along each pile segment and pile tip are modelled to consist of static and dynamic damping resistance. The resistance at the pile point includes the side resistance of the bottom most segment. Also, the point bearing force is prevented from exerting tension on the pile. The detail soil models along pile shaft and tip are shown in Figure (5.3). The soil model is assumed to be weightless, ie, the pile moves through the soil mass and does not move the adjacent soil mass, and is





(a) Actual pile and soil — (b) Idealized pile and soil

Figure 5.2 Smith's Mathematical Model of Pile and Soil

simulated by a spring and dashpot on each pile segment. Stiffness of the soil spring corresponding to each pile segment is given by the Equation (4.4). Based on the proposed model, loading and unloading at the pile point will occur along OABCB. Loading and unloading in shaft friction will occur along OABCDEF.

## 5.2 Numerical Treatment

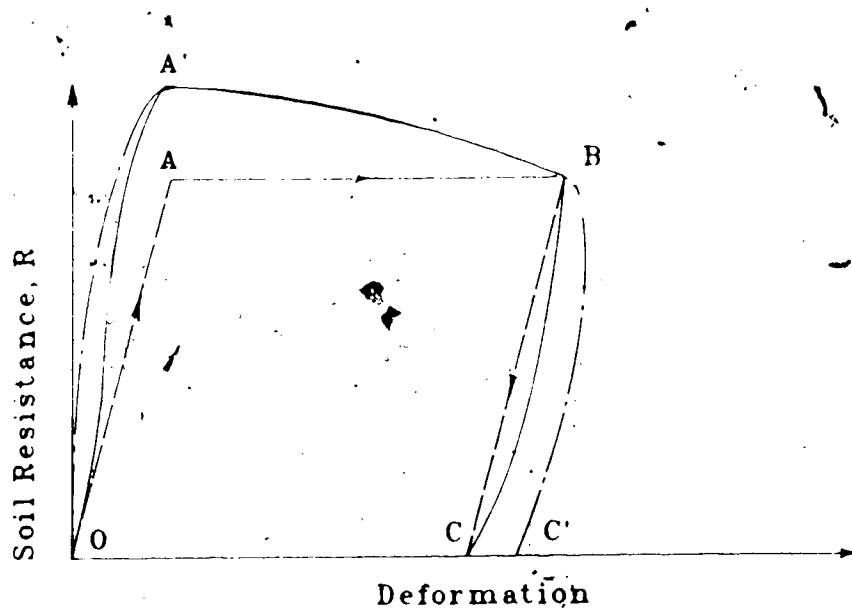
### 5.2.1 Development of Basic Formulae

The time during which the action occurs is divided into small time intervals  $\Delta t$  such as 1/4000 seconds. It is assumed that all the velocities, forces and displacements have fixed values during any particular time interval. In Figure (5.4), the instantaneous displacement  $D_{(m,t)}$  of any element is the sum of the displacement one time interval back  $D_{(m,t-1)}$  plus the product of instantaneous velocity  $V_{(m,t)}$  and time interval  $\Delta t$ .

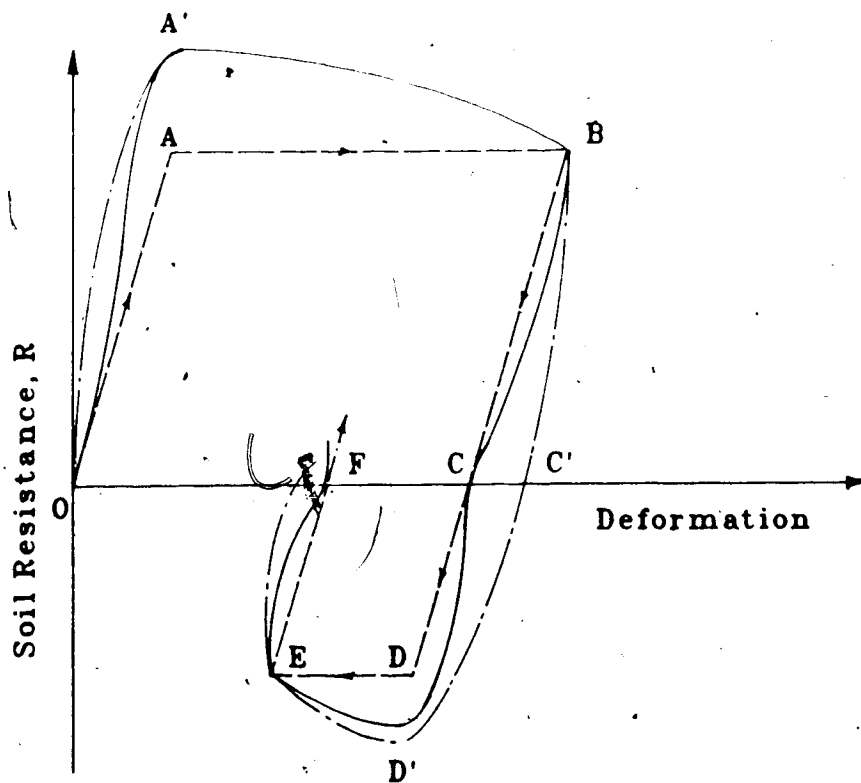
$$D_{(m,t)} = D_{(m,t-1)} + V_{(m,t)} \cdot \Delta t \quad (5.3)$$

$(m,t)$  represents a functional designation;  $m$  denotes the element number;  $t$  denotes the time interval number;  $\Delta t$  is the size of time interval.

The net compression  $C_{(m,t)}$  of the element spring is computed from Figure (5.4). Initial length of the spring  $m$  is  $l$  and  $l'$  is the length after time interval  $t=n$ .



(a) At pile point



(b) Along pile shaft

Figure 5.3 Representation of Soil Model

$$C_{(m,t)} = l - l' ; \text{ but}$$

$$l + D_{(m+1,t)} = l' + D_{(m,t)} ; \text{ Hence}$$

$$C_{(m,t)} = D_{(m,t)} - D_{(m+1,t)} \quad (5.4)$$

The resulting force  $F_{(m,t)}$  in the element spring is given by

$$F_{(m,t)} = K_{(m)} C_{(m,t)} \quad (5.5)$$

Referring to Figure (5.5b), it may be noted that the element  $m$  is acted upon by springs  $m$  and  $m-1$ , and soil resistance  $R_m$ . The accelerating force  $F_{am}$  is given by

$$F_{am} = F_{(m-1,t)} - F_{(m,t)} - R_{(m)} \quad (5.6)$$

The element velocity  $V_{(m)}$  of element  $m$  is computed from the conventional velocity equation as

$$V_{(m,t)} = V_{(m,t-1)} + a\Delta t \quad (5.7)$$

where,  $a = \frac{F_{am}g}{W_{(m)}}$

$W_{(m)}$  = Weight of pile element

$F_{am}$  = Force due to acceleration

Multiplying Equation (5.7) by  $\Delta t$  and substituting for  $a$  leads to

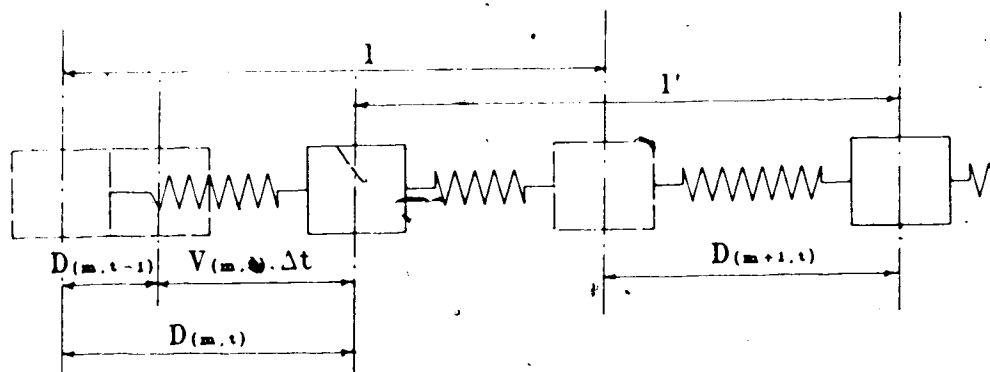


Figure 5.4 Element Displacements

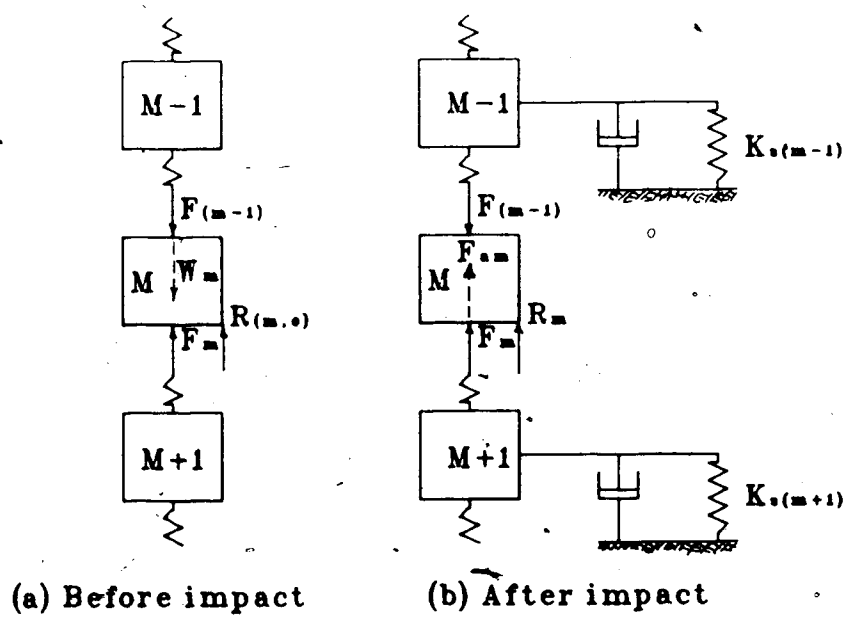


Figure 5.5 Element Forces

$$V_{(m,t)}\Delta t = V_{(m,t-1)}\Delta t + \frac{F_{am}g}{W_{(m)}}(\Delta t)^2 \quad (5.8)$$

Rearranging Equation (5.3) leads to

$$V_{(m,t)}\Delta t = D_{(m,t)} - D_{(m,t-1)} \quad (5.9a)$$

By analogy displacement at time interval  $t = t-1$  can be written as

$$V_{(m,t-1)}\Delta t = D_{(m,t-1)} - D_{(m,t-2)} \quad (5.9b)$$

By substituting for  $V_{(m,t)}\Delta t$  and  $V_{(m,t-1)}\Delta t$  in Equation (5.8), and by rearranging one gets

$$\frac{D_{(m,t)} - 2D_{(m,t-1)} + D_{(m,t-2)}}{(\Delta t)^2} = \frac{F_{am}g}{W_{(m)}} \quad (5.10)$$

If the soil resistance along the pile is considered in formulating Equation (2.5), the resulting equation will be in the form

$$\frac{\partial^2 u}{\partial t^2} - c^2 \frac{\partial^2 u}{\partial x^2} + R_{(m)} = 0$$

$\frac{\partial^2 u}{\partial t^2}$  can be expressed in finite difference form using the first-backward difference equation

$$U''_n = \frac{U_n - 2U_{n-1} + U_{n-2}}{(\Delta t)^2} \quad (5.11)$$

Comparison of Equations (5.10) and (5.11) indicate that the simplification of Equation (2.5) which describes the stress wave transmission through a pile is justified. Also, this shows that these five basic equations are equivalent to the wave equation for purposes of numerical computation.

By substituting  $F_{am} = a \frac{W_{(m)}}{g}$  in Equation (5.6) and replacing  $a$  in Equation (5.7) we get

$$V_{(m+1)} = V_{(m)} + \left[ F_{(m+1)} - F_{(m)} - R_{(m)} \right] \frac{g}{W_{(m)}} (\Delta t) \quad (5.12)$$

#### 5.2.1.1 Gravity Effect

The procedure presented by Smith (1962) does not account for static weight of the pile, weight of hammer housing and in the case of diesel hammer, gas pressure prior to ram impact. In other words, all the internal and external springs exert zero force prior to impact. If the effect of gravity is to be included, these forces must be given initial values to produce equilibrium of the system. Strictly speaking, these initial values should be those in effect as a result of the previous blows. However, it should be recognized that the solution obtained with the program represents the results for one blow of the hammer at the specified soil embedment and soil resistance.

As an approximate method it is assumed (H.Samson,Jr.et al, 1963) that the soil springs resist

the static weight of the system according to the relationship

$$R_{(m,0)} = \frac{R_{u(m)}}{R_u} \cdot W_T \quad (5.13)$$

where,  $R_{(m,0)}$  = Static weight resisted by soil corresponding to the pile segment  $m$

$R_{u(m)}$  = Ultimate soil resistance on the pile segment  $m$

$W_T$  = Total static weight resisted by soil

$$W_T = W_a + F_p + \sum_{m=4}^{m-1} W_{(m)}$$

$W_a$  = Weight of hammer assembly excluding ram

$F_p$  = Gas pressure prior to impact

The internal forces that initially exist in the pile may be obtained from Figure (5.5a) and in general it is given by

$$F_{(m,0)} = F_{(m-1,0)} + W_{(m)} - R_{(m,0)} \quad (5.14)$$

Thus, the compression of the internal spring may be expressed as

$$C_{(m,0)} = \frac{F_{(m,0)}}{K_{(m)}} \quad (5.15)$$

The displacement of the pile point may be obtained from



$$D_{(p,0)} = \frac{R_{(p,0)}}{K_{s(p)}} \quad (5.16)$$

In working progressively upward from the pile point, displacement of other springs may be obtained.

$$D_{(m,0)} = D_{(m+1,0)} + C_{(m,0)} \quad (5.17)$$

Equation (5.12) should be rearranged as follows to include the gravity effect.

$$V_{(m,t)} = V_{(m,t-\Delta t)} + \left[ F_{(m+1,t)} - F_{(m,t)} - R_{(m)} + W_{(m)} \right] \frac{g}{W_{(m)}} (\Delta t) \quad (5.18)$$

### 5.2.2 Computer Solution

The initial velocity  $V_h$  of ram at impact is determined from the properties of the pile driving hammer as explained in Chapter 3. Other time dependent quantities are initialized at zero or to produce equilibrium of forces under gravity. The action of each weight and spring is then calculated separately in each and every time interval. In this way a mathematical determination may be made of stresses and plastic deformation or pile penetration against any amount of soil resistance.

Prior to hammer impact, internal forces, compressions and displacements of the internal springs are calculated by Equations (5.13) to (5.16). However, the external springs to be compatible with the assumed initial forces  $R_{(m,0)}$  and initial displacement  $D_{(m,0)}$ , plastic displacement  $D'_{(m,0)}$

should be set equal to

$$D'_{(m,0)} = D_{(m,0)} - \frac{R_{(m,0)}}{K_{S(m,0)}} \quad (5.19)$$

Displacements  $D_{(m,1)}$  are calculated by Equation (5.3). The initial velocity of the ram is the velocity  $V_h$  at impact. Depending on the type of hammer it will be initialized as follows.

Drop and Steam hammers  $V_{(2,1)} = V_h$

Diesel hammers  $V_{(1,1)} = V_h$

Compression of the internal springs are calculated using Equation (5.4). Forces in the pile segments are calculated by Equation (5.5). However, to calculate the forces in the internal springs which exhibit internal damping, Equation (5.5) is used until  $C_{(m,t)} - C_{(m,t-1)}$  becomes negative. This last value of  $C_{(m,t-1)}$  is thereafter treated as a constant called  $C_{1max}$  which is same as  $C_{max}$  in Figure (4.9b). Time dependent variable  $C_{(m,t)}$  in Equation (4.13) is replaced as follows.

$$F_{(m,t)} = \frac{K_{(m)}}{e_m^2} C_{(m,t)} - \left[ \frac{1}{e_m^2} - 1 \right] K_{(m)} C_{1max} \quad (5.20)$$

When  $C_{(m,t)} - C_{(m,t-1)}$  becomes negative Equation (5.20) is used to calculate the force in the springs  $SP_1$ ,  $SP_2$  and  $SP_3$  until  $C_{(m,t)} - C_{1max}$  becomes positive. Thereafter Equation (5.5) is again used until  $C_{(m,t)} - C_{(m,t-1)}$  again becomes negative. This gives a new value for  $C_{1max}$  equal to the latest value of  $C_{(m,t-1)}$ . Then Equation (5.20) is used with

new value of  $C_{max}$  as a constant. If additional recompression occurs, the above procedure is repeated. In the case of diesel hammers  $F_{(1,t)}$  includes the explosive force which is computed by Equations (3.5) to (3.8) depending on the lapsed time after the ram impact.

All the basic Equations (4.3, 4.5 & 4.6) discussed under Section 4.1.1 for purposes of calculating the dynamic resistance  $R_{(m)}$  are modified as follows to include the pile displacement and plastic displacement of the soil.

$$R_{(m)} = (D_{(m,t)} - D'_{(m,t)})K_{s(m)} (1 + J_{(m)}V_{(m,t-1)}) \quad (5.21a)$$

$$R_{(m)} = (D_{(m,t)} - D'_{(m,t)})K_{s(m)} (1 + J_{(m)}V_{(m,t-1)}^N) \quad (5.21b)$$

$$R_{(m)} = (D_{(m,t)} - D'_{(m,t)})K_{s(m)} + J_{c(m)}\left(\frac{AE}{C}\right)V_{(m,t-1)} \quad (5.21c)$$

Depending on the method of choice, Equation (5.21) is used to calculate the forces in the external springs. Velocities  $V_{(m,t)}$  are calculated by Equation (5.18).

It may be noted that Equations (5.21a) and (5.21b) produce no damping when  $D_{(m,t)} - D'_{(m,t)}$  becomes zero. To overcome this occurrence, these two equations are modified based on Smith's (1960) recommendation. In such occurrence, the following equations will replace Equations (5.21a) and (5.21b).

$$R_{(m)} = (D_{(m,t)} - D'_{(m,t)})K_{s(m)} + J_{(m)}Q_{(m)}K_{s(m)}V_{(m,t-1)}$$

$$R_{(m)} = (D_{(m,t)} - D'_{(m,t)})K_{s(m)} + J_{(m)}Q_{(m)}K_{s(m)}V^N_{(m,t-1)}$$

Displacements, velocities and forces at every time interval are calculated by assigning 1 for beginning and 2 for the current time interval. All the time dependent parameters for the current time interval are computed based on the previous time interval results and the cycle is repeated by initializing the current time dependent quantities to begin the next cycle of computations. This process is repeated until the plastic deformation (permanent set) of the soil reach a maximum value and also the velocities of all the elements are simultaneously become negative or zero. By combining the foregoing formulae and routines a complete computer program is prepared.

#### 5.2.2.1 Selection of Time Interval and Segment Length

In wave equation calculations, care must be taken to make certain that the time interval used is not too large. On the other hand, the time interval should not be unnecessarily small, because this would use an unnecessarily large amount of time in computation with little or no increase in accuracy. Consequently, the choice of the correct time interval becomes an important consideration. Smith (1960) suggested that the best time interval  $\Delta t$ , for use in making a pile calculation, may be defined as the largest interval that will produce a completely stable calculation. Each spring in the model has a "critical" time interval

which is the time that it would require for a sound or stress wave to traverse this particular spring and its associated weight. Considering the possibility of sound or stress wave travelling in both directions, Smith (1955) recommended two formulae for the critical time interval. These are as follows.

$$T_n = \frac{1}{19.648} \sqrt{\frac{W_{(n+1)}}{K_{(n)}}} \quad (5.22a)$$

$$T_r = \frac{1}{19.648} \sqrt{\frac{W_{(r)}}{K_{(r)}}} \quad (5.22b)$$

The minimum value of  $T_m$  that can be obtained by using these formulae is the "critical" time  $T_{cr}$

Smith (1960) and Samson, et al.(1963) recommended to use one half of critical value so as to prevent instability from arising due to other factors not included in Equation (5.22), such as the effects produced by coefficient of restitution  $e$ , ground quake  $Q$  and damping constants.

The length of the pile segments chosen must be considerably shorter than the wave length of the stress or impact wave produced by the hammer. Usually pile driving hammers produce fairly long wave form. Division of the pile into lengths of the order of 5 to 10 ft was recommended by Smith (1960) and Samson, et al.(1963).

### 5.3 Summary

Basic equations and routines which are required to develop a wave equation computer program have been derived. For this purpose, the hammer components and pile are represented by masses and weightless springs and the soil is simulated by dashpot and spring on each pile segment. Also, it was assumed that the mass elements are infinitely stiff and their actual stiffness is represented by the springs.

Gravity effect has also been included by considering the equilibrium of the system before impact. Based on the information gathered from various studies cited indicate that the choice of the correct time interval is an important consideration to produce a complete stable calculation. Also, these studies indicate that one half of the critical time interval will prevent any instability in computations.

## 6. CHARACTERISTICS OF ALWAP AND INPUT INFORMATION

### 6.1 Program Flow

ALWAP is a computer program written in FORTRAN 77 code which performs a wave equation analysis of the pile driving problem. Details of ALWAP such as basic flow chart, listing of the program, input data sheet and other informations related to the program are given in appendix A-1 to A-4. This program will solve problems in either imperial units or metric units, as specified by the user through input data. The program will compute segment weights and spring constants for constant section piles of any shape. It will also compute average properties for round tapered hollow or solid piles and allow reading individual segment areas and weights for stepped piles. Velocity of ram at impact will be calculated by the program from the hammer properties.

Several output options control the amount and type of printed results. Prior to the results of the analysis, the input parameters and the computed pile properties will be printed to verify the accuracy of the input data. Analysis is made for each ultimate soil resistance and depending on the option, output may be pile segment forces, stresses, velocities, displacements and plastic deformations at each time interval, as well as pile point displacement and plastic deformation of soil, and maximum stresses in a segment at each time interval. Also given is the maximum stress ever obtained in any pile segment and corresponding

time interval and, as a check, the last stress and segment velocity. If specified, program will obtain maximum tensile stress in the pile and corresponding pile segment where the maximum tensile stress is obtained. Finally summary of results include assigned ultimate soil resistance, number of blows required to drive per ft or 300mm and corresponding maximum compressive stress ever obtained in the pile. Also, if specified maximum tensile stress ever obtained in the pile.

Graphic output option is also included for bearing graphs obtained for blow count, maximum compressive stress and tensile stress in the pile. On the activation of the option the following graphs will be plotted on separate pages. The graphs are (1) Assigned ultimate soil resistance versus number of blows (2) Maximum compressive stress versus number of blows (3) Maximum tensile stress versus number of blows

In application a set of soil forces  $R_{u(m)}$  are assigned at each element. Computed ram velocity at impact is given and the dynamic computation is continued through successive time increment until all soil forces are less than  $R_u$ , where,

$$R_u = \sum_{m=1}^{m=p} R_{u(m)}$$

For the purposes of computing the permanent displacement, the program scans the pile point plastic deformation  $D'_{(n,t)}$  (permanent set) for the five largest values unless values



differ by more than 0.005 unit, sums the values and divides by the number of values used. The blow count is obtained from the calculated permanent set. In this way the permanent set (or blow count) is determined for a set of assigned soil resistances. The total shape of the bearing graph can be obtained by using variety of  $R_u$  values.

The wave equation bearing graph obtained is associated with a single driving hammer and its accessories, pile type, soil profile and particular pile penetration. If any one of the above items are changed, the bearing graph will change.

The program is designed to stop when the plastic deformation at the pile point in the previous time interval is greater than at current ( $D'_{(m,t-1)} > D'_{(m,t)}$ ) and all pile segment velocities are simultaneously zero or negative. These conditions are based on the permanent set reaching a maximum value from which it should not decrease and pile does not come out of the ground. If the ground resistance  $R_u$  is too low or time interval is too small, the conditions outlined above will be met only after high number of iterations. Under such conditions the program will stop if the number of iterations exceeds 250. Also, if the ground resistance is high or the capacity of the hammer is too low, the program will stop with the suggestion in the output to change one of them. The program is also designed to stop, if the number of blows required to penetrate one ft or 300mm exceeds 1200. Blow counts becoming greater than this value result in very small increase in capacity and often referred

to as "at refusal".

## 6.2 Input Informations

In this program the input parameters such as pile segment lengths, shaft friction distribution and hammer details have to be used directly. Also, the program requires that the user obtain the hammer details from the manufacturers or dealers. In the case of diesel hammers, informations such as lapsed time in each phases and bottom diameter of the ram are difficult to obtain. No computations can be made without these details. Assigning zero for these parameters will make the computer to make use of the values assigned in the program to continue with the computations.

Program input data falls in the general categories of pile characteristics and pile capacity desired, hammer details, soil properties and pile soil interactions. Considering the possible variation of some of the input parameters, a study was performed to adjudge the sensitivity of the program to these parameters. Results of this study is discussed in subsequent sections of this chapter and comparison is also made with the previously published results by various authors.

### 6.2.1 Input Data

The wave equation analysis requires certain input data. Manufacturers' catalogs may be consulted for the details of pile and hammer to be used in the analysis. It is important

to note that the reliability of predicted bearing capacity and predicted driving stress is primarily a function of the accuracy of the soil parameters. Also proper assessment of the pile soil interaction is very important.

#### 6.2.1.1 Pile Properties and Time Interval

Pile details include number of pile segments including ram, cap block, helmet, anvil and cushion if used. Some engineers are of the opinion that the first pile segment in the ground may not have a soil resistance due to driving and other surface disturbances. Also, if the pile is driven through very soft (peat) soil or water surface, the pile segments within the soft strata will not have soil resistance. Considering these possibilities, provision is made in the program to include pile segments which will not be subjected to shaft resistance.

Pile properties required by the computer are modulus of elasticity and wave velocity of pile material, pile cross-sectional area, segment length, weight of unit length and wall thickness if pipe pile is used. If the pipe pile is driven open ended, a soil plug exists when the soil does not move relative to the pile. It may be assumed that the soil has a negligible stiffness compared to the pile stiffness and therefore only pile unit weight is affected. If soil plug is to be considered in the analysis, it should be added to the weight of the pile.

If any pile drive point or driving shoe is used, it can be accommodated in the input data and this will be included in the weight of last pile segment for computational purposes. Usually the pile segment length is not too critical. However, too few elements may not yield the desired computational accuracy. Number of pile segments 8 to 10 with segment length not exceeding 10 ft will be satisfactory.

As explained in Section 5.2.2.1, one should be aware that the minimum number of iterations occurs when the correct value of  $\Delta t$  is used; but if  $\Delta t$  is too big, the computations diverge; if it is too small, it will take many iterations. The program requires constant time interval to be used. If zero is assigned in the input data for time interval, the program will compute and use one half of the critical time ( $T_{cr}^1$ ) for the analysis. However, in the case of pipe piles, if soil plug is included in the weight of the pile, it is important to specify the time interval in the input data.

If a composite pile is analysed, the input parameters such as weight per unit length, area of cross-section, modulus of elasticity and wave velocity of pile material of each segment should be specified irrespective of the shape of pile.

In practice splice or connectors are used to connect concrete piles. In such case, the program

requires informations such as maximum slag or movement allowed in the joint, maximum tensile force that can be transmitted through the joint and the location of the joint. Springs other than the joints should be assigned zero value for slag and tensile force.

#### 6.2.1.2 Soil Properties

Soil data consists of quake, damping values and ultimate soil resistance. However, if Coyle & Gibson's method is used, value of  $N$  appropriate to the soil in which pile is driven is required. In practice, pile point may be founded in a soil strata different from that of shaft and also the soil is remoulded along the shaft during driving. For these reasons, quakes are generally specified for skin and toe separately. This program requires the quake values to be specified separately for skin and toe. Also, an option is available to analyse pile with various quake values keeping other parameters constant.

Most of the published results (Coyle & Gibson (1972), Heerema (1979 & 1981), Litkouhi & Poskitt (1980)) related to damping parameter reveal that in sand, pile toe should be given relatively higher value than shaft whereas in clay it is the opposite. For these reasons the soil damping values are specified by two parameters. By activating the option, the user of this program can select any one of the method discussed in Section 4.1.1 to compute the dynamic resistance. If

the soil strata is considered as a single layer for the purposes of analysis, the program requires separate damping values to be specified for skin and toe and if number of soil layers are considered, damping and N values for each pile segment should be specified. However, this facility is limited to Smith and Coyle's approaches only.

The desired ultimate soil resistance at the pile point is assigned as percentage of total resistance. The computer will determine the resistance at the pile point. The ultimate shaft friction distribution can be of any form. If the distribution is triangular, the program requires only the ultimate soil capacity and percentage of soil resistance at the pile point and by activating the option the computer determine the soil resistance in each pile segment. Soil resistance distribution other than triangular needs detail input.

#### 6.2.1.3 Hammer Details

As mentioned before, the program requires the user to obtain the hammer details. Based on the construction and method of operation of hammers, these are categorised into steam and diesel hammers.

Steam hammer units are not as complicated as diesel hammer units are. However, proper choice of efficiency is very important. For example, a thick cushion may produce a reduced stroke while a thin cushion may allow early air/steam injection because of

self cushioning. Double acting hammers are even more difficult to evaluate since they are extremely sensitive to air/steam pressure changes.

Single acting air/steam hammer data consists of weight of ram, weight of hammer assembly excluding ram weight, rated hammer energy output and efficiency. Hammer efficiencies which are recommended by the manufacturers reflect ideal conditions that are usually not present in the field. Provision is made in the program to assign the stroke observed in the field. If no value is assigned for stroke, the computer will determine the stroke from the input data. The double acting hammers require the following details in addition to the information required in single acting hammers. The details are maximum stroke, operating air steam pressure, and manufacturer's rated limiting pressure. In the absence of any value for observed stroke, the program will compute the stroke from the hammer properties.

Drop hammers are modelled like single acting air/steam hammer. Stroke is usually rather variable and efficiency is often unknown because of a dependency on inertia, operator skill, friction or other quantities that are hard to evaluate. Option is available in the program, either to specify observed stroke or to determine the stroke from the hammer details.

Working principle of diesel hammers varies depending on the type of hammer. All types of diesel hammers are generalised to avoid complications arising from various modifications and detail thermodynamic modelling of its operation. The program requires fairly extensive details of the hammer including maximum explosive force at the impact, top and bottom diameters of the ram, volume of combustion chamber, distance between the exhaust port and anvil top, lapsed time after impact in each phase, length of ram and also other details such as weights and rated energy.

Hammer stroke varies widely in the field depending on the soil resistance, combustion delay, fuel type and preignition. The program requires either rated energy to calculate the stroke or observed stroke to continue the computations. If, there are no values assigned to lapsed time in each phase, the computer will use the values which are assigned in the program itself. Some manufacturers provide the combined stiffness of ram and anvil. This can be directly specified without giving detail physical dimensions of ram and anvil. If there are no values for combined stiffness  $SP_{(1)}$  and bottom diameter of the ram, the stiffness will be calculated assuming that the bottom diameter of the ram is equal to one tenth of top diameter.

Details of hammer accessories such as anvil, cap block and cushion consist of modulus of elasticity of



the material, area of cross-section, thickness and coefficient of restitution. Other details such as weight of anvil and helmet are also required. The stiffness of these components will be calculated by the program along with other calculations.

In the process of driving, the cap block usually gets burnt or crushed if wooden material is used. Considering this possibility, facilities are available in the program to specify change in thickness or modulus of elasticity along with the ultimate soil resistance to which analysis is made. Usually cushions are used only for concrete piles and if steel piles are to be analysed, it can be simulated by specifying zero for modulus of elasticity, thickness and area of cross-section and assigning one for coefficient of restitution of the cushion.

### 6.3 Program Limitations

Usage of this program is limited to impact type hammers with pile head driving. Also, modelling of diesel hammers do not include the thermodynamic action of these hammers to determine the hammer stroke and gas pressure stage by stage.

The program exclude the residual stresses in the pile as well as in the soil. Residual stresses in the pile may develop either during manufacture or from previous hammer blows. Holloway et al. (1978) concluded that for impact driven displacement piles, a significant residual point load

often develops, depending primarily on pile-soil system and this is independent of pile driver. Authier and Fellenius (1983) suggested that the residual stresses are rarely of any significant magnitude and they are of much greater importance for the evaluation of static load test. However, by the time the computations are terminated, the major driving force has been expended and only secondary or residual forces are acting. These are of little interest and no attempt is made to include these in the program.

#### 6.4 Gravity Effect

Five cases indicated in Figure (6.1) are considered to study the effect of gravity on permanent set and stresses in the pile. All calculations associated with this pile were performed on the basis of the following data: Quake = 0.10 in. for side and point; Damping values side = 0.05 sec/ft and point = 0.15 sec/ft; Weight of ram = 5.0 kips; weight of helmet = 0.70 kips; Cap block spring stiffness = 2000 kips/in; Coefficient of restitution = 0.50; Hammer stroke = 2.40 ft; Total ground resistance = 200 kips. Case 3 was further extended to study the effect of ignoring gravity on the blow count diagram. Results of this analysis are shown in Fig. (6.2) and (6.3).

The plots of soil resistance versus number of blows required to penetrate one foot (Figures (6.2) & (6.3)) indicate that the effects of gravity are in the range of 6% to 11% below 120 blows/ft and it varies from 17% to 25% as

the soil resistance reaches the hammer capacity. Increase in compressive stress (Figure (6.2)) due to the influence of gravity effect is in the range of 4% to 12% when the soil resistance is below 100 kips and the difference is negligible (1.7% to 2%) with the increase in soil resistance. The analysis without the gravity (Figure (6.3)) indicates no tensile stress in the pile when the soil resistance exceeds 150 kips. However, when gravity is included, the increase in tensile stress is in the range of 5% to 11% below 150 kips and when soil resistance exceeds this value, significant amount of tensile stress is observed. Its influence on tensile stress can become significant, specially for prestressed concrete piles.

Table 6.1 Gravity Effect on Maximum Forces and Permanent Set

Case No	Maximum Compressive Force in Pounds		Maximum Tensile Force in Pounds		Permanent set in inches	
	Gravity neglected	Gravity included	Gravity neglected	Gravity included	Gravity neglected	Gravity included
1	405640	411685	0	0	0.2057	0.2231
2	291630	297360	0	9460	0.2949	0.3156
3	291100	296750	0	9770	0.2744	0.2940
4	287030	290210	80950	82150	0.4836	0.5152
5	286020	291030	76980	77560	0.4262	0.4553

Results of the analysis carried out for different cases of soil resistance are given in Table 6.1. The gravity effect on compressive forces in all the cases analysed is small (1.5% to 2%). In all the cases, except case 1, the inclusion of gravity produced significant amount of tensile forces. However, this is not evident from the analysis

without the gravity effect and also only case 4 & 5 produced tensile force in the pile. Gravity effect on permanent set varies between 6.5% and 8.5% depending on the load at the pile point.

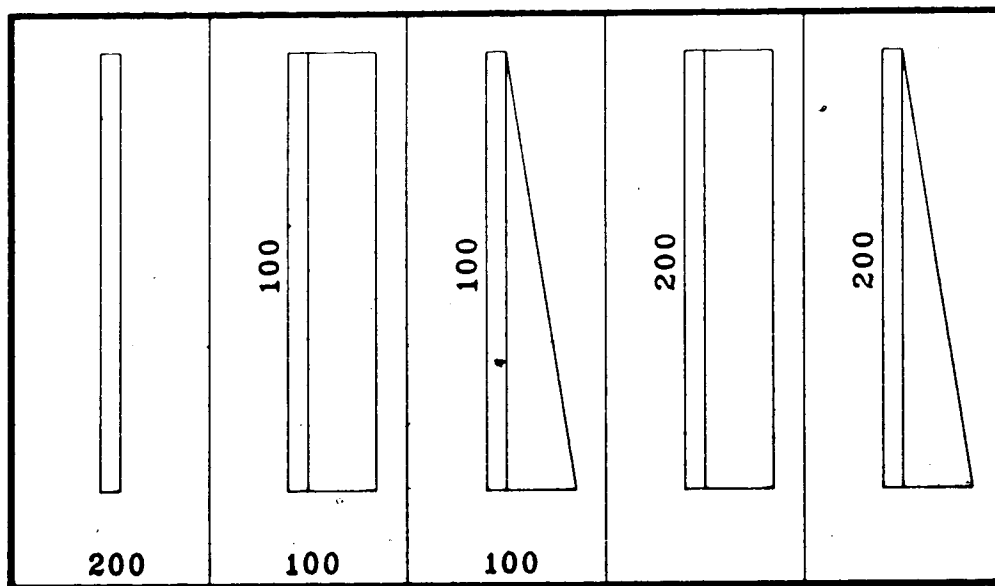
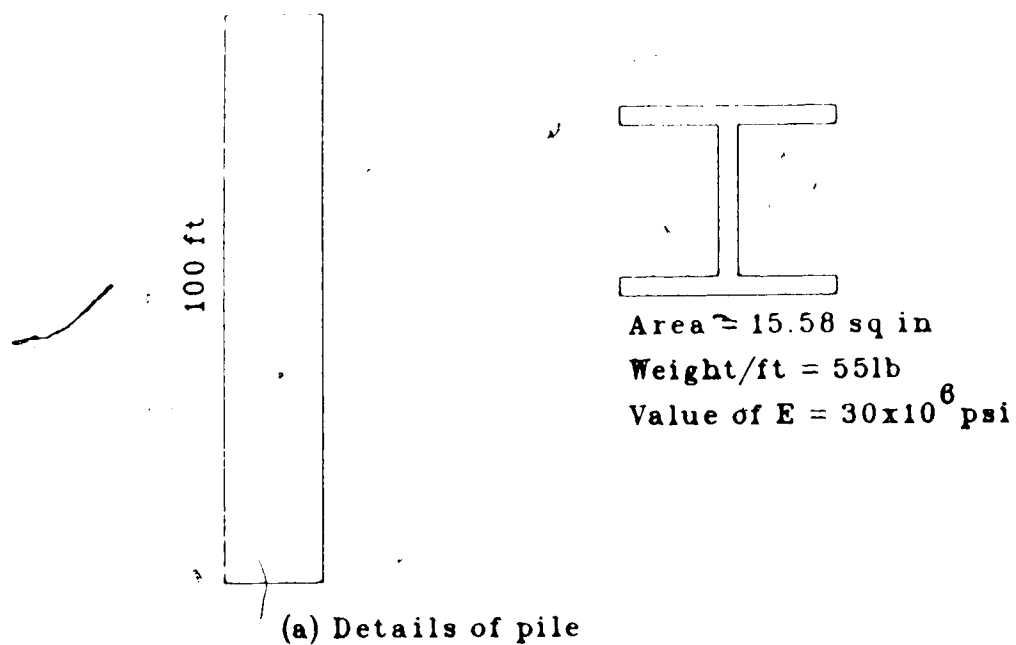
### 6.5 Influence of Input Parameters

The computer program developed requires several input parameters to analyse pile driving problems. Because of the potentially large variation of the values of the parameters, such as hammer energy, quake, properties of cushion materials, percentage of load at the pile point and damping values, a study was performed to adjudge the sensitivity of the program to these parameters. Case 3 shown in Figure (6.1) was selected to perform this study. In each case, all variables other than the parameter under study were held constant.

#### 6.5.1 Hammer Selection

One of the most important question to be answered in the installation of piles is the selection of a hammer to drive the pile to the required penetration successfully. The driving capability of any hammer is greatly influenced by numerous factors. In order to study the effect of driving with varying energy, ram drop of 2, 4 and 6ft were used.

As shown in Figures (6.4) and (6.5), although the energy output of 4ft and 6ft drop of ram are respectively



(b) Details of soil resistance

Figure 6.1 Details of Pile and Soil Resistance

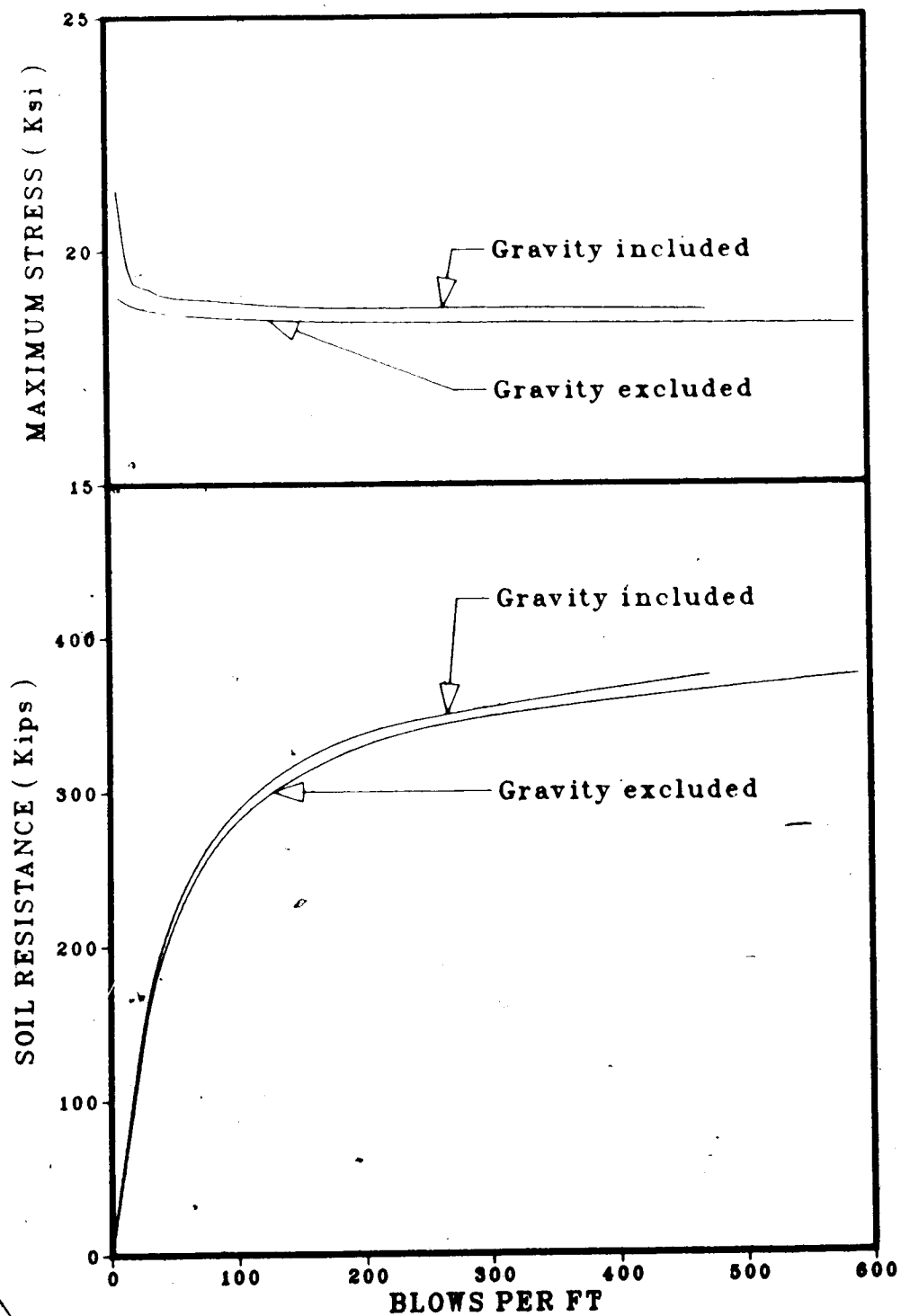


Figure 6.2 Effect of Gravity on Blow Count and Compressive Stress

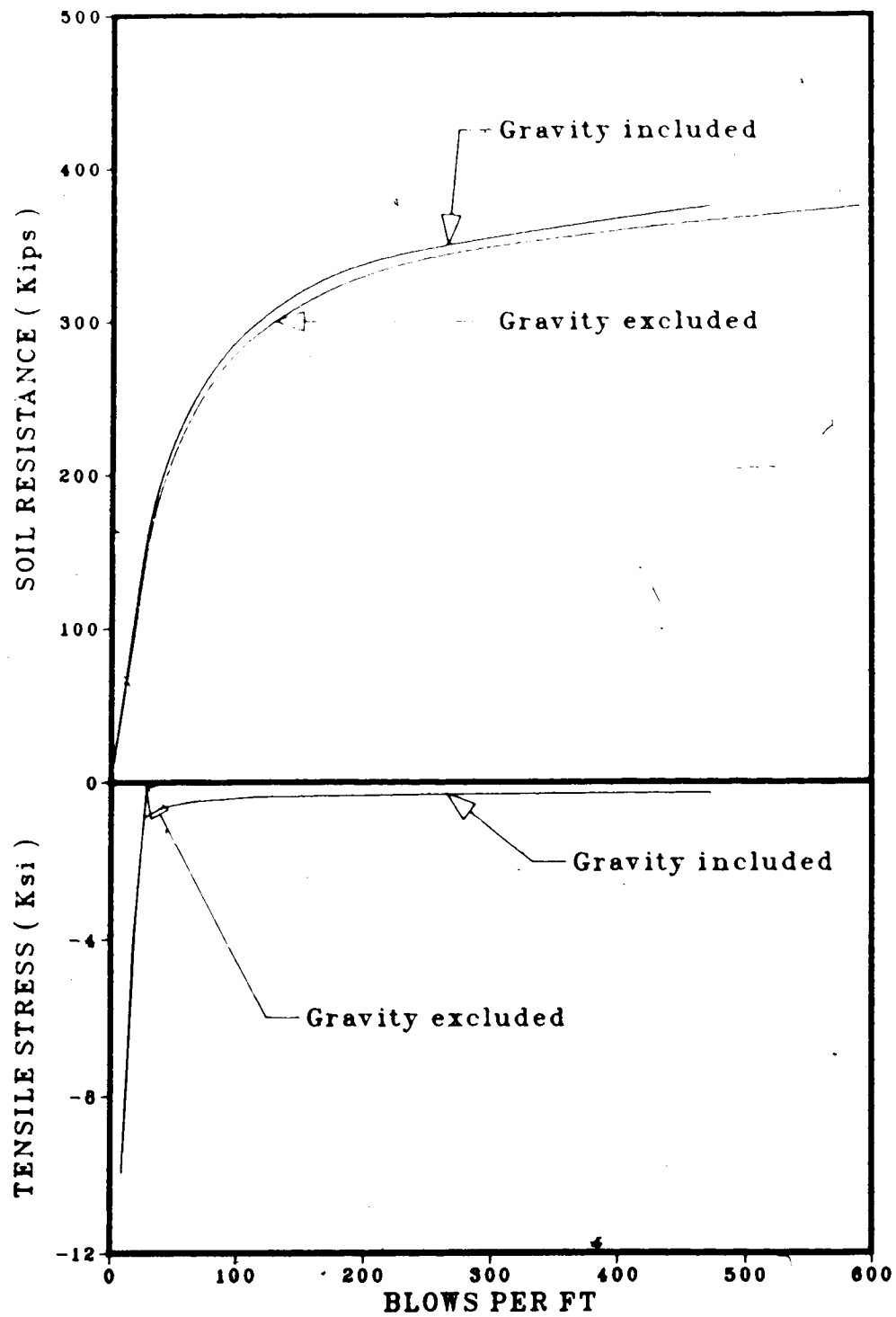


Figure 6.3. Effect of Gravity on Blow Count and Tensile Stress

two and three times that of the 2ft drop, in no case was the driving capacity of the 2ft drop doubled or tripled by use of the higher stroke. Actually, the 100 percent increase in energy from 2ft to 4ft drop increased the driving resistance by 46% and also 50 percent increase in energy from 4ft to 6ft drop increased the driving resistance by only 24%.

Figure (6.4) shows that the increase in energy output by 100 percent (2ft to 4ft) increased the compressive stress in the pile by 40 percent and also an increase in energy by 50 percent (4ft to 6ft) increased the stress by 22 percent. Increase in stresses in the pile is substantial compared to the ability to drive the pile. However, increase in tensile stress (Figure (6.5)) is not significant after the initial stage of driving. Usually high stresses are induced in the pile during driving and therefore any increase in stress beyond the design limit due to improper hammer selection or operation can cause damage to the pile.

#### 6.5.2 Cap Block Properties

Cap blocks are normally used to reduce the stresses in the pile and hammer during driving. The most significant properties of a cap block include its stiffness and coefficient of restitution.

Figure (6.6) indicates that the driving resistance is not sensitive to the cap block stiffness. Also, 100 percent increase in stiffness increased the driving resistance by only 2% to 4% in the possible range of blow counts usually



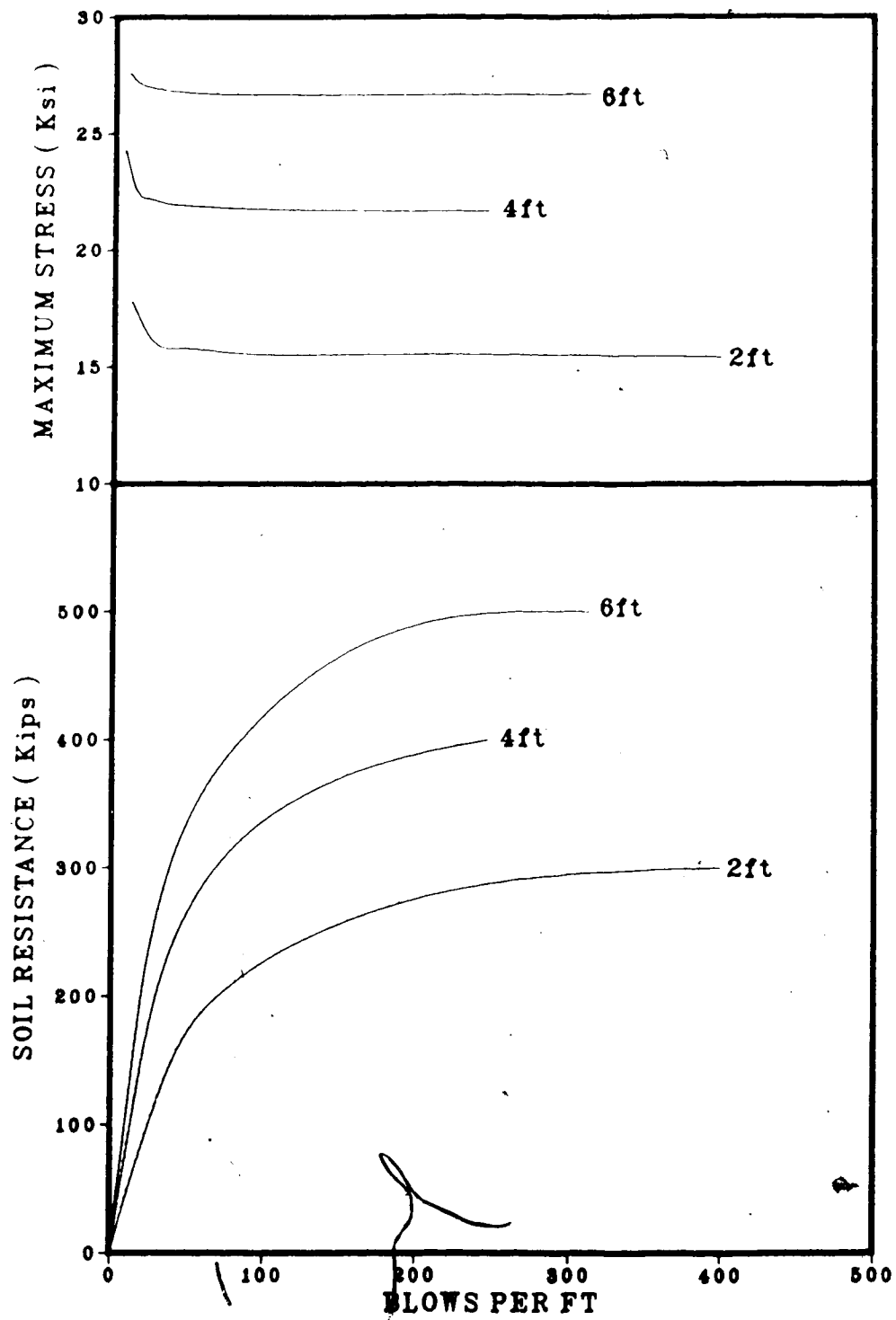


Figure 6.4 Effect of Driving Energy on Blow Count and Compressive Stress

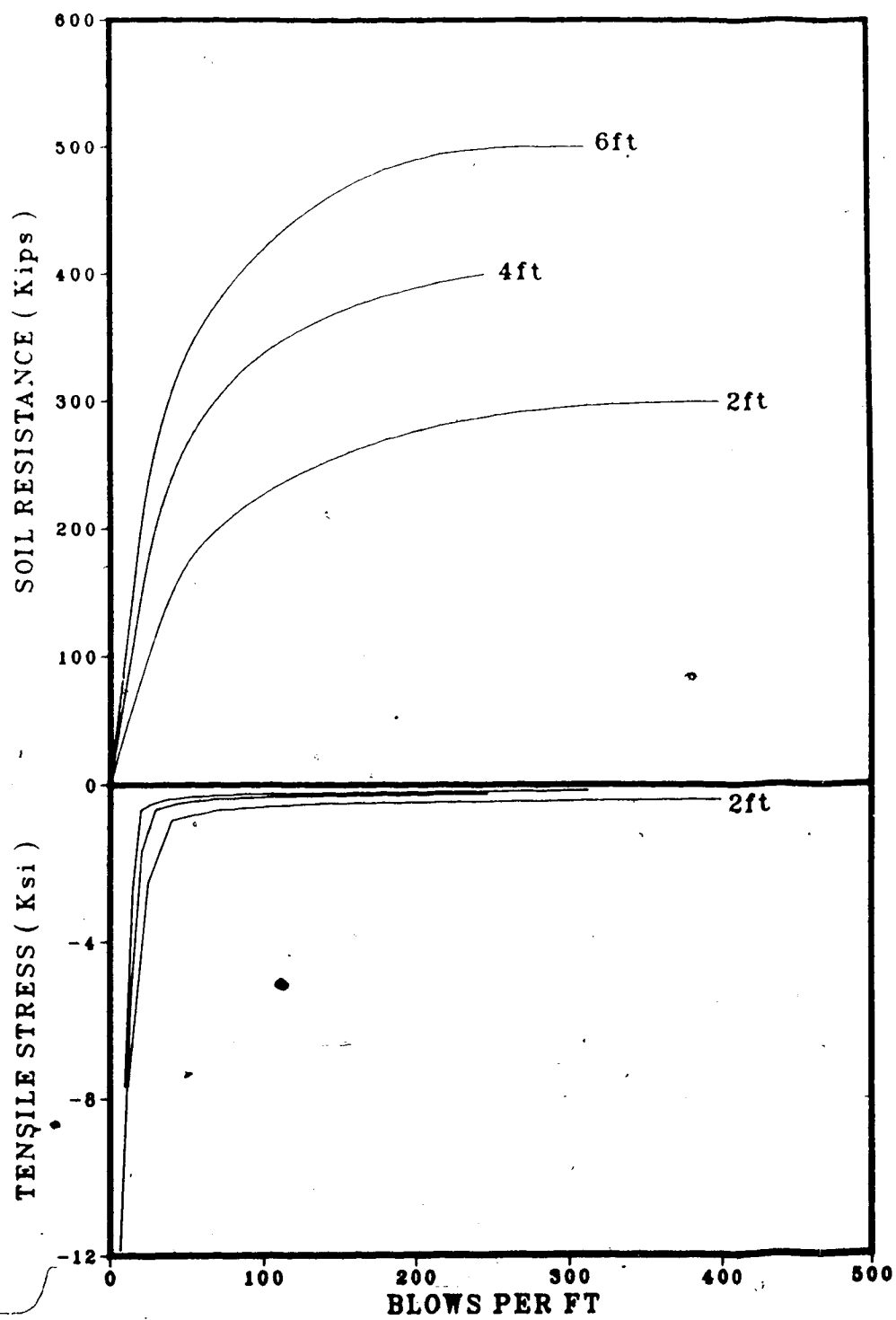


Figure 6.5 Effect of Driving Energy on Blow Count and  
Tensile Stress

employed in pile driving practice. However, 50 percent increase (2000 to 3000) produced almost negligible effect on driving resistance.

Increase in stiffness from 1000 kips/in to 2000 kips/in (Figure (6.6)) increased the compressive stress in the pile by 15 percent and increase from 2000 to 3000 produced 10 percent increase. Also, stiffer cap block produced higher tensile stress at the initial stage of driving and there is no noticeable effect after the soil resistance exceeds 200 kips (Figure(6.7))

Figures (6.8) and (6.9) show the effect of varying the coefficient of restitution of the cap block. The more efficient cap block increases the ability to drive the pile at all levels of resistance since less energy is absorbed in the cap block. However, the effect is not as pronounced as one expects. This can be observed in Figures (6.8) and (6.9). Increase in coefficient of restitution by about 80% produced only 4% to 5% increase in driving ability of hammer. Corresponding increase in compressive stress is only 2 percent. Change in coefficient of restitution has no effect on tensile stress developed in the pile.

### 6.5.3 Soil Properties

Several authors had recommended values for  $\mu$  to be used in the wave equation analysis. These values vary depending on the type of soil and the method of evaluation used by the authors. The results discussed herein are based

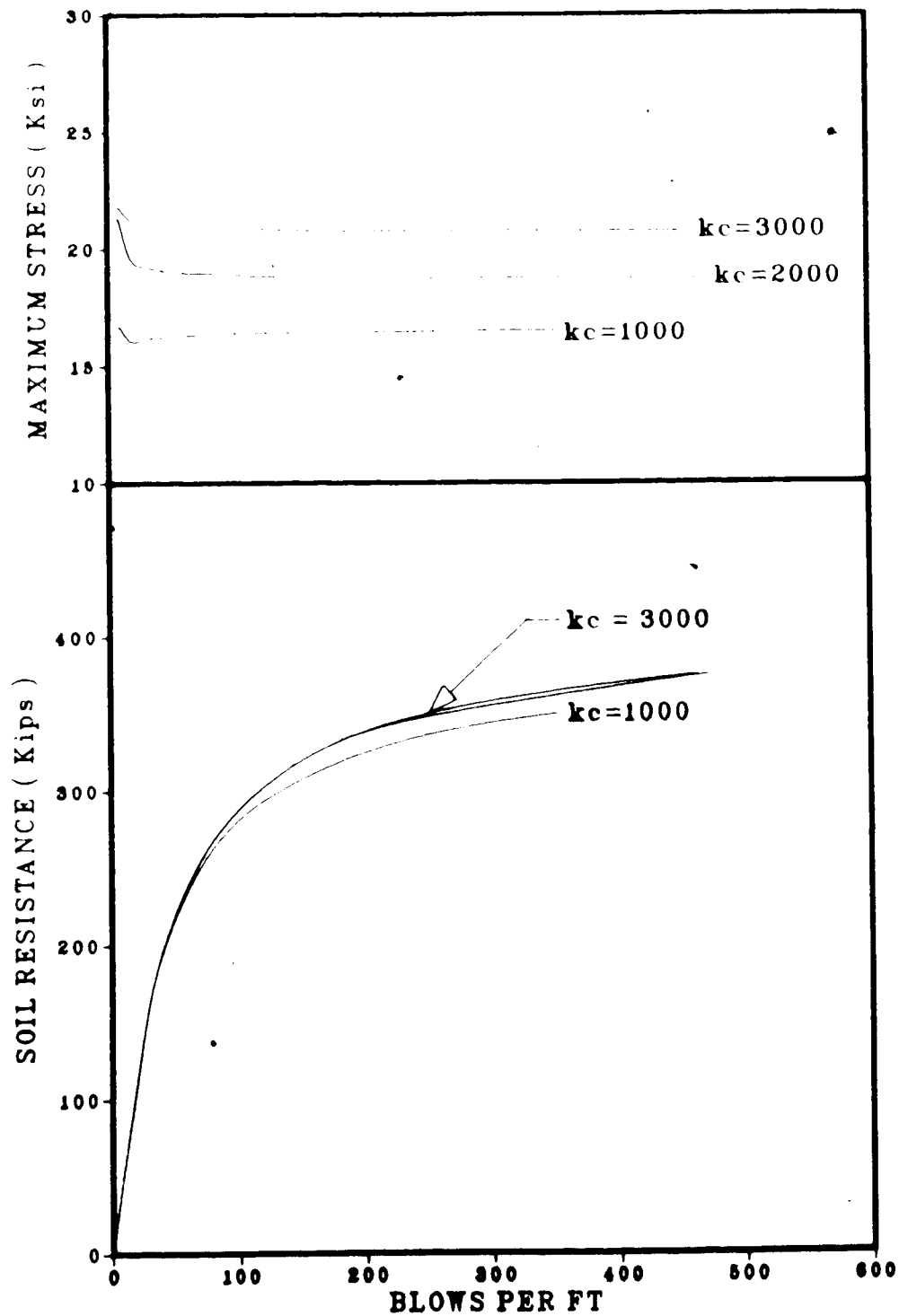


Figure 6.6 Effect of Cap Block Stiffness on Blow Count and Compressive Stress

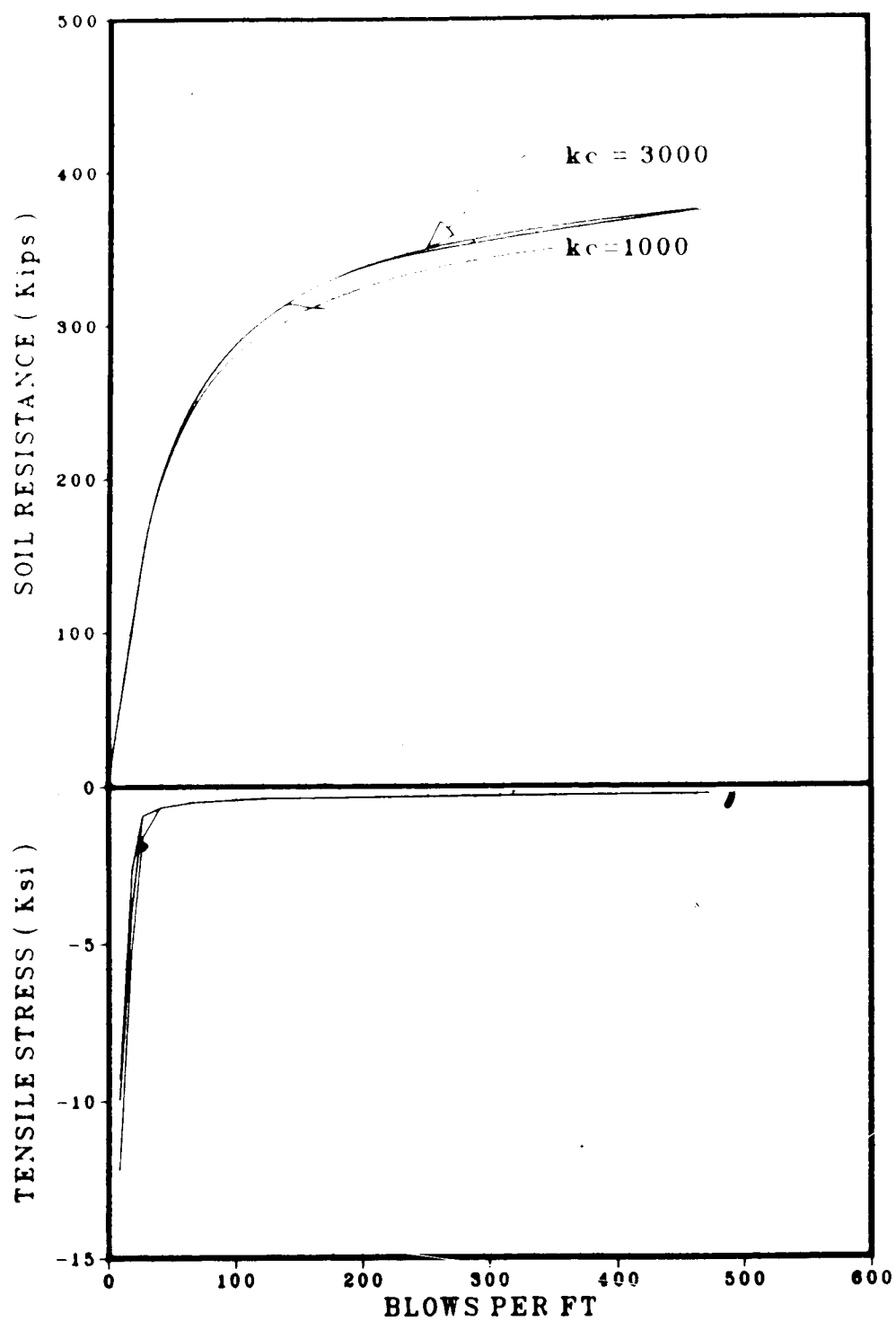


Figure 6.7 Effect of Cap Block Stiffness on Blow Count and Tensile Stress

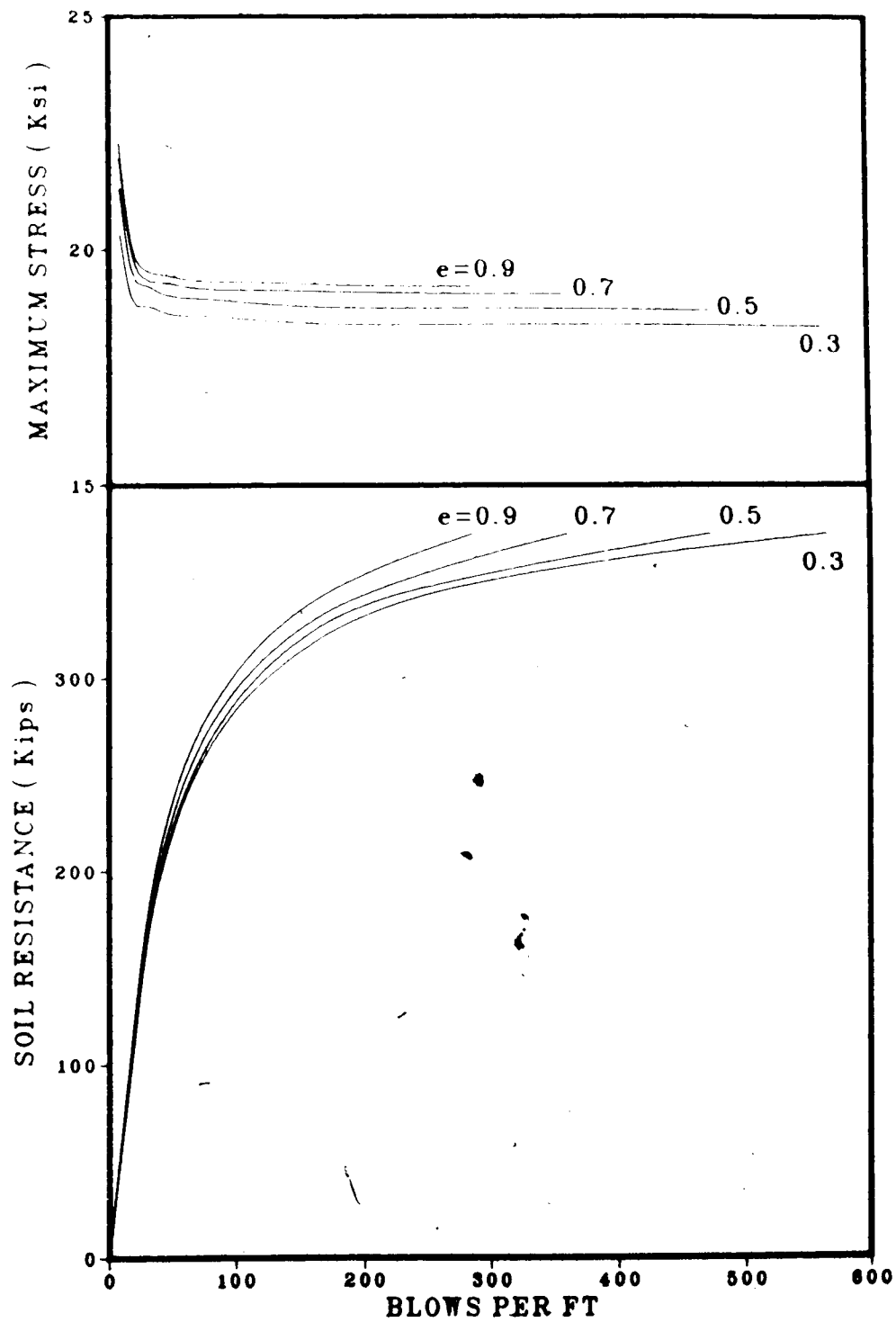


Figure 6.8 Effect of Coefficient of Restitution on Blow Count and Compressive Stress

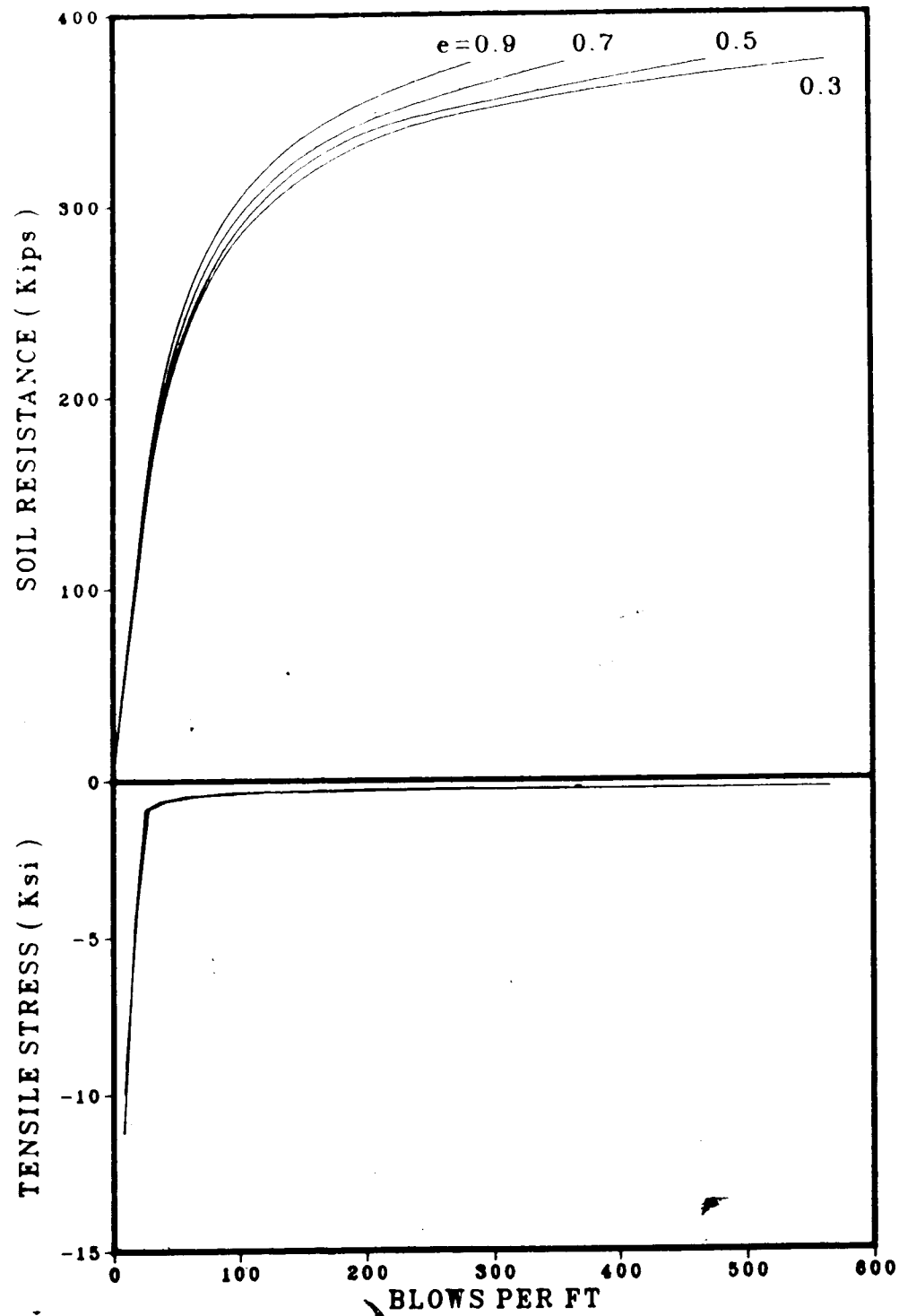


Figure 6.9 Effect of Coefficient of Restitution on Blow Count and Tensile Stress

on the analysis carried out using the same quake value for skin and pile point.

Figures (6.10) and (6.11) show the results of the analysis for various quake values. Variation of  $\pm 50$  percent in quake value produced only 6% reduction in driving resistance corresponding to 100 blows/ft and when the quake value was increased by 100 percent, the driving ability was reduced by only 11 percent. However, changes in quake value did not produce any pronounced effect on compressive stresses (Figure (6.10)). Figure (6.11) indicates that the change in quake values produced appreciable variation in maximum tensile stress. Maximum tensile stress increases with increase in quake. Change in quake value from 0.10in. to 0.15in. produced 93% increase in maximum tensile stress. Variation of this nature can prove significant for prestressed concrete piles.

Varying the percentage of load applied to the pile point influences both the maximum pile stresses and the maximum point set (Figures (6.12) & (6.13)). The percentage increase in maximum compressive stress and the corresponding percentage of total load at pile point are given in Table 6.2.

The pronounced effect on the maximum stress at 100 percent point load is actually due to the complete loss of side resistance and damping.



Table 6.2 Change in Compressive Stress

Percentage $R_u$ on pile point	Change in stress (%)
0 - 50	3 - 4
50 - 75	23 - 37
75 - 100	27 - 32

Pile set or resistance to penetration depends heavily on the assumed ultimate soil resistance  $R_u$  and the assumed point resistance. Varying the percent of point load from 0% to 50% can vary the set 40 to 100 percent and the variation of point load from 50% to 100% can vary the set 20 to 37 percent. Also, it can be noted in Figure (6.12) that the ability of hammer to drive the pile decreases with the increase in percent of point load.

The pronounced effect on the maximum tensile stress is when the load at pile point is zero. Varying the percentage of point load in the range of 0 to 25 percent can vary the maximum tensile stress 90 to 95 percent. However, this variation is not significant when the percentage of point load exceeds 25 percent.

All three approaches discussed in Section 4.1.1 to handle damping in wave equation analysis were employed to study the effect of varying damping values on pile driveability and stress in the pile. Damping values applicable for sandy soils were chosen for this study.

The results of the analysis using damping values recommended by Smith ( Figure (6.14) ) indicate that the

increase in damping value reduces the pile driveability. Variation of  $\pm 50$  percent in damping value can vary the driving resistance 8% to 12%. However, 150% variation in damping value had no effect on maximum compressive stress developed in the pile.

Figure (6.15) shows the results of the analysis using the damping values recommended for sand by Gibson and Coyle. Variation of damping value in the range of 40% to 50% can vary the driving resistance 13 to 17 percent and also, variation of this magnitude in damping value can vary the compressive stress by about 12 percent.

Results of the analysis using Case damping values are shown in Figure (6.16) which indicates that this approach is fairly sensitive to the change in damping values. Variation of  $\pm 30$  percent in damping value can change the driving resistance from 13 to 26 percent. However, no effect on compressive stress can be observed within the range of damping values varied (50%). Figure (6.17) showing the percentage increase in damping value versus number of blows per ft for  $R_u = 150$  kips and  $R_u = 250$  kips was plotted to compare and also examine the approach which is least sensitive to the change in damping value. It can be observed that the values recommended by Smith as well as Gibson and Coyle are not sensitive in the lower range and noticeable change can be observed as the soil resistance ( $R_u$ ) becoming closer to the hammer capacity to drive the pile. In contrast to these two approaches, Case damping factor is fairly

sensitive in the lower range and it becomes very sensitive as the soil resistance increases. Also, with Case damping, the soil damping force becomes dependent on the particular pile material and cross sectional area.

## 6.6 Summary

The computer program has been used to study the effect of gravity on predicted results and also to adjudge the sensitivity of the program to minor variations in the input parameters. The following have been observed from this study.

- 1) For the case considered, permanent set and compressive stress are not significantly influenced by the gravity effect. However, influence on the tensile stress is significant.
- 2) Increase in the hammer energy is not expected to increase the pile driveability proportionally but this can cause excessive compressive stress. However, tensile stress is not significantly influenced after the initial stage of driving.
- 3) Variation in cap block stiffness does not influence the driveability of the hammer. But the increase in stiffness produces higher compressive stress in the pile. Also, stiffer cap blocks produce higher tensile stress at the initial stage of driving.

More efficient cap block increases the ability to drive the pile at all level of resistance. However, the

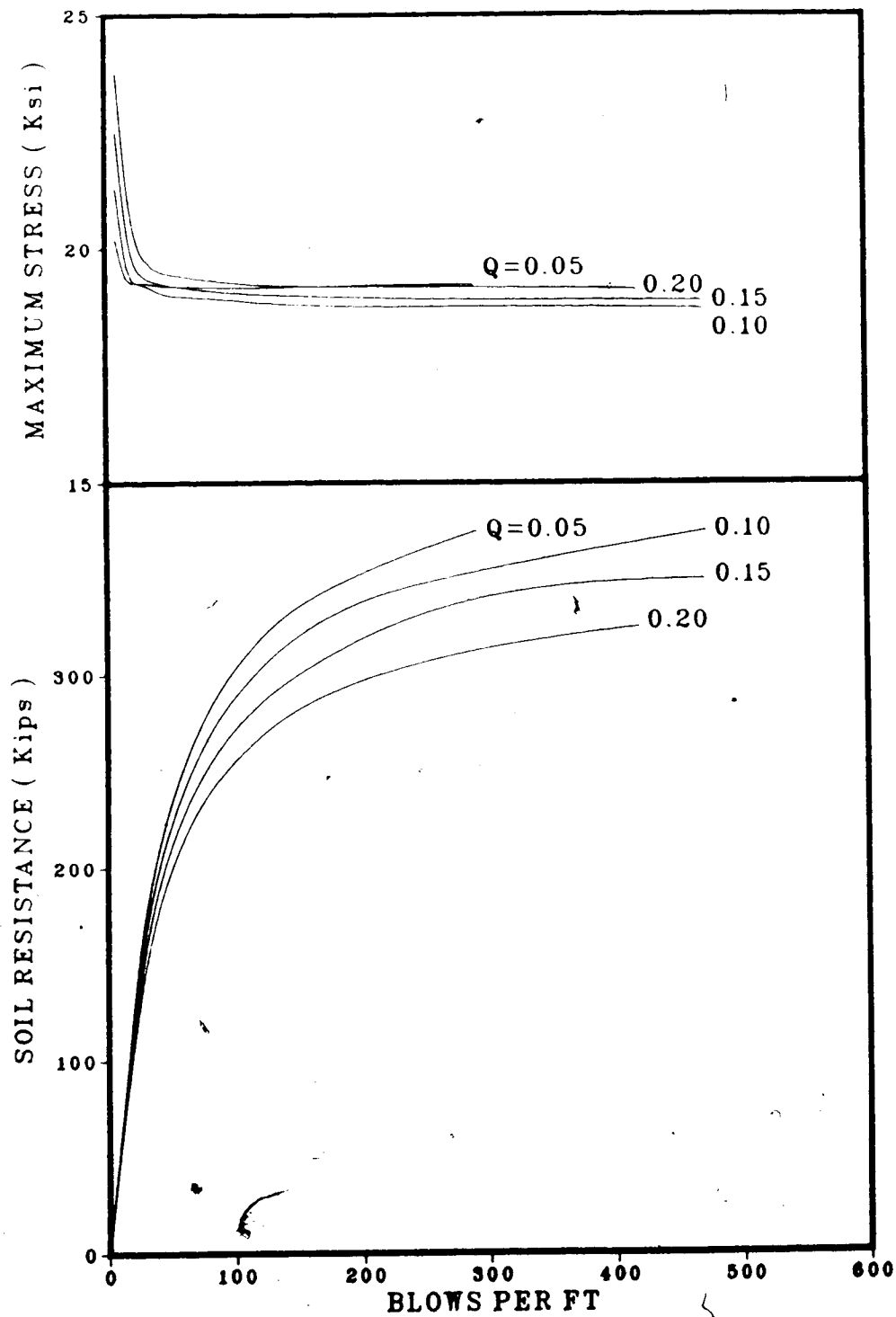


Figure 6.10 Effect of Quake on Blow Count and Compressive Stress

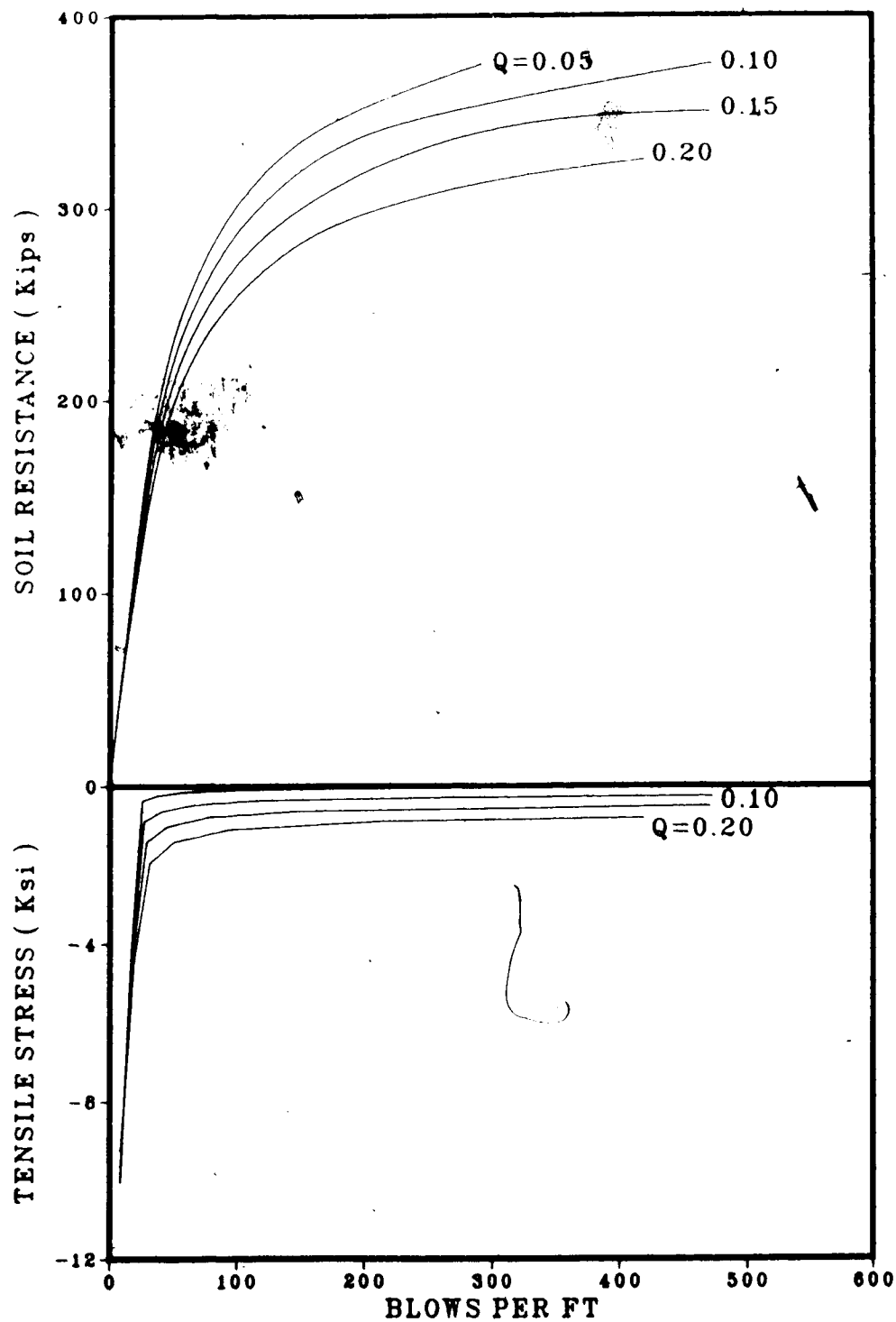


Figure 6.11 Effect of Quake on Blow Count and Tensile Stress

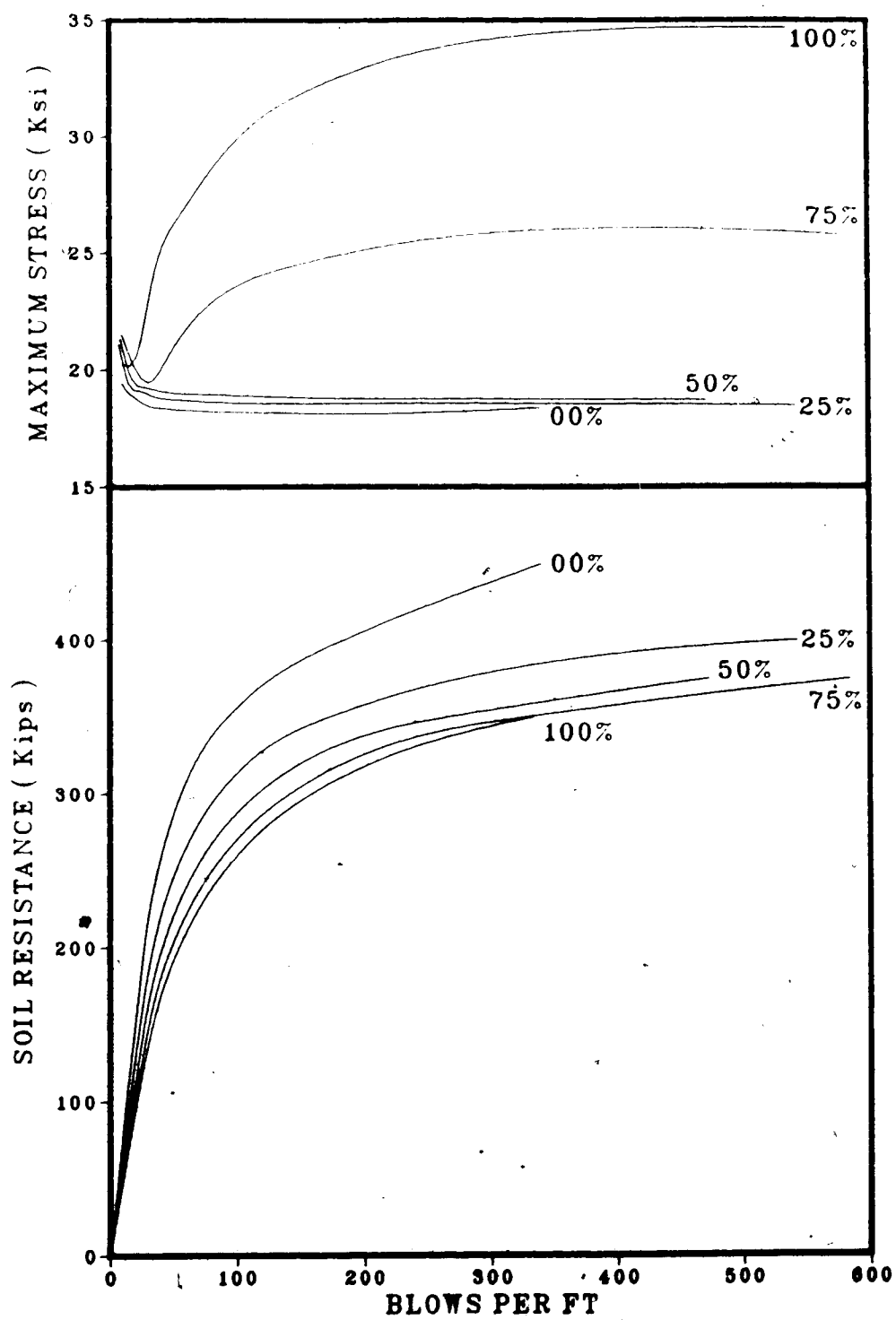


Figure 6.12 Effect of Percent of Point Load on Blow Count and Compressive Stress

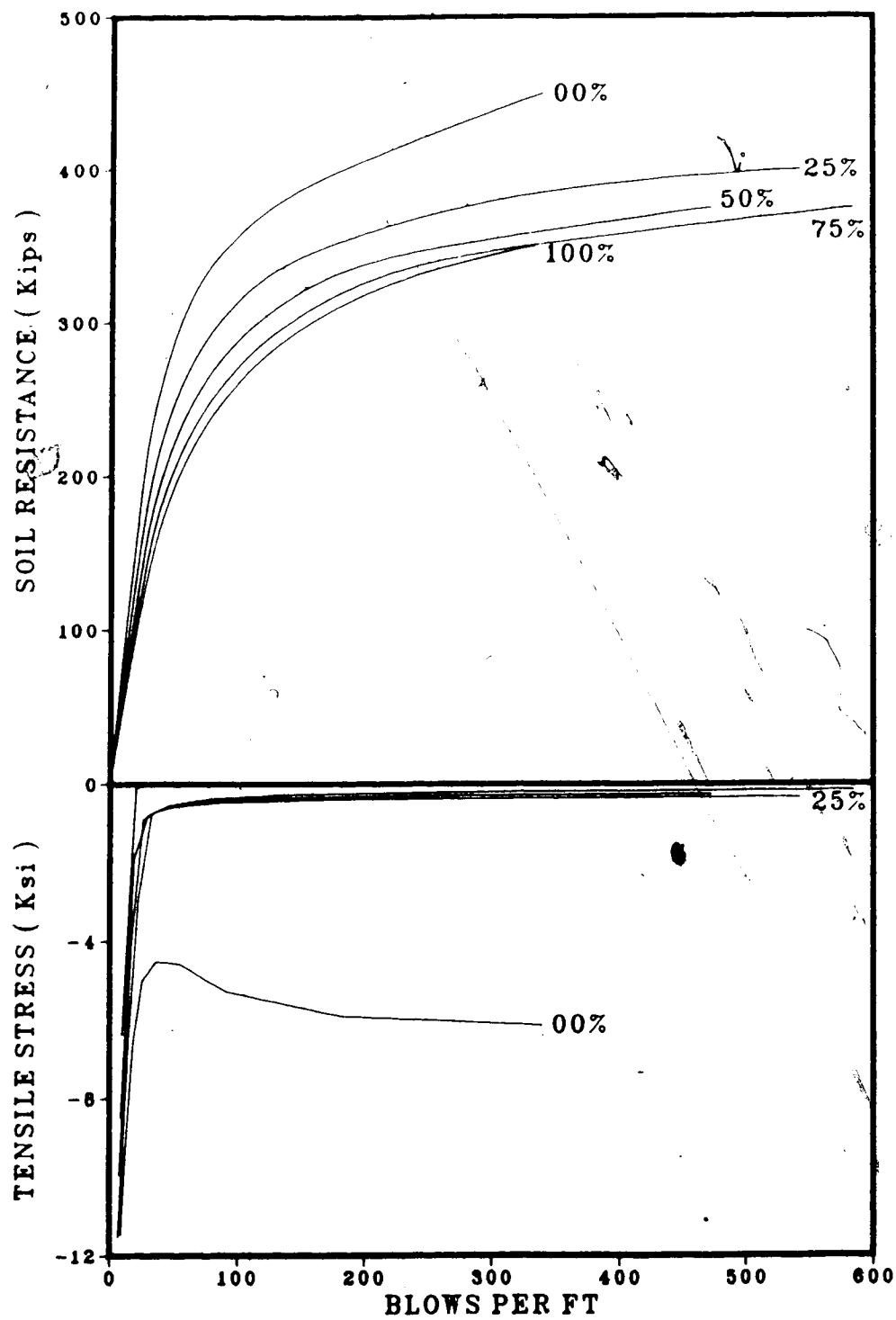


Figure 6.13 Effect of Percent of Point Load on Blow Count and Tensile Stress

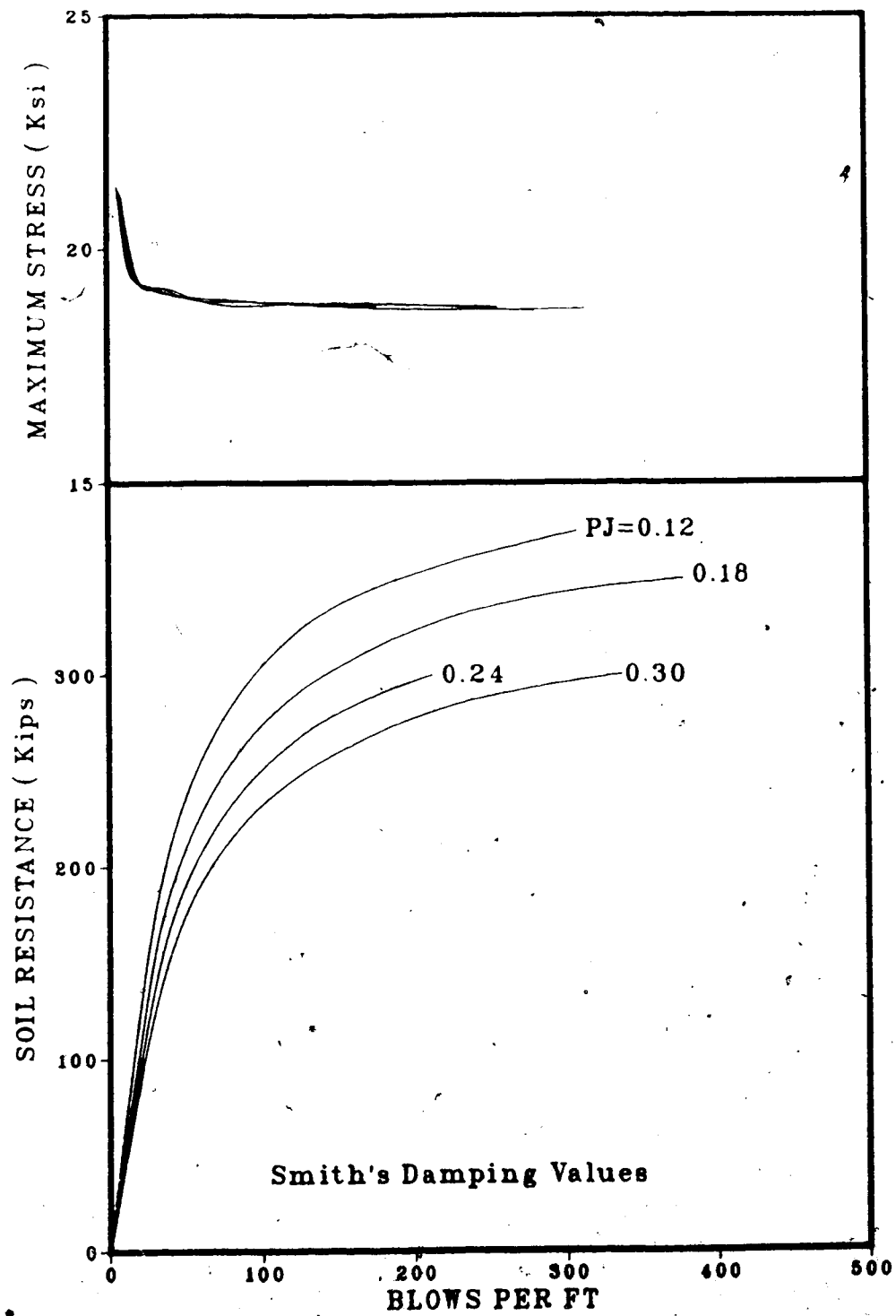


Figure 6.14 Effect of Varying Smith Damping Value



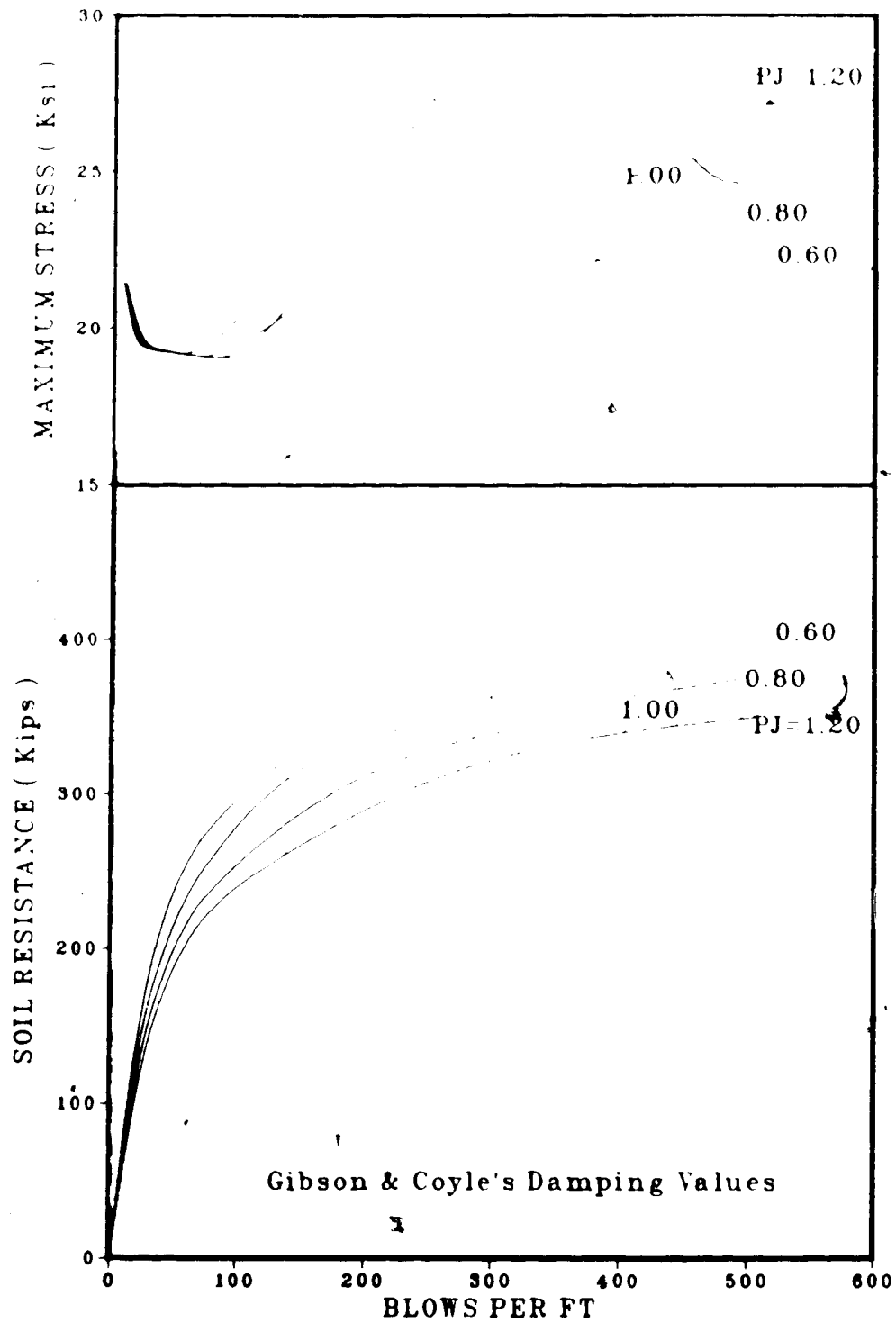


Figure 6.15 Effect of Varying Gibson & Coyle Damping Value

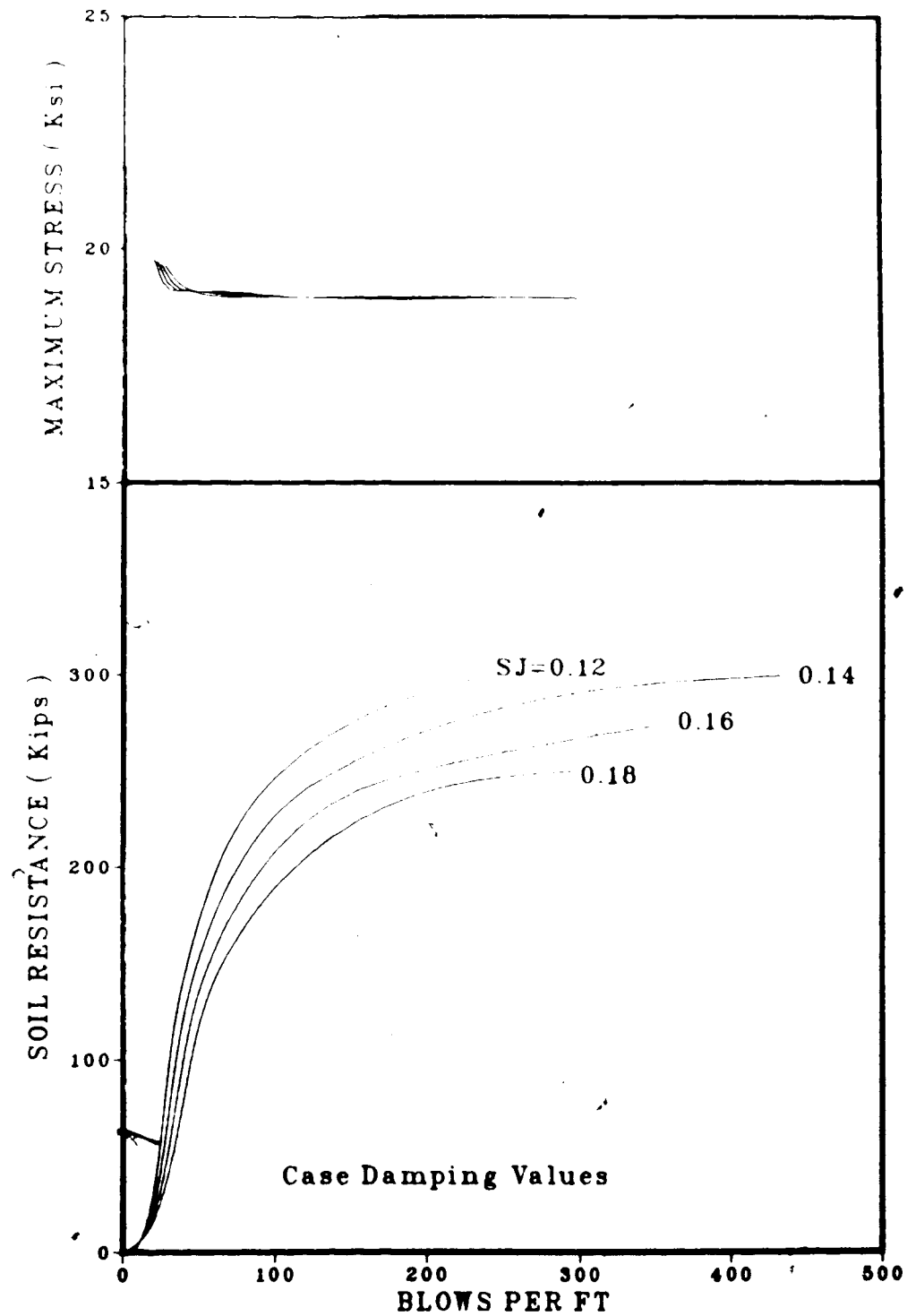


Figure 6.16 Effect of Varying Case Damping Value

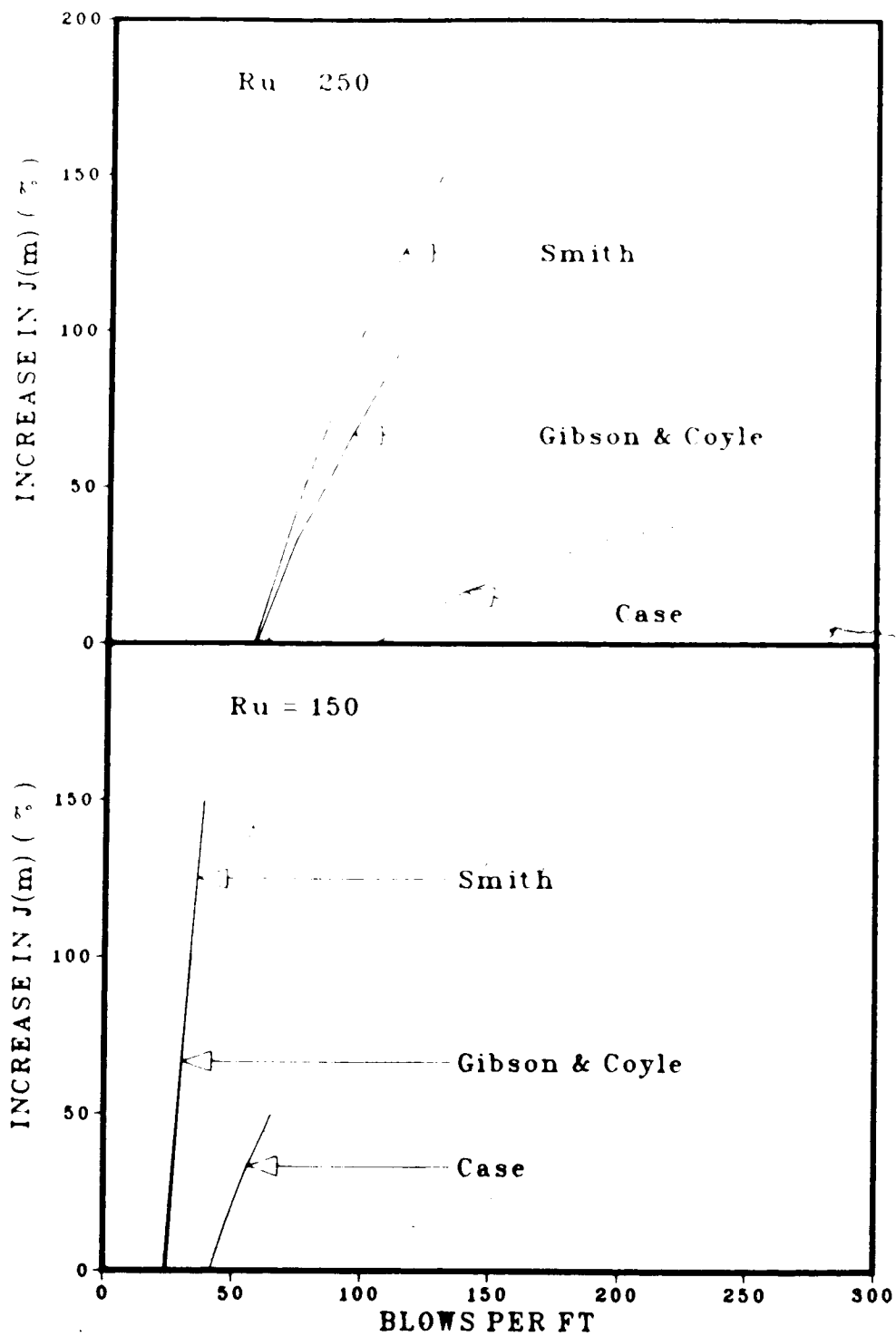


Figure 6.17 Effect of Damping Factors on Blow Count

effect is not as pronounced as one expects. Tensile stress is insensitive to any variation in coefficient of restitution. But the increase in efficiency of the cap block produces higher compressive stress.

4) Minor variations in quake values do not affect the pile penetration or compressive stress significantly. However, this produces appreciable variation in tensile stress and this may be significant for concrete piles.

5) Percentage of load at pile point influence the pile driveability, compressive stress and tensile stress very significantly. Proper assesement of pile point load is very important.

6) Variation in Smith and Case damping has no effect on compressive stress. However, the compressive stress predicted by Coyle and Gibson method is fairly sensitive to minor variations. Driveability of pile is least affected by minor variations in Smith damping parameters.

## 7. PROGRAM PERFORMANCE

### 7.1 Introduction

The successful application of wave equation analysis requires a knowledge of static and dynamic soil properties, dimensions of pile and properties of the material from which it is made, and information on the physical properties of the pile driver and associated equipment used. The overall consideration is to relate the dynamic behaviour of the driving equipment-pile-soil system, with due consideration to changes in properties of the soil during and after driving of the piles.

The program performance is tested using five case histories obtained from Geotechnical Engineering Division of CN Rail and other published records. The informations required for program testing consisted of three different groups.

- 1) Driving system data such as helmet weight and material, properties of cap block and cushion. These were chosen from manufacturers' catalogue and large range of possible values published by various institutions. Material properties such as elastic modulus and coefficient of restitution often proved to be difficult to obtain. However, study on the input parameters indicated that the variation in cap block properties have marginal effect on the predicted results.
- 2) Hammer data including physical dimensions of the ram and other details such as efficiency, peak explosive force and

volume of combustion chamber were obtained either from manufacturers' catalogue or from published records. Values recommended by Rempe and Davisson (1977) for delay time ( $t_d$ ), rise time ( $t_r$ ) and minimum hold time ( $t_h$ ) in combustion phase of diesel hammers were used in the analysis.

3) Soil data such as skin and toe quakes and skin and toe damping values were chosen from the published literatures by various authors. The quakes were mostly chosen at 0.1 inches. Selection of damping parameters in wave equation analysis are dictated by the type of soil in which the pile is driven and the damping model intent to use. The distribution of the soil resistance forces affected the shape of the force and velocity curves as well as stress in the pile and blow count diagram. The ratio between the load at the pile point and total resistance (percent) was observed to influence the predicted pile capacity. In the absence of field measurements, percentage of load at pile point was calculated using various static formulae and possible pile-soil interface failure mode during driving. The final analyses were carried out for most suitable combinations of soil resistance distribution along the pile shaft and percentage of load at the pile point.

In order to place the wave equation in context, it is appropriate to use dynamic formula and compare the results. A number of dynamic pile driving formulae are used in practice to predict the load carrying capacity of piles. Hiley's formula was developed to eliminate some of the

errors associated with the theoretical evaluation of energy absorption by a pile soil-system during driving. The Hiley's formula has been used extensively in practice. This formula is included in this study to examine whether there is any direct correlations existing between Hiley's formula and wave equation analysis. A computer program was written for Hiley's formula to make the computations easy. Listing of the program and other details related to this program are given in appendix B-1 to B-3.

Formula for use with drop hammers and single-acting hammers

$$R_u = \frac{e_f W_r h}{s + 1/2(c_1 + c_2 + c_3)} \frac{W_r + e^2 W_p}{W_r + W_p} \quad (7.1a)$$

Formula for use with double acting and differential-acting hammers and diesel hammers.

$$R_u = \frac{12e_f E_n}{s + 1/2(c_1 + c_2 + c_3)} \frac{W_r + e^2 W_p}{W_r + W_p} \quad (7.1b)$$

where

$R_u$  - Ultimate carrying capacity of pile in lb

$W_r$  - Weight of ram in lb

$E_n$  - Rated energy of hammer per blow in ft-lb

$h$  - Length of free fall for drop hammers and stroke of ram for single-acting hammers in inches

$e_f$  - Hammer efficiency

$W_p$  - Weight of pile in lb

$l$  - Length of pile in inches

$e$  - Coefficient of restitution

$s$  - Permanent set in inches

$c_1$  - Temporary compression allowance for pile head and cap in inches

$$c_2 = \frac{R_u l}{AE}$$

$c_3$  - Temporary compression allowance for quake of ground

$A$  - Average cross-section area in sq-in

$E$  - Elastic modulus of pile material in psi

#### 7.1.1 Interpretation of Load Test Results

The results from the load tests carried out by the respective organizations from which the case histories were obtained are used to compare with the wave equation analysis. The results of these tests have been replotted and reanalysed for this report.

The interpretation of the results from test loading can be made according to many methods. Pile capacity may be viewed either in terms of "failure", that is, rapid progressive settlement at constant load, or as a load satisfying a particular settlement criteria. Each approach has its uses, especially when correlated with local experience, however, the fraction of the failure load obtained from any settlement criterion depends greatly on the pile type, diameter, length, and method of installation



and on the soil conditions at the site. In any case, a failure definition must be based on some mathematical rule and generate a repeatable value that is independent of scale relations and the opinions of the individual interpreter.

Van de Veen (1953) was probably the first to deal with this problem in a rational manner. He postulated that the relation between the tip load  $P_t$  and the tip deflection  $\delta$  could be expressed by

$$P_t = P_{tult} (1 - e^{-\omega \delta}) \quad (7.2)$$

where

$P_{tult}$  - Ultimate pile capacity at the tip

$e$  - Base of natural logarithms

$\omega$  - Arbitrary constant

If it is assumed that a relation of this form is also applicable to the butt load  $P$  and butt displacement  $\delta$  then

$$\ln(1 - P/P_{ult}) = - \omega \delta \quad (7.3)$$

Where  $P_{ult}$  is the ultimate capacity of the pile. Accordingly, a value of  $P_{ult}$  is selected and  $\ln(1 - P/P_{ult})$  versus  $\delta$  is plotted. The correct value of  $P_{ult}$  has been assumed when a straight line plot is obtained.

Davisson (1972) suggested the determination of a limit load calculated as the load for a pile head movement

corresponding to the elastic column compression plus an offset,  $x$ , equal to 0.15 inch plus  $\frac{1}{120}$  times the pile diameter.

$$\delta = \Delta_e + \Delta_s + \Delta_{sp} \quad (7.4)$$

where

$\Delta_e$  - Elastic compression of the pile

$\Delta_s$  - Elastic compression of the soil at the pile tip

$\Delta_{sp}$  - Limiting plastic compression of soil at the pile tip

Chin (1970 & 1971) proposed that, as an approximation, the butt load versus butt displacement could be expressed by a hyperbola of the form

$$P = \frac{\delta}{m\delta + b} \quad (7.5)$$

Where the asymptote  $P_{ult} = \frac{1}{m}$ , and  $b$  is a constant.

Rearranging Equation (7.5) leads to

$$\frac{\delta}{P} = m\delta + b \quad (7.6)$$

After some initial variation, the plot of  $\frac{\delta}{P}$  versus  $\delta$  fall on a straight line. The inverse slope of this line is the Chin failure load ( $P_{ult} = \frac{1}{m}$ ).

Fuller & Hoy (1970) proposed a simple definition for the failure load. The failure load in their method is defined as the load equal to the test load at which the load

movement curve slopes 0.05in./Ton (0.14mm/kN).

Butler & Hoy (1977) defined the failure load as the load at the intersection of the tangent sloping 0.05in./Ton, and the tangent to the initial straight portion of the curve or to a line that is parallel to the rebound portion of the curve.

Each method has its advantages and disadvantages. The Davisson limit was developed in conjunction with the wave equation analysis of driven piles and has gained wide spread use in phase with the increasing popularity of this method of analysis. The Davisson limit results normally in a load which is smaller than a subjectively evaluated failure load. It is intended for use in the evaluation of quick tests, but it is commonly applied to evaluate results from slow tests.

The actual Chin value has very little bearing on the estimate of the pile capacity. The advantage of the Chin method is that it can be used to support the judgement of the quality of the pile test and other evaluations. This method allows a continuous check on the load test results. Check is made by observing sudden kinks or slope changes in the Chin line.

The Fuller & Hoy method penalise the long pile, because the larger elastic movements occurring for a long pile as opposed to a short pile, causes the slope of 0.05in./Ton to occur sooner. The Butler & Hoy development takes the elastic deformations into account and this offset the length effect substantially. However, the slope of 0.05in./Ton is

approached only if failure is imminent.

It is difficult to make a rational choice of the best criterion to use, because the one preferred is heavily dependent on one's past experience. Methods of evaluation discussed above result in upper and lower limits of the ultimate pile capacities estimated from load test results. Considering the purpose of the study and the merits of the methods, all five methods discussed above will be applied to obtain the ultimate static bearing capacity from the load tests.

#### 7.1.2 Damping Models

Three approaches were discussed in Section 4.1.1 to handle damping parameters in wave equation analysis. Options built into the program allow the user to choose the method of analysis depending on the availability of relevant soil informations to select the damping parameters. The study on the effect of varying damping parameters revealed that the Case method is very sensitive to minor changes in damping values and other two methods are insensitive.

In the Case method, selection of damping values impose a greater problem because they affect the blow count result to a much larger degree. Smith's damping values were relatively well proven during several years of use. Gibson & Coyle's damping parameters are related to the basic soil properties such as liquidity index and angle of internal friction. Also, use of this approach and the damping

parameters recommended for this approach are examined in this study. However, the damping parameters recommended for this method were derived from triaxial tests and those are available only for highly compressible clay (CH) and sandy soils. Successful application of the program requires reliable informations and methods which are least sensitive to minor variations. Hence, Smith's and Coyle's approaches are chosen to test the performance of the program.

### 7.1.3 Representaion of Results

The results of the wave equation analysis and Hiley's formula can be represented by the curves. The design pile capacity is given as a function of blow count (blows/ft) and is known as bearing graph. Results of the wave equation analysis and Hiley's formula are given in the form of bearing graphs. Also, the number of blows required during the last foot of driving and the corresponding soil resistance are indicated in these plots. Maximum stresses obtained in the piles are also given as a function of blow count. However, considering the importance of tensile stress in concrete piles during driving, the details of tensile stress are limited to concrete piles only,

In addition to the maximum stress in the pile, maximum stresses obtained in each pile segment are plotted against the pile length. As a means of checking the numerical error in the computation and representing the results, the time dependent variables such as force and velocity of pile head

and toe corresponding to the soil resistance during the last foot of driving are given as a function of time interval, and for pile toe, displacement and permanent set are also included in these plots. These plots are instructive where wave propagation considerations are concerned and also, force and velocity plots are indicative of boundary conditions at pile toe.

Finally the predicted static bearing capacities by the wave equation analysis and evaluated pile capacities from load tests are compared to aid in determining degrees of accuracy obtainable and expectable. Results of Hiley's formula are also compared with Davisson limit load and the pile capacities predicted by the wave equation analysis. In addition to these details, a summary of results are also given in Table 7.1.

## 7.2 Edmonton Rapid Transit 112-Avenue Station

The test pile for the above project selected was a 40ft long W12x65 H Section. The pile was driven with a Delmag D 12 diesel hammer to a depth of 36ft and driving was terminated with an average blow counts of 18 per inch (216/ft). Details of pile driving record are given in the appendix C-1-B.

Pile borehole log close to the test pile indicates presence of 15ft depth of fill underlain by about 6ft thick clay. This is followed by till which extends up to the depth of penetration. Also pile driving data indicate that there was soil resistance starting from 10ft depth. Detail soil informations are given in the appendix C-1-A.

### 7.2.1 Pile Capacity From Static Formula

Site investigation report (Eisenstein and Thomson (1976)) suggested 500lb/sq ft for Lake Edmonton clay and 1000lb/sq ft for till to be used to estimate the frictional resistance of the pile shaft. Presence of fill is not expected to provide any support and no soil resistance was assumed up to a depth of 15ft from ground level.

The ultimate load capacity of a single pile is given by the sum of the ultimate shaft and base resistances. For piles in clay, the undrained load capacity is generally taken to be the critical value unless the clay is highly overconsolidated. If the clay is saturated, the undrained angle of friction  $\phi_u$  is zero. The load capacity of a pile in

saturated clay is given by

$$R_u = R_{u(p)} + \sum_{m=4}^{m=p-1} R_{u(m)} \quad (7.7)$$

where

$$R_{u(p)} = N_c C_u A_b + \sum_{m=p-1}^{m=p} R_{u(m)}$$

$$R_{u(m)} = c_a C_u CL$$

$c_a$  = Undrained pile-soil adhesion

$C_u$  = Undrained shear strength of the soil

$C$  = Perimeter of the pile segment

$L$  = Length of the pile segment

$N_c$  = Bearing capacity factor

$A_b$  = Base cross-sectional area of the pile

The ultimate pile capacity based on static formula was estimated assuming two failure modes of pile-soil interface.

1) The development of the limiting pile-soil shear strength along the entire surface area of the pile. The ultimate capacity of pile estimated based on this failure mode gave 114 kips with 9 percent of the total soil resistance acting at the pile point.

2) The development of the limiting pile-soil shear strength along the outer parts of the flange, plus the development of the full shear strength of the soil along the plane joining



the tips of the flanges (ie, the soil within the outer boundaries of the pile effectively forms part of the pile shaft). This approach gave an ultimate capacity of 379 kips with 5 percent of the total resistance at the pile toe.

#### 7.2.2 Wave Equation Analysis and Hiley's Formula

Soil informations available are inadequate to use Gibson & Coyle's approach and as such, the wave equation analysis was carried out only with Smith's damping parameters. The difference between both failure modes considered to estimate the percentage of load at the pile point was marginal. Hence, the soil resistance distribution with 9 percent at pile point was considered for the analysis.

Results of the analysis are shown in Figure (7.1). Pile driving records indicate that 216 blows were required for last foot of driving and this corresponds to an ultimate pile capacity of 392 kips. The maximum stress in the pile during last foot of driving is computed as 36 ksi. Figure (7.2) indicates that the maximum stress in the pile occurs at 16ft from the pile head and reduces towards the pile toe to 6 ksi. The time dependent variables such as force, velocity and displacement are given as a function of time interval in Figure (7.3) which indicates that there are no possible numerical errors in the computations.

Results obtained from Hiley's formula indicate ultimate soil resistance of 465 kips at 216 blows per ft. In practice

a minimum factor of safety of 6 is employed with this formula. However, the results of Hiley's formula shown in Figure (7.1) do not include any factor of safety.

### 7.2.3 Summary

In the absence of load test, no comparison can be made with the predicted pile capacity. However, the ultimate static bearing capacity estimated assuming the limiting pile-soil shear strength along plane joining the tips of the flanges plus the outer parts of the flanges is 379 kips and it is very close to the ultimate pile capacity (392 kips) predicted by the wave equation analysis.

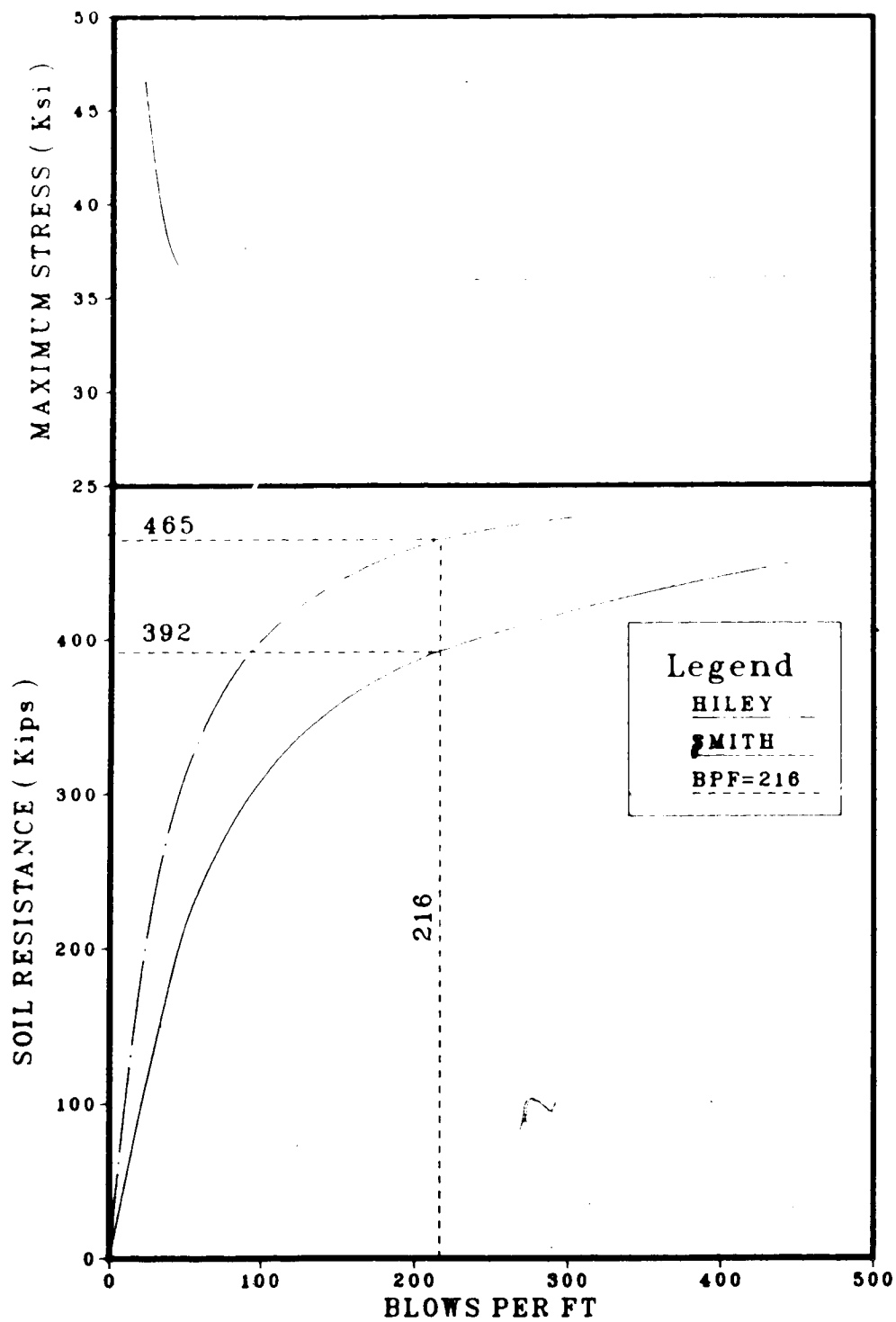


Figure 7.1 Bearing Graphs for Blow Count and Maximum Stress

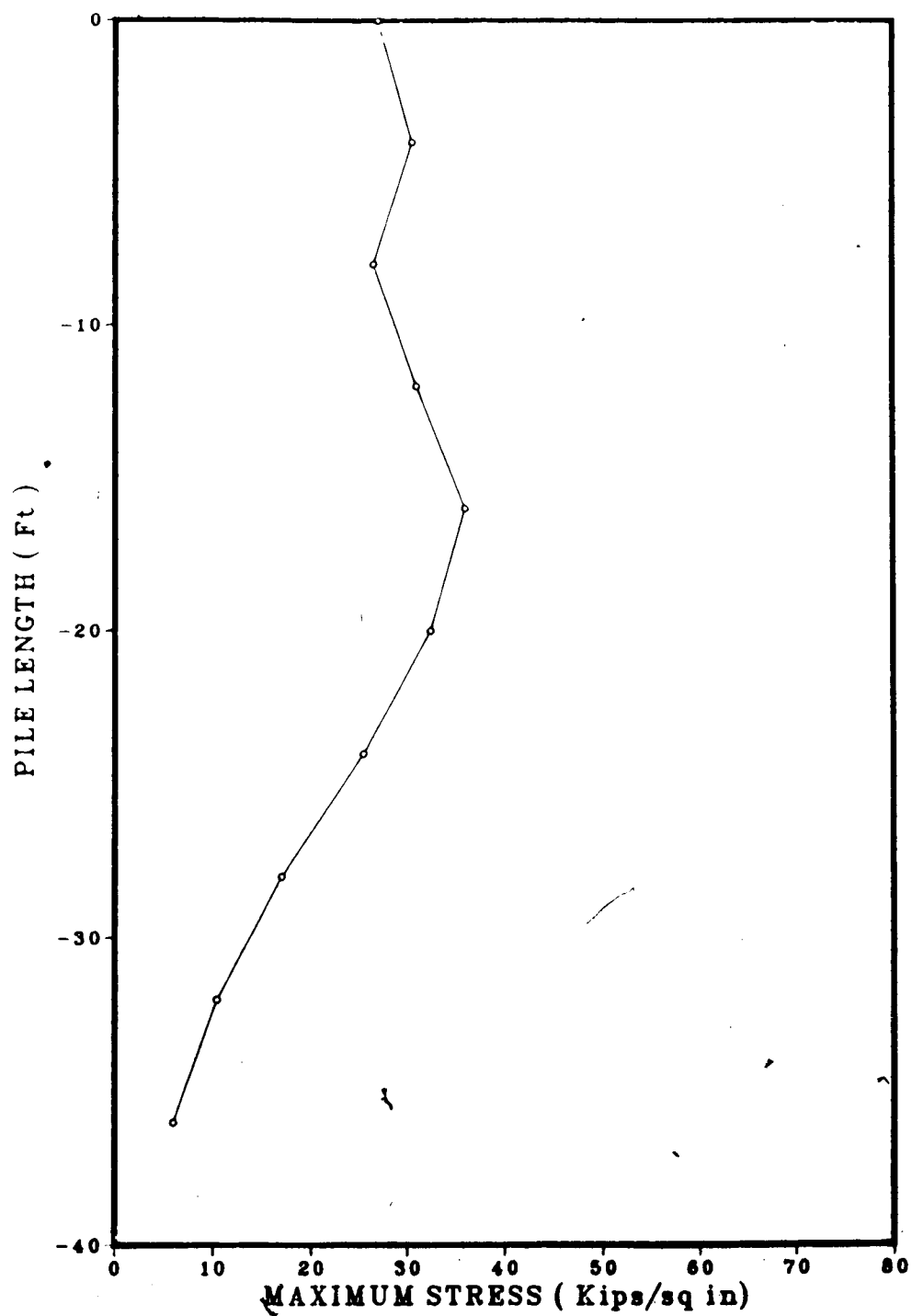


Figure 7.2 Maximum Stress in Pile Segments

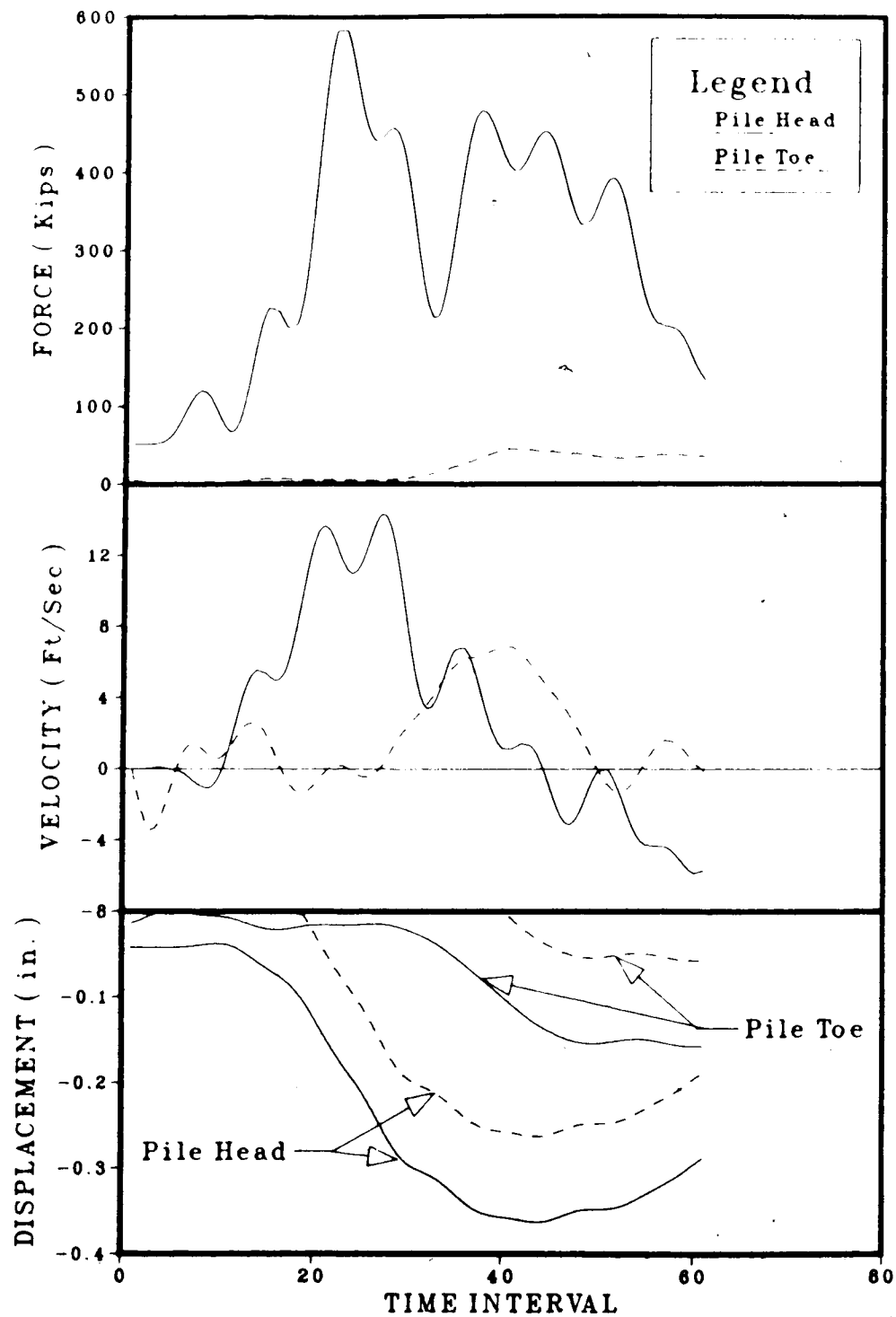


Figure 7.3 Variation of Force, Velocity and Displacements  
with Time Interval

### 7.3 Test Pile At Beaumont, Texas

The pile selected was a 16-in. diameter, 3/8-in. wall thickness, steel pipe pile 53ft long. The strain gauge data from the field tests indicated that 15 percent of the total load applied at the head of the pile during the static load test was carried in point bearing at the tip of the pile. Also, the driving record indicated 28 blows per ft were required during last foot of driving. The pile was driven with a Delmag D-12 diesel hammer.

The soil profile at the test site is given in the appendix C-2-A. Details of soil informations include unit dry weight, Atterberg limits, moisture content and unconfined compressive strength at every 5ft interval. The clay layers presence upto 9ft depth and from 32 to 50ft depth may be classified as highly compressible clay (CH), and the clay soil extends from 9ft to 28ft depth may be classified as low compressible clay (CL) using the unified soil classification system. Unconfined compressive strength ( $C_u$ ) varies between 1750lb/sq ft and 2910lb/sq ft and natural moisture content varies between 20.8% and 56.5%.

#### 7.3.1 Damping Parameters and Soil Set-Up Factor

The plasticity index (PI) of the clay layers presence at the test site varies from 12 to 66 and the liquidity index varies from 0.036 to 0.575. Pile point was founded in highly compressible stiff clay with liquidity index 0.224. Upper and lower limits of damping parameters corresponding

to liquidity index 0.224 are 0.977 sec/ft and 0.707 sec/ft (see Figure (4.5)). An average value of 0.84 sec/ft was chosen for the pile point. In the case of pile shaft, it passes through CH and CL materials. However, 60 percent of the pile shaft is embeded in CH material. Damping value for pile shaft was chosen based on an average liquidity index of 0.316 which corresponds to an upper limit of 1.061 sec/ft and lower limit of 0.784 sec/ft. Analysis was carried out using an average value of 0.92 sec/ft.

Damping parameters for Smith's approach were selected from range of values. Damping values of 0.20 sec/ft for skin and 0.02 sec/ft for toe were used in the analysis.

Consistency of clay presence at this test site varies from medium to stiff. Soil set-up factor of this type of clay is expected to vary between 2 and 3 over a considerable period of time. Based on the experience of the authors (Coyle, et.al 1970b) with this soil and other geological conditions of the test site and the time allowed for soil to regain its strength before load test (13 days), they recommended a set-up factor of 2.

### 7.3.2 Pile Capacity From Static Formula

The test pile was driven open ended. Considering the possibility of forming soil plug in the pile, the ultimate pile capacity and the percentage of load at pile point was calculated for both plugged and unplugged conditions.

Ultimate capacity of pile for plugged condition estimated

based on the lambda method suggested by Vijayvergiya and Focht (1972) gave 354 kips with 10 percent of the total resistance acting at the pile point and for unplugged condition this method gave total resistance of 320 kips with 1% of the total resistance at toe. In the absence of any informations about the ground water condition, pore pressure was assumed hydrostatic for the purpose of estimating the effective stress at the pile point.

Ultimate pile capacity was also estimated using the relationships between the adhesion factor and undrained shear strength suggested by Tomlinson (1970). For plugged condition, this method gave an ultimate capacity of 328 kips with 11% of the total resistance at the toe and for unplugged condition the total resistance was 295 kips with 1.5% at the pile point. However, the strain gauge data indicated 15% of the total resistance was acting at the pile point.

### 7.3.3 Pile Capacity From Load Test

The load test at this test site was performed 13 days after driving and the static bearing capacity obtained from this test was 240 kips. The method of evaluation used to obtain this pile capacity as well as the details of the test results are not available to replot and evaluate by any of the methods used in this study.



#### 7.3.4 Wave Equation Analysis and Hiley's Formula

Wave equation analysis was carried out using Smith's as well as Gibson & Coyle's damping parameters. Computer run was made for both plugged and unplugged conditions assuming 15 percent of the total resistance acting at the pile point. Ultimate soil resistance corresponding to each pile segment was assigned based on the shaft frictional resistance estimated from static formulae.

Bearing graphs obtained from wave equation analysis are shown in Figures (7.4) and (7.5). From Figure (7.4), for Smith's and Coyle's approach, the total soil resistance at 28 blows/ft is 118 kips. Assuming a soil set-up factor of 2, the predicted ultimate static bearing capacity is computed as  $118 \times 0.85 \times 2 + 118 \times 0.15 = 218$  kips.

Results of the analysis for plugged condition are shown in Figure (7.5) which indicates total resistance of 117 kips at 28 blows/ft for both approaches. Ultimate static bearing capacity for soil plugged condition is computed as  $117 \times 0.85 \times 2 + 117 \times 0.15 = 216$  kips.

Results obtained from Hiley's formula are represented by the bearing graph in Figures (7.4) & (7.5). These figures indicate an ultimate soil resistance of 228 kips at 28 blows/ft. Generally a minimum factor of safety of 6 is employed with this formula to estimate the design pile capacity and no set-up factor is applied to dynamic formulae.

Maximum compressive stress obtained in the pile are also shown in Figures (7.4) & (7.5). It can be observed that the plugged condition predict higher stresses in the pile than the unplugged condition. Also, it can be noticed in Figure (7.6) that stresses in the pile segments for plugged condition are 66% to 77% higher than the unplugged condition. This may be attributed to the inertia effect resulted from increase in weight per unit length of pile. Gibson & Coyle's approach predicts slightly higher stresses than Smith's approach. The location of the maximum stress in the pile for unplugged condition is also different from that of plugged condition. In the case of plugged condition, the maximum stress occurred at the location (20ft) where the high frictional resistance is offered by soil, whereas in unplugged condition, it is located close to the pile head (8 to 12ft). However, in both cases the maximum stress varies according to the shaft friction:

Variation of time dependent variables such as displacement, velocity and force with time interval are given in Figure (7.7). The force and velocity diagrams reflect the boundary conditions at the pile toe. Higher velocities in the pile are accompanied by low resistance to penetration. This condition is reflected in the pile point velocity and force diagrams. Also, it can be noticed that the pile head velocity and force increase steadily to a maximum value until the ram impact is made and after that it varies according to the reflected waves.

### 7.3.5 Summary

Ultimate static bearing capacity predicted by the wave equation analysis varies only by 10 percent from the load test result. However, for clay soils proper assessment of the soil set-up factor is very essential. Ultimate pile capacity estimated from static formulae are 23 to 47 percent higher than the load test result. One of the reason for this variation may be the lack of time period allowed for soil to gain its strength.

Results of this analysis indicate that the analysis should be performed for possible combinations of driving conditions to avoid high driving stresses in the pile as well as to select suitable pile driving system.

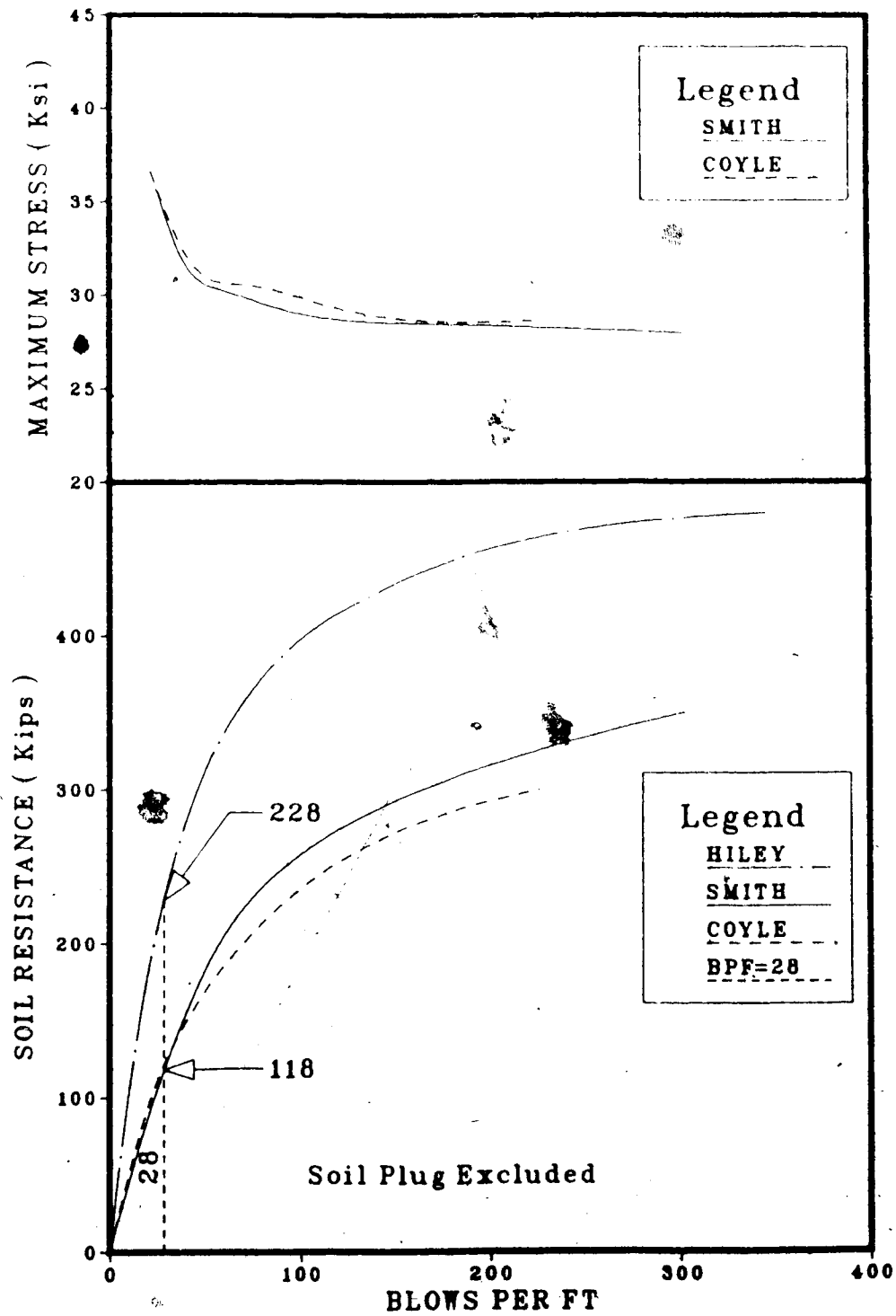


Figure 7.4 Bearing Graphs for Blow Count and Maximum Stress

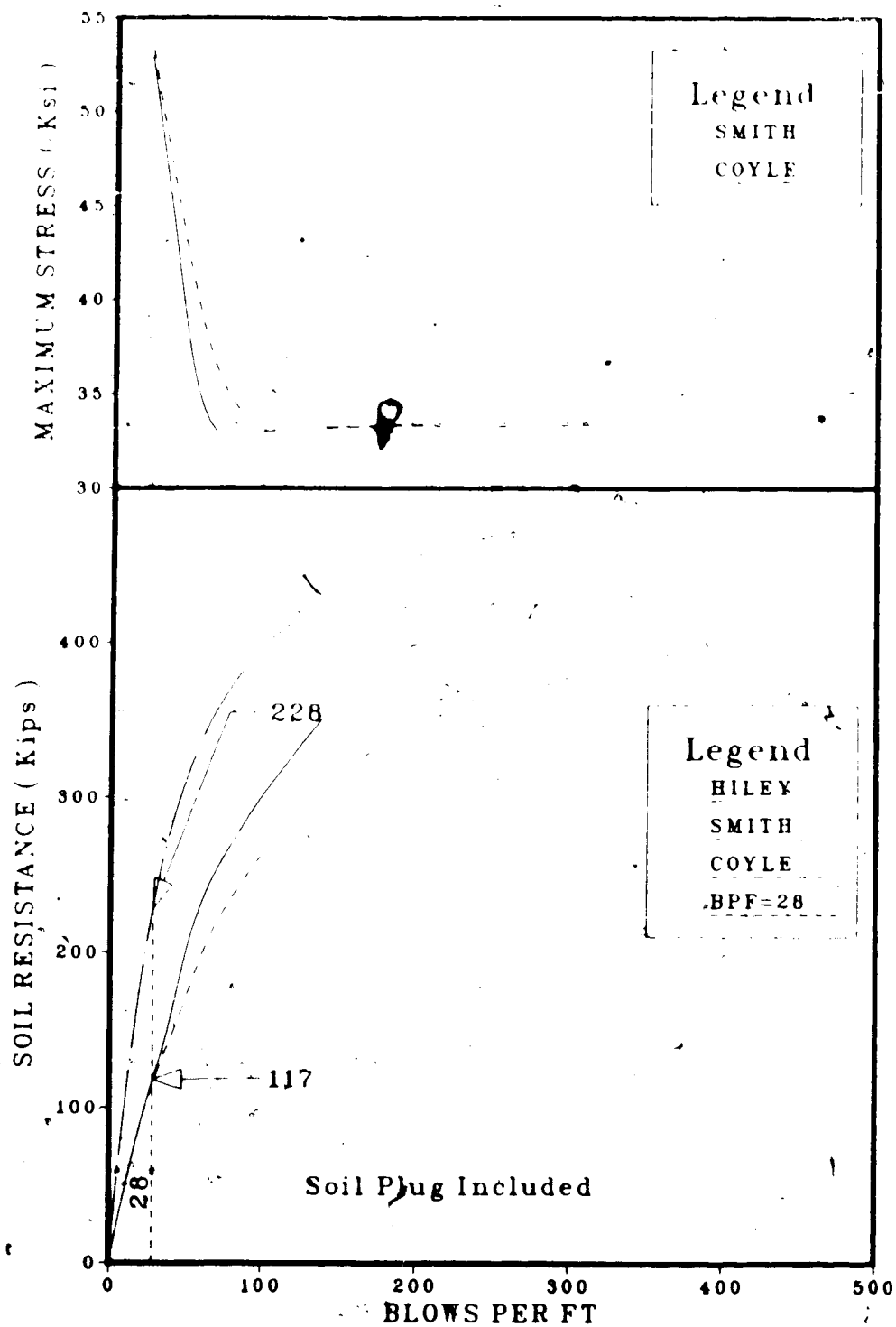


Figure 7.5 Bearing Graphs for Blow Count and Maximum Stress

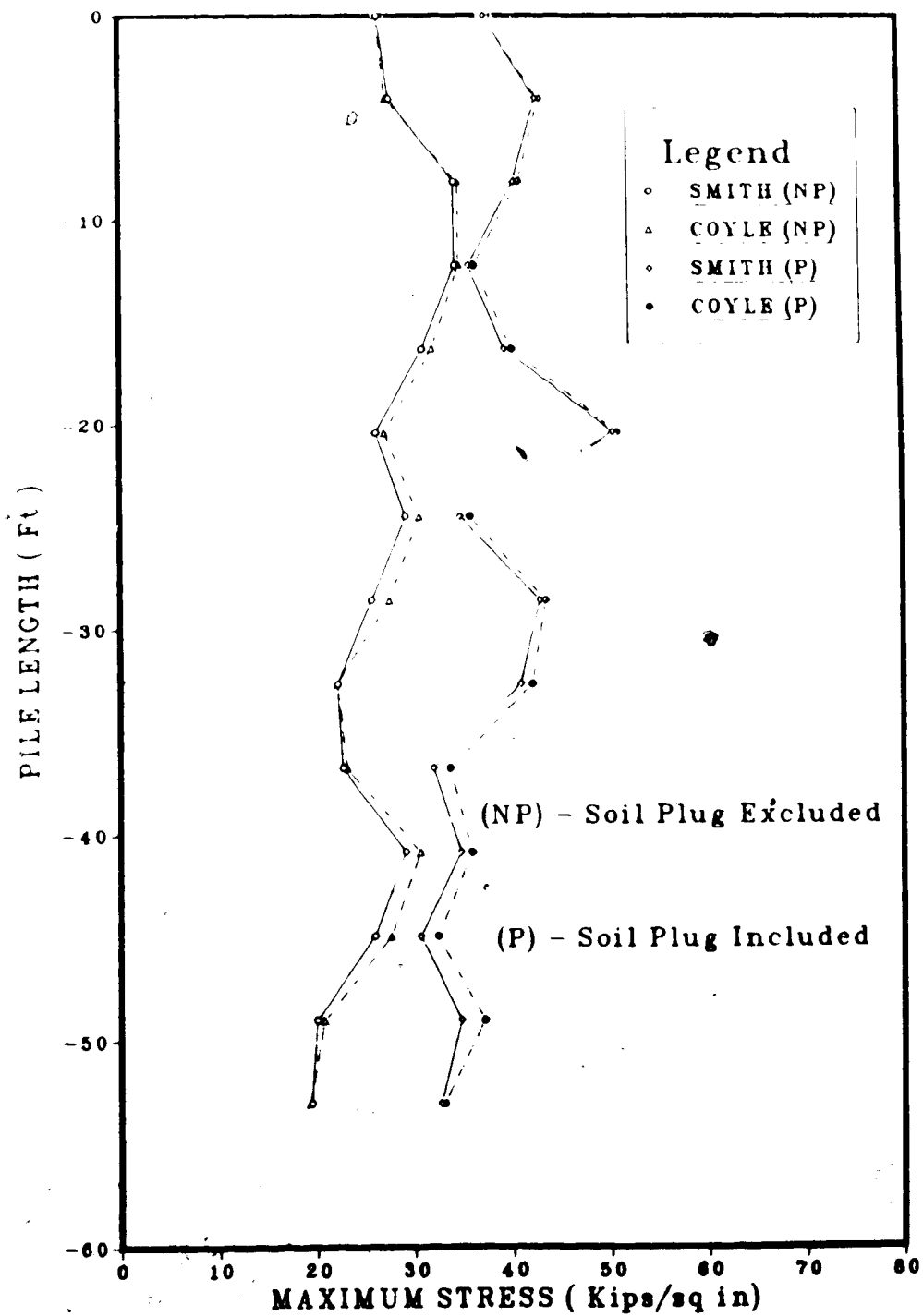
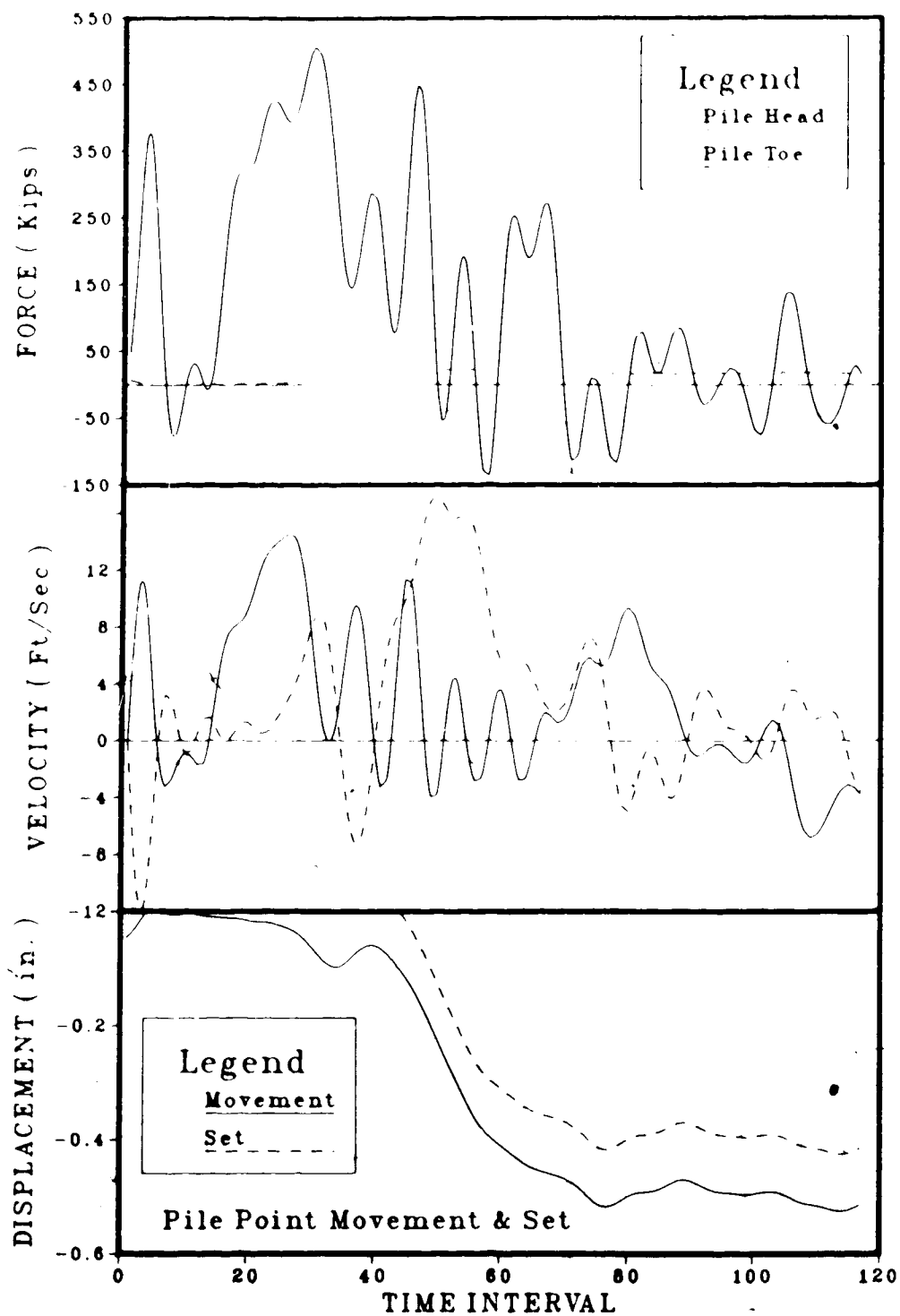


Figure 7.6 Maximum Stress in Pile Segments



#### 7.4 Test Pile No V11-9-22C Thornton Yard

The test pile selected was a 75ft long, 15-in. square precast concrete pile. The pile was driven to a depth of 57ft below ground level. The driving record indicates that 163 blows/ft were required during the last foot of driving. Pile was driven with a Vulcan-0 single-acting steam hammer. Details of driving record are given in the appendix C-3-B.

The subsurface stratigraphy (ref. Appendix C-3-A) indicates presence of 5ft thick sandy fill. This is followed by thick layers of peat and mixture of clay and silt upto a depth of 47ft below ground level. This is underlain by fine sand in medium to dense state of compaction. This sandy layer extends upto the depth of bore hole termination. Also, pile driving record indicates that there was little or no resistance to pile driving upto the depth of 45ft (2 to 8 blows/ft)

##### 7.4.1 Damping Parameters

Considering the relative density of sand presence from 47ft to the depth of penetration of the pile, effective internal friction angle of 36 degrees was assumed for selection of damping parameters. For sandy soils, the wall friction does not depend on velocity ( $J_s=0$ ) and point bearing depend on velocity. Analysis using Gibson & Coyle's approach was performed with pile point damping value of 0.88 sec/ft corresponding to  $\phi' = 36$  (see Figure (4.4)) and skin damping value of 0.001 sec/ft.



Damping parameters for Smith's approach were chosen from range of values. This method generally assumes that the damping values for cohesionless materials at pile point are three times of those in skin. Analysis using Smith's approach was performed with  $J_p = 0.20$  sec/ft for pile point and  $J_s = 0.06$  sec/ft for skin.

#### 7.4.2 Pile Capacity From Static Formula

Based on the subsurface stratigraphy and pile driving record, no shaft resistance was assumed upto a depth of 47ft. Also, ground water level was assumed at 5ft below ground level. The ultimate pile capacity from static formula was estimated by two different methods. The method using Berezantev's bearing capacity factor ( $N_q = 85$ ) corresponding to  $\phi' = 36$  resulted in an ultimate pile capacity of 270 kips with 87 percent of the total resistance acting at the pile point.

Second method is based on the correction factors recommended by Kishida (1967) for effect of pile driving in sand and the relationship between  $K_s \tan \phi'_a$  and angle of internal friction suggested by Meyerhof (1976). Use of this approach resulted in an ultimate pile capacity of 415 kips with 86 percent of the total resistance acting at the pile point.

#### 7.4.3 Pile Capacity From Load Test

The test pile was loaded to a maximum of 350 kips and the corresponding pile butt settlement was 0.44 inches. The load test was not taken to failure and the details of the load test were not sufficient to evaluate the pile capacity. The load settlement curve was extrapolated beyond 350 kips using Chin's method. However, ultimate capacity of pile was estimated using modified Van de Veen's method independent of extrapolated values.

Load settlement curve of the load test is given in Figures (7.8) & (7.9). From Figure (7.8), the Davisson limit load is estimated as 369 kips. Davisson limit load is influenced by the elastic modulus of the pile material from which it was made and in this case a value of 5000 ksi was used. Ultimate failure load according to Butler & Hoy's definition is 480 kips (see Figure (7.9)). Also, Figure (7.9) indicates an ultimate failure load of 520 kips according to Fuller & Hoy's definition.

Evaluation of load test results by modified Van de Veen's method is given in Figure (7.10). Use of this method resulted in an ultimate capacity of 450 kips. Chin's method of evaluation is given in Figure (7.11) and this method estimates the ultimate pile capacity as 656 kips.

#### 7.4.4 Wave Equation Analysis and Hiley's Formula

Results of the wave equation analysis are represented by curves in Figure (7.12) and (7.13): The analysis was

carried out assuming no shaft resistance upto a depth of 47ft below ground level and 86 percent of the total soil resistance acting at the pile point.

Bearing graph obtained using Smith's damping parameters indicates that the total soil resistance at 163 blows/ft is 552 kips. The analysis using Gibson & Coyle's damping parameters indicates total resistance of 404 kips at 163 blows/ft. In sandy soils no soil set-up is expected to occur. However, relaxation may be expected in dense fine grained sand. Hence, the ultimate pile capacity from Smith's and Coyle's approaches are 552 kips and 404 kips, respectively.

Results obtained from Hiley's dynamic formula are also plotted in Figures (7.12) & (7.13). This formula estimates the ultimate soil resistance as 301 kips at 163 blows/ft.

Maximum compressive stress in the pile corresponding to each design pile capacity is given as a function of blow count in Figure (7.12). Gibson & Coyle's method predicts slightly higher stress than Smith's method. As far as concrete piles are concerned, the development of stresses are of concern and in this case, the maximum compressive stresses predicted by Smith's and Coyle's methods during last foot of driving are 3500 psi and 3600 psi, respectively.

In addition to compressive stresses, maximum tensile stresses are also given as a function of blow count in Figure (7.13). This indicates high tensile stresses during

the initial stage of driving and reduces as the soil resistance increases. Maximum tensile stress during last foot of driving for Smith's and Coyle's methods are 320 psi and 470 psi, respectively.

Maximum compressive stress obtained in each pile segment is shown in Figure (7.14). Highest stress in the pile is located about 4 to 8ft from the toe of the pile. Figure (7.14) indicates, in both methods, the stress is fairly uniform (2500 psi) up to about 25ft and then gradually increases towards pile toe to about 3500 psi in Smith's method and 3600 psi in Gibson & Coyle's method.

Time dependent variables are given in Figure (7.15). High soil resistance at pile point (86%) results in low pile toe velocity and higher forces at pile toe. This condition is reflected in force and velocity diagrams. Also, variation of force with time interval indicates (Figure (7.15)) very high force in pile toe at the time of termination of computations.

#### 7.4.5 Summary

Wave equation analysis using Gibson & Coyle's method predicted ultimate static bearing capacity of 404 kips which is about 9.5% higher than Davisson limit load and about 11% lower than Van de Veen's failure load. However, Smith's method predicted about 15% higher than Butler & Hoy's failure load and 6% higher than Fuller & Hoy's failure load.

Static bearing capacity predicted by Smith's method is 37% higher than that of Gibson & Coyle's method. Generally stress measurements are made close to the pile head. In this case maximum compressive stress as well as tensile stress are located close to the pile toe. Analysis of this nature will help to plan the location of the stress measurement and also to avoid any pile damage close to the pile toe.

Ultimate pile capacity estimated using the recommendations of Kishida (1967) and Meyerhof (1976) is 415 kips and this is within close range of pile capacities obtained from load test. This may be due to the fact that their recommendations take into account of the changes that take place during pile driving in sand.

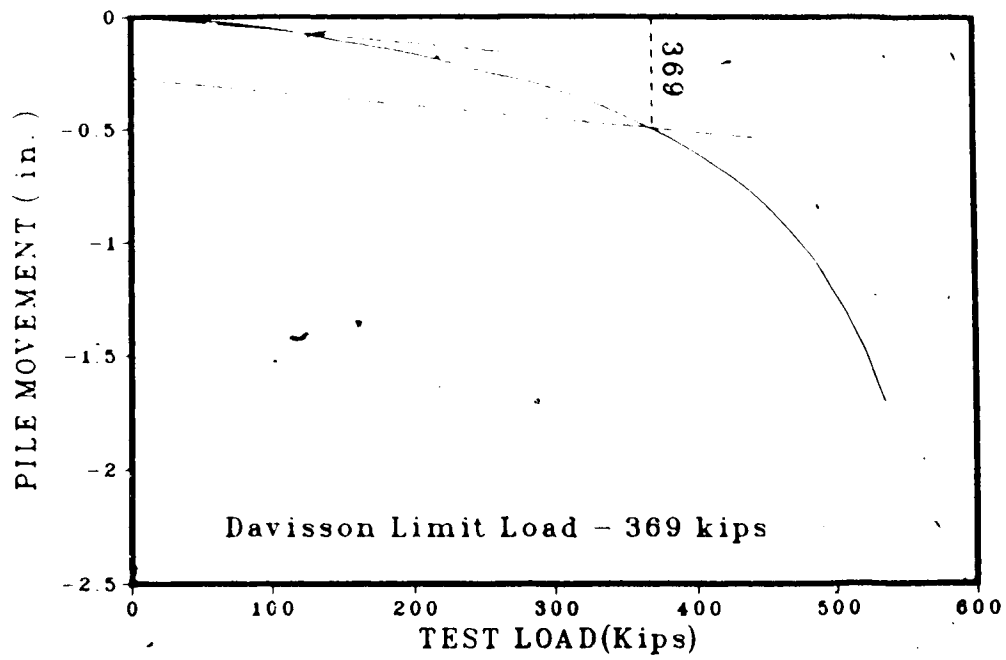


Figure 7.8 Construction of Davisson Limit Load

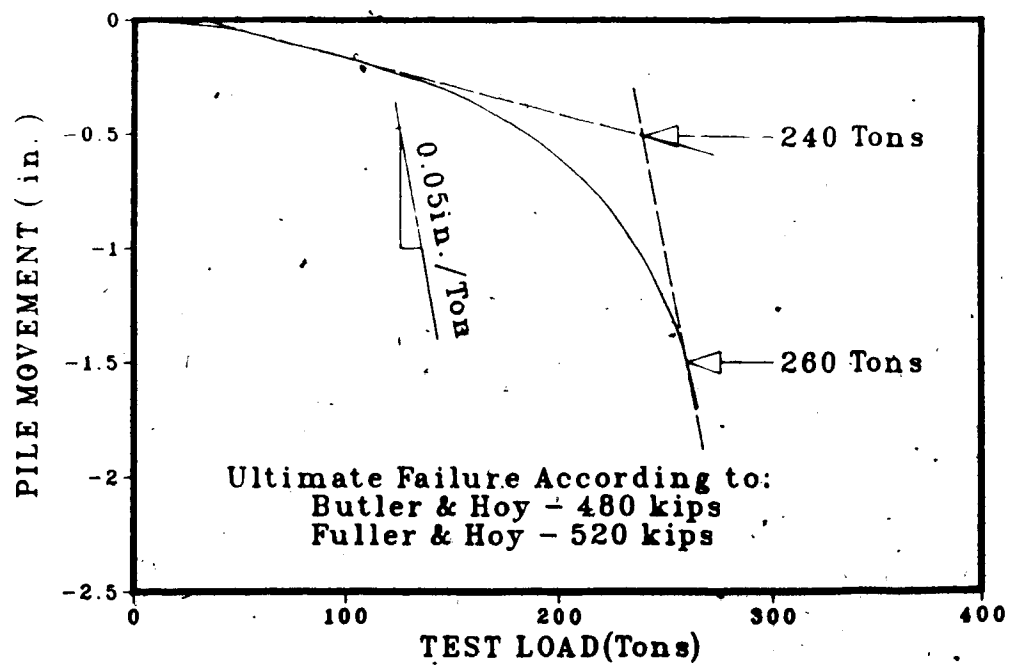


Figure 7.9 Failure Loads According to Butler & Hoy and Fuller & Hoy

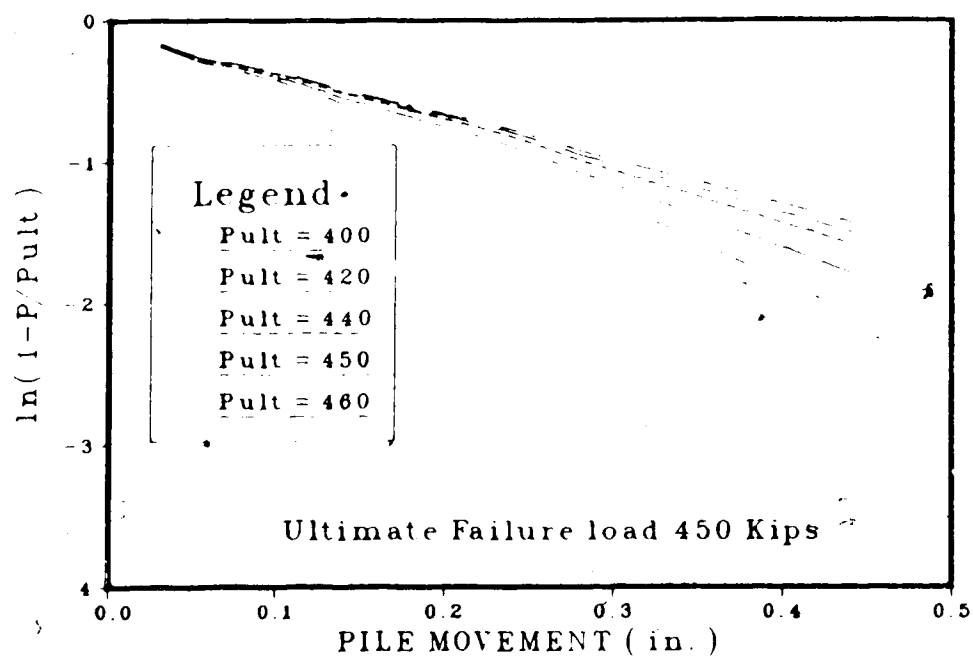


Figure 7.10 Construction of Failure Load According to Van de Veen

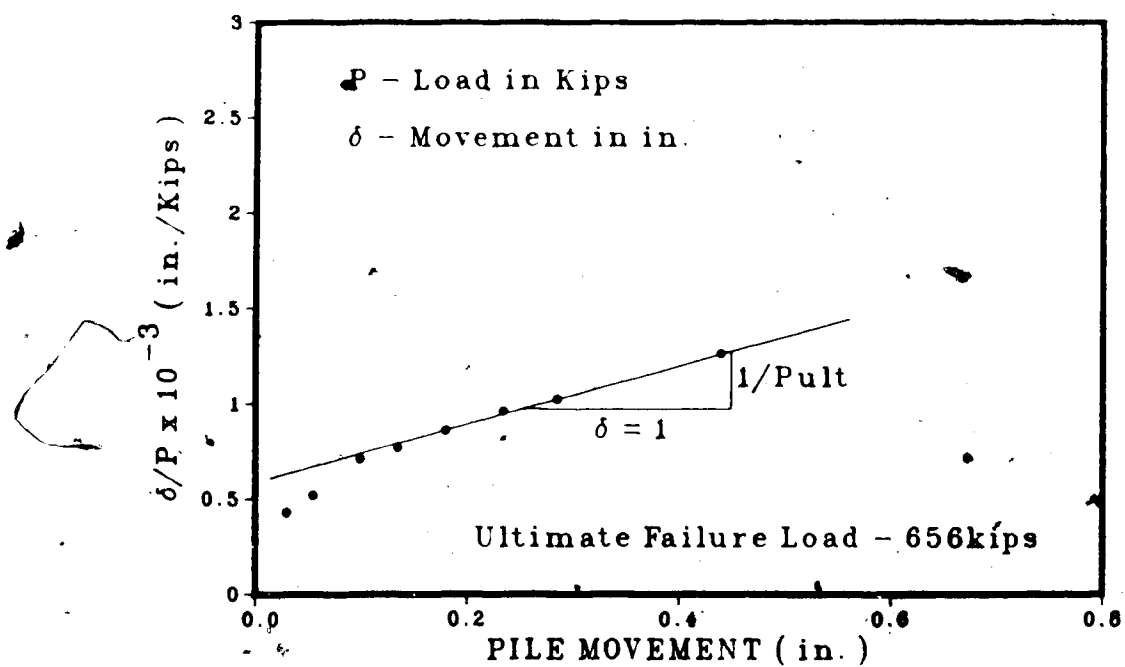


Figure 7.11 Construction of Failure Load According to Chin

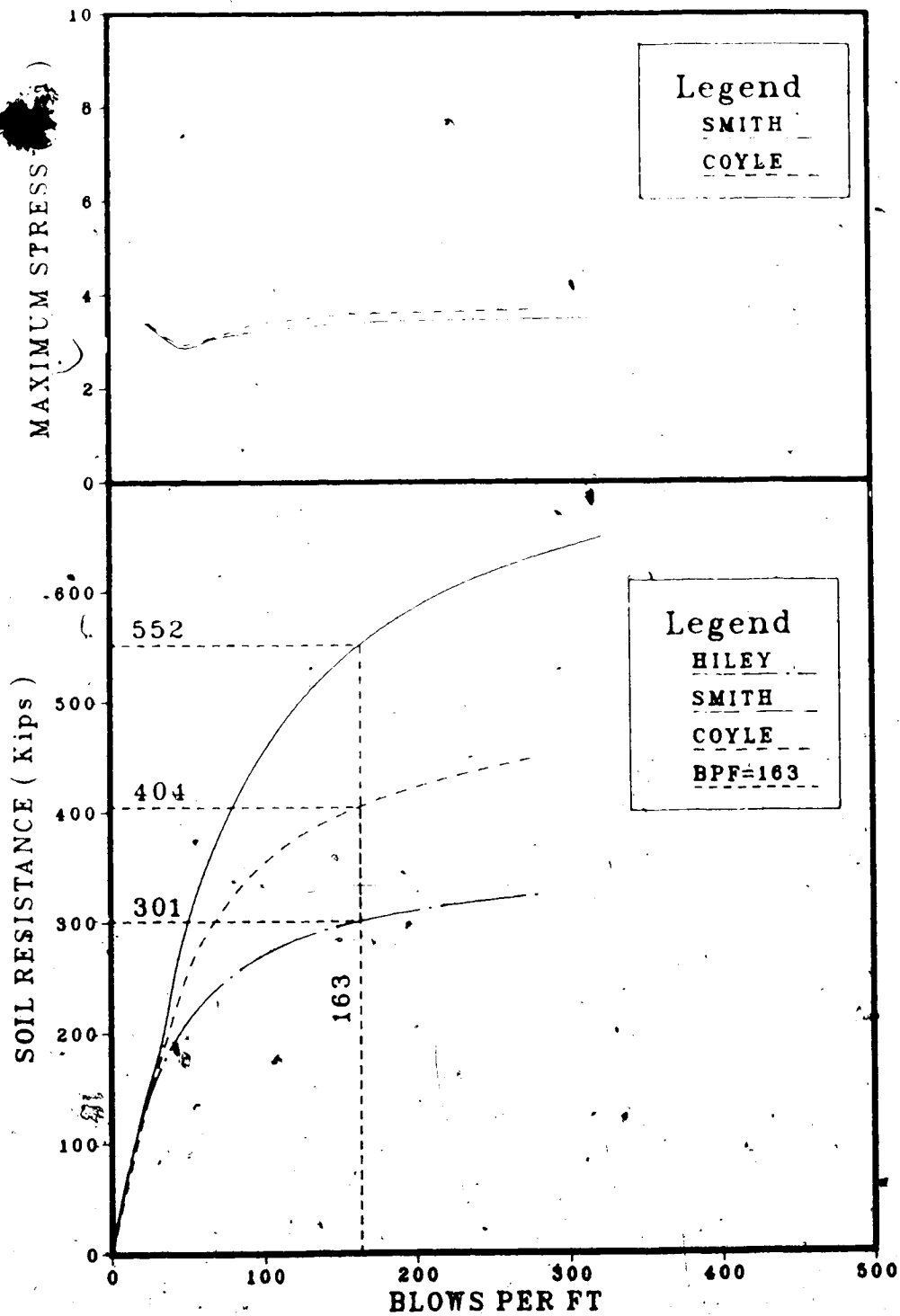


Figure 7.12 Bearing Graphs for Blow Count and Maximum Stress



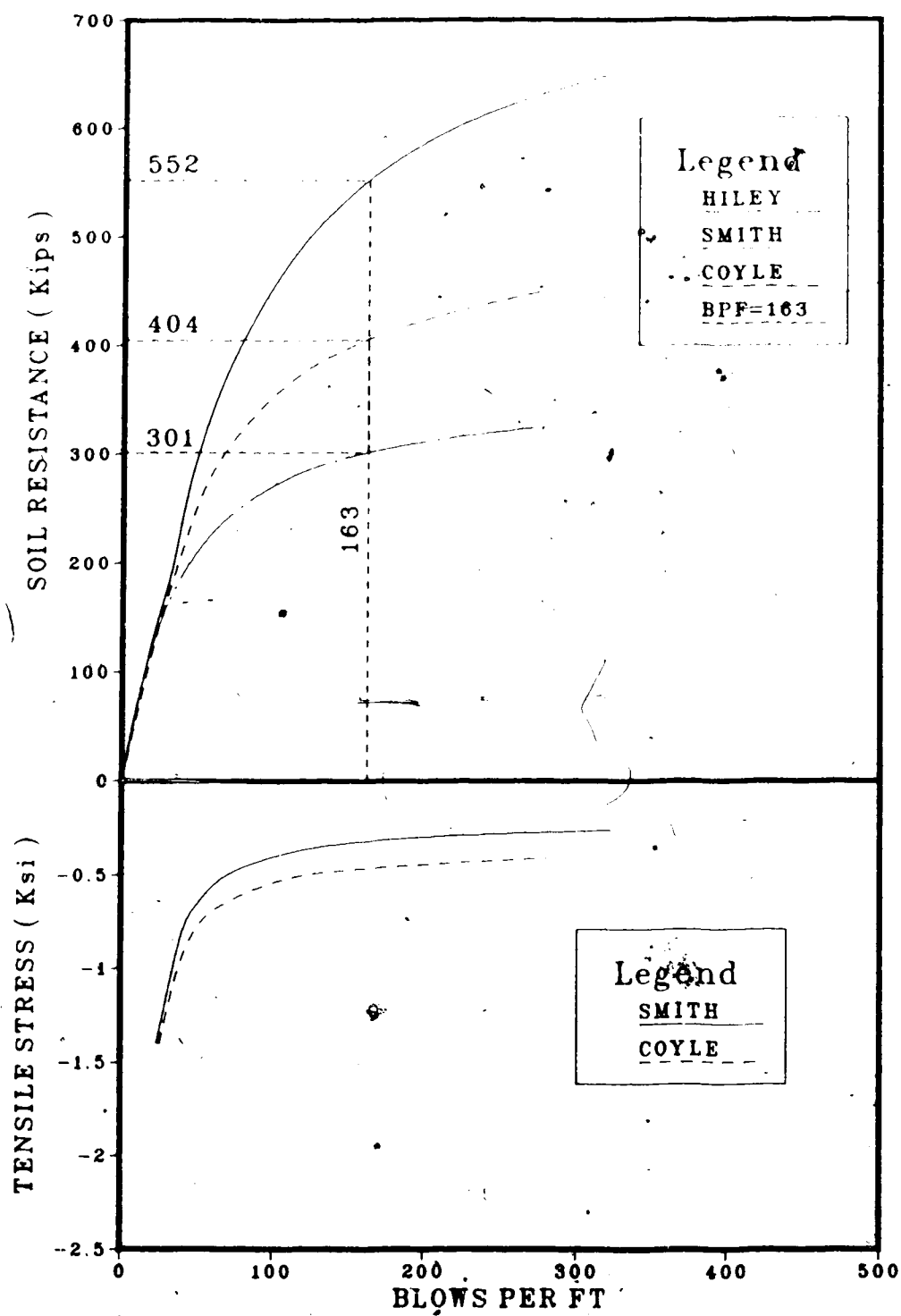


Figure 7.13 Bearing Graphs for Blow Count and Maximum  
Tensile Stress

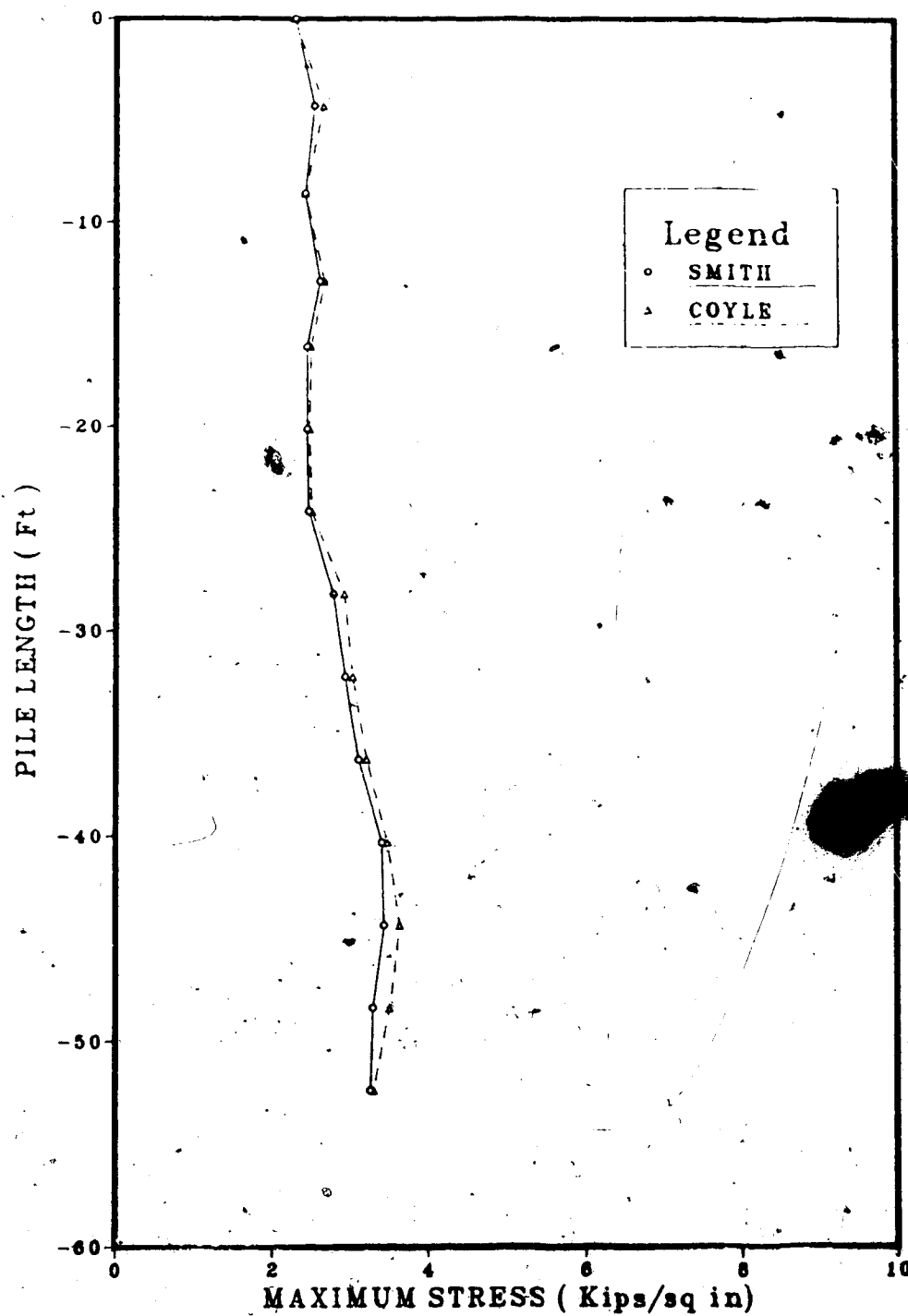


Figure 7.14 Maximum Stress in Pile Segments

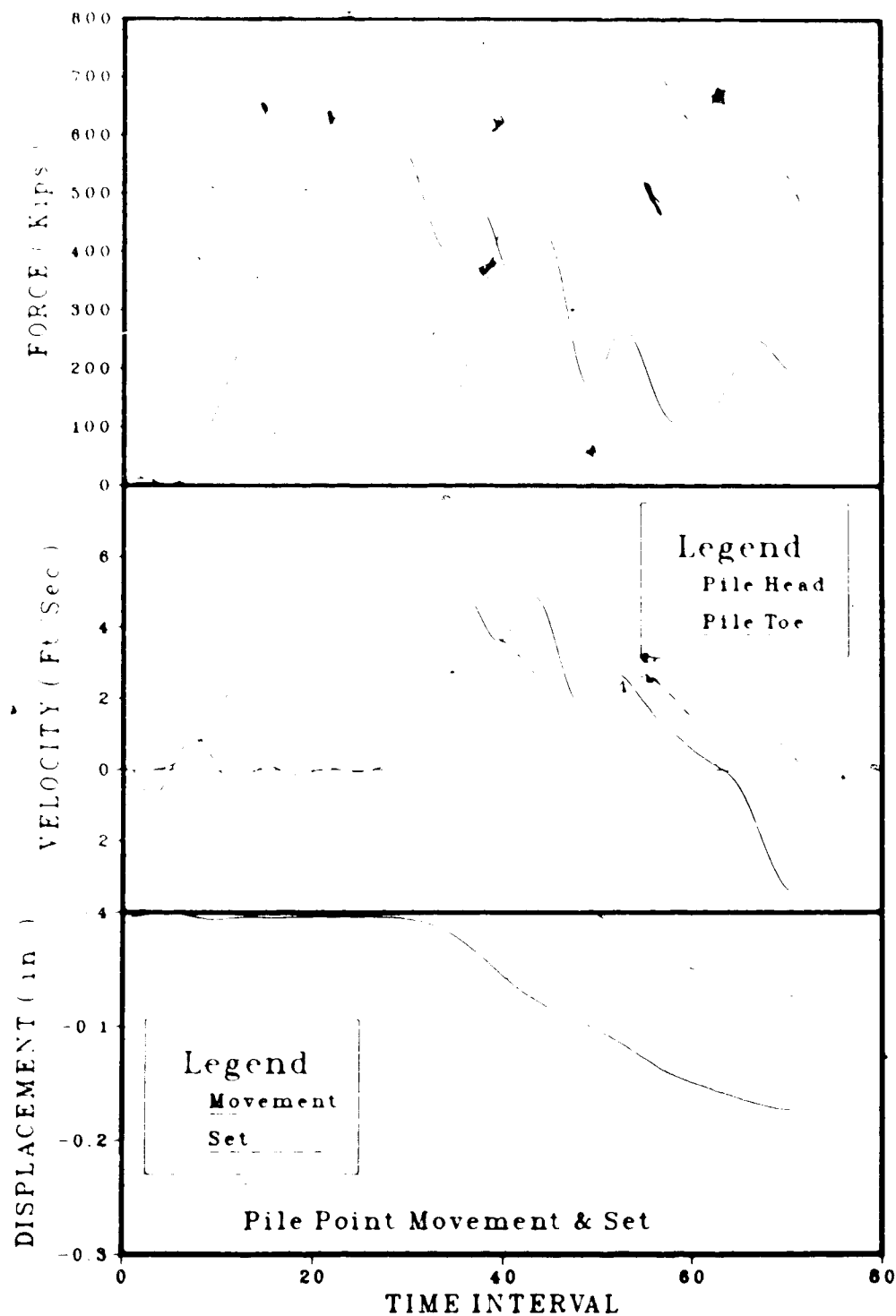


Figure 7.15 Variation of Force, Velocity and Displacements  
with Time Interval

### 7.5 Test Pile at M.6.6, Fraser Subdivision

The test pile selected for this project was a 60ft long LBPB3 (W12x53) H pile with 50ft of penetration into the ground. The pile was driven with a Link Belt LB 312 diesel hammer. The driving record from the field test indicated 36 blows ft were required during the last foot of driving. Pile driving records are given in the appendix C 4 B.

Bore hole informations include in situ as well as remoulded vane shear stress, natural moisture content at every 5ft depth interval and Atterberg limits at 5ft and 40ft depth below ground level. Detail informations are given in the appendix C 4 A.

The bore hole data indicate presence of very soft organic clay upto a depth of 10ft below ground level. Moisture content of this strata is in the range of 70% and the vane shear strength is in the range 940lb/sq ft. This organic clay layer is followed by stiff to very stiff clay which extends beyond the depth of pile penetration. In situ vane shear strength of this layer varies between 2470lb/sq ft and 3060lb/sq ft and remoulded strength varies between 530lb/sq ft and 820lb/sq ft. Natural moisture content of this clay layer varies between 27% and 45%.

Atterberg limits are available only at two locations (15ft & 40ft) as such proper assessment of clay type (CH or CL) is very difficult. Sensitivity of clay was calculated from vane shear test results. Sensitivity of clay presence below 10ft depth varies between 3.0 and 4.8 with an average

value of 4.1. This may be classified as low to medium sensitive clay.

#### 7.5.1 Damping Parameters and Set-Up Factor

Inadequate informations to assess the clay type impose greater difficulty in choosing damping parameters for Gibson and Coyle's method. Liquidity index at 15ft and 40ft depth are 0.50 and 0.36, respectively. Considering the variation of liquidity index with depth and the nature of clay presence at this site (CH & CL), lower limit of the damping values correspond to the liquidity indexes were chosen. Damping parameter of 0.95 sec/ft for skin and 0.70 sec/ft for pile point were used in the analysis.

In Smith's approach, damping forces are distributed proportional to the static resistance. Damping parameters for this method were chosen from range of values. Damping values of 0.20 sec/ft for skin and 0.04 sec/ft for pile point were selected for the analysis.

Informations about the soil set-up factor of the soil or redriving records of the test pile are not available to estimate the static bearing capacity. However, the results published by Cooke, et.al (1979) based on tests carried out on jacked piles in london clay with compressive load testing indicate that the percentage of increase in pile capacity with time vary between 20% and 50%. Considering the type of clay presence at this test site, a soil set-up factor of 1.4 is assumed to estimate the static bearing capacity of the

pile.

#### 7.5.2 Pile Capacity From Static Formula

The pile driving record indicates no resistance to penetration upto a depth of 10ft. Considering the resistance to driving and presence of organic clay upto 10ft depth, no shaft resistance was assumed upto a depth of 10ft from ground level. For purposes of estimating the pile capacity, it was assumed that the unconfined compression strength is equal to one half of vane shear strength.

The ultimate static bearing capacity of pile based on static formulae was estimated using two different failure modes of shaft.

- 1) The development of the limiting pile-soil shear strength along the entire surface area of the pile. Use of this mode of failure resulted in an ultimate pile capacity of 106 kips with 1.5% of the total resistance acting at the pile point.
- 2) The development of the limiting pile-soil shear strength along the outer parts of the flanges, plus the development of the full shear strength of the soil along the plane joining the tips of the flanges (ie, the soil with in the outer boundaries of the pile effectively, forms part of the pile shaft). Estimation of ultimate pile capacity using this mode of failure gave 156 kips with 9% of the total resistance acting at the pile point.

### 7.5.3 Pile Capacity From Load Test

The test pile was loaded to a maximum of 195 kips and the corresponding pile butt movement was 1.79 inches. The load settlement curve of the load test is shown in Figures (7.16) & (7.17). From Figure (7.16), the Davisson limit load was estimated as 159 kips. Estimation of ultimate failure load according to Butler & Hoy and Fuller & Hoy are shown in Figure (7.17). Ultimate failure load according to Butler & Hoy is 150 kips and according to Fuller & Hoy is 172 kips.

Van de Veen's method of estimating ultimate failure load is shown Figure (7.18) and this method gave an ultimate failure load of 150 kips. Use of Chin's method resulted in an ultimate failure load of 214 kips (see Figure (7.19)).

### 7.5.4 Wave Equation Analysis and Hiley's Formula

The analysis was carried out for the total length of the pile (60ft) that was in leads during driving. Computer run was made for both modes of failure those were discussed in Section 7.5.2. No soil resistance was assigned to the pile segments within 20ft from the pile head and rest of the pile segments were assigned based on the skin friction obtained from static formulae.

Bearing graphs obtained using Smith's damping parameters are given in Figure (7.20). Results of both failure modes are almost identical. From Figure (7.20), for both failure modes, the total soil resistance at 36 blows/ft is 115 kips. Assuming a soil set-up factor of 1.4, the

predicted ultimate bearing capacities for failure modes 1 and 2 are computed as  $115 \times 0.985 \times 1.4 + 115 \times 0.015 = 160$  kips and  $115 \times 0.91 \times 1.4 + 115 \times 0.09 = 157$  kips, respectively.

Results of wave equation analysis using Gibson & Coyle's damping parameters are shown in Figure (7.21). In this method the bearing graphs deviate from each other as the soil resistance increases. However, both failure modes predicted total soil resistance of 107 kips at 36 blows/ft. The ultimate static bearing capacities are computed as  $107 \times 0.985 \times 1.4 + 107 \times 0.015 = 149$  kips and  $107 \times 0.91 \times 1.4 + 107 \times 0.09 = 146$  kips, respectively.

Results obtained from Hiley's formula are shown in Figures (7.20) & (7.21). This formula estimates an ultimate soil resistance of 205 kips at 36 blows/ft.

Maximum stress in the pile is given as a function of blow count. Smith's method predicts about 31.5 ksi at 36 blows/ft and Gibson & Coyle's method predict it as 32.5 ksi. Maximum stress in each pile segment is given in Figure (7.22). It can be noticed that the maximum stress close to the pile head reduces upto 15ft as there is no soil resistance and beyond this length, it fluctuates as the skin friction varies.

Time dependent variables such as force, velocity and displacement are given in Figure (7.23). As expected, pile toe has high velocity and low force. Pile head force as well as velocity increase initially until the ram impact is made and then the force and velocity varies according to the



reflected stress waves.

#### 7.5.5 Summary

Smith's method predicted ultimate static bearing capacities of 160 kips and 157 kips for failure modes 1 and 2, respectively. Gibson & Coyle's method predicted 149 kips and 146 kips, respectively. Davisson limit load, Butler & Hoy and Van de Veen ultimate failure loads are in the range of 150 to 159 kips. In clay soils, proper assessment of soil set-up factor is very essential. Also, ultimate bearing capacity estimated from static formula using second failure mode (156 kips) is within the range of failure loads obtained from load test.

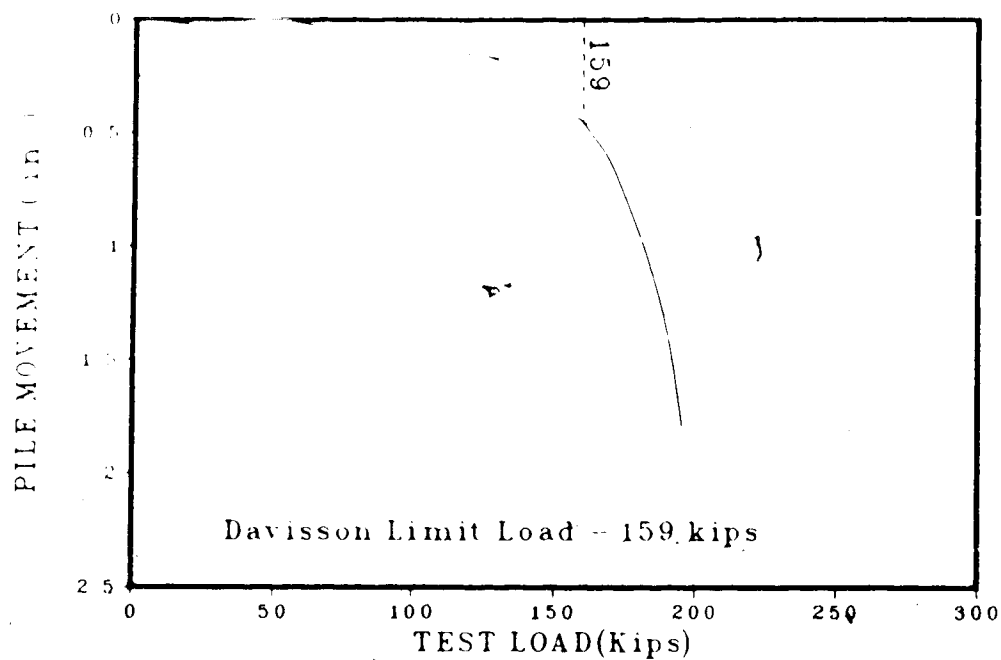


Figure 7.16 Construction of Davisson Limit Load

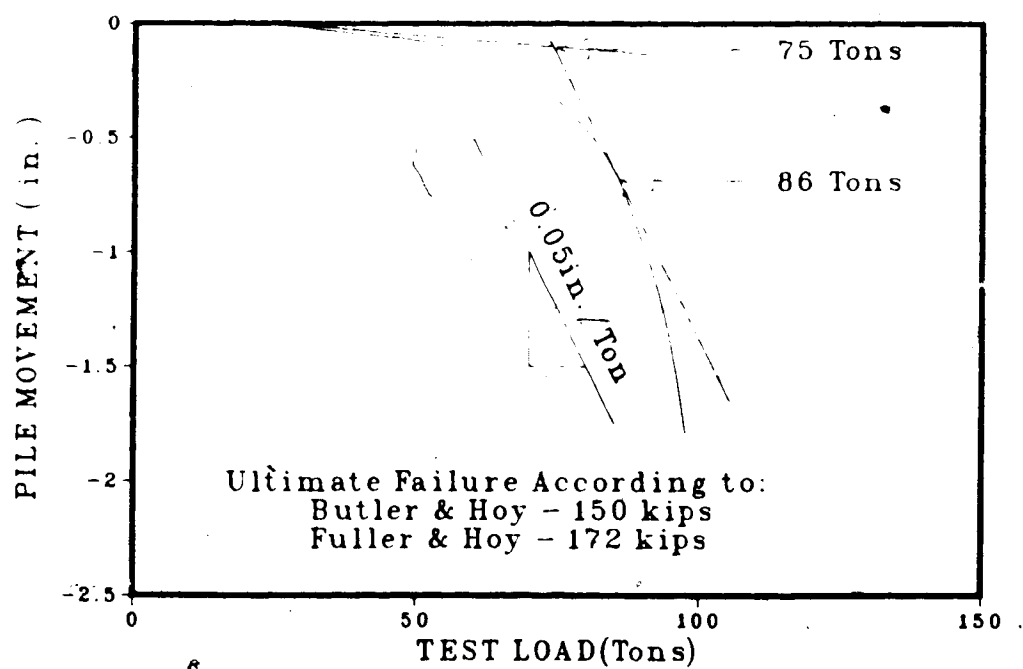


Figure 7.17 Failure Loads According to Butler &amp; Hoy and Fuller &amp; Hoy

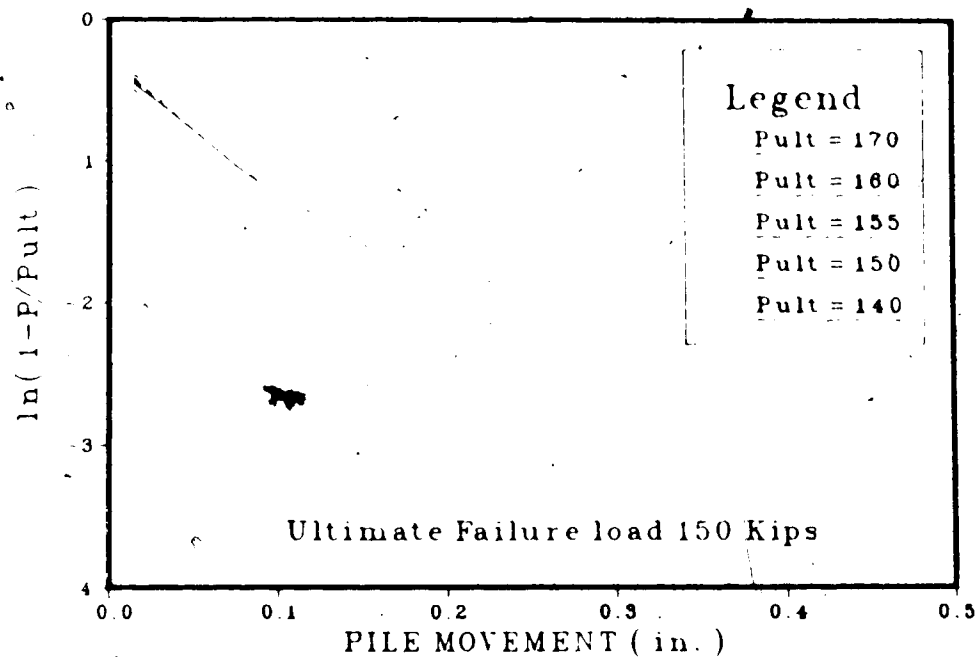


Figure 7.18 Construction of Failure Load According to Van de Veen

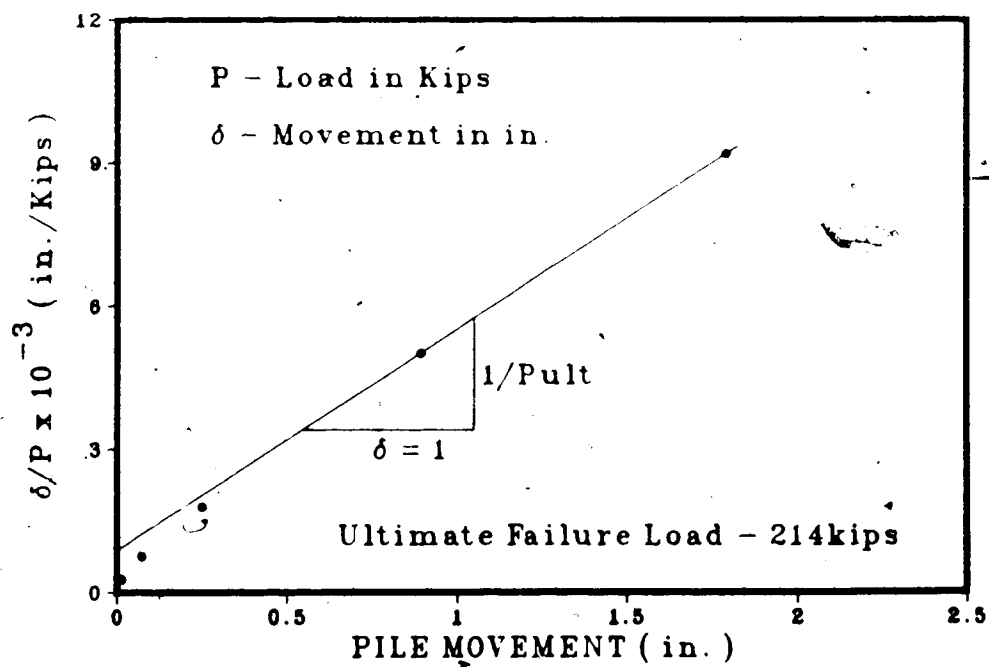


Figure 7.19 Construction of Failure Load According to Chin

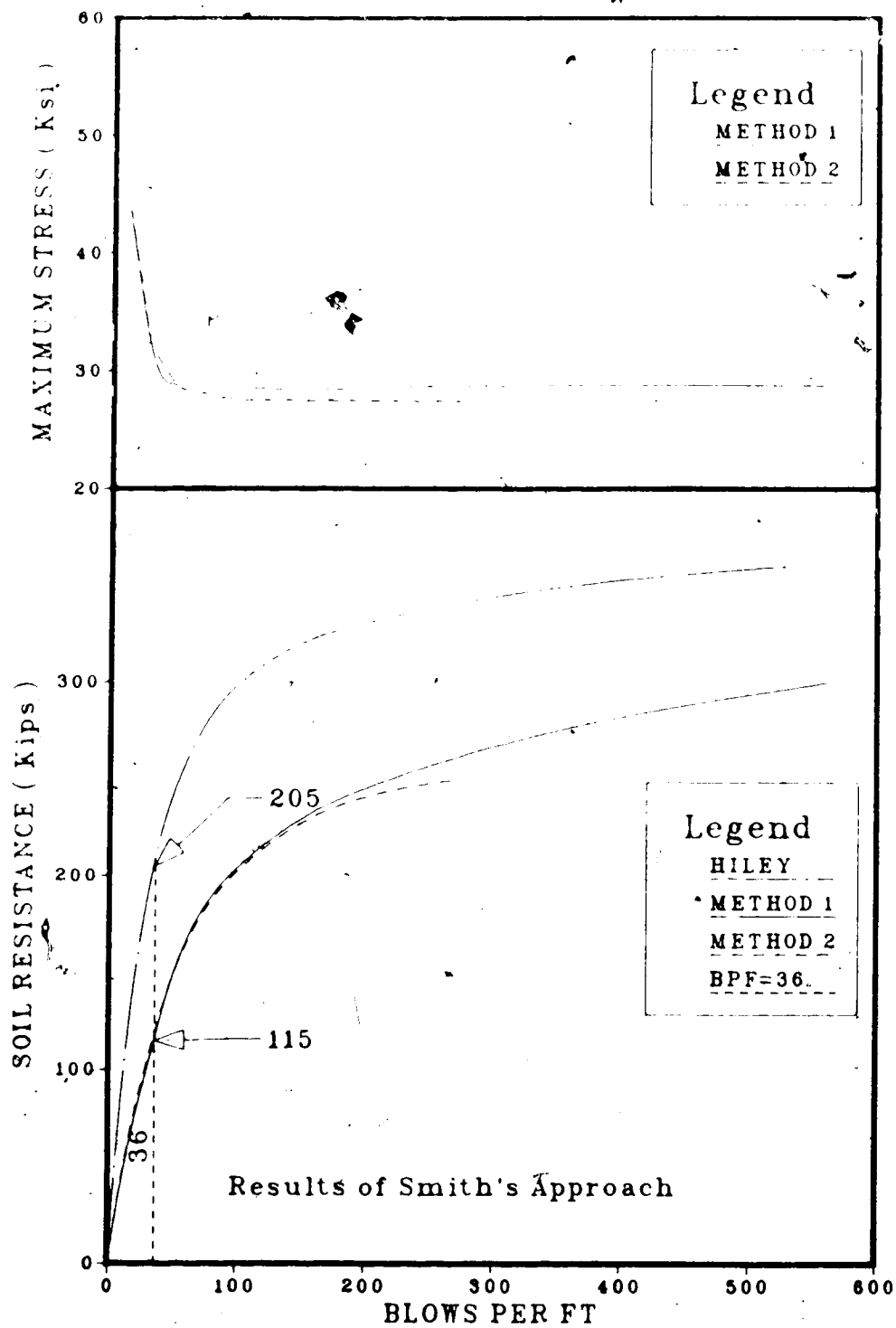


Figure 7.20 Bearing Graphs for Blow Count and Maximum Stress

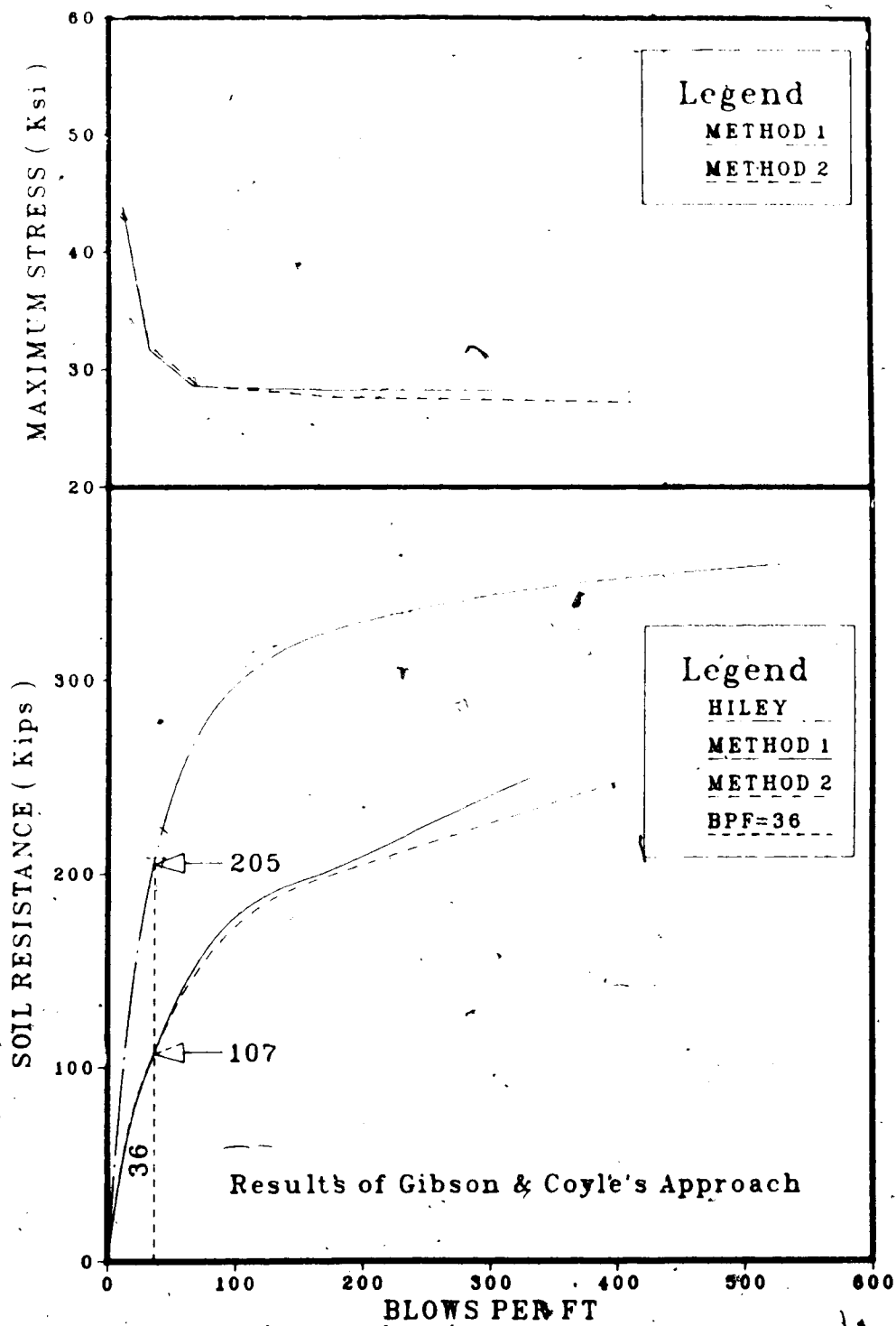


Figure 7.21 Bearing Graphs for Blow Count and Maximum Stress

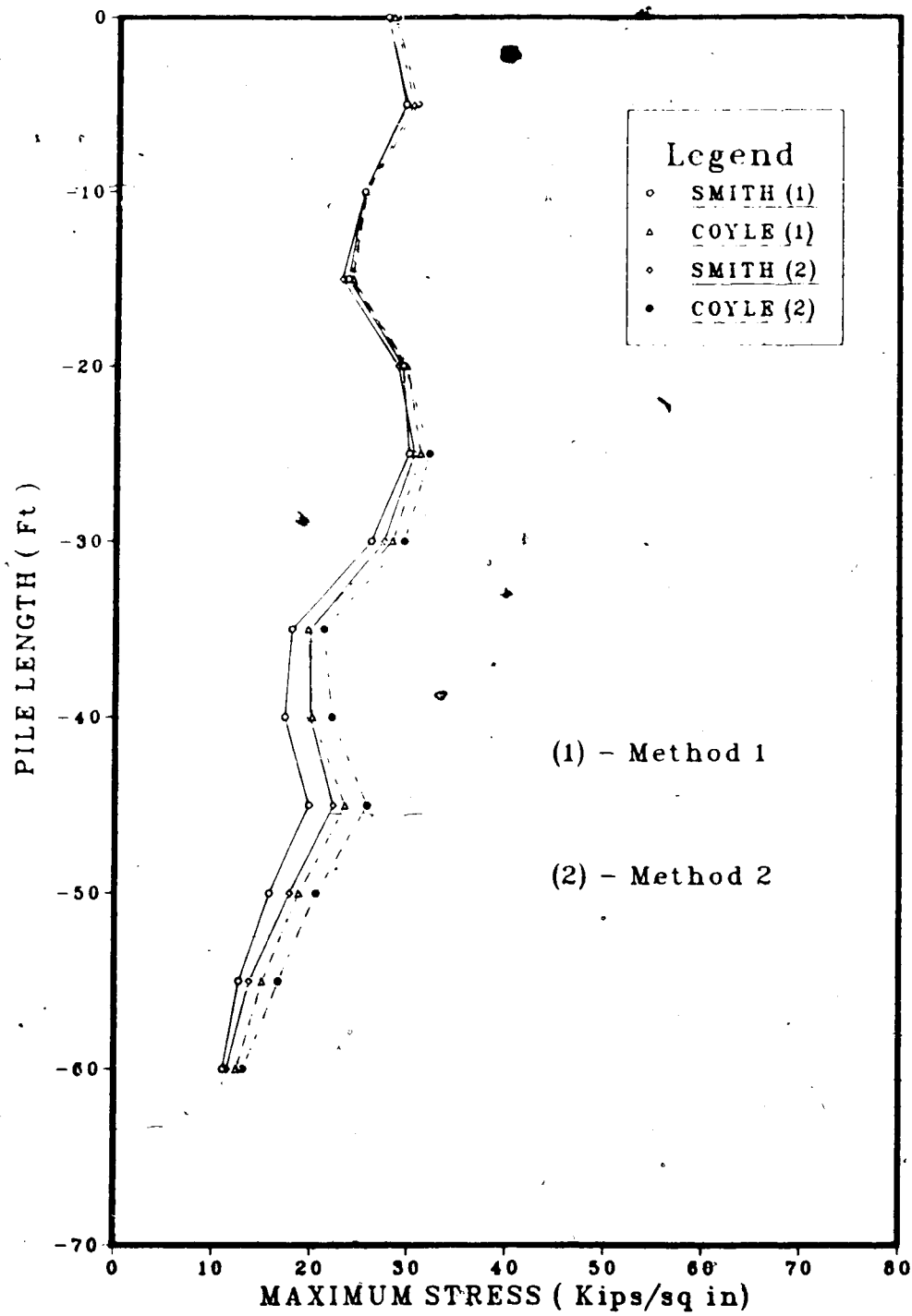


Figure 7.22 Maximum Stress in Pile Segments

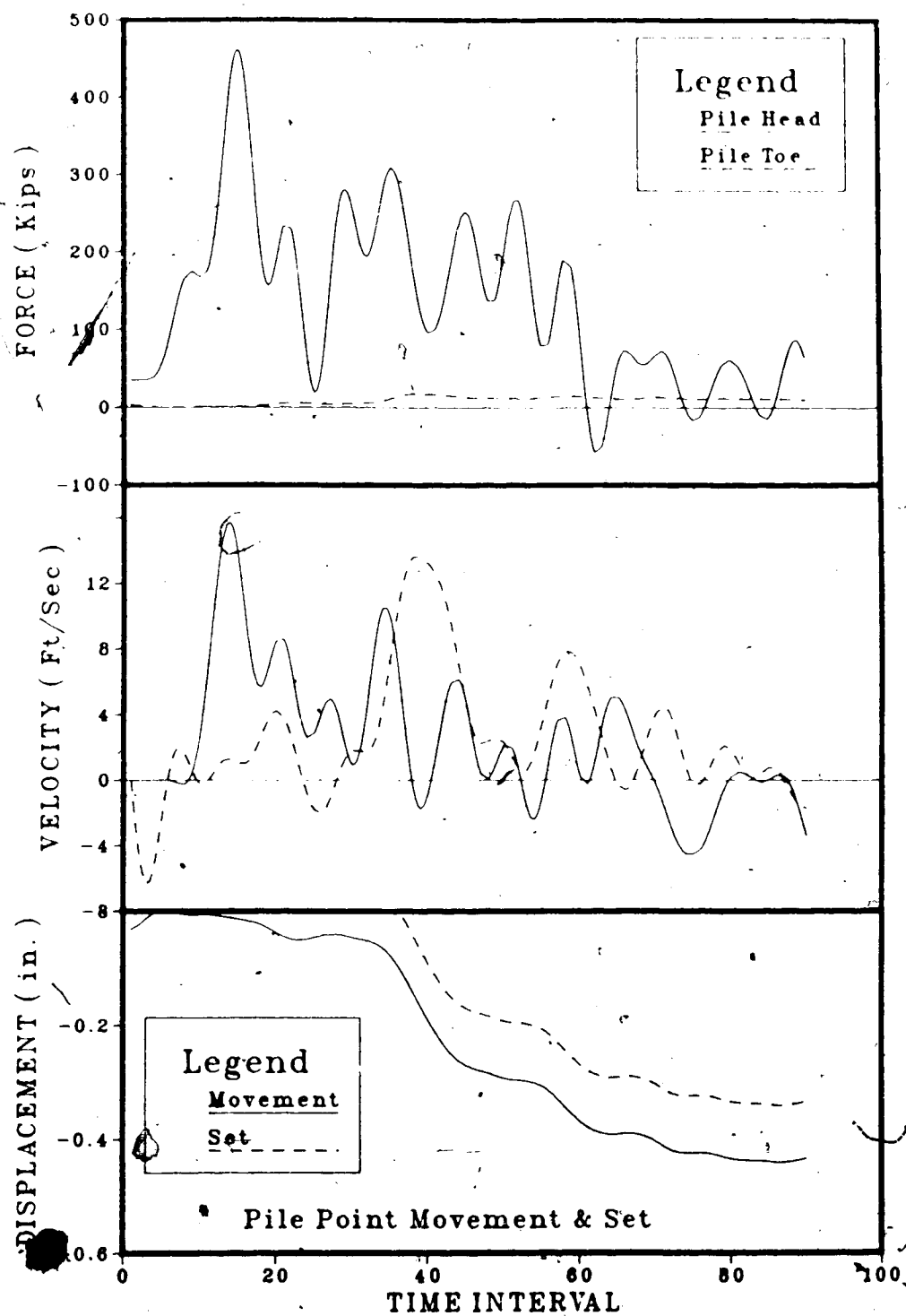


Figure 7.23 Variation of Force, Velocity and Displacements  
with Time Interval

### 7.6 Test Pile No. U, Research Project Report

Test pile selected was a 10.75 in. diameter, 0.23 in. wall thickness, closed end 5ft long steel pipe pile. A pile analyzer was used to monitor the stress in the pile during driving. The analyzer monitoring showed that the driving stresses at refusal were about 30 ksi. Drop hammer with ram weight 620 lbs and height of fall 3ft was used to drive the pile. The driving resistance at the time of termination was 2 blows/inch (84 blows/ft).

The soil profile at test site is given in the appendix C.5.A. Standard penetration tests were carried out at every 5ft interval up to a depth of 25ft and beyond this depth, the test was conducted at every 10ft interval. Bore hole data indicates presence of grey silty sand in loose to medium state of compaction upto a depth of 36ft. The N values in this layer varies between 10 and 35. This layer is underlain by mixture of sand and gravel in dense state of compaction. This layer extends upto a depth of 45ft and N value in this strata ranges from 39 to refusal. Bore hole was terminated at 80ft depth in very dense sandy layer which contains gravel and cobbles.

#### 7.6.1 Damping Parameters

The blow counts derived from the standard penetration test are a means by which the angle of internal friction of sand may be assessed. Pile passes through medium dense sand and the toe is founded in dense sand. An internal friction



angle of 36 degrees was assumed up to the depth of 34 ft below ground level. Beyond this depth a corresponding value of 40 degrees was assumed.

In sandy soil wall friction does not depend on velocity ( $\alpha = 0$ ) but point bearing depends strongly on velocity. A damping value of 0.588 sec/ft corresponding to  $\phi' = 40$  for pile point was used in Gibson & Coyle's method of analysis.

Smith's method generally assumes that the damping values for cohesionless materials at pile point are three times of those in friction. Damping parameters of 0.15 sec/ft for pile point and 0.05 sec/ft for skin were assumed in the analysis.

#### 7.6.2 Pile Capacity From Static formula

The static bearing capacity from static formula was estimated by two different methods. The method using Berzantev's bearing capacity factor ( $N_q = 137$ ) corresponding to  $\phi' = 40$  degrees and values suggested by Tomlinson (1977) for earth pressure coefficient ( $K_a = 1.0$ ) and angle of wall friction ( $\delta = 20$ ) resulted in an ultimate pile capacity of 205 kips with 83% of the total resistance acting at the pile point.

Second method is based on the critical depth approach and the relationship between  $K_s \tan \phi'_a$  and  $\phi'$  suggested by Vesic (1967). Use of this approach resulted in an ultimate pile capacity of 317 kips with 75% of the total resistance acting at the pile point.

### 7.6.3 Pile Capacity From load Test

The test pile was loaded to a maximum of 160 Tons and the corresponding butt settlement was 1.10 inches. When the pile was unloaded, the pile head rebound by 0.40 inches. The corresponding load settlement curve is shown in Figures (7.24) & (7.25). From Figure (7.25), ultimate failure load according to Butler & Hoy is 302 kips and failure load according to Fuller & Hoy is 320 kips. Davisson limit load from Figure (7.24) was estimated as 258 kips.

Van de Veen's method of estimating the ultimate failure load from the load test is shown in Figure (7.26). This figure indicates the ultimate failure load as 336 kips. Use of Chin's method resulted in an ultimate failure load of 420 kips (see Figure (7.27)).

### 7.6.4 Wave Equation Analysis and Hiley's Formula

Percentage of load at pile point was assumed 79% for the analysis. Damping parameters appropriate to sandy soils recommended to use with Smith's as well as Gibson & Coyle's method were used in the analysis. Bearing graphs obtained from these analysis are given Figure (7.28).

Analysis using Smith's damping parameters gave total soil resistance of 247 kips at 84 blows/ft. Bearing graph obtained using Gibson & Coyle's damping parameters indicates total soil resistance of 220 kips at 84 blows/ft. In sandy soils, depending on its structure and relative density relaxation may be expected but no freezing. Therefore, the

ultimate static bearing capacities from Smith's and Coyle's methods are 247 kips and 220 kips, respectively.

The bearing graph obtained from Hiley's formula is also shown in Figure (7.28). This formula predicted an ultimate soil resistance of 321 kips at 84 blows ft.

Maximum stress in the pile is given as a function of blow counts in Figure (7.28). This indicates that the stresses predicted by Gibson & Coyle's approach is considerably higher than the stresses predicted by Smith's method. Stresses close to the pile head predicted by Smith's and Coyle's method during the last foot of driving are 41.5 ksi and 44.5 ksi, respectively. These values are about 38% and 48% greater than the stress measured by the analyser monitoring. Stresses obtained at every 4ft interval are given in Figure (7.29). This indicates higher stresses close to the pile head and reduces slightly towards the toe. However, the reduction is not appreciable and the stress at toe is almost equal to the stress at the pile head.

Variation of force and velocity of pile head and toe at time interval are given in Figure (7.32). Also, displacement and permanent set of pile toe are given in this figure. It can be noticed that the velocity of pile head and force increase gradually until the ram impact is made and then the force diagram varies with time, depending on the soil resistance. Velocity diagram of pile toe and head as well as pile toe displacement diagram indicate that very little penetration is achieved and this results in higher

stresses in the pile.

Considering the wide variation between the predicted pile capacity and the bearing capacities evaluated from the load test results and presence of gravel at the founding level of the pile toe, analysis was repeated with damping values lower than the values used for sandy soil.

There are no proven damping values available for gravel. However, Goble et al. (1976) recommended values in the range of 0.05 to 0.10 sec/ft for Smith's method. As explained before, in sandy soil wall friction does not depend on velocity. After several trial runs, a damping value of 0.30sec/ft for pile point was used in Gibson & Coyle's method of analysis. A damping value of 0.05sec/ft for skin as well as for pile toe was used in Smith's method of analysis.

Bearing graphs obtained from the second set of computer runs are given in Figure (7.30). Analysis using Smith's method gave a total soil resistance of 276kips at 84blows/ft. Bearing graph obtained from Gibson & Coyle's method indicates total soil resistance of 243kips at 84blows/ft. Also, Figure (7.30) indicates that the stresses predicted by both methods are very close compared to the results of the previous analysis.

Stresses obtained at every 4ft interval during the last foot of driving are given in Figure (7.31). Stresses close to the pile head predicted by Smith's and Coyle's methods during the last foot of driving are 41.6ksi and 42.8ksi,

respectively. These values are 38% and 42% greater than the stress measured by the analyser monitoring.

#### 7.6.5 Summary

Ultimate static bearing capacities predicted by Smith's method in the first and second set of runs are 247kips and 276kips, respectively. Gibson & Coyle's method predicted 220kips and 243kips. Ultimate bearing capacity predicted by Smith's method in the second run is 16% lower than Fuller & Hoy's failure load compared to 30% in the first set of run. In Gibson & Coyle's method, the ultimate bearing capacity corresponds to 0.30sec/ft is 6% lower than Davisson limit load compared to 17% corresponds to the damping value of 0.588sec/ft. Both methods predicted stresses higher than the analyser monitoring showed. However, in Gibson & Coyle's method, stress predicted in the second run is 6% lower than that of first run.

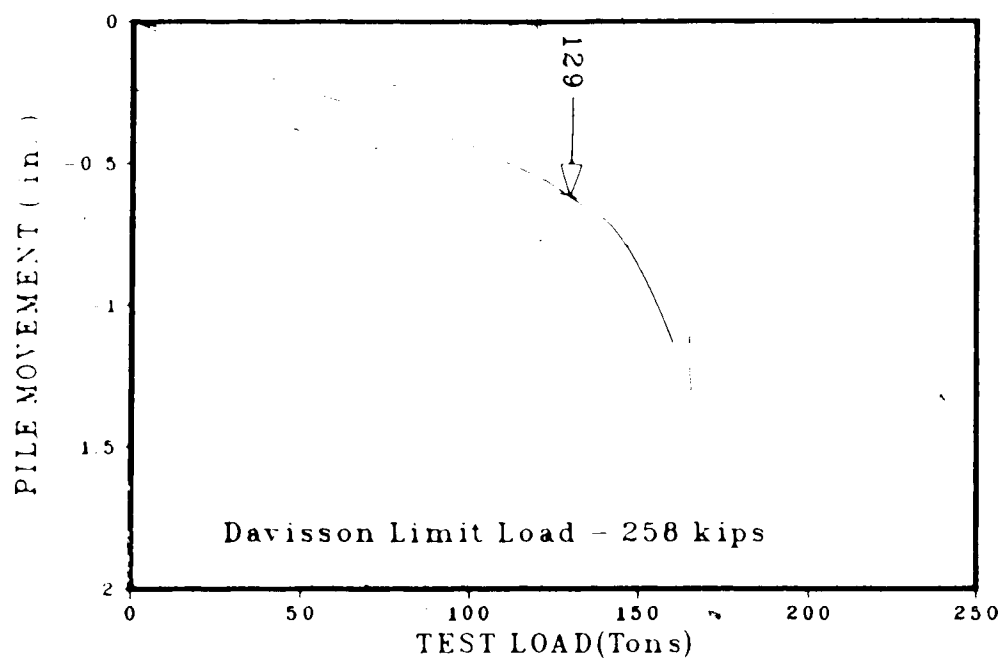


Figure 7.24 Construction of Davisson Limit Load

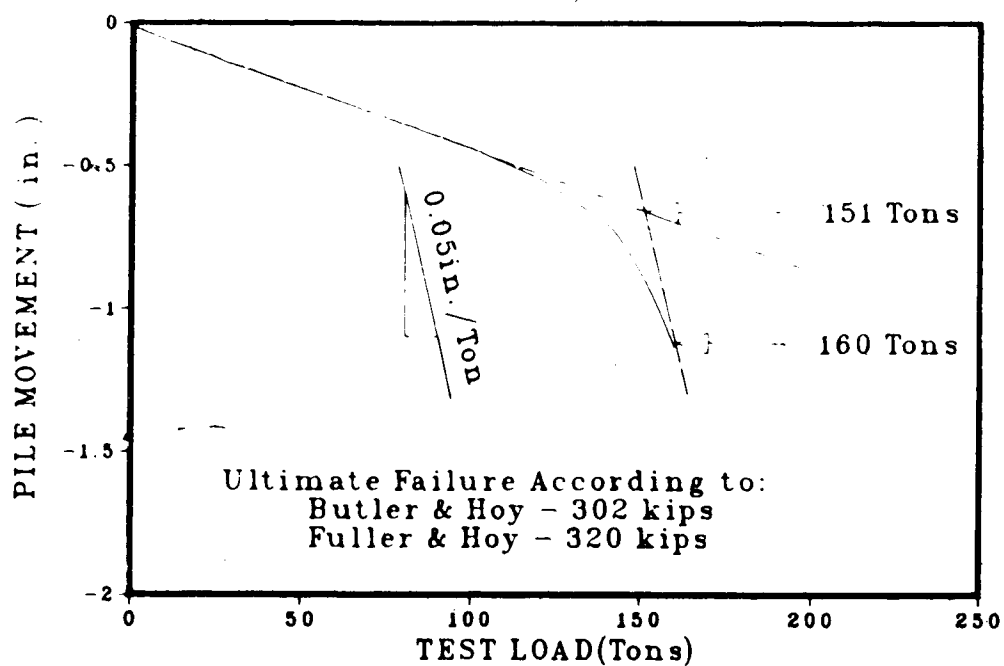


Figure 7.25 Failure Loads According to Butler & Hoy and Fuller & Hoy

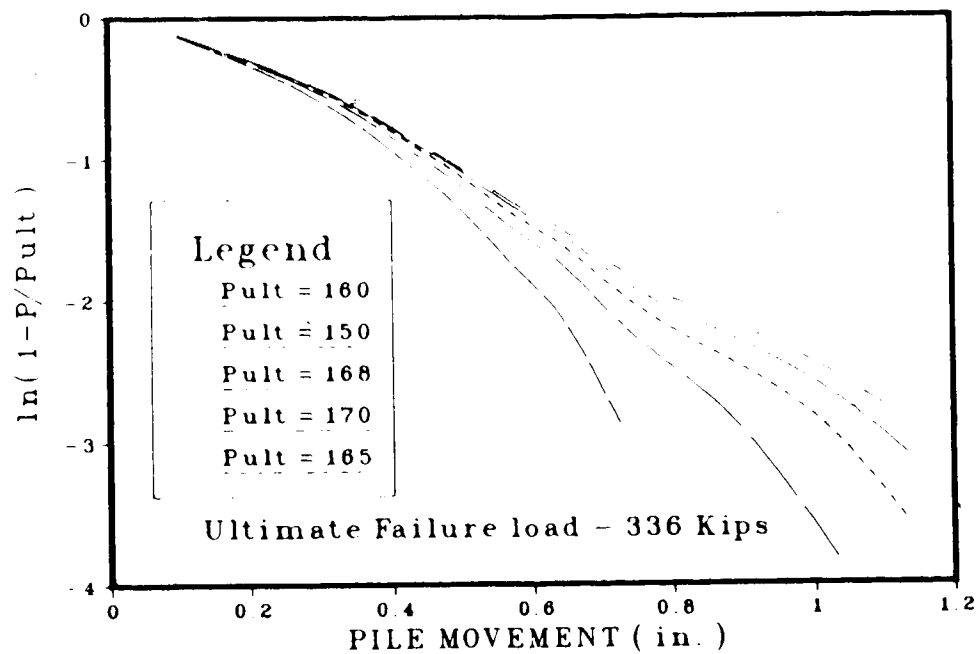


Figure 7.26 Construction of Failure Load According to Van de Veen

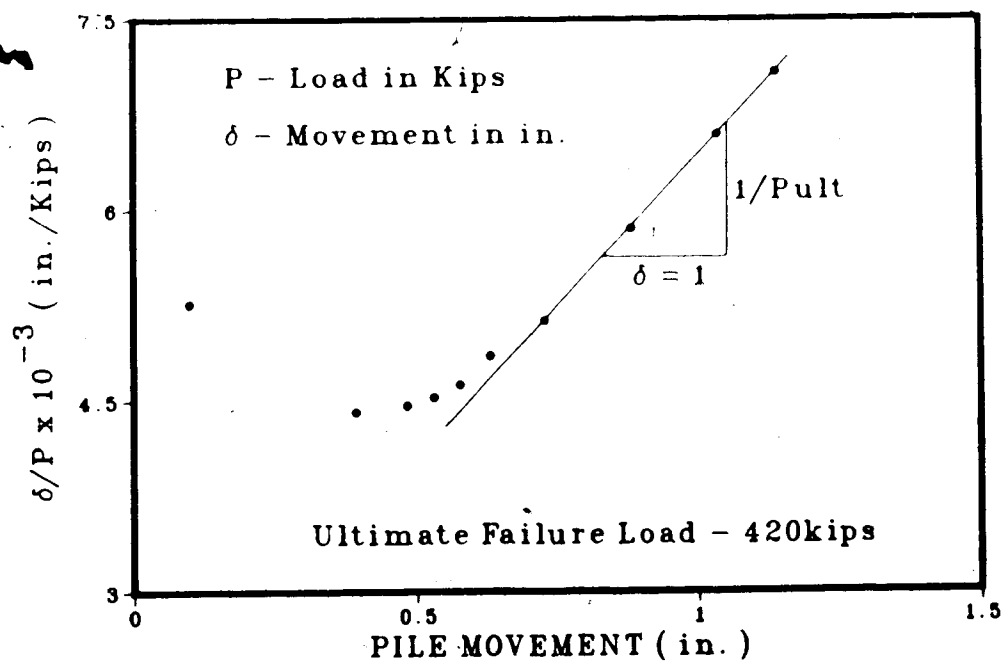


Figure 7.27 Construction of Failure Load According to Chin

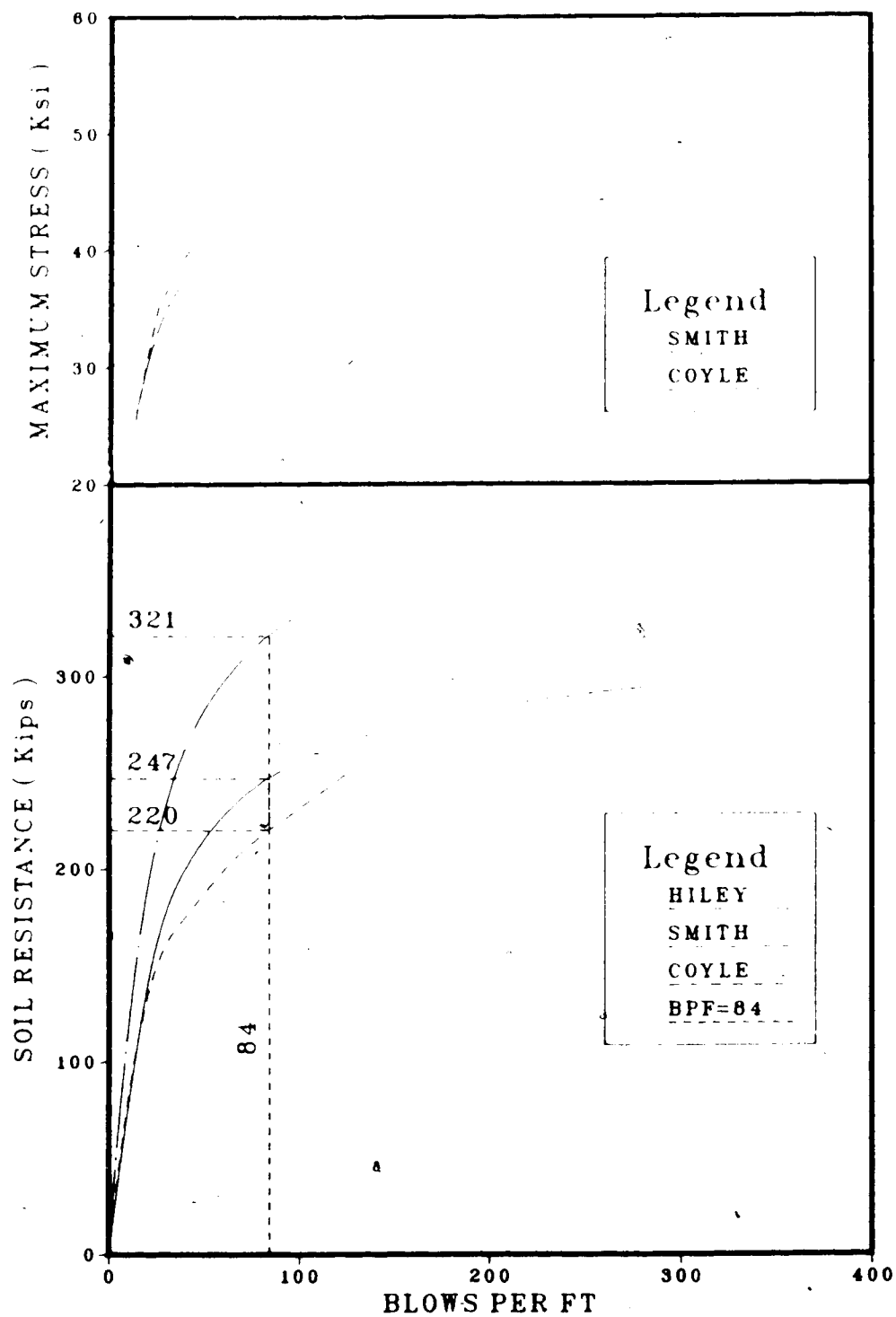


Figure 7.28 Bearing Graphs for Blow Count and Maximum Stress



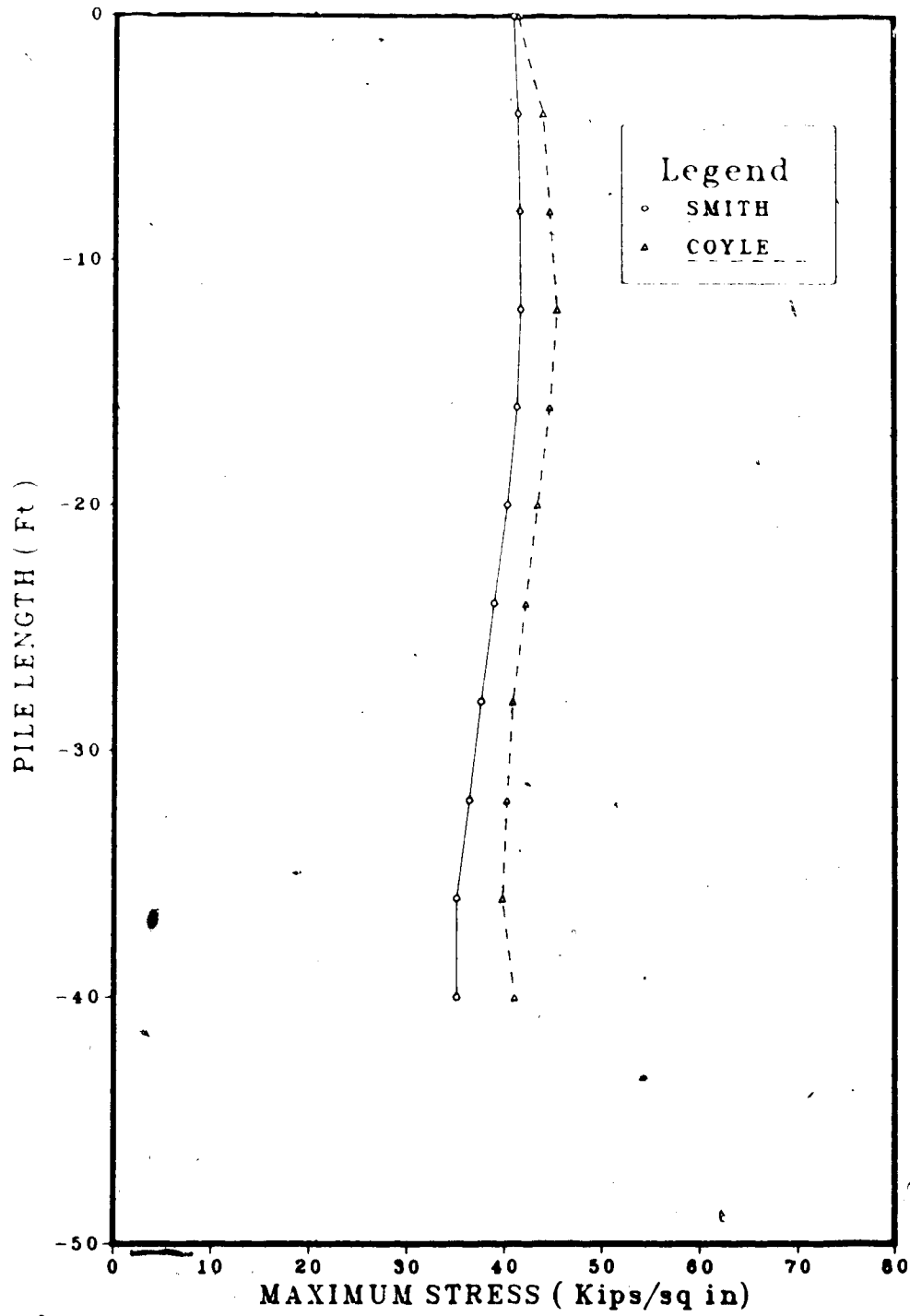


Figure 7.29 Maximum Stress in Pile Segments

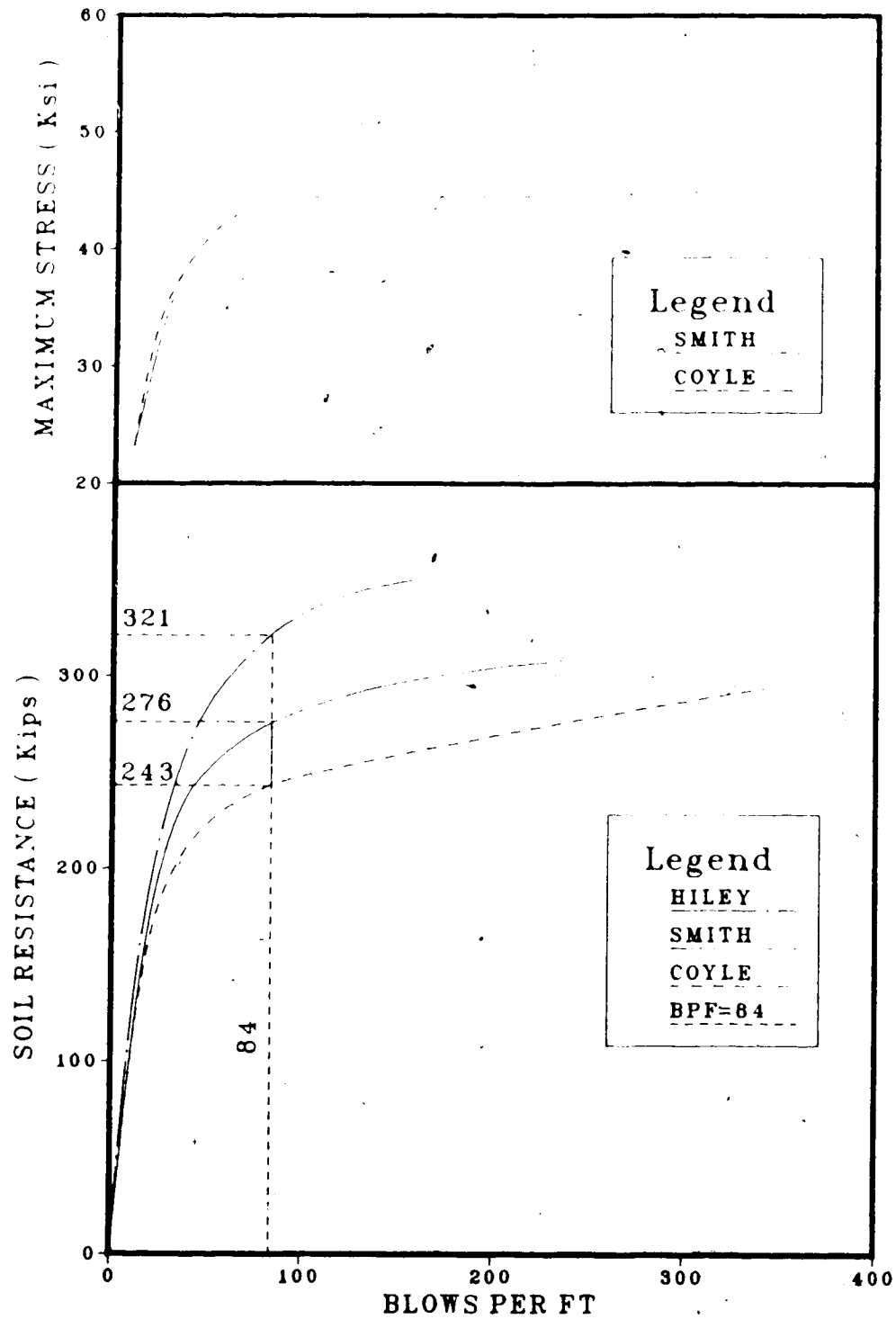


Figure 7.30 Bearing Graphs for Blow Count and Maximum Stress

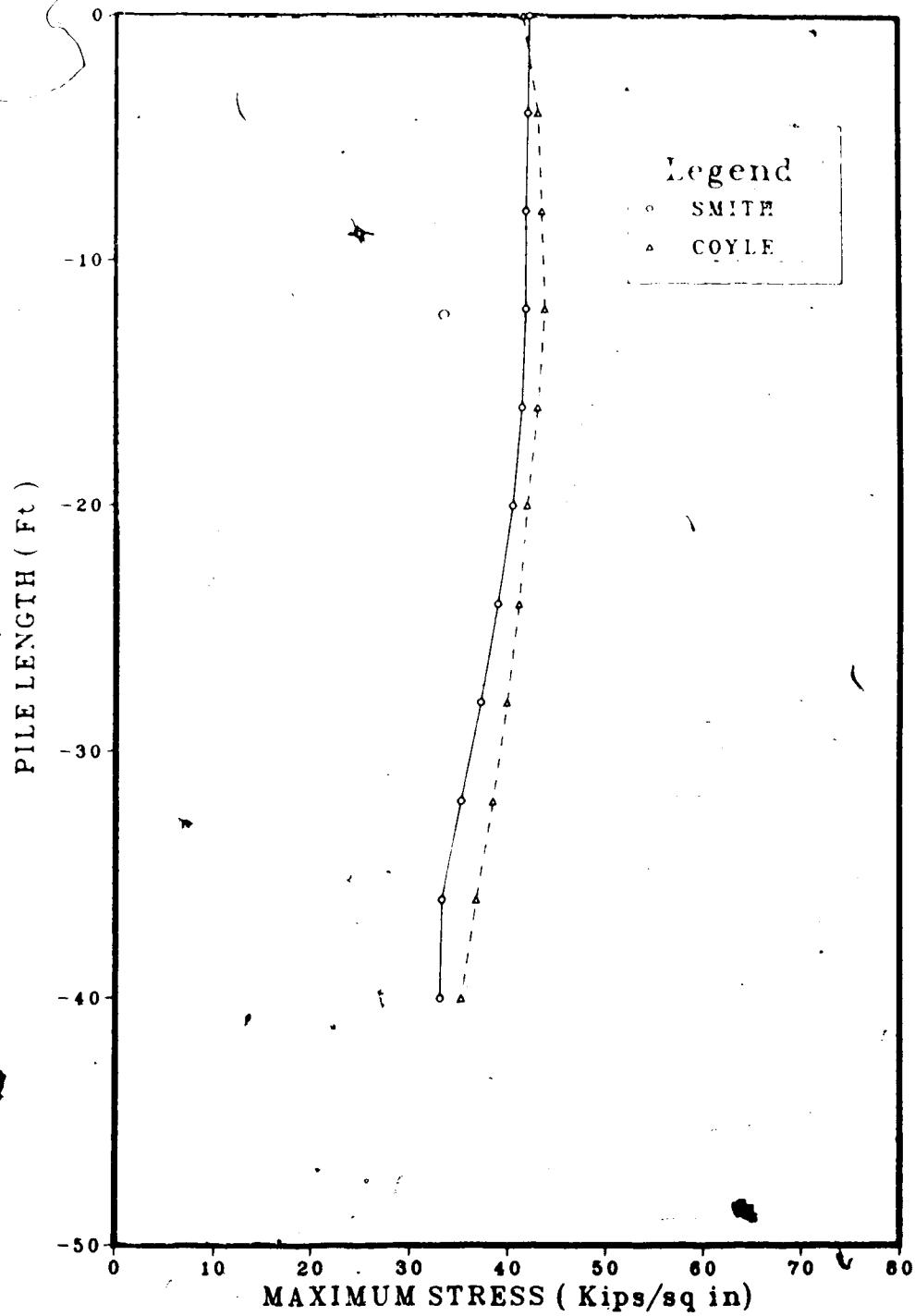


Figure 7.31 Maximum Stress in Pile Segments

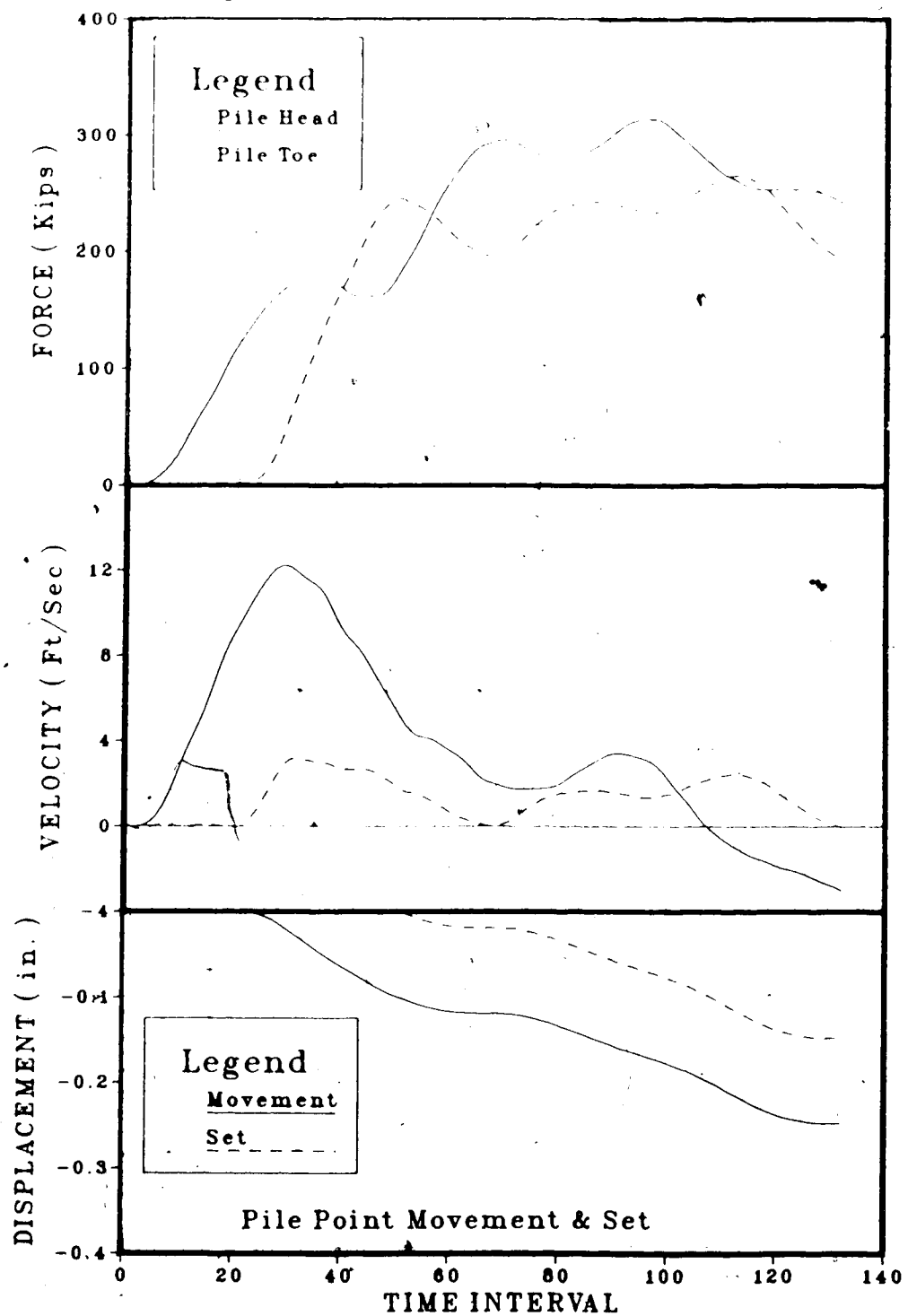


Figure 7.32 Variation of Force, Velocity and Displacements with Time Interval

## 7.7 Discussion of Results

Testing of the computer program involved study of five case histories with different soil conditions and various type of hammers and piles. Pile driving hammers used in this study include diesel hammers, single-acting steam hammer and drop hammer. Type of piles selected for this study include H-sections, closed-end pipe pile, open-end pipe pile and concrete pile. In the following the results are examined in relation to the ultimate static bearing capacities obtained from load tests by applying various methods of evaluation and also, stresses in the pile during driving.

Ultimate static bearing capacities predicted by Smith's and Coyle's methods are compared with the pile capacities estimated using Davisson method and failure criteria suggested by Fuller & Hoy, Butler & Hoy and Van de Veen. Detail results of the study are given in Table 7.1. Comparison of predicted pile capacities with Davisson limit loads are given in Figure (7.33). This indicates that the ultimate pile capacities predicted by Gibson & Coyle's method vary by  $\pm 10\%$  from Davisson limit loads. Predicted pile capacity of site U assuming damping value that is appropriate for sand varies by 17%. Ultimate pile capacities predicted by Smith's method for clayey soils are about 10% lower than the Davisson limit loads. However, for sandy soils, pile capacities predicted by Smith's method vary considerably.

Figure (7.34) is the plot of predicted pile capacities versus Butler & Hoy's failure loads. Smith's method predicted about 4 to 15 percent higher than Butler & Hoy's failure loads. In the case of site U, the pile capacity predicted using damping parameter of sand is 22% lower than Butler & Hoy's failure load. Ultimate pile capacities predicted by Gibson & Coyle's approach for clayey soils are very close to (less than 3%) Butler & Hoy's failure loads but for sandy soils, the variation is considerable (19% to 47%).

In Figure (7.35), predicted pile capacities versus failure loads according to Van de Veen's are plotted. This plot indicates that the pile capacities predicted by Gibson & Coyle's method, except for site U, are about 11% lower than Van de Veen's failure loads. The predicted pile capacity of site U in the first set of computer run is 53% lower than Van de Veen's failure load compared to 38% in the second set of run. However, ultimate pile capacities predicted by Smith's method are 4% to 22% higher than Van de Veen's failure loads.

Ultimate bearing capacities predicted by Smith's method, except for site U, vary only by  $\pm 8$  percent from Fuller and Hoy's failure loads. However, in the case of site U, if presence of gravel is considered, the predicted pile capacity is only 16% lower than Fuller & Hoy's failure load compared to 29% when it was not accounted. Pile capacities predicted by Gibson & Coyle's method vary by about 15% to

28% from Fuller & Hoy's failure loads (see Figure 7.36)).

The ultimate pile capacity predicted by Smith's as well as Gibson & Coyle's method for site U assuming damping values of sand vary considerably from those of load test values. The bore hole data indicates that the sandy soil presence at the founding level of the pile toe contains mixture of gravel and cobbles. Presence of gravel and cobbles in sand was not taken into account in choosing the damping parameters for the first set of analysis and in this case the influence of gravel may be the reason why the predicted pile capacities of site U is inconsistent with the predicted pile capacities of other sites. The damping value is expected to decrease with the increase in consistency of clay or density of sand, hence the damping values lower than those were used in the analysis will be more appropriate. This fact is evident from the pile capacity predicted using damping values lower than those were used in the previous set of run.

Examination of the ultimate pile capacities predicted by the wave equation analysis and the static bearing capacities evaluated from load tests reveal that the ultimate capacities predicted by Gibson & Coyle's method vary marginally from Davisson limit load and failure loads evaluated using Butler & Hoy's as well as Van de Veen's failure criteria. Also, ultimate capacities predicted by Smith's method are comparable with Fuller & Hoy's failure load ( $\pm 8\%$  variation) and the capacities predicted by this

method for clayey soils vary by maximum of 10% from those of failure loads evaluated from load test results.

As mentioned before the actual Chin value has very little bearing on the estimate of the pile capacity other than having a check on the quality of the load test. The failure loads evaluated using this method were not used for comparison.

The ultimate soil resistance obtained by Hiley's formula varies widely depending on the pile length and hammer type. The ultimate soil resistance predicted by Hiley's formula are within the range of values evaluated from the load tests. However, in practice a minimum factor of safety of 6 is employed with this formula and this result in very conservative estimate of the pile capacity.

Figure (7.37) is the plot of Davisson limit load versus ultimate soil resistance predicted by the Hiley's formula. As expected, there is no particular trend and the results of Hiley's formula varies between 29% and 5% from those of Davisson limit loads. Comparison of wave equation analysis values with results of Hiley's formula are given in Figure (7.38). Basic approaches of these two methods are completely different and also, Hiley's formula ignores the type of soil in which pile is driven. Figure (7.38) indicates that the results are scattered and variations are wide.

Maximum stresses developed close to the pile head during the last foot of driving are given in Table 7.1. Except for site U, there are no stress measurements available



to compare with the predicted stresses. The difference between the stresses predicted by Smith's method and Gibson & Coyle's method was considerable in the case of sandy soils. In both approaches, damping forces are distributed proportional to the static resistance. However, damping forces in Smith's method vary linearly with the velocity but in Gibson & Coyle's method it varies non linearly and also, in sandy soils, the distribution of dynamic forces vary considerably from one another. In sandy soils, Smith's method distributes considerable proportion of the damping forces along pile shaft, whereas in Gibson & Coyle's method, almost all the damping forces are concentrated at the pile point.

Analysar monitoring of test pile at site U showed a maximum stress of 30 ksi. Maximum stresses predicted by Smith's and Coyle's methods are 41.5 ksi and 42.8 ksi, respectively. Predicted stresses vary by about 38% to 42% from measured stress. However, the stress predicted in the first set of run is 44.5ksi (48% higher) which is 6% higher than the stress predicted in the second set of run. The variation between the measured and predicted stresses may be attributed to mushrooming of the pile head during driving and also some energy loss in plastifying the hammer accessories such as cap block and cushion is not accounted in the model. This problem can be resolved by introducing a cushion in series with cap block or helmet for qualitative purposes. In the absence of any stress measurements, no

analysis of this nature can be under taken to match the measured stresses.

It was observed in all the cases that the stresses were high when the soil resistance was low and the stress reduces as the soil resistance increases. This may be due to inadequate soil resistance at the initial stage of pile driving to transfer the energy imparted to the pile by the hammer. This explains why the hammer stroke should be reduced ("cold blow") at the initial stage of pile driving and in the case of diesel hammer, it is used as a drop hammer by shutting off the diesel injection to the combustion chamber.

The force and velocity diagrams of the piles which carry higher proportion of the load at pile point (end bearing piles) indicated that the pile points are highly stressed and possible damage may be expected if excessive number of blows are used during the last foot of driving.

Table 7.1 Summary of Test Piles Analysed by the Program

Test Location		112 Avenue Edmonton	Beaumont Texas	Thornton Yard	* Fraser Subdivision	Site No. 11
Soil Type		Clay & Till	Clay	Peat & Sand	Clay	Sand, Gravel & Cobble
Pile Type		H Section W12x65	Pipe Pile Open End	Precast Concrete	H Section 12BP53	Pipe Pile Closed End
Hammer Type		Diesel Delmag 12	Diesel Delmag 12	Steam Vulcan 0	Diesel LB - 312	Drop Hammer 6250 lbs
Stress in Ksi	1)	114	320 , 354	270	106	205
	Static Formula					
	2)	379	295 , 328	415	156	317
	Smith:	392	218 , 216	552	160 , 157	247 , 276
	Wave analysis					
	Coyle:		218 , 216	404	149 , 141	220 , 241
	Hiley's Formula	465	228	301	205	321
	Load Test		240			
	Davisson			369	159	258
	Butler & Moy			480	150	302
	Van De Veen			450	150	336
	Fuller & Moy			520	172	320
	Chin			656	214	420
Stress in Ksi	Smith	36	34.3 , 42.6	3.4	29.6	41.5 , 41.6
	Coyle		34.7 , 42.9	3.6	30.6	44.5 , 42.8

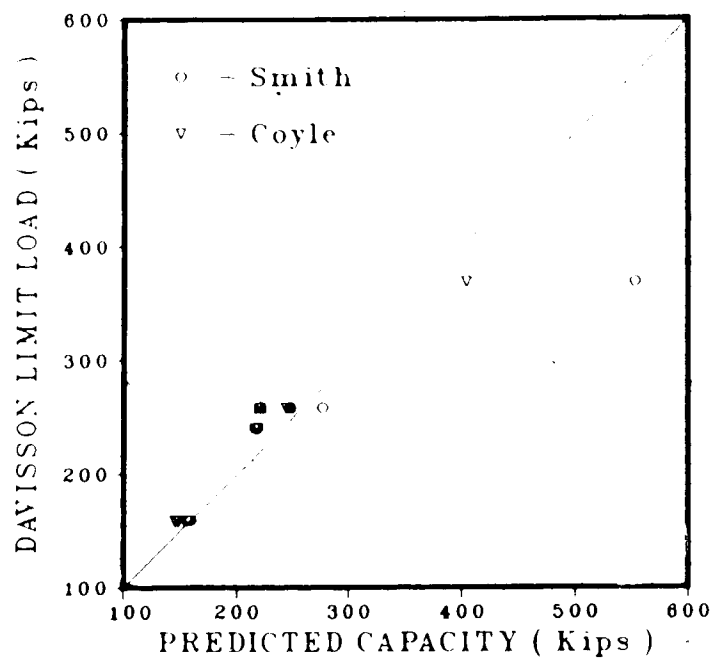


Figure 7.33 Davisson Limit Load Versus Predicted Pile Capacity

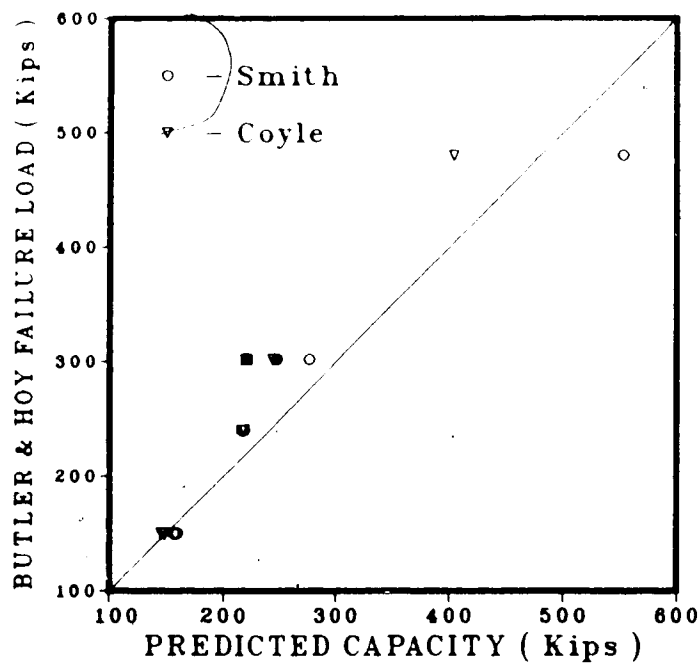


Figure 7.34 Butler & Hoy's Failure Load Versus Predicted Pile Capacity

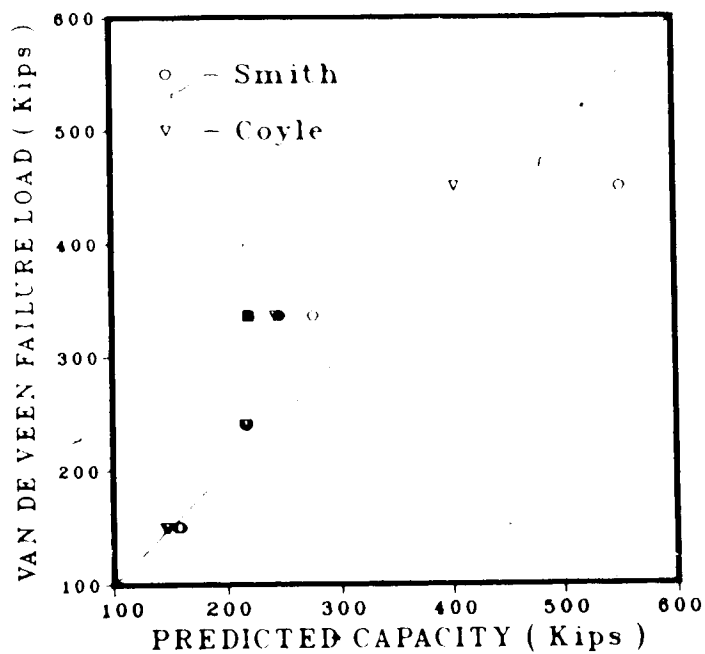


Figure 7.35 Van de Veen's Failure Load Versus Predicted Pile Capacity

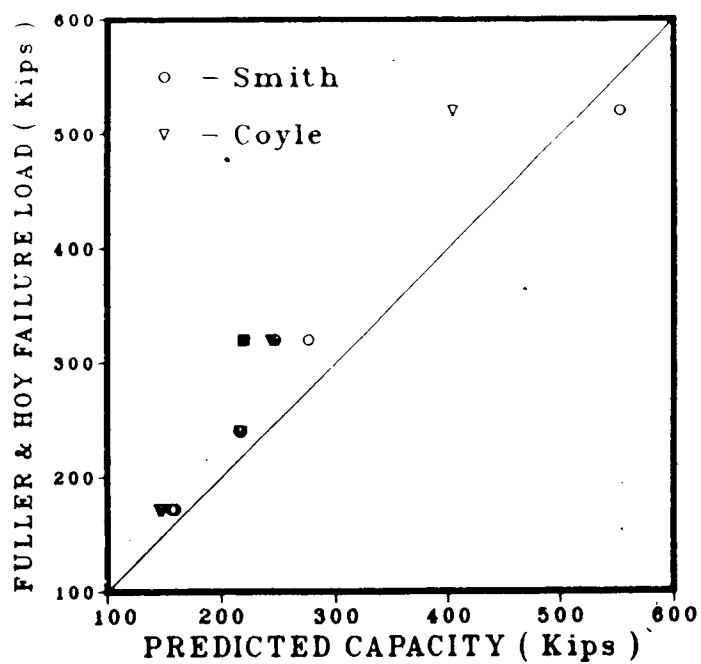


Figure 7.36 Fuller & Hoy's Failure Load Versus Predicted Pile Capacity

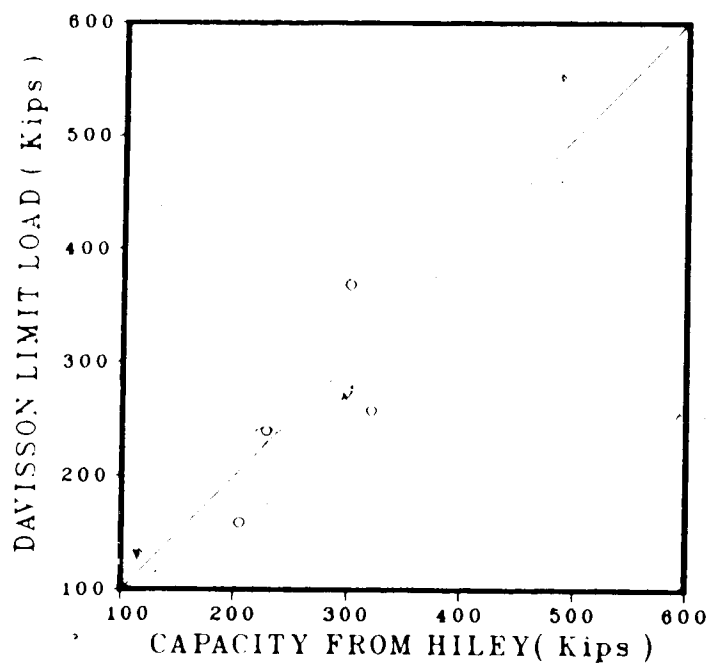


Figure 7.37 Davisson Limit Load Versus Hiley's Ultimate Soil Resistance

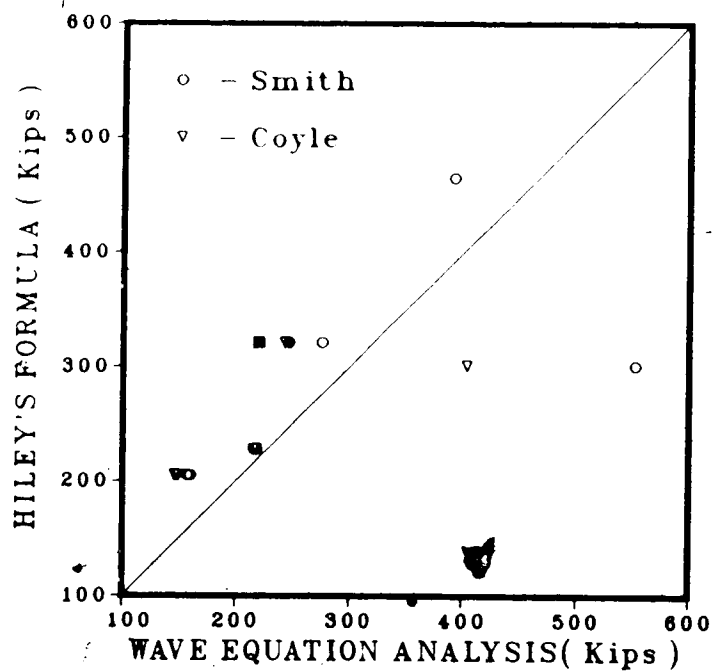


Figure 7.38 Comparison between Wave Equation and Hiley's Formula

## 8. CONCLUSIONS AND RECOMMENDATIONS

The prime objectives of this study were:

- to produce a computer program which includes options of using the damping parameters suggested by Smith, Case Western University and Gibson & Coyle.
- to examine the possibility of using Gibson and Coyle's recommendations
- to test the performance of the program by comparing the predicted ultimate static bearing capacities with the failure loads obtained from load tests.

A computer program capable of solving pile driving problems in either imperial units or metric units has been developed. The results of the parametric study and case histories obtained using the program support the following conclusions:

- 1) The program can be used very easily for most of commonly encountered dynamic pile analysis.
- 2) It is well known that steel piles are bent or damaged at the pile point when driven through hard strata. The program can be used to determine the stresses in the pile and thereby establish a driving procedures to help eliminate these difficulties.
- 3) Precast concrete piles are sometimes cracked or broken

due to excessive compressive stresses caused by the hammer blow. In some cases excessive tensile stresses may also result from the hammer blow, especially if the pile is long. The program can be used to determine the correct reinforcement and driving procedures to help eliminate these troubles.

4) If the soil resistance distribution, soil properties and the driving system properties are accurately known, the static bearing capacities can be predicted within  $\pm 10\%$  of the failure loads obtained from load test.

5) The method suggested by Gibson and Coyle predicted ultimate static bearing capacities within  $\pm 10\%$  of Davisson limit loads.

6) Prediction of ultimate static bearing capacities by Smith's method are within  $\pm 8\%$  of Fuller & Hoy's failure loads.

It should be mentioned that the Case damping values are non-dimensionalized by pile properties. Thus, different values may need to be used in the same soil for different types of pile. Also, the Case method is very sensitive to minor errors in choosing damping values. It is for these reasons that Smith's or Gibson and Coyle's damping should be used whenever no experience with Case damping exists.



7) The program is well suited to solve the driveability problem since it uses the actual hammer potential for a given soil condition. Also, it can be used to establish the driving criteria.

It should be remembered that all the damping parameters recommended by Gibson & Coyle were the result of triaxial tests conducted on prepared samples. Also, the failure mechanism occurring in the soil sample tested in the laboratory may not be the same as the failure mechanism occurring at the pile tip of a full scale pile in the field. Use of this method requires further work to establish damping parameters for low compressible clay (CL) and gravels.

Accuracy of compressive as well as tensile stress prediction by this program can be improved by introducing a cushion in series with helmet or cap block for qualitative purposes. Examination of this possibility needs measurement of stresses during pile driving.

## BIBLIOGRAPHY

- Agerschou, H.A. "Analysis of the Engineering News Pile Formula.", ASCE, SM5, October, 1962.
- Authier, J. & Fellenius, B.H. "Dynamic measurements as an Inspection Tool for Discovering Damage to Spliced and Unspliced Precast Concrete Piles. Two case Histories.", Proc. International Seminar on the Application Stress Wave Theory on Piles, Stockholm, PP.121-127, 1980.
- Authier, J. & Fellenius, B.H. "Quake Values Determined from Dynamic Measurements.", Proc. International Seminar on the Application of Stress Wave Theory on Piles, Stockholm, PP.197-216, 1980.
- Authier, J. & Fellenius, B.H. "Wave Equation Analysis and Dynamic Monitoring of Pile Driving.", Civil Engineering Practicing and Design Engineers.", V2n, PP.387-407, 4, July, 1983.
- Bent Hansen & Hans Denver. "Wave Equation Analysis of a Pile-An Analytical Model.", Proc. International Seminar on the Application of Stress Wave Theory, Stockholm, June, 1980.
- Bowles, J.E. Analytical and Computer Methods in Foundation Engineering. New York: McGraw-Hill, 1974.
- Bergdahl, U. & Hult, G. "Load Tests on Friction Piles in

- Clay.", Proc. International Conference on Soil Mech and Found. Eng., Stockholm, Vol.2, PP.625-630, 1981.
- Bredenberg,H. "Response of Pile Points on Rock During Driving.", Proc. International Seminar on the Application of Stress Wave Theory, Stockholm, June, 1980.
- Broms,B.B. & Bredenberg,H. "Application of Stress Wave Theory on Pile Driving. A State of the Art Report.", Proc. of the Seventh Southeast Asian Geotechnical Conference, HonKong, PP.195-238, November, 1982.
- Butler,H.D. & Hoy,H.E. "Users Manual for the Texas Quick-Load Method for Foundation Load Testing.", Federal Highway Administration Offices of Research and Development, 1977.
- Chellis,R.D. Pile Foundations. New York: McGraw-Hill, 1961.
- Chida,S. & Tsukada,Y. "Driveability of Hydraulic Pile Hammers.", Proc. of the International Symposium on Penetrability and Driveability of Piles, San Francisco, Vol.1,PP.129-132, August, 1985.
- Chin,F.K. "Estimation of the Ultimate Load of Piles not Carried to Failure.", Proc. 2nd Southeast Asian Conf. on Soil Engineering, pp. 81-90, 1970.
- Chin,F.K. "Pile tests Arkansas River Project.", J.S.M.F.D, ASCE, Vol 97, No. SM6, pp. 930-932, 1971.

Clough, R.W. & Penzien, J. Dynamics of Structures., New York:  
McGraw Hill, 1975.

Cooke, R.W., Price, G., & Tarr, K. "Jacked Piles in London  
Clay: a Study of Load Transfer and Settlement Under  
Working Conditions.", Geotechnique, 29(2), PP.113-147,  
1979.

Coyle, H.M. & Reese, L.D. "Load Transfer for Axially Loaded  
Piles in Clay.", J.S.M.F.D, ASCE, Vol.92, SM2, pp.1-26,  
1966.

Coyle, H.M. & Gibson, G.C. "Empirical Damping Constants for  
Sands and Clays.", J.S.M.F.D, ASCE, Vol.96, SM3,  
PP.949-965, 1970.

Coyle, H.M., Bartoskewitz, R.E. & Lowery, L.L. "Prediction of  
Static Bearing Capacity from wave Equation Analysis.",  
Offshore Technology Conference, Texas, 2nd, No. OTC  
1202, April, 1970.

Das, B.M., Fundamentals of Soil Dynamics., New York:  
Elsevier, 1983.

Davisson, M.T. "High Capacity Piles.", Proc. ASCE Lecture  
Series, Innovation in Foundation Construction, Illinois  
Section, 1972.

Davisson, M.T. "Stress in Piles.", ASTM STP670, pp.64-83,  
1979.

- Desai, C.S. & Christian, J.T., Numerical Methods in Geotechnical Engineering, New York: McGraw Hill, 1977.
- Dismuke, T.D., "Behaviour of Steel Piles During Installation and Service.", ASTM STP 670, PP.282-299, 1979.
- Eisenstein, Z. & Thomson, S. " Foundation Investigation Edmonton Rapid Transit 112th Avenue Station.", Site Investigation Report, April, 1976.
- Etter, D.M., Structured Fortran 77 for Engineers and Scientists, California: Benjamin/Cummings, 1983.
- Fellenius, B.H., "Test Loading of Piles - Methods, Interpretation, and Proof Testing.", GT9, ASCE, Vol.101, pp.855-869, 1975.
- Fellenius, B.H., Samson, L., Thompson, P.E. & Trow, W. "Dynamic Behaviour of Foundation Piles and Driving Equipment.", Research Project, Department of Supply and Services, Ottawa, Contract No. IST77.00045, Vol.1&2, 1978.
- Fellenius, B.H. "The Analysis of Results from Routine Pile Test loading.", Ground Engineering, London, Vol.13, No.6, pp.19-31, 1980.
- Fellenius, B.H. "Geotechnically Allowable Stress for Driven Piles.", ASCE, Vol.54, No.11, pp.72-75, 1984.
- Flaate, K. "Effects of Pile Driving in Clays.", Canadian Geotechnical Journal 9(1), pp.81-88, 1972.

Fuller, R.M. & Hey, H.E. "Pile Load Test Including Quick Load Test Method, Conventional Methods and Interpretations.", Highway Research Board No. 333, Pile Foundations, pp. 74-86, 1970.

Fuller, F.M. Engineering of Pile Installations., New York: McGraw Hill, 1983.

George, A.B., Sherrell, F.W., & Tomlinson, M.J. "The Behaviour of Steel H Piles in Slaty Mudstone.", Geotechnique, 26(1), pp. 95-104, 1976.

Gerwick, B.C & Brauner, H.A. "Design of High Performance Prestressed Concrete Piles for Dynamic Loadings.", ASTM STP670, pp. 323-334, 1979.

Goble, G.G., Rausche, F. & Moses, F. "Dynamic Studies on the Bearing Capacity of Piles. Phase 3.", Report No.48, Vol.1&2, Division of Solid Mechanics, Structures, and Mechanical Design, Case Western Reserve University, Cleveland, 1970.

Goble, G.G. & Rausche, F. "Wave Equation Analysis of Pile Driving. WEAP program.", Vol.1-3, US Dept. of Transp. FHWA, off. of Res. and Dev., Vol.76-14.1-76-14.3, Washington, 1976.

Goble, G.G. & Rausche, F. "Pile Driveability Predictions by CAPWAP.", Institution of Civil Engineers, London, 1980.

Goble, G.G., Rausche, F. & Likins, G.E. "The Analysis of Pile Driving - A State of the Art.", Proc. International Seminar on the Application of Stress Wave Theory, Stockholm, June, 1980.

Heerema, E.P. "Relationship Between Wall Friction, Displacement, Velocity and Horizontal Stress in Clay and in Sand for Pile Driveability Analysis.", Ground Engineering, Vol. 12, pp. 55-58, 61, 65, 1, January, 1979.

Heerema, E.P. & Jong, A.De. "An Advanced Wave Equation Computer Program which Simulates Dynamic Plugging through a Coupled Mass-Spring System.", Institution of Civil Engineers, London, 1980.

Heerema, H.P. "Dynamic Point Resistance in Sand and in Clay for Pile Driveability Analysis.", Ground Engineering, Vol. 14, 6, September, 1981.

Hirsch, T.J., Carr, L. & Lowery, L.L. "Pile Driving Analysis. Wave Equation User's Manual. TTI Program.", Vol. 1-3, US Dept. of Transp., FHWA, off. of Res. and Dev., Washington, 1976.

Holloway, D.M. "Pile Driving analysis Using the One Dimensional Wave Equation." Technical Report S-75-5., U.S. Army Engineers Waterways Experiment Station, Vicksburg, MS., 1975.

Holloway, D.M., Clough, G.W. & Vesic, A.S. "The Effects of

- Residual Driving Stresses on Pile Performance under Axial Loads.", Proc. Offshore Technology Conference, Houston, OTC 3306, 1978.
- Housel, W.S. "Michigan Study of Pile Driving Hammers.", Proc. of the ASCE, SM5, pp.37-65, September, 1965.
- Isaacs, D.V. "Reinforced Concrete Pile Formulae.", Transactions of The Institution of Engineers, Australia, Vol XII, No. 370, pp. 312-323, 1931.
- Kishida, H. "Ultimate Bearing Capacity of Piles Driven into Loose Sand.", S.M & F.E, Vol 7, No.3, pp. 20-29, 1967.
- Leonards, G.A. & Lovel, D. "Interpretation of Load Tests on High Capacity Driven Piles.", ASTM STP670, pp. 388-415, 1979.
- Litkouhi, S. & Poskitt, T.J. "Damping Constants for Pile Driveability Calculations.", Geotechnique, Vol.30, No.1, pp.77-86, 1980.
- Lowery, L.L., Hirsch, T.J., Edwards, T.C., Coyle, H.M. & Samaon, C.H. "Use of the Wave Equation to Predict Soil Resistance on a Pile During Driving.", Special Session No.8, 7th Int. Conf. S.M.&F.E., Mexico, 1969.
- Marchetti, S. "Improving the Quality of input Data for the Wave Equation Analysis of Driven Piles.", Canadian Geotechnical Journal, V17n, pp.286-291, 2, May, 1980.



McClelland, B., Focht, J.A., Emrich, W.J. "Problems in Design and Installation of Offshore Piles.", J.S.M.F.D., ASCE, Vol 95, SM6, pp.1491-1514, 1969.

Meyerhof, G.G. "Bearing Capacity and Settlement of Pile Foundations.", GT3, ASCE, Vol 102, pp. 195-228, 1976.

Novak, M. "Soil-Pile Interaction Under Dynamic Loads.", Institution of Civil Engineers, London, 1980.

Olson, R.E. & Flaate, K.S. "Pile Driving Formulas for Friction Piles in Sand.", Proc. ASCE, SM6, November, 1967.

Poulos, H.G. & Davis, E.H. Pile Foundation Analysis and Design., John Wiley & Sons, 1980.

Ramey, G.E. & Hudgins, A.P. "Sensitivity and Accuracy of the Pile Wave Equation.", Ground Engineering, Vol.10, No.7, pp.45-47, 1977.

Rausche, F., Moses, F. & Goble, G.G. "Soil Resistance Prediction from Pile Dynamics.", Proc. ASCE, SM9, September, 1972.

Rempe, D.M. & Davisson, M.T. "Performance of Diesel Pile Hammers.", Proc. of the Int. Conf. on Soil Mech. and Found. Eng., 9th, Tokyo, pp.347-354, July, 1977.

Samson, C.H., Hirsch, T.J. & Lowery, L.L. "Computer Study of Dynamic Behaviour of Piling.", J. Structural Division, ASCE, Vol.89, ST4: 418-449, 1963.

- Samson, L. & Authier, J. "Change in Pile Capacity with Time: Case Histories.", Can. Geotech. J. 23, pp. 174-180, 1986.
- Skempton, A.W. & Northey, R.D. "Sensitivity of Clays.", Geotechnique, Vol. 3, pp. 40-51, 1952.
- Smith, E.A.L. "Impact and Longitudinal Wave Transmission.", Trans. ASME, pp. 963-973, August, 1955.
- Smith, E.A.L. "Pile Driving Analysis by the Wave Equation.", J.S.M.F.D., ASCE, Vol. 86, SM4, pp. 35-61, 1960.
- Smith, E.A.L. "Pile Driving Analysis by the Wave Equation.", J.S.M.F.D., ASCE, Vol. 127, Part 1, pp. 1145-1193, 1962.
- Tada, H., Oshima, K., Kaminaga, K., Ueki, Y. & Fukuwaka, M. "New Dynamic Formula Applied to Hydraulic Pile Hammers.", Proc. of the Int. Symposium on Penetrability and Driveability of Piles, San Francisco, Vol. 1, pp. 197-200, 10, August, 1985.
- Tavenas, F. & Audy, R. "Limitations of the Driving Formulas for Predicting the Bearing Capacities of Piles in Sand.", Can. Geotech. J. 9, 1972.
- Tavenas, F.A. & Audibert, J.M.E. "Application of the Wave Equation Analysis to Friction Piles in Sand.", Can. Geotech. J., V14, 1977.
- Thompson, C.D. & Murty, D. "Evaluation of Ultimate Bearing

Capacity of Different Piles by Wave Equation Analysis.", Proc. of the Int. Seminar on the Application of Stress Wave Theory, Stockholm, June, 1980.

Thompson, C.D. & Thompson, D.E. "Real and Apparent Relaxation of Driven Piles.", Proceedings ASCE, GT, Vol. 111, NO. 2, February, 1985.

Tomlinson, M.J. "Some effects of Pile Driven in Clay Soils.", Conf. on behaviour of Piles, Institution of Civil Engineers, London, pp. 59-66, 1970.

Tomlinson, M.J. Pile Design and Construction Practice, 3rd Ed, London: Pitman, 1977.

Van de Veen, C. "The Bearing Capacity of Pile.", Proc. of the Int. Conf. on Soil Mech. and Found. Eng., 3rd, Zurich, Vol 2, pp. 84-90, 1953.

Van Koten, H. & Middendrop, P. "Interpretation of Results from Integrity Tests and Dynamic Load Test.", Proc. of the Int. Seminar on the Application of Stress Wave Theory, Stockholm, June, 1980.

Vesic, A.S. "A Study of Bearing Capacity of Deep Foundations.", Final Report, Project. B-189, School of Civil Engineering, Georgia Inst. of Tech., Atlanta, 1967.

Vesic, A.S. "Tests on Instrumented Piles, Ogeechee River

Site." , Proceedings ASCE, Vol 96, SM2, pp. 561-584, 1970.

Vijayvergiya,V.N. & Focht,J.A.Jr. "A New Way to Predict the Capacity of Piles in Clay.", Offshore Technology Conference, Houston, Vol 2, pp. 865-874, 1972.

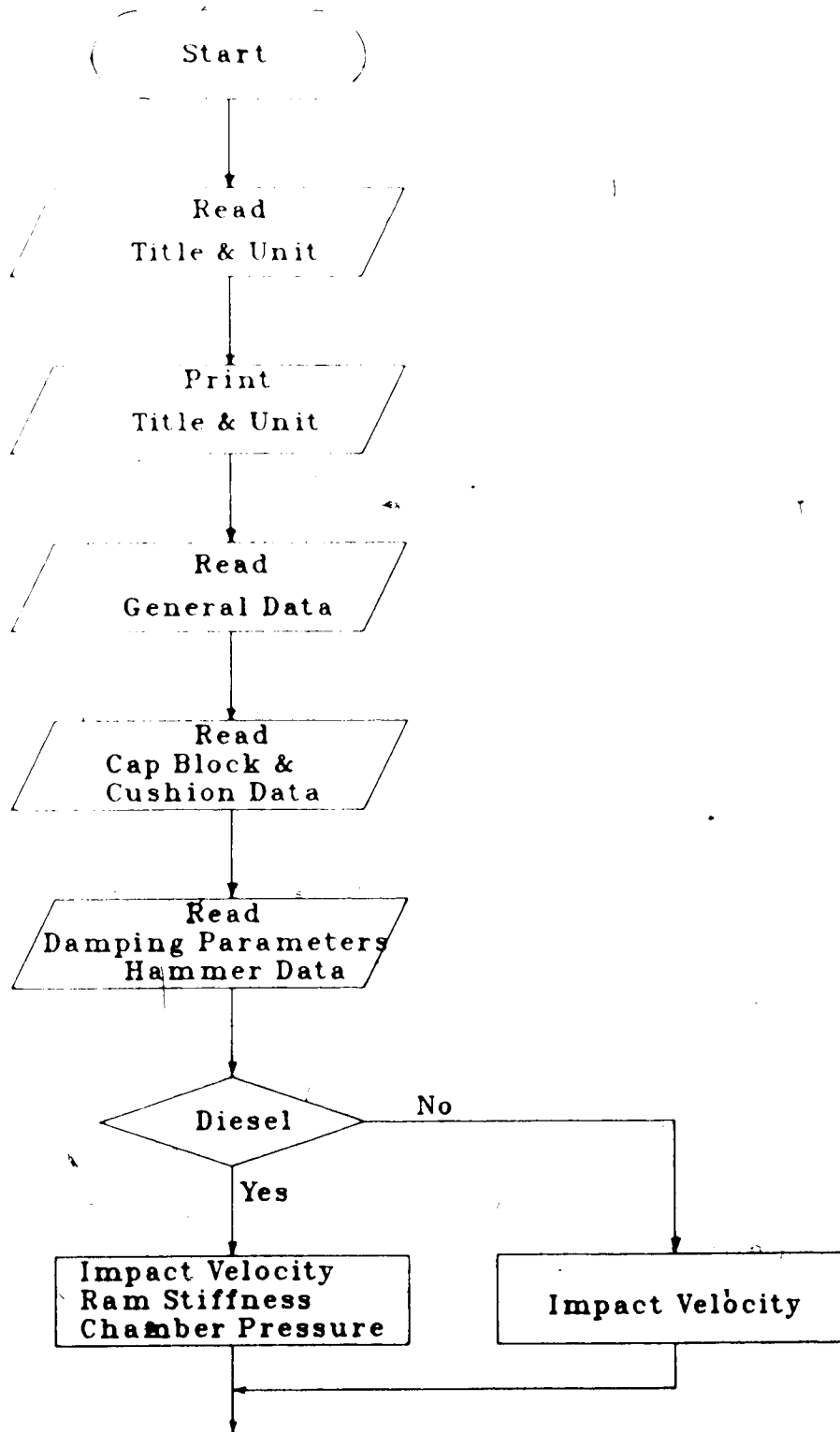
Vijayvergiya,V.N. "Soil Response During Pile Driving.", Institution of Civil Engineers, London, 1980.

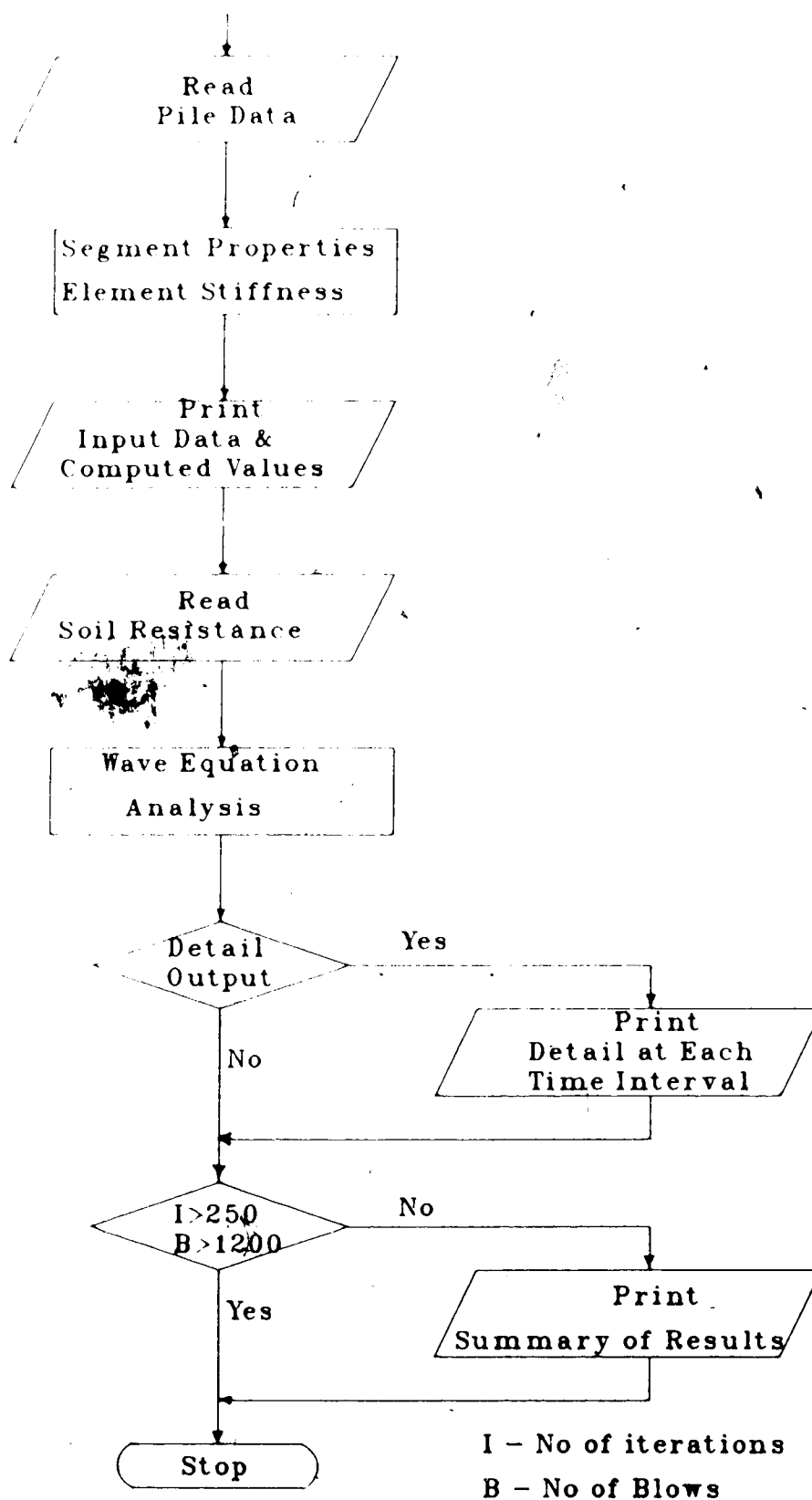
Winterkorn,H.F. & Fang,H.Y. Foundation Engineering Hand Book, Van Norstrand Reinhold Company: New York, 1975. ◆

Yang,N.C. "Relaxation of Piles in Sand and Inorganic Silts.", ASCE, 96, SM2, pp.395-409, 1970.

APPENDIX A-1

Basic Flow Chart





## APPENDIX A-2

### List of Common Variables in "ALWAP"

**TITLE:** Project title not exceeding eighty characters.

**UT1-UT8:** Read the choice of unit (fps or metric); the order is as follows

FT, IN, KIPS, KIPS/IN, K/SQ IN, FT/SEC, SQ IN, CU IN  
M, CM, KN, KN/CM, KN/SQ CM, M/SEC, SQ CM, CU CM

**FU1:** Conversion factor equivalent to ft in inches or meter in centimeters (fps=12 & metric=100)

**FU2:** -do- for area (fps=144 & metric=10000)

**FU3:** Acceleration of gravity in  $\text{ft/sec}^2$  or  $\text{m/sec}^2$  depending on the choice of unit ( $32.2 \text{ ft/sec}^2$  or  $9.807 \text{ m/sec}^2$ ).

**NELEM:** Number of elements including ram and cap; in the case of diesel hammer ram, cap and anvil

**NSAS:** Number of pile segments above ground level or number of pile segments from pile head have no soil resistance

**NSOIL:** Control to activate the selection of damping parameter;  $<1$  read only skin and toe damping values;  $>1$  read damping value of all the pile segments including pile point

**MDR:** Control to choose the method to compute the dynamic

resistance; =1 Case method; =2 Smith's or Gibson and  
Coyle's method

ELEML: Length of pile segment in ft or meter

TWALL: Wall thickness of pipe pile in inches or cms

PILTYP: Pile type; >0 constant area of cross-section; =0  
read area and weight of each pile segment; <0 compute  
average area and weight of each pile segment

IFHTYP: Type of pile driving hammer; =5 drop hammer or  
single/double acting air/steam hammer; =7 diesel hammer

NCOM: To identify the nature of pile (composite); >0 read  
weight, area of cross-section, modulus of elasticity  
and stress wave velocity of each pile segment; <0 read  
elastic modulus and stress wave velocity of pile  
material

STEAM: Differentiate between drop or single acting hammer  
and double/differential acting hammer; >0 drop hammer  
or single acting hammer; <0 double acting or  
differential acting hammer

DIESEL: To specify diesel hammer; >0 read stroke; <0 read  
indicated ram energy output and compute stroke

NPLOT: To identify output option; >0 bearing graph is  
produced in addition to the results; <0 only results

NW: Control to activate the output option if detail of any



pile element is required; this option can be activated by specifying the element number in question; force, velocity, displacement and set of the specified pile segment and the pile point at each time interval will be included in the output

IFD: Control to activate the output option of pile point; >0 maximum stress in the pile, and pile point displacement and set at each time interval will be included in the output

JJS: Identify the shaft soil resistance distribution; =0 to compute linear distribution of shaft resistance on sides of pile segments; =1 read distribution of shaft resistance on the sides of the pile segments

NCHECK: Counter in computed GO TO statement; 1= vary quake values keeping other parameters constant; 2= vary percentage of ultimate soil resistance at pile point keeping other parameters constant; 3= vary ultimate soil resistance and cap block properties keeping other parameters constant; 4= change all problem data including TITLE; 5= stop after one run

IFWRIT: Control to write element forces, stresses, velocities, displacements and sets; 0= does not write; >1 depending on the choice, writes element forces or velocities or displacements or sets

IFFSV: Identify the output requirement; 1= writes element

1- writes stresses at each time interval; 2- writes stresses at each time interval; 3- writes velocities at each time interval; 4- writes displacements at each time interval; 5- writes set at each time interval

**NRU:** Total number of ultimate soil resistance values used in the analysis (RUPOT)

**NJOINT:** Identify whether there is any splice or joint in the pile; -0 read element No., maximum tensile force that can be transferred through the joint and maximum movement allowed in the joint

**COMEM:** Control to compute tension forces in the pile; 0 tension forces not required; -0 compute and obtain tension forces

**W(3):** Weight of pile cap (helmet) in Kips or Kn

**DRIVPT:** Weight of drive point (shoe) in Kips or Kn

**DT:** Time interval in seconds; 0= to compute by the program; for pipe piles it should be specified

**NE:** If NCOM>0; pile joint number

**ECOM(M):** -do- ; E value of pile elements in Ksi or Kn/sq cm

**VCOM(M):** -do- ; stress wave velocity of pile elements in ft/sec or m/sec

**EMOD:** If NCOM<0; E value of pile material in Ksi or Kn/sq cm

**WVEL:** -do- ; stress wave velocity of pile material in ft/sec  
or m/sec

**ECAP:** E value of cap block in Ksi or Kn/sq cm

**ACAP:** Cross sectional area of cap block in sq in or sq cm

**THCAP:** Thickness of cap block in inches or cms

**EPCB:** Coefficient of restitution of cap block

**ECUS:** E value of pile cushion in Ksi or Kn/sq cm

**ACUS:** Cross sectional area of pile cushion in sq in or sq cm

**THCUS:** Thickness of pile cushion in inches or cms

**EPC:** Coefficient of restitution of pile cushion

**SJ:** If NSOIL=1; skin damping constant in sec/ft or sec/m

**PJ:** -do- ; pile point damping constant in sec/ft or sec/m

**RS,RP:** -do- ; velocity exponention of side and pile point,  
respectively; for Case and Smith methods RS = RP = 1.0;  
for Gibson & Coyle's method it is dictated by the soil  
type

**NS:** If NSOIL>1; pile segment number

**D(M):** -do-; damping constants of pile elements in sec/ft or  
sec/m

**RX(M):** -do- ; velocity exponention of pile elements

depending on the soil type

**W(2):** If IFHTYP=5; weight of ram in Kips or Kn

**WH:** Total weight of hammer housing in Kips or Kn; for diesel hammer less weight of ram

**RENG:** If STEAM=0; rated hammer energy in Kips-in or Kn-cm

**EFF:** Hammer efficiency

**STROKE:** Ram fall of drop hammer; observed field stroke of single or double acting and diesel hammer in ft or m;  
0 to compute by the program from the hammer properties

**STRMAX:** If STEAM=0; maximum stroke of double/differential acting hammer in ft or m as indicated by the manufacturer

**POP:** -do- ; operating air steam pressure in Ksi or Kn/sq cm

**PRLIM:** -do- ; manufacturer's rated limiting pressure in Ksi or Kn/sq cm

**W(1):** If IFHTYP=7; weight of ram in Kips or Kn

**EXPF:** -do- ; maximum explosive force in Kips or Kn

**RENOP:** -do- ; rated hammer energy output

**DHK:** -do- ; stiffness of ram in Kips/in, or Kn/cm

**DRAM:** -do- ; top diameter of ram in inches or cms

**DBT:** do ; bottom diameter of ram; if DBT 0, 10% of DRAM  
will be assigned

**DAEP:** do ; distance from anvil to exhaust port in ft or m

**TD, TI, TL, TR:** do ; delay time, rise time, peak time and  
exhaust time of explosive force at impact; if zero is  
specified for all these parameters, program will assume  
these values

**VFIN:** do ; volume of combustion chamber in cu in or cu cm

**PAT:** do ; atmospheric pressure in Ksi or KN/sq cm

**ERAM:** E value of the ram material in Ksi or Kn/sq cm; read  
if DHK<0

**EEAN:** E value of anvil material in Ksi or Kn/sq cm; read if  
DHK<0

**RAML:** Ram length in ft or m; read if DHK<0

**ANL:** Length of anvil in inches or cms; read if DHK<0

**DAN:** Diameter of anvil in inches or cms; read if DHK<0

**WAN:** Weight of anvil in Kips or Kn

**EAN:** Coefficient of restitution of anvil

**RIENP:** Indicated ram energy in Kips-ft or Kn-m; read if  
DIESEL<0

**WFT:** Weight per unit length of pile in Kips or Kn

AREA: Cross sectional area of pile in sq in or sq cm

IC: If NCOM=0; read composite pile segment number

WCOM(M): Weight per unit length of composite pile segment in  
Kips or Kn

A(M): Cross sectional area of pile segment in sq in or sq  
cm; read if NCOM=0 or PILTYP=0

W(M): Weight of pile segment in Kips or Kn; read if PILTYP=0

DIAT: Top outside diameter of pile in inches or cms; read  
if PILTYP=0

DIAB: Bottom do

UNITWT: Unit weight of pile material in Kips/cu ft or Kn/cu  
m; read if PILTYP=0

IU: If NCOM=0 & PILTYP=0; read pile element number

UWCOM(M): -do- ; unit weight of pile segment in Kips/cu ft  
or Kn/cu m

MN: If NJOINT=0; read pile element number

SPLICE(M): -do- ; read maximum tensile force of joint in  
Kips or Kn

SLACK(M): -do- ; read maximum movement allowed in the joint  
in inches or cms

**QS:** Quake value of ground adjoining the pile shaft in inches  
or cms

**QP:** -do- pile point

**PER:** Percentage of ultimate soil resistance at pile point

**RUTOT:** Assumed ultimate pile resistance in Kips or Kn

**IP:** If JJS=1; read pile segment number

**RU(I):** -do- ; read distribution of pile resistance on sides  
of the pile segments (Kips or Kn)

# APPENDIX A-3

## Listing of Program "ALWAP"

```

1      C      WAVE EQUATION FOR PILE RESPONSE TO IMPACT TYPE DRIVING
2      C      PILE MAY BE STRAIGHT, TAPERED, STEPPED OR H-SECTION, ALSO
3      C      PILE MAY BE WITH JOINTS CAPABLE OF TRANSMITTING
4      C      TENSILE FORCE UNDER SPECIFIED CONDITION.
5      C      *****
6      C      THIS PROGRAM WILL COMPUTE THE FOLLOWING.
7      C      1) SEGMENTS WEIGHT AND SPRING CONSTANT
8      C      2) PILE SEGMENT FORCE, STRESS AND VELOCITY AT
9      C      EACH TIME INTERVAL DEPENDING ON THE OPTION.
10     C      3) POINT DISPLACEMENT, NO OF BLOWS REQUIRED TO
11     C      PENETRATE ONE FT AND MAXIMUM STRESS IN A SEGMENT
12     C      AT EACH TIME INTERVAL
13     C      4) MAXIMUM STRESS EVER OBTAINED IN ANY PILE SEGMENT
14     C      AND AS A CHECK, THE LAST STRESS AND ELEMENT VELOCITY
15     C      COMPUTATIONS
16     C      5) IF SPECIFIED TENSILE STRESS FOR CONCRETE PILE
17     C      6) SUMMARY OF RESULTS INCLUDING ULTIMATE SOIL RESISTANCE
18     C      NO OF BLOWS REQUIRED TO PENETRATE, MAXIMUM COMPRESSIVE
19     C      STRESS IN THE PILE AND IF SPECIFIED MAXIMUM TENSILE
20     C      STRESS IN THE PILE.
21     C
22     C      DIMENSION C(40, 4), F(40, 2), V(40, 2), B(40, 7), W(40), SP(40),
23     C      D(40, 2), DE(40, 2), EK(40), R(40), IX(40), RU(40),
24     C      AF(40, 2), DE1(400), D1(400), KKK(40), FMAX(400),
25     C      JX(400), FM(40), A(40), DB(40), D1(40), FMIN(40, 2),
26     C      TITLE(40), ES(40, 2), RV(40, 7), BF(40, 7), REU(40),
27     C      BPF(40), CSMAX(40), CTS(40), SPLICE(40), SLACK(40),
28     C      ECOM(40), VCOM(40), CAS(40), WCOM(40), UWCOM(40),
29     C      ED(40, 7), RS(40, 7), FP(40, 250), STP(40, 250),
30     C      VP(40, 250), DP(40, 250), SSP(40, 250), RO(40), FO(40),
31     C      DO(40), CO(40), DEO(40), XS(40), YS(40), DC(40), RX(40),
32     C      XT(40), YT(40)
33     C
34     C      DOUBLE PRECISION UT4, UT5, UT6, UT7, UT8
35     C
36     C      COMMON EXPT, DT, INTV, TD, TI, TL, TR, TIND, TINI, TINI, TINI
37     C
38     2000 READ(6, 10, END=150) TITLE, UT1, UT2, UT3, UT4, UT5, UT6, UT7, UT8
39     10   FORMAT(20A4, /, 3(A4, 1X), 5(AH, 1X))
40     WRITE(6, 20) TITLE
41     20   FORMAT('1', //, 10X, 20A4)
42     READ(5, 30) FU1, FU2, FU3
43     30   FORMAT(3F11.3)
44     WRITE(6, 40) UT1, UT2, UT3, UT4, UT5, UT6, UT7, UT8, FU1, FU2, FU3
45     40   FORMAT(//, 5X, 3(A4, 3X), 5(A10, 3X), /, /, 5X, 3(F10.3, 3X))
46     2100 READ(5, 50) NELEM, NSAS, NSOIL, MDR, ELEML, TWALL, PILTYP
47     50   FORMAT(4I5, 2F7.3, F5.2)
48     READ(5, 70) IFHTYP, NCOM, STEAM, DIESEL
49     70   FORMAT(2I5, 2F5.1)
50     READ(5, 90) NPILOT, NW, IFD
51     90   FORMAT(3I5)
52     READ(5, 110) JJS, NCHECK, IFWRIT, IFFSV, NRU, NJOINT, COMPM
53     110  FORMAT(6I5, F7.2)
54     READ(5, 130) W(3), DRIVPT, DT
55     130  FORMAT(2F10.3, F10.8)
56     IF(NCOM.GT.0) THEN
57         DO 15, M = 3, NELEM
58         READ(5, 170) NE, ECOM(M), VCOM(M)

```



```

59      170  FORMAT(13,F10.2,F10.2)
60      CAS(M) = ECUM(M)/VCOM(M)
61      180  CONTINUE
62      CAS(LA) = CAS(LA-1)
63      ELSE
64      READ(5,190)EMOD,WVH1
65      190  FORMAT(2F10.2)
66      ENDIF
67      IF(1FHTYP.EQ.5)FO = NELEM - 2
68      IF(1FHTYP.EQ.7)FO = NELEM - 4
69      X = KO
70      LA = NELEM + 1
71      READ(5,210)ECAP,ACAP,THCAP,EPCB
72      210  FORMAT(4F10.4)
73      READ(5,230)ECUS,ACUS,THCUS,EPC
74      230  FORMAT(4F10.4)
75      IF(NSOIL.LT.1)READ(5,250)SJ,PJ,RS,RP
76      250  FORMAT(4F6.3)
77      IF(NSOIL.GT.1.AND.MDR.EQ.2)THEN
78      READ(5,270)(NS,DC(M),RX(M), M = 4,LA)
79      270  FORMAT(2(15,F5.3,F5.3))
80      ENDIF
81      IF(1FHTYP.EQ.5)THEN
82      IF(STEAM.GT.0.)THEN
83      READ(5,290)W(2),WH,RENG,EFF,STROKE
84      290  FORMAT(5F10.2)
85      IF(STROKE.EQ.0.0)STROKE = (RENG)/(W(2)*FU1)
86      ELSE
87      READ(5,310)W(2),WH,STRMAX,POP,PRELM,EFF
88      310  FORMAT(6F10.2)
89      READ(5,330)STROKE
90      330  FORMAT(F8.3)
91      IF(STROKE.EQ.0.0)THEN
92      STROKE = (STRMAX)*(1 + ((POP)*(WH))/((PRELM)*(W(2))))
93      ELSE
94      STROKE = STROKE
95      ENDIF
96      ENDIF
97      VIMP = SQRT(.2*FU1*EFF*STROKE)
98      ENDIF
99      IF(1FHTYP.EQ.7)THEN
100     READ(5,350)W(1),WH,EXPF,RENOP,DHF
101     350  FORMAT(5F10.2)
102     READ(5,370)DRAM,DBT,DAEP,TD,TI,TL,TR,EFF
103     370  FORMAT(3F7.3,4F8.5,F5.3)
104     READ(5,390)VFIN,PAT
105     390  FORMAT(F10.2,F10.5)
106     IF(TD.EQ.0)TD=0.001
107     IF(TI.EQ.0)TI=0.005
108     IF(TL.EQ.0)TL=0.005
109     IF(TR.EQ.0)TR=0.0025
110     IF(DBT.EQ.0)DBT = 0.1*(DRAM)
111     ARAM = 0.7854*(DRAM)**2
112     VIN = (DAEP)*(ARAM)*(FU1)
113     IF(VFIN.GT.0)FC = (PAT)*(((VIN/VFIN)+1)**1.30)*(ARAM)
114     IF(DHK.LE.0)THEN
115     READ(5,410)ERAM,EEAN,RAML,ANL,DAN
116     410  FORMAT(2F10.2,3F8.3)

```

```

117      KAN = (0.7654*(DAN)**.
118      DBE = (0.2*(KAM)*(DBAM/DBT)/(DB*(KAM+DBT))
119      ANE = (1EAN)*(KAN)/(ANE)
120      ENDDIF
121      READ(5,460)WAN,LAN
122      460  FORMAT(F10.2,F10.2)
123      IF(DIE.LL.GT.0.0)THEN
124      READ(5,450)STROFF
125      450  FORMAT(F10.2)
126      VIMP = SQRT(2*E*E*(STROFF - DARE)*EIE)
127      ELSE
128      READ(5,470)KIEFF
129      470  FORMAT(F10.2)
130      STROFF = (KIEFF)/W(1)
131      VIMP = SQRT(2*E*E*(STROFF - DARE)*EIE)
132      ENDDIF
133      ENDDIF
134      WRITE(6,600)X,ELEM,UT0,NELEM,NSAS
135      600  FORMAT(1X,/,10X,'** GENERAL INPUT DATA **',/,/,5X,'ELEMENT'
136      *      ,1X,'DETAILS',/,/,9X,'NO OF PILE SEGMENTS - ',F5.1,
137      *      /,9X,'LENGTH OF PILE ELEMENT - ',F7.3,1X,A2,/,9X,'NO'
138      *      ,1X,'OF ELEMENTS INCLUDING RAM AND CAP - ',14,/,9X,
139      *      'NO OF PILE SEGMENTS ABOVE GROUND LEVEL OR',/,9X,
140      *      'ASSUMED ZERO SIDE RESISTANCE ON PILE SEGMENTS'
141      *      ,1X,'- ',14,/)
142      IF(NCOM.LE.0)THEN
143      WRITE(6,800)EMOD,UT5,WVEL,UT6
144      800  FORMAT(1X,/,5X,'PILE DETAILS',/,/,9X,'PILE MODULUS OF',1X,
145      *      'OF ELASTICITY - ',F11.1,1X,A8,/,9X,'STRESS WAVE',
146      *      ,1X,'VELOCITY - ',F11.1,1X,A8,/)
147      ELSE
148      WRITE(6,100)UT5,UT6
149      100  FORMAT(9X,'SEGMENT NO',1X,'E VALUE',10X,'WAVE VELOCITY',/
150      *      ,24X,A10,10X,A10,/)
151      WRITE(6,120)(1,ECOM(1),VCOM(1),1-3,NELEM)
152      120  FORMAT(12X,14,1X,F12.2,1X,F12.2)
153      ENDDIF
154      IF(PILTYP.GT.0.0)THEN
155      IF(NCOM.LE.0)THEN
156      READ(5,490)WFT,AREA
157      490  FORMAT(2F10.4)
158      DO 25, 1 = 3,NELEM
159      A(1) = AREA
160      25  CONTINUE
161      ELSE
162      READ(5,510)(10,WCOM(M+1),A(M),M=3,NELEM)
163      510  FORMAT(13,F10.3,F10.3)
164      ENDDIF
165      GO TO 2200
166      ELSEIF(PILTYP.EQ.0.0)THEN
167      READ(5,530)(W(M+1),A(M),M=3,NELEM)
168      530  FORMAT(2F10.3)
169      GO TO 2200
170      ELSE
171      READ(5,550)DIAT,DIAB,UNITWT
172      550  FORMAT(3F10.3)
173      IF(NCOM.GT.0)READ(5,570)(IU,UWCOM(1),1-3,NELEM)
174      570  FORMAT(13,F10.4)

```

```

135      WRITE(6,140)DIAT,UT1,DIAB,UT2,TWALL,UT2,UNITWT
136      140  FORMAT(/,9X,'TOP DIAMETER = ',F10.3,1X,A2,/,9X,'BOTTOM'
137      *      ,1X,'DIAMETER = ',F10.3,1X,A2,/,9X,'WALL THICKNESS'
138      *      ,1X,' = ',F10.3,1X,A2,/,9X,'UNIT WEIGHT = ',F10.3/)
139      IF(NCOM.GT.0)THEN
140      WRITE(6,100)
141      100  FORMAT(/,9X,'SEGMENT NO',1X,'UNIT WEIGHT')
142      WRITE(6,180)(M,UWCOM(M),M=3,NELEM)
143      180  FORMAT(/,12X,13,12X,F10.3)
144      ENDF
145      DELD = (DIAT - DIAB)/X
146      BB = 0.5
147      DO 35, I = 1,E0
148      DB(I) = DIAT - BB*DELD
149      DI(I) = DB(I) - 0.5*TWALL
150      IF(TWALL.EQ.0)THEN
151      A(I) = .7854*((DB(I))**2)
152      ELSE
153      A(I) = 0.7854*((DB(I))**2 - (DI(I))**2)
154      ENDF
155      IF(NCOM.LE.0)THEN
156      W(I+1) = A(I)*UNITWT*ELEM1/FU1
157      SP(I+1) = A(I)*EMOD/(ELEM1*FU1)
158      ELSE
159      W(I+1) = A(I)*UWCOM(M)*ELEM1/FU1
160      SP(I+1) = A(I)*ECOM(M)/(ELEM1*FU1)
161      ENDF
162      BB = BB + 1
163      35  CONTINUE
164      ENDF
165      GO TO 2300
166      2200  DO 45 M = 3,NELEM
167      IF(NCOM.LE.0)THEN
168      SE(M) = A(M)*EMOD/(ELEM1*FU1)
169      ELSE
170      SE(M) = A(M)*ECOM(M)/(ELEM1*FU1)
171      ENDF
172      45  CONTINUE
173      IF(FILTYP.LE.0.0)GO TO 2300
174      DO 55 M = 4,LA
175      IF(NCOM.LE.0)THEN
176      W(M) = ELEM1*WFT
177      ELSE
178      W(M) = ELEM1*WCOM(M)
179      ENDF
180      55  CONTINUE
181      2300  W(LA) = W(LA) + DRIVPT
182      WP = 0
183      DO 65 M = 4,LA
184      WP = WP + W(M)
185      65  CONTINUE
186      IF(IFHTYP.EQ.5)WTO = WH + WP + W(3)
187      IF(IFHTYP.EQ.7)WTO = WH + WP + FC
188      IF(DHK.GT.0.AND.ANK.GT.0)THEN
189      AHK = 1./DHK + 1./ANK
190      SP(1) = 1./AHK
191      ELSE
192      SP(1) = DHK

```

```

233      ENDDIF
234      SP(1) = (ECAP) * (ACAP) / (THCAP)
235      IF (THBU,GT,0) SP = (LBU) * (ACUS) / (THBU)
236      IF (SC,GT,0) THEN
237          SPX = (1./SP(1)) * (1./SC)
238          SP(1) = 1./SPX
239      ENDDIF
240      IF (DT,EQ,0) DT = ((W(4)/(C(4)*FU*(BU))**0.5)/2.0
241      IF (ERTYPE,LE,0) EPC1 = 1./EPC**2
242          EPC = 1./EPC**2
243          EPC2 = 1./EPC**2
244          T = DT*FU
245          G = DT*FU*
246          INTV = 0
247          IEN = 0
248          NMF = 0
249          KBF(1) = 0
250          BPF(1) = 0
251          CMAX(1) = 0
252          CTN(1) = 0
253          IF (NMAINT,GT,0) THEN
254              DO 255 M = 4, NELEM
255          READ(5,500) MN, SPICE(M), SLACK(M)
256          FORMAT(15,F10.2,F8.5)
257          IF (SPICE(M),GT,0) SPICE(M) = SPICE(M)
258          IF (SLACK(M),GT,0) SLACK(M) = SLACK(M)
259          CONTINUE
260      ENDDIF
261          DO 262 M = NELEM, LA
262          SPICE(M) = 0
263          SLACK(M) = 0
264      CONTINUE
265      IF (FILTYPE,LE,0) THEN
266          WRITE(6,200) UT1, (A(N), N = 1,EO)
267          FORMAT(10X,'** COMPUTED PILE SEGMENT PROPERTIES **',/,5X,
268          * 'AREAS',1X,A6,1X,'= ',5F10.4/,20X,5F10.4/,
269          * '20X,5F10.4/,20X,5F10.4/,20X,5F10.4/,20X,5F10.4)
270          WRITE(6,220) UT3, (W(M), M = 4,LA)
271          FORMAT(5X,'WEIGHT',1X,A4,1X,'= ',5F10.4/,20X,5F10.4/,20X,
272          * '5F10.4/,20X,5F10.4/,20X,5F10.4/,20X,5F10.4)
273      ENDDIF
274      IF (FILTYPE,GT,0) THEN
275          IF (NCOM,LE,0) THEN
276              WRITE(6,240) UT1,WFT,UT3,AREA,UT7,TWALL,UT2
277          FORMAT(/,9X,'WT/',A2,1X,'OF PILE = ',F9.4,1X,A4/,9X,
278          * 'PILE X-SECTION AREA = ',F8.3,1X,A5/,9X,'WALL',1X,
279          * 'THICKNESS = ',F10.3,1X,A4,/)
280      ELSE
281          WRITE(6,260) UT1,UT3,UT7
282          FORMAT(/,9X,'WEIGHT/',A2,1X,'IN',1X,A4,7X,'AREA IN',1X,A8)
283          WRITE(6,280) (WCOM(M+1),A(M),M=3,NELEM)
284          FORMAT(/,12X,F10.3,15X,F8.3)
285      ENDDIF
286      ENDDIF
287      WRITE(6,300) UT3,W(3),DRIVPT,W(LA),WP,WTO
288      FORMAT(/,5X,'ELEMENT WEIGHTS IN',1X,A4,':',/,9X,'PILE CAP'
289      * '1X,'= ',F8.4/,9X,'WT OF DRIVE POINT = ',F9.4/,9X,
290      * 'WT OF BOTTOM ELEMENT + DRIVE POINT = ',F9.4/,9X,

```

```

291      * 'TOTAL WEIGHT OF PILE - ',F12.3,/,9X,'TOTAL STATIC',1X,
292      * 'LOAD RESISTED BY SOIL - ',F12.2,/)
293      WRITE(6,320)ECAP,UT5,ACAP,UT7,THCAP,UT2,SP(2),UT4,EPCB
294 320   FORMAT(5X,'CAP BLOCK DETAILS',1X,':',/,9X,'MODULUS OF',1X,
295      * 'ELASTICITY - ',F11.1,1X,A8,/,9X,'AREA OF X-SECTION'
296      * ',1X, - ',F8.3,1X,A8,/,9X,'THICKNESS - ',F6.3,1X,A4,/,
297      * '9X,'SPRING CONSTANT - ',F12.3,1X,A8,/,9X,'COEFFICIENT'
298      * ',1X,'OF RESTITUTION - ',F6.3,/)
299      IF(THCUS.GT.0)THEN
300      WRITE(6,340)ECUS,UT5,ACUS,UT7,THCUS,UT2,SC,UT4,EPC
301 340   FORMAT(5X,'PILE CUSHION DETAILS',1X,':',/,9X,'MODULUS OF',
302      * '1X,'ELASTICITY - ',F11.1,1X,A8,/,9X,'AREA OF',1X,
303      * 'X SECTION - ',F8.3,1X,A8,/,9X,'THICKNESS - ',
304      * 'F6.3,1X,A4,/,9X,'SPRING CONSTANT - ',F12.3,1X,A8,/,
305      * '9X,'COEFFICIENT OF RESTITUTION - ',F6.3,/)
306      ENDIF
307      WRITE(6,360)SP(3),UT4,SP(4),UT4
308 360   FORMAT(/,5X,'PILE SPRING CONSTANTS',1X,':',/,9X,'1ST PILE'
309      * ',1X,'SEGMENT - ',F12.3,1X,A8,/,9X,'2ND PILE SEGMENT'
310      * ',1X, - ',F12.3,1X,A8,/)
311      IF(NSOIL.LT.1)WRITE(6,380)SJ,PJ,RS,RP
312 380   FORMAT(1X,/,5X,'ASSUMED DAMPING CONSTANTS',1X,':',/,9X,
313      * 'SIDE - ',F6.3,/,9X,'POINT - ',F6.3,/,5X,
314      * 'VELOCITY EXPONENTION',1X,':',/,9X,'SIDE - ',F6.3,
315      * '/,9X,'POINT - ',F6.3,/)
316      IF(NSOIL.GT.1)THEN
317      WRITE(6,400)
318 400   FORMAT(1X,/,5X,'ASSUMED DAMPING CONSTANTS',1X,':',/,9X,
319      * 'ELEMENT NO',5X,'DAMPING CONSTANT',5X,
320      * 'EXPONENTION',/)
321      WRITE(6,420)(M,DC(M),RX(M),M-4,LA)
322 420   FORMAT(10X,15,14X,F6.3,12X,F6.3)
323      ENDIF
324      IF(MDR.EQ.1)WRITE(6,440)
325 440   FORMAT(/,12X,'** DYNAMIC RESISTANCE IS COMPUTED **',/
326      * ',12X,'** USING CASE-METHOD **',/)
327      IF(MDR.EQ.2.AND.RS.EQ.1.0)WRITE(6,460)
328 460   FORMAT(/,12X,'** DYNAMIC RESISTANCE IS COMPUTED **',/
329      * ',12X,'** USING SMITH'S PROPOSAL **',/)
330      IF(NSOIL.LT.1.AND.RS.LT.1.0)WRITE(6,480)
331 480   FORMAT(/,12X,'** DYNAMIC RESISTANCE IS COMPUTED USING **',
332      * '/,12X,'** SMITH'S EQUATION WITH VELOCITY',1X,
333      * 'EXPONENTION **',/)
334      IF(NSOIL.GT.1.AND.RS.LT.1)WRITE(6,500)
335 500   FORMAT(/,12X,'** DYNAMIC RESISTANCE IS COMPUTED USING **',/
336      * '12X,'NON LINEAR RELATIONSHIP FOR MORE THAN ONE',1X,
337      * 'SOIL LAYER **')
338      WRITE(6,520)DT
339 520   FORMAT(/,9X,'TIME INTERVAL - ',F10.8,1X,'SEC',/)
340      IF(1FHTYP.EQ.5)THEN
341      IF(STEAM.GT.0.)THEN
342      WRITE(6,540)W(2),UT3,WH,UT3,RENG,UT4,EFF,STROKE,UT1,VIMP,UT6
343 540   FORMAT(1X,/,5X,'DROP OR SINGLE ACTING HAMMER DETAILS',1X,':',
344      * '/,9X,'WT OF RAM - ',F10.2,1X,A4,/,9X,'WT OF HOUSING',
345      * '1X, - ',F10.2,1X,A4,/,9X,'RATED HAMMER',
346      * '1X,'ENERGY - ',F12.2,1X,A8,/,9X,'HAMMER EFFICIENCY',
347      * '1X, - ',F5.3,/,9X,'HAMMER STROKE - ',F7.2,1X,A4,
348      * '/,9X,'VELOCITY AT IMPACT - ',F7.2,1X,A8,/)

```

```

141      ELSE
142      WRITE(6,560)W(2),UT1,WH,UT3,STRMAX,UT1,POP,UT5,PRELIM,UT5,EFF
143      FORMAT(1X,/,5X,'DOUBLE OR DIFFERENTIAL ACTING HAMMER DETAILS'
144      *      ', ',/,9X,'WEIGHT OF RAM - ',F10.2,1X,A4,/,9X,'WEIGHT'
145      *      ', ',/,9X,'OF HOUSING - ',F10.2,1X,A4,/,9X,'MAXIMUM HAMMER',
146      *      '1X,'STROKE - ',F7.2,1X,A4,/,9X,'OPERATING AIR/STEAM',
147      *      '1X,'PRESSURE - ',F12.2,1X,A10,/,9X,'MANUFACTURER'S',1X,
148      *      'RATED LIMITING PRESSURE - ',F12.2,1X,A10,/,9X,'HAMMER'
149      *      ', ',/,9X,'EFFICIENCY - ',F5.3,/)
150      WRITE(6,580)STROKE,UT1,VIMP,UT6
151      FORMAT(1X,/,9X,'HAMMER STROKE - ',F7.2,1X,A4,/,9X,'VELOCITY'
152      *      '1X,'AT IMPACT - ',F7.2,1X,A8,/)
153      ENDIF
154      ENDIF
155      IF(IFHTYP.EQ.7)THEN
156      WRITE(6,600)W(1),UT3,WH,UT3,EXPF,UT3,RENOP,DRAM,UT2,DET,UT3
157      FORMAT(1X,/,5X,'DIESEL HAMMER DETAILS : ',/,9X,'WEIGHT OF',
158      *      '1X,'RAM - ',F10.2,1X,A4,/,9X,'WEIGHT OF HOUSING - ',
159      *      'F10.2,1X,A4,/,9X,'EXPLOSIVE FORCE AT IMPACT - ',F10.2,
160      *      '1X,A4,/,9X,'RATED HAMMER',1X,
161      *      '1X,'ENERGY OUTPUT - ',F10.2,/,9X,'TOP DIAMETER OF RAM - '
162      *      ',F7.3,1X,A4,/,9X,'BOTTOM DIAMETER OF RAM - ',F7.3,1X,A4,/)
163      WRITE(6,620)FC,UT3,PAT,UT5,DHK,UT4,DAEP,UT1,ARAM,UT7,EPF
164      FORMAT(9X,'FORCE EXERTED BY COMPRESSED GAS - ',F10.3,1X,
165      *      'A4,/,9X,'ATMOSPHERIC PRESSURE - ',F10.5,1X,A8,
166      *      ',/,9X,'STIFFNESS OF RAM - ',F10.2,1X,A10,/,9X,
167      *      'DISTANCE FROM ANVIL TO EXHAUST PORT - ',F5.2,1X,
168      *      'A4,/,9X,'RAM AREA OF CROSS-SECTION - ',F8.2,1X,A6,
169      *      ',/,9X,'HAMMER EFFICIENCY - ',F5.3,/)
170      WRITE(6,640)WAN,UT3,EAN,TD,TI,TL,TR,VIN,UTH,VFIN,UTH
171      FORMAT(1X,/,9X,'WEIGHT OF ANVIL - ',F10.2,1X,A4,
172      *      ',/,9X,'COEFFICIENT OF RESTITUTION - ',F5.3,/,9X,
173      *      'DETAILS OF EXPLOSIVE FORCE EFFECTIVE TIME: ',/,12X,
174      *      '1) DELAY TIME - ',F8.5,1X,'SEC',/,12X,
175      *      '2) RAISE TIME - ',F8.5,1X,'SEC',/,12X, '3) PEAK TIME - ',
176      *      'F8.5,1X,'SEC',/,12X, '4) EXHAUST TIME - ',F8.5,1X,'SEC',/,
177      *      '9X,'INITIAL VOLUME OF GAS - ',F10.2,1X,A6,/,9X,
178      *      'VOLUME OF COMBUSTION CHAMBER - ',F10.3,1X,A6,/)
179      IF(ANK.GT.0)THEN
180      WRITE(6,660)ERAM,UT5,EEAN,UT5,RAML,UT1,ANL,UT2,DAN,UT2
181      FORMAT(/,9X,'ELASTIC MODULUS OF RAM MATERIAL - ',F10.2,
182      *      '1X,A10,/,9X,'ELASTIC MODULUS OF ANVIL MATERIAL - ',
183      *      'F10.2,1X,A10,/,9X,'LENGTH OF RAM - ',F7.2,1X,A4,/,9X,
184      *      'LENGTH OF ANVIL - ',F7.2,1X,A4,/,9X,'DIAMETER OF',1X,
185      *      'ANVIL - ',F7.2,1X,A4,/)
186      WRITE(6,680)DHK,UT4,ANK,UT4,SP(1),UT4,AAN,UT7
187      FORMAT(1X,/,10X,'** COMPUTED HAMMER DETAILS **',/,9X,
188      *      'STIFFNESS OF RAM - ',F10.2,1X,A10,/,9X,
189      *      'STIFFNESS OF ANVIL - ',F10.2,1X,A10,/,9X,
190      *      'COMBINED STIFFNESS OF RAM AND ANVIL - ',F10.2,1X,A10
191      *      ',/,9X,'ANVIL AREA OF CROSS-SECTION - ',F8.2,1X,A6,/)
192      ENDIF
193      IF(DIESEL.GT.0)THEN
194      WRITE(6,700)STROKE,UT1,VIMP,UT6
195      FORMAT(9X,'OBSERVED RAM TOTAL STROKE - ',F7.2,1X,A4,/,9X,
196      *      'VELOCITY AT IMPACT - ',F7.2,1X,A10,/)
197      ELSE
198      RIENP = 12*RIENP

```

```

407      WRITE(6,720)RIENP,UT4,STROKE,UT1,VIMP,UT6
408 720  FORMAT(1X,/,9X,'INDICATED RAM ENERGY =',F10.2,1X,A10,/,9X,
409      'EQUIVALENT STROKE =',F7.2,1X,A4,/,9X,'VELOCITY AT',
410      1X,'IMPACT =',F7.2,1X,A10,/)
411      ENDIF
412      ENDIF
413      IF(NSJOINT.GT.0)THEN
414      WRITE(6,740)UT3,UT2
415 740  FORMAT(/,5X,'SPlice DETAILS',/,/,10X,'SPRING NO',5X,'SPlice'
416      ,1X,'FORCE',5X,'SLACK ALLOWED',/,25X,'IN',1X,A6,9X,
417      'IN',1X,A4,/)
418      WRITE(6,760)(M,SPlice(M),SLACK(M),M = 4,LA)
419 760  FORMAT(10X,15,7X,F10.2,10X,F8.5)
420      ELSE
421      WRITE(6,780)
422 780  FORMAT(/,20X,'** NO SPLICE OR CONNECTOR USED **')
423      ENDIF
424 2400  READ(5,610)QS,QP
425 610  FORMAT(2F8.3)
426      IF(QS.LE.0.AND.QP.LE.0)GO TO 2000
427 2500  READ(5,630)PER
428 630  FORMAT(F8.3)
429      IF(PER.LT.0.0)GO TO 2000
430 2600  READ(5,650)RUTOT,ECAP,ACAP,THCAP
431 650  FORMAT(F12.3,3F10.2)
432      SP(2) = (ECAP)*(ACAP)/(THCAP)
433      NPS = 0
434      NZS = 0
435      IF(RUTOT.GT.0.0)NSR = NSR + 1
436      IF(RUTOT)150,2000,2700
437 2700  WRITE(6,800)PER
438 800  FORMAT(/,9X,'***** % OF RUTOT CARRIED BY PILE POINT = ',
439      F6.3,/)
440      WRITE(6,820)RUTOT,UT3,SP(2)
441 820  FORMAT(/,9X,'***** ASSUMED ULTIMATE PILE RESISTANCE = ',
442      F10.2,1X,A4,/,9X,'***** CAP BLOCK = ',F12.3,/)
443      WRITE(6,840)UT3
444 840  FORMAT(15X,'I',4X,'R(U) IN',1X,A4)
445      IF(JJS.EQ.1.)THEN
446      READ(5,670)(IP,RU(1),I = 4,NELEM)
447 670  FORMAT(4(15,F10.4))
448      ELSE
449      DO 95, M = 4,NELEM
450      RU(M) = (1. - PER)*RUTOT/(X - (NSAS+1))
451 95  CONTINUE
452      ENDIF
453      DO 105, M = 1,NSAS
454      RU(M+3)=0
455 105  CONTINUE
456      RU(LA) = RUTOT*PER
457      WRITE(6,860)(M,RU(M),M = 4,LA)
458 860  FORMAT(14X,12,F12.2)
459      DO 115, M = 3,LA
460      IF(M.GT.3)EK(M) = RU(M)/QS
461      V(M,1) = 0
462 115  CONTINUE
463      IF(QS.NE.QP)EK(LA)=RU(LA)/QP
464      IF(IFHTYP.EQ.7)THEN

```

```

400000      A(1) = A(1)
400001      A(2) = A(2)
400002      A(3) = A(3)
400003      A(4) = A(4)
400004      A(5) = A(5)
400005      A(6) = A(6)
400006      A(7) = A(7)
400007      A(8) = A(8)
400008      A(9) = A(9)
400009      A(10) = A(10)
400010      A(11) = A(11)
400011      A(12) = A(12)
400012      A(13) = A(13)
400013      A(14) = A(14)
400014      A(15) = A(15)
400015      A(16) = A(16)
400016      A(17) = A(17)
400017      A(18) = A(18)
400018      A(19) = A(19)
400019      A(20) = A(20)
400020      A(21) = A(21)
400021      A(22) = A(22)
400022      A(23) = A(23)
400023      A(24) = A(24)
400024      A(25) = A(25)
400025      A(26) = A(26)
400026      A(27) = A(27)
400027      A(28) = A(28)
400028      A(29) = A(29)
400029      A(30) = A(30)
400030      A(31) = A(31)
400031      A(32) = A(32)
400032      A(33) = A(33)
400033      A(34) = A(34)
400034      A(35) = A(35)
400035      A(36) = A(36)
400036      A(37) = A(37)
400037      A(38) = A(38)
400038      A(39) = A(39)
400039      A(40) = A(40)
400040      A(41) = A(41)
400041      A(42) = A(42)
400042      A(43) = A(43)
400043      A(44) = A(44)
400044      A(45) = A(45)
400045      A(46) = A(46)
400046      A(47) = A(47)
400047      A(48) = A(48)
400048      A(49) = A(49)
400049      A(50) = A(50)
400050      A(51) = A(51)
400051      A(52) = A(52)
400052      A(53) = A(53)
400053      A(54) = A(54)
400054      A(55) = A(55)
400055      A(56) = A(56)
400056      A(57) = A(57)
400057      A(58) = A(58)
400058      A(59) = A(59)
400059      A(60) = A(60)
400060      A(61) = A(61)
400061      A(62) = A(62)
400062      A(63) = A(63)
400063      A(64) = A(64)
400064      A(65) = A(65)
400065      A(66) = A(66)
400066      A(67) = A(67)
400067      A(68) = A(68)
400068      A(69) = A(69)
400069      A(70) = A(70)
400070      A(71) = A(71)
400071      A(72) = A(72)
400072      A(73) = A(73)
400073      A(74) = A(74)
400074      A(75) = A(75)
400075      A(76) = A(76)
400076      A(77) = A(77)
400077      A(78) = A(78)
400078      A(79) = A(79)
400079      A(80) = A(80)
400080      A(81) = A(81)
400081      A(82) = A(82)
400082      A(83) = A(83)
400083      A(84) = A(84)
400084      A(85) = A(85)
400085      A(86) = A(86)
400086      A(87) = A(87)
400087      A(88) = A(88)
400088      A(89) = A(89)
400089      A(90) = A(90)
400090      A(91) = A(91)
400091      A(92) = A(92)
400092      A(93) = A(93)
400093      A(94) = A(94)
400094      A(95) = A(95)
400095      A(96) = A(96)
400096      A(97) = A(97)
400097      A(98) = A(98)
400098      A(99) = A(99)
400099      A(100) = A(100)

```



```

512      ENCL
513      NLELEM
514      DEGLA(1) = DEGLA
515      DEFORMED EQUATION = 0
516      DEFORMED EQUATION = 1
517      DO 205, M = 1, NLELEM
518          CDM(1) = CDM
519      IF (CDM(1) .EQ. 0) THEN
520          CDM(1) = CDM
521      ELSE
522          CDM(1) = CDM
523      ENDIF
524      ENCL
525      CONTINUE
526      DEGLA(1) = 0
527      ** INITIAL MOTIVATION CONSTANT TO PERFORM
528      NC = 0
529      FL = 0
530      PMIN = 0
531      NMIN = 0
532      IMIN = 0
533      EMIN = 0
534      EMAX = 0
535      EFCUT = 0
536      DEMAX = 0
537      CMAXY = 0
538      CMAX = 0
539      CMAXX = 0
540      DEFORM EQUATION OVERLAP = 0.004
541      DEFORM EQUATION PERIM = 0.0
542      DEFORM EQUATION PERI = 0.49
543      DEFORM EQUATION PERI = 0.0
544      ** INITIALIZE TO COMPUTE FILE SEGMENT PERI AND PERI
545      I = 0
546      J = 1
547      MM = 1
548      INUM = 0
549      IF (CDM(1) .EQ. 0) THEN
550          INTV = 1
551          TINI = (TI) / (CI)
552          TINI = (TI + TI) / (CI)
553          TINI = (TI + TI + TI) / (CI)
554          TINI = (TI + TI + TI + TI) / (CI)
555      ENDIF
556      ** (LA) IS THE INSTANT POINT DISPLACEMENT **
557      IF (CDM(1) .EQ. 0) THEN
558          DO 205, M = 1, NLELEM
559              D(M,2) = D(M,1) + V(M,1)*T
560          CONTINUE
561      ENDIF
562      IF (CDM(1) .EQ. 0) THEN
563          DO 215, M = 1, NLELEM
564              D(M,2) = D(M,1) + V(M,1)*T
565          CONTINUE
566      ENDIF
567      DO 225, M = 1, NLELEM
568          DE(M,2) = 0
569      IF (PER.EQ.1) GO TO 225
570      ** TO OBTAIN PLASTIC DEFORM OF TOTAL DEFORM **
571      IF ((QS - D(M,2)) .GT. 0.0) GO TO 2900

```



```

637         ENDDI
638         IF (V(LA,1) .GE. 0) THEN
639             R(LA) = (D(LA,2) - DE(LA,2)) * EF(LA) * (1. - DC(LA,1)) * RX(LA)
640             IF (V(LA,1) .LT. 0) THEN
641                 V(LA,1) = ABS(V(LA,1))
642                 R(LA) = (D(LA,2) - DE(LA,2)) * EF(LA) * (1. - DC(LA,1)) * RX(LA)
643                 V(LA,1) = -V(LA,1)
644             ENDIF
645         ENDIF
646     ENDDI
647     IF (MPE .EQ. 0.0 .AND. NSOIL .GT. 0) THEN
648         IF ((QP - D(LA,2)) .GT. 0.0) GO TO 3250
649         DE(LA,2) = D(LA,2) - QP
650         IF (PEE .EQ. 0) GO TO 3350
651         DO 344, M = 4, NELEM
652             IF (Q(M,1) - DE(M,2)) .EQ. 0 THEN
653                 IF (V(M,1) .GE. 0) THEN
654                     R(M) = (D(M,2) - DE(M,2)) * EF(M) * QP * DC(M) * (1. - DC(M,1)) * RX(M)
655                     IF (V(M,1) .LT. 0) THEN
656                         V(M,1) = ABS(V(M,1))
657                         R(M) = (D(M,2) - DE(M,2)) * EF(M) * QP * DC(M) * (1. - DC(M,1)) * RX(M)
658                         V(M,1) = -V(M,1)
659                     ENDIF
660                 ELSE
661                     IF (V(M,1) .GE. 0) THEN
662                         R(M) = (D(M,2) - DE(M,2)) * EF(M) * (1. - DC(M,1)) * DC(M) * (V(M,1) * RX(M))
663                     ELSE
664                         V(M,1) = ABS(V(M,1))
665                         R(M) = (D(M,2) - DE(M,2)) * EF(M) * (1. - DC(M,1)) * DC(M) * (V(M,1) * RX(M))
666                         V(M,1) = -V(M,1)
667                     ENDIF
668                 ENDIF
669             CONTINUE
670             IF ((D(LA,2) - DE(LA,2)) .EQ. 0) THEN
671                 IF (V(LA,1) .GE. 0) THEN
672                     R(LA) = (D(LA,2) - DE(LA,2)) * EF(LA)
673                     * QP * DC(LA) * EF(LA) * (V(LA,1) * RX(LA))
674                 ELSE
675                     V(LA,1) = ABS(V(LA,1))
676                     R(LA) = (D(LA,2) - DE(LA,2)) * EF(LA)
677                     * QP * DC(LA) * EF(LA) * (V(LA,1) * RX(LA))
678                     V(LA,1) = -V(LA,1)
679                 ENDIF
680             ELSE
681                 IF (V(LA,1) .GE. 0) THEN
682                     R(LA) = (D(LA,2) - DE(LA,2)) * EF(LA) * (1. + DC(LA,1)) * (V(LA,1) * RX(LA))
683                 ELSE
684                     V(LA,1) = ABS(V(LA,1))
685                     R(LA) = (D(LA,2) - DE(LA,2)) * EF(LA) * (1. - DC(LA,1)) * (V(LA,1) * RX(LA))
686                     V(LA,1) = -V(LA,1)
687                 ENDIF
688             ENDIF
689         ENDIF
690     CALL OVERFL(IV)
691     IF (IV .NE. 2) GO TO 5900
692     C FIND MAXIMUM POINT SET VALUE FOR LATER AVERAGING OF SET
693     C VALUE (DE(LA,2))

```

```

737      IF (D(1,2).LT.DELIMANE) NEN = NEN + 1
738      IF (D(1,2).LT.DENZ) = NEN + 1
739      NEN = NEN - NEN
740      D(1,1) = D(1,2)
741      IF (D(1,1).LT.DEMAX) GO TO 3400
742      DEMAX = D(1,1)
743      D(1,1) = D(1,2)
744      IF (IHTYPE.EQ.5) THEN
745      DO 205, M = 2, NITEM
746      C(M,2) = D(M,2) - D(CM(1),2)
747      CONTINUE
748      ENDF
749      IF (IHTYPE.EQ.7) THEN
750      DO 205, M = 1, NITEM
751      C(M,2) = D(M,2) - D(CM(1),2)
752      CONTINUE
753      ENDF
754      C ***** COMPUTE FORCES AND STRESSES IN PILE CAP *****
755      IF (IHTYPE.EQ.7) THEN
756      IF (I.EQ.1) GO TO 3500
757      IF (C(1,2).LT.C(1,1).AND.EN.EQ.0) GO TO 3600
758      IF (C(1,2).LT.CMAX) GO TO 3600
759      IF (C(1,2).GT.C(1,1)) EN = 0
760      F(1,2) = C(1,2)*SP(1)
761      ES(1,2) = F(1,2)/(ACAP)
762      GO TO 3700
763      IF (EN.EQ.1)
764      IF (EN.EQ.1) CMAXH = C(1,1)
765      IF (EN.GE.1) CMAX = CMAXH
766      F(1,2) = SP(1)*CMAX + SP(1)*ECB*(C(1,2) - CMAX)
767      ES(1,2) = F(1,2)/(ACAP)
768      IF (F(1,2).LT.0.) F(1,2) = 0.0
769      IF (ES(1,2).LT.0.) ES(1,2) = 0.0
770      ENDF
771      IF (I.EQ.1) GO TO 3800
772      IF (C(2,2).LT.C(2,1).AND.IM.EQ.0) GO TO 3900
773      IF (C(2,2).LT.CMAX) GO TO 3900
774      IF (C(2,2).GE.C(2,1)) IM = 0
775      F(2,2) = C(2,2)*SP(2)
776      ES(2,2) = F(2,2)/(ACAP)
777      GO TO 4000
778      IF (IM.EQ.1)
779      IF (IM.EQ.1) CMAXH = C(2,1)
780      IF (IM.GE.1) CMAX = CMAXH
781      F(2,2) = SP(2)*CMAX + SP(2)*ECB*(C(2,2) - CMAX)
782      ES(2,2) = F(2,2)/(ACAP)
783      IF (F(2,2).LT.0.) F(2,2) = 0
784      IF (ES(2,2).LT.0.) ES(2,2) = 0
785      C ***** COMPUTE FORCE AND STRESS IN FIRST PILE SEGMENT. PILE
786      C CAP CANNOT CARRY TENSION. *****
787      IF (I.EQ.1) GO TO 4100
788      IF (C(3,2).LT.C(3,1).AND.KM.EQ.0) GO TO 4200
789      IF (C(3,2).LT.CMAX) GO TO 4200
790      IF (C(3,2).GE.C(3,1)) KM = 0
791      F(3,2) = C(3,2)*SP(3)
792      IF (ACUS.GT.0) ES(3,2) = F(3,2)/(ACUS)
793      GO TO 4300
794      IF (KM.EQ.1)
795      IF (KM.EQ.1) CMAXH = C(3,1)
796      IF (KM.GE.1) CMAX = CMAXH
797      F(3,2) = SP(3)*CMAX + SP(3)*ECB*(C(3,2) - CMAX)
798      ES(3,2) = F(3,2)/(ACUS)
799      IF (F(3,2).LT.0.) F(3,2) = 0
800      IF (ES(3,2).LT.0.) ES(3,2) = 0

```

```

755      IF (FM.EQ.1) CMAXXH = C(1,1)
756      IF (FM.GE.1) CMAXX = CMAXXH
757      F(1,2) = SP(4)*CMAXX + SP(3)*FV1*(C(1,2)-CMAXX)
758      IF (ACUS.GT.0) THEN
759          ES(1,2) = F(1,2)/(ACUS)
760      ELSE
761          ES(1,2) = F(1,2)/(A(4))
762      ENDIF
763      4400 IF (F(1,2).LT.0) F(1,2) = 0
764      IF (ES(1,2).LT.0) ES(1,2) = 0
765      ** COMPUTE FORCES AND STRESSES IN REMAINING FILE SEGMENTS **
766      KL = KL + 1
767      IX(KL) = 1
768      DO 775, M = 4, NELEM
769          F(M,2) = C(M,2)*SP(M)
770      IF (NJOINT.GT.0) THEN
771          IF (C(M,2).LT.0.AND.C(M,2).GT.SLACK(M)) F(M,2) = 0
772          IF (C(M,2).LT.SLACK(M)) F(M,2) = (C(M,2)-SLACK(M))*SP(M)
773          IF (F(M,2).LT.SPLICE(M).AND.SPLICE(M).LT.0.0) F(M,2) = SPLICE(M)
774      ENDIF
775          ES(M,2) = F(M,2)/A(M)
776          BF(M,KL) = F(M,2)
777          B(M,KL) = ES(M,2)
778          BV(M,KL) = V(M,1)
779          BD(M,KL) = D(M,2)
780          BS(M,KL) = DE(M,2)
781      775 CONTINUE
782      F(LA,2) = R(LA)
783      ES(LA,2) = F(LA,2)/A(LA,1)
784      IF (ECOUN.IE.0) GO TO 4400
785      KKK(2) = 0
786      ** TEST FOR TENSION (NEGATIVE) SEGMENT STRESS **
787      IF (IFHTYP.EQ.7) IL = 1
788      IF (IFHTYP.EQ.5) IL = 2
789      DO 285, M = 1L, LA
790          FM(M) = ES(M,2)
791      IF (ES(M,2).GE.FM(M)) GO TO 285
792      IF (ES(M,2).LT.ES(M,1)) KKK(2) = KKK(1) + 1
793      285 CONTINUE
794      4400 IF (IFHTYP.EQ.5) THEN
795          B(2,KL) = ES(2,2)
796          B(3,KL) = ES(3,2)
797          B(LA,KL) = ES(LA,2)
798          BF(2,KL) = F(2,2)
799          BF(3,KL) = F(3,2)
800          BF(LA,KL) = F(LA,2)
801          BV(2,KL) = V(2,1)
802          BV(3,KL) = V(3,1)
803          BV(LA,KL) = V(LA,1)
804          BD(2,KL) = D(2,2)
805          BD(3,KL) = D(3,2)
806          BD(LA,KL) = D(LA,2)
807          BS(LA,KL) = DE(LA,2)
808      ENDIF
809      IF (IFHTYP.EQ.7) THEN
810          B(1,KL) = ES(1,2)
811          B(2,KL) = ES(2,2)
812

```

```

807          B(1,FI) = B(1,2)
808          B(1A,FI) = B(1A,2)
809          BF(1,FI) = F(1,2)
810          BF(2,FI) = F(2,2)
811          BF(3,FI) = F(3,2)
812          B(1A,FI) = F(1A,2)
813          BV(1,FI) = V(1,2)
814          BV(2,FI) = V(2,2)
815          BV(3,FI) = V(3,2)
816          BV(1A,FI) = V(1A,2)
817          BD(1,FI) = D(1,2)
818          BD(2,FI) = D(2,2)
819          BD(3,FI) = D(3,2)
820          BD(1A,FI) = D(1A,2)
821          BD(1A,FI) = D(1A,2)
822          EN11F
823          IF(IFHTYPE.EQ.7)FF=1
824          IF(IFHTYPE.EQ.5)FF=2
825          NC = NC + 1
826          DO 295, M = KP,LA
827          FP(M,NC) = F(M,2)
828          STP(M,NC) = ES(M,2)
829          VP(M,NC) = V(M,2)
830          DP(M,NC) = D(M,2)
831          IF(M.GE.4)SSP(M,NC) = D(M,2)
832          CONTINUE
833          IF(I.GT.3)GO TO 4500
834          IF(IFHTYPE.EQ.7)LN = 1
835          IF(IFHTYPE.EQ.5)LN = 2
836          DO 305, N = LN,LA
837          AF(N,1) = B(N,FI)
838          FMIN(N,1) = B(N,KL)
839          FMIN(N,2) = 1
840          AF(N,2) = 1
841          CONTINUE
842          ** FIND MAXIMUM ELEMENT STRESS AND CORRESPONDING DT **
843          4500 IF(IFHTYPE.EQ.7)LI = 1
844          IF(IFHTYPE.EQ.5)LI = 2
845          DO 315, N = 11,LA
846          IF(B(N,KL).LE.AF(N,1))GO TO 4600
847          AF(N,1) = B(N,FI)
848          AF(N,2) = 1
849          4600 IF(COMPM.LE.0)GO TO 315
850          IF(B(N,KL).GT.FMIN(N,1))GO TO 4700
851          FMIN(N,1) = B(N,KL)
852          FMIN(N,2) = 1
853          4700 IF(N.LT.4.OR.N.GT.NELEM)GO TO 315
854          IF(B(N,KL).GE.BMIN)GO TO 315
855          BMIN = B(N,KL)
856          NMIN = N
857          IMIN = 1
858          315 CONTINUE
859          IF(KCOUN.LE.0)GO TO 4800
860          IF(KKK(2).LE.KKK(1))GO TO 5700
861          KKK(1) = KKK(2)
862          4800 FMAX(1) = B(4,KL)
863          JX(1) = 4
864          DO 325, K = 5,LA

```

```

871      IF(B(F,FI).GT.FMAX(1))FMAX(1) = B(F,KL)
872      IF(B(F,FI).EQ.FMAX(1))IX(1) = F
873      CONTINUE
874      IF(KL.LT.7)GO TO 5000
875      IF(1.LT.8.AND.(IFWRITE.GT.0)THEN
876      IF(IFFSV.EQ.1)WRITE(6,880)UT3
877      880  FORMAT(//,15X,'COMPUTED SEGMENT FORCE IN',1X,A4,/)
878      IF(IFFSV.EQ.2)WRITE(6,900)UT5
879      900  FORMAT(//,15X,'COMPUTED SEGMENT STRESS IN',1X,A6,/)
880      IF(IFFSV.EQ.3)WRITE(6,920)UT6
881      920  FORMAT(//,15X,'COMPUTED SEGMENT VELOCITY IN',1X,A6,/)
882      IF(IFFSV.EQ.4)WRITE(6,940)UT2
883      940  FORMAT(//,15X,'COMPUTED SEGMENT DISPLACEMENT IN',1X,A2,/)
884      IF(IFFSV.EQ.5)WRITE(6,960)UT7
885      960  FORMAT(//,15X,'COMPUTED PILE SEGMENT SET IN',1X,A2,/)
886      ENDIF
887      IF(IFWRITE.LE.0)GO TO 4900
888      WRITE(6,980)(1X(NN),NN = 1,7)
889      980  FORMAT(//,7X,'DT-',3X,14,6(7X,14))
890      IF(IFHTYP.EQ.7)NL = 1
891      IF(IFHTYP.EQ.5)NL = 2
892      IF(IFFSV.EQ.1)WRITE(6,1000)((B(11,JJ),JJ=1,7),11-NL,LA)
893      1000  FORMAT(9X,7F11.2)
894      IF(IFFSV.EQ.2)WRITE(6,1020)((B(11,JJ),JJ=1,7),11-NL,LA)
895      1020  FORMAT(9X,7F11.2)
896      IF(IFFSV.EQ.4)WRITE(6,1040)((BV(11,JJ),JJ=1,7),11-NL,LA)
897      1040  FORMAT(9X,7F11.2)
898      IF(IFFSV.EQ.4)WRITE(6,1060)((BD(11,JJ),JJ=1,7),11-NL,LA)
899      1060  FORMAT(12X,7F10.5)
900      IF(IFFSV.EQ.5)WRITE(6,1080)((BS(11,JJ),JJ=1,7),11-4,LA)
901      1080  FORMAT(12X,7F10.5)
902      4900      KL = 0
903      5000  IF(IFHTYP.EQ.5)THEN
904          DO 345, M = 2,LA
905          IF(M.EQ.LA)GO TO 5100
906          V(M,2) = V(M,1)+(F(M-1,2)+W(M)-F(M,2)-R(M))*G/W(M)
907          GO TO 5200
908      5100  V(M,2) = V(M,1)+(F(M-1,2)+W(M)-R(M))*G/W(M)
909      5200  CALL OVERFL(IV)
910          IF(IV.NE.2)GO TO 5900
911          IF(V(M,2).GT.0.0)GO TO 345
912          LSUM = LSUM + 1
913      335  CONTINUE
914      ENDIF
915      IF(IFHTYP.EQ.7)THEN
916      F(1,2) = F(1,2) + FFEX(INTV)
917      DO 345, M = 1,LA
918      IF(M.EQ.LA)GO TO 5300
919      V(M,2)=V(M,1)+(F(M-1,2)+W(M)-F(M,2)-R(M))*G/W(M)
920      GO TO 5400
921      5300  V(M,2)=V(M,1)+(F(M-1,2)+W(M)-R(M))*G/W(M)
922      5400  CALL OVERFL(IV)
923      IF(IV.NE.2)GO TO 5900
924      IF(V(M,2).GT.0.0)GO TO 345
925      LSUM = LSUM + 1
926      345  CONTINUE
927      ENDIF
928      IF((LSUM+1 - LA).LT.0)GO TO 5500

```

```

939      IF(DE(LA,2).LE.DE(LA,1))GO TO 5600
940      5500      LSUM = 0
941      IF(NCON.EQ.0)GO TO 5550
942      IF(NCON.GT.50.AND.DE(LA,2).LT.FE(LM))GO TO 5600
943      5550      IF(IFHTYP.EQ.7)N1 = 1
944      IF(IFHTYP.EQ.5)N1 = 2
945      DO 355, M = N1,LA
946      D(M,1) = D(M,2)
947      F(M,1) = F(M,2)
948      ES(M,1) = ES(M,2)
949      IF(M.NE.LA)C(M,1) = C(M,2)
950      V(M,1) = V(M,2)
951      355      CONTINUE
952      DE(LA,1) = DE(LA,2)
953      IF(1.GE.250)IEX = IEX + 1
954      NEX = NSR - IEX
955      IF(NEX.GT.0.AND.1.GE.250)GO TO 5900
956      IF(KCOUN.EQ.0.AND.1.EQ.250)GO TO 5800
957      IF(1.LT.250)GO TO 2800
958      C      END OF SEGMENT FORCE LOOP AND SET FOR 500 ITERATIONS
959      C      FIND LARGEST SET VALUES IF NOT LESS THAN 100% OF
960      C      MAXIMUM VALUE
961      5600      DSET = 0
962      LL = 0
963      IF(DEMAX.LE.FE(LM))THEN
964      IF(FU1.EQ.12.)THEN
965      WRITE(6,1100)
966      1100      FORMAT(/,10X,'** NO OF BLOWS MORE THAN 1200/F1 **')
967      ELSE
968      WRITE(6,1120)
969      1120      FORMAT(/,10X,'** NO OF BLOWS MORE THAN 1200/100MM **')
970      ENDIF
971      ENDIF
972      IF(DEMAX.LT.FE(LM))GO TO 6000
973      DO 365, L = 1,MM
974      DIFF = DEMAX - DE(L)
975      IF(ABS(DIFF).GT.0.005)GO TO 365
976      DSET = DSET + DE(L)
977      LL = LL + 1
978      365      CONTINUE
979      SET = DSET/LL
980      IF(SET.EQ.0.0)SET = 0.001
981      BLOW = (UNL)/(SET)
982      IF(NSR.GT.0.AND.1.LT.250)THEN
983      BPF(NSR) = BLOW
984      REU(NSR) = RUTOT
985      CTS(NSR) = BMIN
986      CSMAX(NSR) = AF(4,1)
987      DO 375, M = 4,LA
988      IF(AF(M,1).GT.CSMAX(NSR))THEN
989      CSMAX(NSR) = AF(M,1)
990      ELSE
991      CSMAX(NSR) = CSMAX(NSR)
992      ENDIF
993      375      CONTINUE
994      ENDIF
995      IF(BMIN.GE.0.0)THEN
996      NMIN = NELEM

```



```

0001      IMIN = 1
0002      ENDIF
0003      IF (NW.GT.0) THEN
0004          WRITE(6,1140) NW
0005          1140  FORMAT(/,10X,'DETAILS OF PILE MOMENT',1X,10X,
0006              *   'FORCE, VELOCITY',/,10X,'DISPLACEMENT, SET AT EACH
0007              *   ,1X,'TIME INTERVAL',//)
0008          WRITE(6,1160) (FP(NW,I),I=1,MM)
0009          1160  FORMAT(5(F10.2,2X))
0010          WRITE(6,1180)
0011          1180  FORMAT(//)
0012          WRITE(6,1200) (VP(NW,I),I=1,MM)
0013          1200  FORMAT(5(F10.2,2X))
0014          WRITE(6,1220)
0015          1220  FORMAT(//)
0016          WRITE(6,1240) (DP(NW,I),I=1,MM)
0017          1240  FORMAT(5(F11.6,2X))
0018          WRITE(6,1260)
0019          1260  FORMAT(//)
0020          IF (NW.GE.4) WRITE(6,1280) (SSP(NW,I),I=1,MM)
0021          1280  FORMAT(5(F11.6,2X))
0022          WRITE(6,1300)
0023          1300  FORMAT(//,10X,'DETAILS OF PILE POINT FORCE, VELOCITY',/,
0024              *   10X,'DISPLACEMENT, SET AT EACH TIME INTERVAL',//)
0025          WRITE(6,1320) (FP(LA,I),I=1,MM)
0026          1320  FORMAT(5(F10.2,2X))
0027          WRITE(6,1340)
0028          1340  FORMAT(//)
0029          WRITE(6,1360) (VP(LA,I),I=1,MM)
0030          1360  FORMAT(5(F10.2,2X))
0031          WRITE(6,1380)
0032          1380  FORMAT(//)
0033          WRITE(6,1400) (DP(LA,I),I=1,MM)
0034          1400  FORMAT(5(F11.6,2X))
0035          WRITE(6,1420)
0036          1420  FORMAT(//)
0037          WRITE(6,1440) (SSP(LA,I),I=1,MM)
0038          1440  FORMAT(5(F11.6,2X))
0039          ENDIF
0040          WRITE(6,1460) MM, QS, UT2, QP, UT2, SET, UT2, LL, BLOW
0041          1460  FORMAT(//,15X,'NUMBER OF ITERATIONS =',14,/,15X,'SIDE',
0042              *   1X,'QUAKE =',F5.3,1X,A2,/,15X,'POINT QUAKE =',F5.3,
0043              *   1X,A2,/,15X,'AVERAGE SET =',F7.4,1X,A2,/,15X,
0044              *   'NO OF VALUES USED =',12,/,15X,'NO OF BLOWS/FT =',
0045              *   FB.2,//)
0046          IF (KCOUN.GT.0) GO TO 5700
0047          IF (IPD.GT.0) THEN
0048              DO 385, M = 1, MM, 11
0049                  M1 = (M+10)
0050                  IF (M1.GT.MM) M1=MM
0051                  WRITE(6,1480) (K,K = M,M1)
0052                  1480  FORMAT(/,4X,'DT =',1X,13,10X,13)
0053                  WRITE(6,1500) (DE1(K), K = M,M1)
0054                  1500  FORMAT(3X,'SET =',1X,11F9.5)
0055                  WRITE(6,1520) (D1(K), K = M,M1)
0056                  1520  FORMAT(5X,'D. =',1X,11F9.5)
0057                  WRITE(6,1540) (FMAX(K), K = M,M1)
0058                  1540  FORMAT(4X,'ES =',1X,11F9.3)

```

```

1045      WRITE(6,1500) (JX(I), F = M, M1)
1046      1500  FORMAT(1X, 'ELNO = ', 1X, I3, 10((CX, 1.0))
1047      100  CONTINUE
1048      ENDIF
1049      WRITE(6,1580) UT5, UT5, UT6
1050      1580  FORMAT(//, 15X, 'THE STRESS IN FILE SEGMENTS ARE AS FOLLOWS',
1051      *      //, 7X, 'ELEMENT', 3X, 'MAXIMUM ELEMENT', 6X, 'TIME', 6X,
1052      *      'LAST STRESS', 6X, 'LAST VELOCITY', /, 8X, 'NO', 8X, 'STRESS',
1053      *      14X, 'INTERVAL', 4X, 'COMPRESSION', 6X, 'V(M,2) IN', /, 16X,
1054      *      'IN', 1X, A8, 20X, 'IN', 1X, A8, 4X, 'IN', 1X, A8, /)
1055      IF (IFHTYP.EQ.7) FC=1
1056      IF (IFHTYP.EQ.5) FC=2
1057      WRITE(6,1600) (N, (AF(N,M), M = 1,2), ES(N,2), V(N,2), N = KC, 1A)
1058      1600  FORMAT(1X, I8, 6X, F10.2, 12X, F6.1, 3X, F10.2, 6X, F10.2)
1059      KCOUN = KCOUN + 1
1060      IF (COMFM.GT.0.0 AND MM.NE.250) GO TO 5500
1061      IF (NSR.EQ.NRU) GO TO 6100
1062      GO TO 6000
1063      5700  WRITE(6,1620) I, UT5, UT6
1064      1620  FORMAT(///, 5X, 'MIN ELEM STRESS (TENSILE STRESS) AT DT = ',
1065      *      15, 3X, 'LAST STRESS COMP', 1X, A8, 4X, 'LAST V(M,2)',
1066      *      1X, A8, /)
1067      IF (IFHTYP.EQ.7) NS=1
1068      IF (IFHTYP.EQ.5) NS=2
1069      WRITE(6,1640) ((FMIN(M,L), L = 1,2), ES(M,2), V(M,2), M = NS, 1A)
1070      1640  FORMAT(5X, F14.3, 12X, F6.1, 18X, F14.3, 10X, F14.5)
1071      WRITE(6,1660) BMIN, UT5, NMIN, IMIN
1072      1660  FORMAT(//, 10X, 'MIN NEG SEGMENT STRESS = ', F12.4, 1X, A8, 3X,
1073      *      'IN ELEMENT', 1X, I3, 1X, 'AT ITERATION NO', 1X, I3, /)
1074      IF (NSR.EQ.NRU) GO TO 6100
1075      IF (KCOUN.GT.0) GO TO 6000
1076      5800  WRITE(6,1680)
1077      1680  FORMAT(////, 8X, '*****PROBLEM UNSTABLE OVER 250 ITERATIONS',
1078      *      'DT TOO SMALL *****', /)
1079      GO TO 6000
1080      5900  WRITE(6,1700)
1081      1700  FORMAT(//, 8X, '***** PROBLEM UNSTABLE CHANGE ONE OF', 1X,
1082      *      'FOLLOWING*****', /, 14X, '1) PILE HAMMER', /, 14X, '2)', 1X,
1083      *      'INCREASE OR DECREASE TIME INTERVAL', /, 14X,
1084      *      '3) DECREASE SOIL RESISTANCE', /, 14X, '4) CHANGE CAP', 1X,
1085      *      'BLOCK OR CUSHION SPRING CONSTANT', /)
1086      GO TO (2400, 2500, 2600, 2000, 150), NCHECK
1087      6000  IF (FU1.EQ.12.0) THEN
1088      IF (COMFM.GT.0.0) THEN
1089      WRITE(6,1720) UT5, UT5, UT5
1090      1720  FORMAT(/, 20X, '***** SUMMARY OF RESULTS *****', //, 6X,
1091      *      'ULTIMATE SOIL', 5X, 'NO OF BLOWS', 13X, 'MAXIMUM', 1X,
1092      *      'STRESS', /, 7X, 'RESISTANCE', 8X, 'PER FT', 11X,
1093      *      'COMPRESSION', 5X, 'TENSION', /, 8X, 'IN', 1X, A4, 26X,
1094      *      'IN', 1X, A10, 4X, 'IN', 1X, A10, /)
1095      WRITE(6,1740) (REU(I), BPF(I), CSMAX(I), CTS(I), I = 1EX, NRU)
1096      1740  FORMAT(4(3X, F12.3, 1X))
1097      ELSE
1098      WRITE(6,1760) UT3, UT5
1099      1760  FORMAT(/, 20X, '***** SUMMARY OF RESULTS *****', //, 10X,
1100      *      'ULTIMATE SOIL', 6X, 'NO OF BLOWS', 6X, 'MAXIMUM', 1X,
1101      *      'COMPRESSIVE', /, 11X, 'RESISTANCE', 8X, 'PER FT', 13X,
1102      *      'STRESS IN', /, 12X, 'IN', 1X, A4, 26X, A12, /)

```

```

1103 WRITE(6,1780) (REU(1),BPF(1),CSMAX(1),I - 1EX,NRU)
1104 1780 FORMAT(3(6X,F12.3,2X))
1105 ENDIF
1106 ELSE
1107 IF (COMFM.GT.0.0) THEN
1108 WRITE(6,1800) UT3,UT5,UT5
1109 1800 FORMAT(/,20X,'***** SUMMARY OF RESULTS *****',//,6X,
1110 * 'ULTIMATE SOIL',5X,'NO OF BLOWS',13X,'MAXIMUM',1X,
1111 * 'STRESS',/,7X,'RESISTANCE',8X,'PER 300MM',11X,
1112 * 'COMPRESSION',5X,'TENSION',/,8X,'IN',1X,A4,26X,
1113 * 'IN',1X,A10,4X,'IN',1X,A10,/)
1114 WRITE(6,1820) (REU(1),BPF(1),CSMAX(1),CTS(1),I - 1EX,NRU)
1115 1820 FORMAT(4(3X,F12.3,1X))
1116 ELSE
1117 WRITE(6,1840) UT3,UT5
1118 1840 FORMAT(/,20X,'***** SUMMARY OF RESULTS *****',//,10X,
1119 * 'ULTIMATE SOIL',6X,'NO OF BLOWS',6X,'MAXIMUM',1X,
1120 * 'COMPRESSION',/,11X,'RESISTANCE',8X,'PER 300MM',13X,
1121 * 'STRESS IN',/,12X,'IN',1X,A4,26X,A12,/)
1122 WRITE(6,1860) (REU(1),BPF(1),CSMAX(1),I - 1EX,NRU)
1123 1860 FORMAT(3(6X,F12.3,2X))
1124 ENDIF
1125 ENDIF
1126 IF (NPLT.GT.0) CALL RBPLT(BPF,REU,NRU,FU1)
1127 IF (NPLT.GT.0) CALL CSPLT(BPF,CSMAX,NRU,FU1,1EX)
1128 IF (NPLT.GT.0.AND.COMFM.GT.0) CALL TSPLT(BPF,CTS,NRU,FU1,1EX)
1129 150 STOP
1130 END
1131 C
1132 FUNCTION FFEX(INTV)
1133 COMMON EXPF,DT,TD,T1,TL,TR,TIND,TINI,TINL,TINR
1134 IF (INTV.LE.TIND) FFEX=FC
1135 * IF (INTV.GT.TIND.AND.INTV.LT.TINI) THEN
1136 FFEX = (EXPF-FC)*((DT*INTV-TD)/(T1)) + FC
1137 ENDIF
1138 IF (INTV.GE.TINI.AND.INTV.LE.TINL) FFEX=EXPF
1139 IF (INTV.GT.TINL.AND.INTV.LE.TINR) THEN
1140 FFEX = EXPF*(1 - (DT*INTV - TD - T1 - TL)/(TR))
1141 ENDIF
1142 RETURN
1143 END
1144 C
1145 SUBROUTINE RBPLT(BPF,REU,NRU,FU1)
1146 C
1147 DIMENSION BPF(30),REU(30),XX(30),YY(30)
1148 C
1149 CALL DSPDEV('PLOTTER ')
1150 CALL PAGE(8.5,11.0)
1151 CALL AREA2D(6.5,8.5)
1152 IF (FU1.EQ.12.0) THEN
1153 CALL XNAME('No of blows per ft$',100)
1154 CALL YNAME('Soil resistance in Kips$',100)
1155 ELSE
1156 CALL XNAME('No of blows per 300mm$',100)
1157 CALL YNAME('Soil resistance in Kn$',100)
1158 ENDIF
1159 XORIG=0.
1160 YORIG=0.

```

```

1161      IF (BPF(NRU) .LE. 600.) THEN
1162      XMAX=600.
1163      XSTP=100.
1164      ELSE
1165      XMAX=1200.
1166      XSTP=150.
1167      ENDIF
1168      IF (REU(NRU) .LE. 1000.) THEN
1169      YMAX=1000.
1170      YSTP=100.
1171      ELSE
1172      YMAX=REU(NRU)
1173      YSTP=250.
1174      ENDIF
1175      CALL GRAF(XORIG,XSTP,XMAX,YORIG,YSTP,YMAX)
1176      CALL THKFRM(.02)
1177      CALL FRAME
1178      XX(1) = 0.0
1179      YY(1) = 0.0
1180      DO 11 , I=1,NRU
1181      IF (BPF(I) .LE. 1200.) THEN
1182      XX(I+1) = BPF(I)
1183      YY(I+1) = REU(I)
1184      ENDIF
1185      11 CONTINUE
1186      CALL SPLINE
1187      CALL CURVE(XX,YY,NRU+1,0)
1188      CALL HEADIN('ASSUMED SOIL RESISTANCES',100,1.25,3)
1189      CALL HEADIN('VERSUS$',100,1.0,3)
1190      CALL HEADIN('NO OF BLOWS $',100,1.25,3)
1191      CALL ENDPL(0)
1192      RETURN
1193      END
1194      C
1195      SUBROUTINE CSPLT(BPF,CSMAX,NRU,FU1,IEX)
1196      C
1197      DIMENSION BPF(30),CSMAX(30),XS(30),YS(30)
1198      C
1199      CALL PAGE(8.5,11.0)
1200      CALL AREA2D(6.5,8.5)
1201      IF (FU1.EQ.12.0) THEN
1202      CALL XNAME('No of blows per ft$',100)
1203      CALL YNAME('Maximum Stress in Kips/sq in$',100)
1204      ELSE
1205      CALL XNAME('No of blows per 300mm$',100)
1206      CALL YNAME('Maximum Stress in Kn/sq cm$',100)
1207      ENDIF
1208      XORIG=0.
1209      YORIG=0.
1210      IF (BPF(NRU) .LE. 600.) THEN
1211      XMAX=600.
1212      XSTP=100.
1213      ELSE
1214      XMAX=1200.
1215      XSTP=150.
1216      ENDIF
1217      CSMAXX=CSMAX(1)
1218      DO 6 , I = IEX,NRU

```

```

1219      IF(CSMAX(1).LT.CSMAXX)THEN
1220      CSMAXX = CSMAXX
1221      ELSE
1222      CSMAXX = CSMAX(1)
1223      ENDIF
1224      CONTINUE
1225      YMAX=CSMAXX + 10.
1226      YSTP=5.
1227      CALL GRAF(XORIG,XSTP,XMAX,YORIG,YSTP,YMAX)
1228      CALL THKFRM(.02)
1229      CALL FRAME
1230      NO = NRU + 1 - IEX
1231      DO 12 , 1-IEX,NRU
1232      IF(BPF(1).LE.1200.0)THEN
1233          K = 1+1-IEX
1234          XS(K) = BPF(1)
1235          YS(K) = CSMAX(1)
1236      ENDIF
1237      CONTINUE
1238      CALL CURVE(XS,YS,NO,0)
1239      CALL HEADIN('MAXIMUM COMPRESSIVE STRESS$',100,1.25,3)
1240      CALL HEADIN('VERSUS$',100,1.0,3)
1241      CALL HEADIN('NO OF BLOW$',100,1.25,3)
1242      CALL ENDPL(0)
1243      RETURN
1244      END
1245
1246      SUBROUTINE TSPLT(BPF,CTS,NRU,FU1,IEX)
1247
1248      DIMENSION BPF(30),CTS(30),XT(30),YT(30)
1249
1250      CALL PAGE(8.5,11.0)
1251      CALL AREA2D(6.5,8.5)
1252      IF(FU1.EQ.12.0)THEN
1253      CALL XNAME('No of blows per ft$',100)
1254      CALL YNAME('Maximum Stress in Kips/sq in$',100)
1255      ELSE
1256      CALL XNAME('No of blows per 300mm$',100)
1257      CALL YNAME('Maximum Stress in Kn/sq cm$',100)
1258      ENDIF
1259      CTSS = CTS(IEX)
1260      DO 11 , 1 = IEX,NRU
1261      IF(CTSS.LT.CTS(1))THEN
1262          CTSS = CTS
1263      ELSE
1264          CTSS = CTS(1)
1265      ENDIF
1266      CONTINUE
1267      XORIG=0.
1268      YORIG=CTSS - 5.
1269      IF(BPF(NRU).LE.600.)THEN
1270      XMAX=600.
1271      XSTP=100.
1272      ELSE
1273      XMAX=1200.
1274      XSTP=150.
1275      ENDIF
1276      YMAX=0.

```

```

12100 Y1=1000
12110 CALL GRAF(X0=10, XNT=1, XMAX=Y1/10, Y0=1, Y1=YMAX)
12120 CALL THERMO(0)
12130 CALL FRAM1
12140 NT = NRG * 100 / HEN
12150 DO 12170, I=1, NRG, NRG
12160 IF (PIEC(I) .EQ. 0) GO TO 12170
12170     F = 100 / FEN
12180     XT(I) = PIE(I)
12190     Y1(I) = CH(I)
12200     ENDF
12210     CONTINUE
12220 CALL CURVE(XA, Y1, NT, 0)
12230 CALL HEADIN('MAXIMUM TENSILE STRESS', 100, 1, 20, 0)
12240 CALL HEADIN('CONVERGENCE', 100, 1, 1, 0)
12250 CALL HEADIN('NO. OF BLOWS', 100, 1, 20, 0)
12260 CALL ENDF(0)
12270 CALL DONEFI
12280 RETURN
12290 END

```

• • • • •

[illegible]

100

[illegible]

சென்னை, 19.05.2023

NELEM	NSAS	NSCIN	MOB	ELEM	NAME
4 C					
5 C	IFHYP	NCOM	STEAM	DISEN	
6 C	NPLO*	NV	IFC		
7 C	JUS	NMCHV	IFHYP	IFHYP	COMIN
8 C					
9 C					
10 C					

60-108000-1000

NE	ECOM	DCM
9 11	3	
9 12	4	
9 13	5	
9 14		
9 15		

Note: m = NELEM  
EMCO

9 20	ECAP	ACAP	ECAP	ECOB
10 0	ECUS	ACUS	ECUS	ECOC
11 0				

Soil damping parameters

NS	DCM	PRIM	NS	DCM	PRIM
12 1					
12 2	4				
12 3	5				
12 4					
12 5					
12 6					
12 7					
12 8					
12 9					
12 10					
12 11					
12 12					
12 13					
12 14					
12 15					
12 16					
12 17					
12 18					
12 19					
12 20					
12 21					
12 22					
12 23					
12 24					
12 25					
12 26					
12 27					
12 28					
12 29					
12 30					
12 31					
12 32					
12 33					
12 34					
12 35					
12 36					
12 37					
12 38					
12 39					
12 40					
12 41					
12 42					
12 43					
12 44					
12 45					
12 46					
12 47					
12 48					
12 49					
12 50					
12 51					
12 52					
12 53					
12 54					
12 55					
12 56					
12 57					
12 58					
12 59					
12 60					
12 61					
12 62					
12 63					
12 64					
12 65					
12 66					
12 67					
12 68					
12 69					
12 70					
12 71					
12 72					
12 73					
12 74					
12 75					
12 76					
12 77					
12 78					
12 79					
12 80					
12 81					
12 82					
12 83					
12 84					
12 85					
12 86					
12 87					
12 88					
12 89					
12 90					
12 91					
12 92					
12 93					
12 94					
12 95					
12 96					
12 97					
12 98					
12 99					
12 100					

Note: m = NELEM

Drop hammer or spring hammer data 1

13 1	W12	W1	RENG	EFF	CHDVE
------	-----	----	------	-----	-------

Double/Differential loading hammer data 3

13 11	W12	W1	SDMAT	POS	DDCM	EFF
13 22	STROKE					





DATE		TIME		PROJECT	
14	4	14	4		
FID		C/COM(1)			
14	5	3			
14	5	4			
14	5	5			
14	5	6			
14	5	7			
14	5	8			
14	5	9			
14	5	10			
14	5	11			
14	5	12			
14	5	13			
14	5	14			
14	5	15			
14	5	16			
14	5	17			
14	5	18			
14	5	19			
14	5	20			
14	5	21			
14	5	22			
14	5	23			
14	5	24			
14	5	25			
14	5	26			
14	5	27			
14	5	28			
14	5	29			
14	5	30			
14	5	31			
14	5	32			
14	5	33			
14	5	34			
14	5	35			
14	5	36			
14	5	37			
14	5	38			
14	5	39			
14	5	40			
14	5	41			
14	5	42			
14	5	43			
14	5	44			
14	5	45			
14	5	46			
14	5	47			
14	5	48			
14	5	49			
14	5	50			
14	5	51			
14	5	52			
14	5	53			
14	5	54			
14	5	55			
14	5	56			
14	5	57			
14	5	58			
14	5	59			
14	5	60			
14	5	61			
14	5	62			
14	5	63			
14	5	64			
14	5	65			
14	5	66			
14	5	67			
14	5	68			
14	5	69			
14	5	70			
14	5	71			
14	5	72			
14	5	73			
14	5	74			
14	5	75			
14	5	76			
14	5	77			
14	5	78			
14	5	79			
14	5	80			
14	5	81			
14	5	82			
14	5	83			
14	5	84			
14	5	85			
14	5	86			
14	5	87			
14	5	88			
14	5	89			
14	5	90			
14	5	91			
14	5	92			
14	5	93			
14	5	94			
14	5	95			
14	5	96			
14	5	97			
14	5	98			
14	5	99			
14	5	100			
14	5	101			
14	5	102			
14	5	103			
14	5	104			
14	5	105			
14	5	106			
14	5				

## APPENDIX B-1

### List of Variables in Hiley's Formula

**TITLE:** project title not exceeding eighty characters

**WR:** Weight of ram in lb

**HATYP:** Hammer type; >0 drop or single acting hammer; <0 double/differential acting or diesel hammer

**EFF:** Hammer efficiency

**CHC:** Temporary compression allowance for pile head and cap in inches ( $C_1$ )

**QC:** Temporary compression allowance for quake of ground in inches ( $C_2$ )

**FS:** Factor of safety desired

**EMOD:** Modulus of elasticity of pile material in psi

**AREA:** Cross-sectional area of pile in sq in

**PLEN:** Length of pile measured from head to center of driving resistance in ft

**PTL:** Total length of pile measured from head to pile toe in ft

**WPFT:** Weight of pile per ft in lb

DRVPT: Weight of drive point (shoe) in lb

ECP: Coefficient of restitution

STROKE: If HATYP=0; length of free fall for drop hammer and  
normal stroke of ram of single acting hammer in inches

WHEL: Weight of helmet in lb

ERN: If HATYP=0; rated energy output of hammer

WAN: do ; weight of anvil in lb

RULT: Ultimate carrying capacity of pile in lb before  
applying factor of safety

## APPENDIX B-2

### Program Listing of Hiley's Formula

```

1      C      THIS PROGRAM WILL COMPUTE PERMANENT SET, NO OF
2      C      BLOWS REQUIRED TO PENETRATE ONE INCH AND STRESS
3      C      IN THE PILE HEAD.
4      C
5      C      DIMENSION TITLE(20)
6      C
7      READ(5,10)TITLE
8      10      FORMAT(20(A4))
9      WRITE(6,20)TITLE
10     20      FORMAT(' ',//,10X,20A4)
11     READ(5,30)WR,HATYP,EFF,CHC,QC,FC
12     30      FORMAT(F10.2,5F5.4)
13     IF(HATYP.GT.0)THEN
14     WRITE(6,40)
15     40      FORMAT(//,10X,'**DROP OR SINGLE ACTING HAMMERS**',/)
16     ELSE
17     WRITE(6,60)
18     60      FORMAT(//,10X,'**DOUBLE/DIFFERENTIAL ACTING OR DIESEL',
19     1X,'HAMMERS',/)
20     , ENDIF
21     WRITE(6,80)WR,EFF,CHC,QC
22     80      FORMAT(/,10X,'WEIGHT OF RAM =',F10.2,1X,'LB',/,10X,
23     1X,'HAMMER EFFICIENCY =',F5.3,/,10X,'TEMPORARY',1X,
24     1X,'COMPRESSION ALLOWANCE =',F5.3,/,10X,
25     1X,'QUAKE OF GROUND =',F5.3,/)
26     READ(5,50)EMOD,AREA,PLEN,PTL,WPFT,DRVPT,ECF
27     50      FORMAT(F12.2,6F8.2)
28     WRITE(6,100)EMOD,AREA,PLEN,PTL,WPFT,DRVPT,ECF
29     100     FORMAT(/,10X,'PILE MODULUS OF ELASTICITY =',F12.2,1X,'PSI'
30     1X,/,10X,'ARE OF X-SECTION OF PILE =',F7.2,1X,'SQ IN'
31     1X,/,10X,'LENGTH OF PILE =',F7.2,1X,'FT',/,10X,
32     1X,'TOTAL LENGTH OF PILE =',F7.2,1X,'FT',/,10X,
33     1X,'WEIGHT OF PILE PER FT =',F7.2,1X,'LB',/,10X,
34     1X,'WEIGHT OF SHOE =',F8.2,1X,'LB',/,10X,
35     1X,'COEFFICIENT OF RESTITUTION =',F5.3,/)
36     C
37     ECR = (ECF)**2
38     IF(HATYP.GT.0)THEN
39     READ(5,70)STROKE,WHEL
40     70      FORMAT(2F10.2)
41     FALL = (STROKE)/(12.0)
42     WRITE(6,120)FALL,WHEL
43     120     FORMAT(/,10X,'HEIGHT OF RAM FALL =',F8.2,1X,'FT',/,10X,
44     1X,'WEIGHT OF HELMET =',F8.2,1X,'LBS',/)
45     WP = (WPFT)*(PTL) + DRVPT + WHEL
46     SEIMP = (EFF)*(WR)*(STROKE)
47     ELSE
48     READ(5,90)ERN,WAN,WHEL
49     90      FORMAT(3F12.2)
50     WRITE(6,140)ERN,WAN,WHEL
51     140     FORMAT(/,10X,'RATED ENERGY OUTPUT =',F12.2,1X,'FT-LB',/,
52     1X,10X,'WEIGHT OF ANVIL =',F10.2,1X,'LBS',/,10X,
53     1X,'WEIGHT OF HELMET =',F10.2,1X,'LBS',/)
54     WP = (WPFT)*(PTL) + DRVPT + WAN + WHEL
55     DEIMP = 12.*(EFF)*(ERN)
56     ENDF
57     WCC = (WR + (ECR)*(WP))/(WR + WP)
58     WRITE(6,160)

```

```

59      100  FORMAT(/,4X,'ALLOWABLE SOIL',5X,'NO OF BLOWS',5X,'NO OF',
60      *    1X,'BLOWS',5X,'STRESS AT',/,5X,'RESISTANCE',9X,'PER INCH'
61      *    ,8X,'PER FT',10X,'PILE HEAD',/,7X,'IN KIPS',40X,
62      *    'IN KIPS/SQ IN',/)
63      15  READ(5,110)RULT
64      110  FORMAT(F12.2)
65      IF(RULT.GT.0)THEN
66          CC = ((RULT)*(PLEN)*12)/((AREA)*(EMOD))
67          CCS = (CHC + QC + CC)/2.0
68      IF(CHATP.GT.0)THEN
69          SET = ((SEIMP)*(WCC)/(RULT))    CCS
70          BLOW = 1./SET
71          BPF = 12.0*(BLOW)
72          PST = (RULT)/((AREA)*1000.0)
73          RALL = (RULT)/((FS)*1000.0)
74      ELSE
75          SET = ((DEIMP)*(WCC)/(RULT))    CCS
76          BLOW = 1./SET
77          BPF = 12.0*(BLOW)
78          PST = (RULT)/((AREA)*1000.0)
79          RALL = (RULT)/((FS)*1000.0)
80      ENDIF
81      IF(SET.LT.0.)GO TO 15
82      WRITE(6,180)RALL,BLOW,BPF,PST
83      180  FORMAT(/,3X,F10.2,10X,F7.3,9X,F10.3,5X,F12.2)
84      GO TO 15
85      ENDIF
86      STOP
87      END

```

# APPENDIX B-3

General Data Sheet For  
WATER FORMER

1	2	3	4	5	6	7	8	9	0	1	2	3	4	5	6	7	8	9	0	1	2	3	4	5	6	7	8	9	0
---	---	---	---	---	---	---	---	---	---	---	---	---	---	---	---	---	---	---	---	---	---	---	---	---	---	---	---	---	---

Project title (not exceeding 80 characters)

TITLE																													
-------	--	--	--	--	--	--	--	--	--	--	--	--	--	--	--	--	--	--	--	--	--	--	--	--	--	--	--	--	--

1	2	3	4	5	6	7	8	9	0	1	2	3	4	5	6	7	8	9	0	1	2	3	4	5	6	7	8	9	0
---	---	---	---	---	---	---	---	---	---	---	---	---	---	---	---	---	---	---	---	---	---	---	---	---	---	---	---	---	---

VR	MTYP	EFF	CHC	OC	FS
----	------	-----	-----	----	----

EMOC	AREA	PLEN	PPL	WPR	DOPT	FCP
------	------	------	-----	-----	------	-----

STROKE	WHEL
--------	------

ERN	WAN	WHEL
-----	-----	------

RULY
------

# APPENDIX C-1-A

SHEET 1 OF 1

## BOREHOLE RECORD

PROJECT: Edmonton Rapid Transit 112-Avenue Station

LOCATION: 112 - Avenue, Edmonton

ELEVATION DATUM: \_\_\_\_\_ CASING SIZE: \_\_\_\_\_

HOLE NO: 2

HOLE DATE: \_\_\_\_\_

DRILLER: HEIGHT: \_\_\_\_\_ LBS.

HANDER: DROP: \_\_\_\_\_ IN

**GROUND WATER**

WL: GROUND WATER LEVEL

**SAMPLE TYPES**

SS: SPLIT SPOON, 2 IN. S.D.

TS: THIN-WALL SAMPLER, \_\_\_\_\_ IN. \_\_\_\_\_ %

PS: PISTON SAMPLER, \_\_\_\_\_ IN. \_\_\_\_\_ %

DC: DIAMOND CORE, \_\_\_\_\_ SIZE

WS: WASH SAMPLE

AS: AUGER SAMPLE

ROD: ROCK QUALITY DESIGNATION (%)

**SAMPLE CONDITIONS**

DETERMINED: ☒ GOOD: ☒ LOST: ☐

**TESTS**

N: STANDARD PENETRATION VALUE (BLows/FT.)

K: PERMEABILITY (CM/SEC.)

V: IN-SITU VALUE (LBS./SQ. FT.)

VR: VALUE ON REMOLDED SOIL (LBS./SQ. FT.)

VL: LABORATORY VALUE (LBS./SQ. FT.)

**TESTS**

GS: GRAIN-SIZE ANALYSIS

S: TOTAL UNIT WEIGHT (LBS./CU. FT.)

U: UNCONFINED COMPRESSION (T./SQ. FT.)

Q: UNDRAINED TRIAXIAL (T./SQ. FT.)

(%) STRAIN AT FAILURE

C: CONSOLIDATION

B: PLASTIC LIMIT

Δ: LIQUID LIMIT

●: NATURAL WATER CONTENT

PROFILE				SAMPLES			TESTS	
DEPTH (FT.)	ELEV. (FT.)	DESCRIPTION	STRAT.	GROUND WATER	COND.	W. & TYPE		
0		Ground surface						
1		Fill						
2								
3								
4		Lake Edmonton clay						
5								
6								
7		Till						
8								
9								
10		End of Borehole						

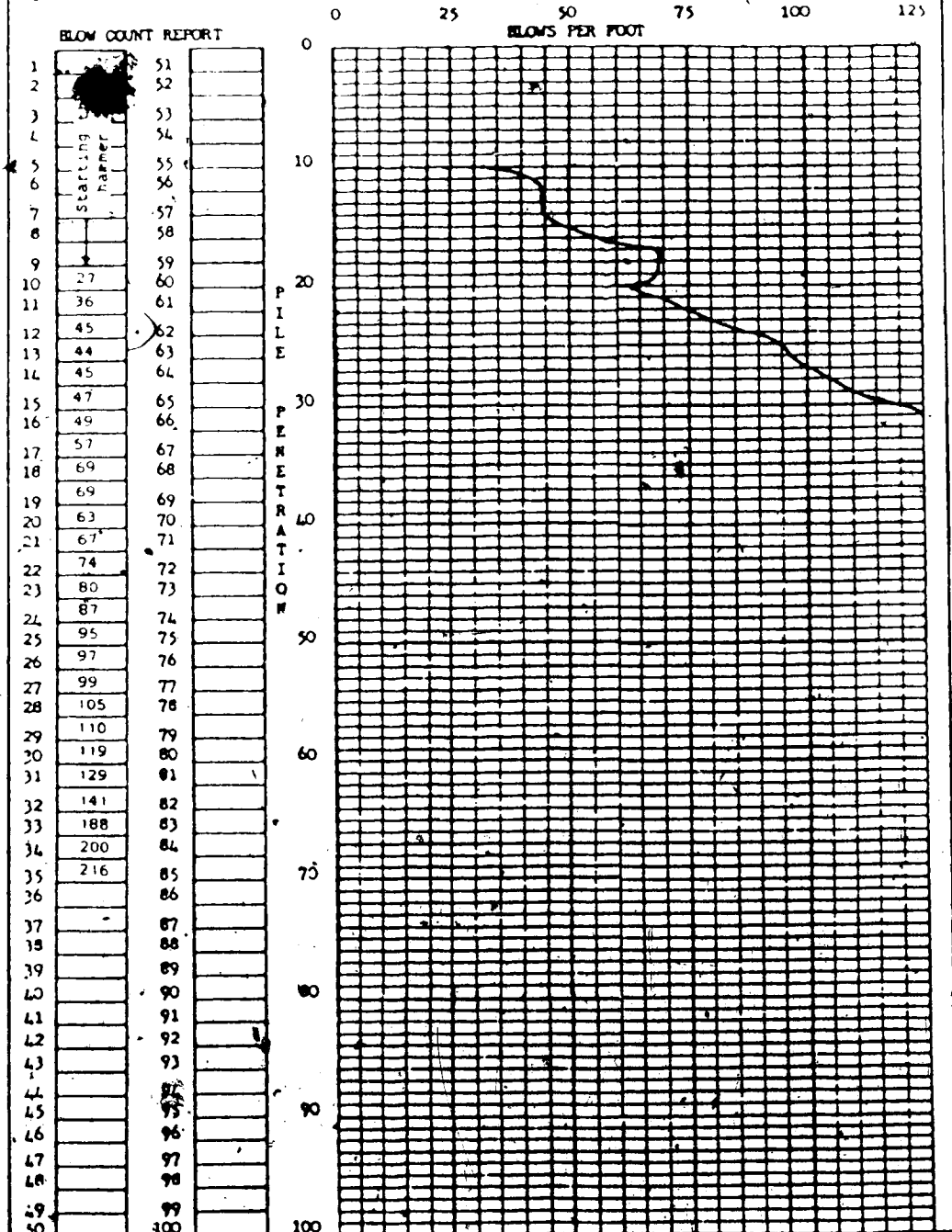
25% 50%



# APPENDIX C-1-B

## PILE DRIVING RECORD

Contractor:	Date:		
Test Pile: A	Size & Type: W12x85 H-Pile	Design Load:	
Gross Lgth:	Out-Off:	Net Lgth:	36 ft
Out-Off Elev:	Ground Elev:	Tip Elev:	
Pen. Final 5 Blows:	Ave. Pen/Blows:	Rebound:	
Hammer Type: Delmag 12	Wght: 2750 lb	Hght. of Fall or Energy:	22500 ft-lb
Formula:	Remarks:		
Inspector:			



# APPENDIX C-2-A

BOREHOLE RECORD									
PROJECT <u>Test Pile</u> LOCATION <u>Beaumont, Texas</u> ELEVATION DATUM _____					SHEET <u>1</u> OF <u>2</u> HOLE NO. _____ HOLE DATE _____ HAMMER - WEIGHT _____ LBS. HAMMER - DROP _____ IN				
GROUND WATER W/L - GROUND WATER LEVEL _____					SAMPLE CONDITIONS DISTURBED <input checked="" type="checkbox"/> GOOD <input checked="" type="checkbox"/> LOST <input checked="" type="checkbox"/>				
SAMPLE TYPES SS - SPLIT SPOON <u>2</u> IN G.S. TW - THIN - WALL SAMPLER _____ IN _____ % PS - PISTON SAMPLER _____ IN _____ % DC - DIAMOND CORE _____ IN _____ % WS - WASH SAMPLE AS - ASHER SAMPLE ROD - ROCK QUALITY DESIGNATION (%)					TESTS GS - GRAIN-SIZE ANALYSIS S - TOTAL UNIT WEIGHT (LBS./CU. FT.) U - UNCONFINED COMPRESSION (T./SQ. FT.) Q - UNDRAINED TRIAXIAL (T./SQ. FT.) (N) STRAIN AT FAILURE C - CONSOLIDATION P - PLASTIC LIMIT L - LIQUID LIMIT W - NATURAL WATER CONTENT				
PROFILE				SAMPLES		TESTS			
DEPTH (FT.)	ELEV. (FT.)	DESCRIPTION	STRT.	END	IN. B TYPE	REC. (%)			
0		Ground surface							
1		Fill organic clay							
2		Stiff tan and grey silty clay with calcareous nodules					$\gamma_d = 98.8$ $U = 0.87$		
3		Tan and grey silty clayey, some sand					$\gamma_d = 96.3$ $U = 0.85$		
4		Soft tan and grey silty sandy clay					$\gamma_d = 107.5$ $U = 1.37$		
5		Soft sandy, silty clay					$\gamma_d = 101.1$ $U = 0.74$		
6		Grey sand					-N=40		
7							$\gamma_d = 73.3$ $U = 1.12$		

PROJECT NO. _____				SHEET 2 of 2					
BOREHOLE RECORD								HOLE NO. _____	
PROFILE			GROUT WATER	SAMPLES			TESTS	<div style="display: flex; justify-content: space-around;"> <span>50%</span> <span>100%</span> </div>	
DEPTH (FT.)	DESCRIPTION	STRAT.		COND.	TYPE	WTC (%)			
33	Firm to stiff dark blue clay with some shells						$\gamma_d = 68.6$ $U = 1.10$		
30									
33									
30									
27									
24									
21									
18									
15									
12									
9									
6									
3									
0									

# APPENDIX C-3-A

BOREHOLE RECORD									
PROJECT: <u>Test File No VII-9-220</u>					HOLE NO: _____				
LOCATION: <u>Timber Yard, CN Rail</u>					HOLE DATE: _____				
ELEVATION DATUM: _____					HOLE DEPTH: _____				
GROUND WATER					SAMPLE CONDITIONS				
WL: GROUND WATER LEVEL					DISTURBED <input checked="" type="checkbox"/> GOOD <input checked="" type="checkbox"/> LOST <input checked="" type="checkbox"/>				
SAMPLE TYPES					TESTS				
SS: SPLIT SPOON <u>2</u> IN O.D.					N: STANDARD PENETRATION VALUE (BLOWS/FT)				
TM: THIN-WALL SAMPLER _____ IN _____ %					K: PERMEABILITY (CM/SEC)				
PS: PILED PISTON SAMPLER _____ IN _____ %					V: IN-SITU VANE (LBS/50 FT)				
CC: CHAMBER CORE _____ SIZE					VN: VANE ON REMOLDED SOIL (LBS/50 FT)				
WS: WASH SAMPLE					VL: LABORATORY VANE (LBS/50 FT)				
AS: AUGER SAMPLE					C: CONSOLIDATION				
ROD: ROCK QUALITY DESIGNATION (%)					P: PLASTIC LIMIT				
					L: LIQUID LIMIT				
					W: NATURAL WATER CONTENT				

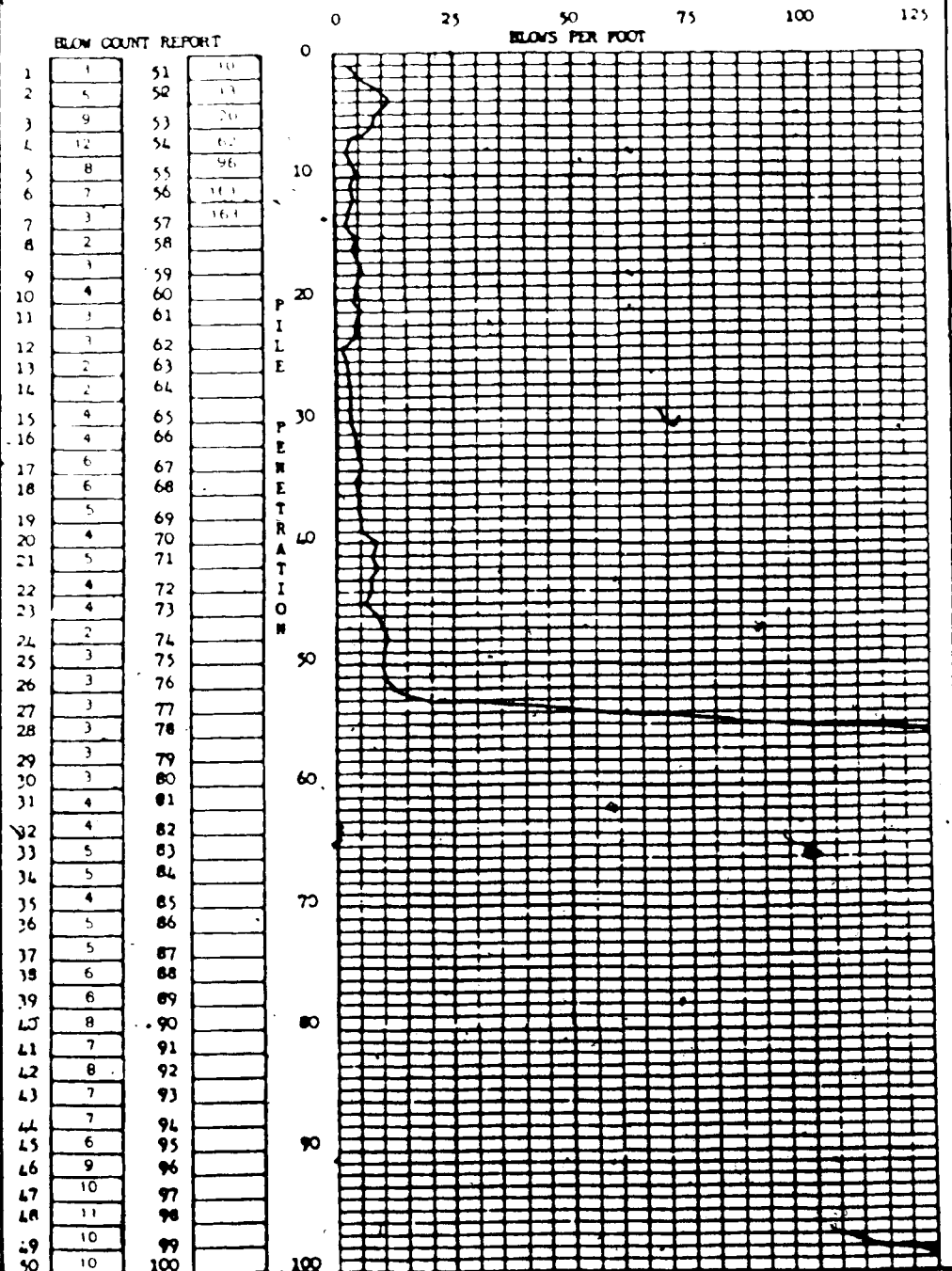
PROFILE			SAMPLES			TESTS	
ELEV (FT)	DESCRIPTION	STRAT.	GROUND WATER	COND.	NO. & TYPE	REC. (%)	TESTS
0	Ground surface						
1	Medium grained compact sand fill						
2							
3	Peat-silty, moist compact woody, brown very clayey						
4							
5							
6							
7							
8							
9							
10	Peat and organic with occasional pockets of clayey silt and sand						
11							
12							
13							
14							
15							
16							
17							
18							
19							
20							
21							
22							
23							
24							
25							
26							
27							
28							
29							
30							

PROJECT NO.		SHEET 2 OF 2		BOREHOLE RECORD		HOLE NO.	
PROFILE			SAMPLES		TESTS		
ELEV FEET	DESCRIPTION	DEPTH FEET	DIAMETER INCHES	NO. & TYPE	TEST		
110							
105							
100							
95							
90							
85							
80							
75							
70							
65							
60							
55							
50							
45							
40							
35							
30							
25							
20							
15							
10							
5							
0							

# APPENDIX C-3-B

## PILE DRIVING RECORD

Contractor: \_\_\_\_\_ Date: July 9, 1975  
 File No.: V118-220 Size & Type: 1510 square cone Design Load: \_\_\_\_\_  
 Gross Lgth: 2571 Out-Off: \_\_\_\_\_ Net Lgth: 576  
 Cut-Off Elev: \_\_\_\_\_ Ground Elev: \_\_\_\_\_ Tip Elev: \_\_\_\_\_  
 Pen. Final 5 Blows: \_\_\_\_\_ Ave. Pen/Blow: \_\_\_\_\_ Rebound: \_\_\_\_\_  
 Hammer Type: Vulcan 0 Wght: 7500 lb. Hght. of Fall or Energy: 24375 ft lb.  
 Formula: \_\_\_\_\_ Remarks: Test Pile  
 Inspector: \_\_\_\_\_



# APPENDIX C-4-A

BOREHOLE RECORD										SHEET 1 OF 2	
PROJECT: Replacement of a 30 Bent Timber Pile Trestle								HOLE NO: 74-4			
LOCATION: Across Bent #22, Fraser, Mile:6.6								HOLE DATE: _____			
ELEVATION DATUM: 85.6								HAMMER WEIGHT: _____ LBS			
CORING SIZE: _____								HAMMER DROP: _____ IN			
GROUND WATER				SAMPLE CONDITIONS				TESTS			
W/L: GROUND WATER LEVEL				<input checked="" type="checkbox"/> RETURNED <input checked="" type="checkbox"/> GOOD <input type="checkbox"/> LOST				GS: GRAIN-SIZE ANALYSIS G: TOTAL UNIT WEIGHT (LBS/CU FT) U: UNCONFINED COMPRESSION (T/50 FT) Q: UNDRAINED TRIAXIAL (T/50 FT) (W): STRAIN AT FAILURE C: CONSOLIDATION B: PLASTIC LIMIT A: LIQUID LIMIT O: NATURAL WATER CONTENT			
SAMPLE TYPES				TESTS							
SS: SPLIT SPOON, 2 IN. O.D. TW: THIN-WALL SAMPLER, _____ IN. _____ % PS: PISTON SPLIT SAMPLER, _____ IN. _____ % DC: DRANDING CORE, _____ SIZE WS: WASH SAMPLE AS: AUGER SAMPLE ROD: ROCK QUALITY DESIGNATION (%)				N: STANDARD PENETRATION VALUE (BLOWS/FT) K: PERMEABILITY (CM/SEC) V: IN-SITU VALUE (LBS/50 FT) VR: VALUE ON REMOLDED SOIL (LBS/50 FT) VL: LABORATORY VALUE (LBS/50 FT)							

PROFILE			SAMPLES		TESTS			
ELEV (FT)	DESCRIPTION	STRAT.	GROUND WATER	CORING	BY & TYPE	REC. (%)		
0	Ground surface						25%	50%
1	Firm medium brownish grey clay, highly plastic, black organic pockets occasional sand grain		V		A.S			
2								
3	Firm to very stiff clay		V		A.S			
4								
5				T.W				
6				A.S				
7				A.S				
8				T.W				
9					A.S			
10								
11								
12								
13								
14								
15								
16								
17								
18								
19								
20								
21								
22								
23								
24								
25								
26								
27								
28								
29								
30								
31								
32								
33								
34								
35								
36								
37								
38								
39								
40								
41								
42								
43								
44								
45								
46								
47								
48								
49								
50								

PROJECT NO. _____				SHEET 2 of 2		BOREHOLE RECORD		HOLE NO. _____	
PROFILE		START	GROUND WATER	SAMPLES		TESTS			
DEPTH (FT.)	DESCRIPTION			NO. & TYPE	REC. (%)				
33			seepage	A.S.		V-2882 VR-823	25%	50%	
30				A.S.		V-4559 VR-941			
25	Medium grey silty clay with mica particles, medium to high plasticity			A.S. T.W.					
20				A.S.		V-3059 VR-706			
15	Stiff to very stiff			A.S.		V-3294 VR-765			
10	Fine sand layers			A.S.		V-3000 VR-765			
5				A.S.		V-3147 VR-706			
0				A.S.		V-3706 VR-882			
5				A.S.		V-3088 VR-765			
10	Occasional silt pockets			A.S.					



# APPENDIX C-4-B

## PILE DRIVING RECORD

Contractor: B & B Forces Date: June 23, 1976

Pile No.: Test Pile Size & Type: 12BF53 H Pile Design Load: \_\_\_\_\_

Gross Lgth: 60ft Cut-Off: 10ft Net Lgth: 50ft

Cut-Off Elev: \_\_\_\_\_ Ground Elev: \_\_\_\_\_ Tip Elev: \_\_\_\_\_

Pen. Final 5 Blows: \_\_\_\_\_ Ave. Pen/Blow: \_\_\_\_\_ Rebound: \_\_\_\_\_

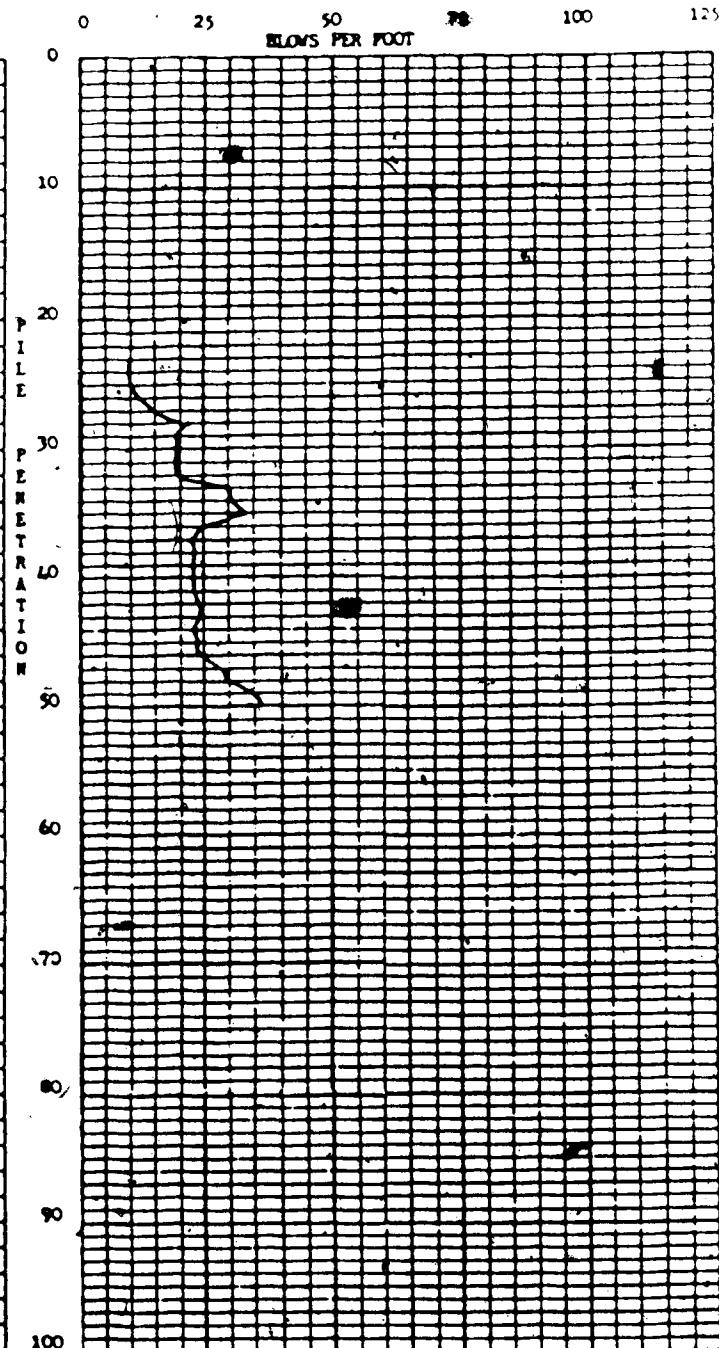
Hammer Type: Link Belt 312 Wght: 3800lb Hght. of Fall or Energy: 18,000 ft-lb

Formula: \_\_\_\_\_ Remarks: \_\_\_\_\_

Inspector: \_\_\_\_\_

### BLOW COUNT REPORT

1		51
2		53
3		54
4		55
5		56
6		57
7		58
8		59
9		60
10		61
11		62
12		63
13		64
14		65
15		66
16		67
17		68
18		69
19		70
20		71
21		72
22	10	73
23	10	74
24	10	75
25	10	76
26	12	77
27	14	78
28	22	79
29	19	80
30	18	81
31	18	82
32	18	83
33	30	84
34	30	85
35	33	86
36	25	87
37	22	88
38	23	89
39	22	90
40	22	91
41	22	92
42	24	93
43	24	94
44	22	95
45	23	96
46	22	97
47	29	98
48	28	99
49	35	100
50	36	100



# APPENDIX C-5-A

BOREHOLE RECORD																																																																																																																																																																
PROJECT <u>Site U</u>					HOLE NO. _____																																																																																																																																																											
LOCATION _____					HOLE DATE _____																																																																																																																																																											
ELEVATION DATUM _____					HARDER: WEIGHT <u>140</u> LBS																																																																																																																																																											
CORING SIZE _____					HARDER: DROP <u>30</u> IN																																																																																																																																																											
GROUND WATER			SAMPLE CONDITIONS			TESTS																																																																																																																																																										
WL: GROUND WATER LEVEL _____			<div style="display: flex; justify-content: space-around;"> <span>✓ DISTURBED</span> <span>✓ GOOD</span> <span>✗ LOST</span> </div>			<div style="display: flex; justify-content: space-between;"> <div> SS: SPLIT SPOON, <u>2</u> IN O.D.  TW: THIS-WALL SAMPLER, _____ IN _____ %  PS: PISTON SAMPLER, _____ IN _____ %  DC: DIAMOND CORE, _____ SIZE  WS: WASH SAMPLE  AS: AUGER SAMPLE  ROD: ROCK QUALITY DESIGNATION (%) </div> <div> N: STANDARD PENETRATION VALUE (BLOWS/FT)  K: PERMEABILITY (CM/SEC)  V: IN-SITU VANE (LBS/100 FT)  VR: VANE ON REMOLDED SOIL (LBS/100 FT)  VL: LABORATORY VANE (LBS/100 FT) </div> <div> GS: GRAIN-SIZE ANALYSIS  S: TOTAL UNIT WEIGHT (LBS/CU FT)  U: UNCONFINED COMPRESSION (T/100 FT)  O: UNBRAINED TRIAXIAL (T/100 FT)  C: STRAIN AT FAILURE  E: CONSOLIDATION  P: PLASTIC LIMIT  L: LIQUID LIMIT  W: NATURAL WATER CONTENT </div> </div>																																																																																																																																																										
<table border="1" style="width: 100%; border-collapse: collapse;"> <thead> <tr> <th colspan="3" style="text-align: center;">PROFILE</th> <th colspan="3" style="text-align: center;">SAMPLES</th> <th colspan="2" style="text-align: center;">TESTS</th> <th colspan="2"></th> </tr> <tr> <th style="width: 5%;">DEPTH (FT)</th> <th style="width: 15%;">ELEV (FT)</th> <th style="width: 35%;">DESCRIPTION</th> <th style="width: 5%;">WATER</th> <th style="width: 5%;">CORR</th> <th style="width: 10%;">NO. &amp; TYPE</th> <th style="width: 10%;">REC. (%)</th> <th style="width: 10%;"></th> <th style="width: 10%;"></th> <th style="width: 10%;"></th> </tr> </thead> <tbody> <tr> <td>0</td> <td></td> <td>Ice surface</td> <td></td> <td></td> <td></td> <td></td> <td></td> <td></td> <td></td> </tr> <tr> <td></td> <td></td> <td>Ice</td> <td style="text-align: center;">▽</td> <td></td> <td></td> <td></td> <td></td> <td></td> <td></td> </tr> <tr> <td></td> <td></td> <td>Water</td> <td style="text-align: center;">1</td> <td></td> <td></td> <td></td> <td></td> <td></td> <td></td> </tr> <tr> <td>0</td> <td></td> <td rowspan="10">Grey silty sand, loose to dense</td> <td></td> <td></td> <td></td> <td></td> <td>N=Refusal</td> <td></td> <td></td> </tr> <tr> <td></td> <td></td> <td></td> <td></td> <td></td> <td></td> <td>-N=10</td> <td></td> <td></td> </tr> <tr> <td></td> <td></td> <td></td> <td></td> <td></td> <td></td> <td>-N=22</td> <td></td> <td></td> </tr> <tr> <td></td> <td></td> <td></td> <td></td> <td></td> <td></td> <td>-N=23</td> <td></td> <td></td> </tr> <tr> <td></td> <td></td> <td></td> <td></td> <td></td> <td></td> <td>-N=25</td> <td></td> <td></td> </tr> <tr> <td></td> <td></td> <td></td> <td></td> <td></td> <td></td> <td>-N=20</td> <td></td> <td></td> </tr> <tr> <td></td> <td></td> <td></td> <td></td> <td></td> <td></td> <td>-N=9</td> <td></td> <td></td> </tr> <tr> <td></td> <td></td> <td></td> <td></td> <td></td> <td></td> <td>-N=28</td> <td></td> <td></td> </tr> <tr> <td></td> <td></td> <td></td> <td></td> <td></td> <td></td> <td>-N=32</td> <td></td> <td></td> </tr> <tr> <td></td> <td></td> <td></td> <td></td> <td></td> <td></td> <td>-N=35</td> <td></td> <td></td> </tr> <tr> <td>20</td> <td></td> <td>Grey silty sand and gravel, dense</td> <td></td> <td></td> <td></td> <td></td> <td></td> <td></td> <td></td> </tr> </tbody> </table>										PROFILE			SAMPLES			TESTS				DEPTH (FT)	ELEV (FT)	DESCRIPTION	WATER	CORR	NO. & TYPE	REC. (%)				0		Ice surface										Ice	▽									Water	1							0		Grey silty sand, loose to dense					N=Refusal									-N=10									-N=22									-N=23									-N=25									-N=20									-N=9									-N=28									-N=32									-N=35			20		Grey silty sand and gravel, dense							
PROFILE			SAMPLES			TESTS																																																																																																																																																										
DEPTH (FT)	ELEV (FT)	DESCRIPTION	WATER	CORR	NO. & TYPE	REC. (%)																																																																																																																																																										
0		Ice surface																																																																																																																																																														
		Ice	▽																																																																																																																																																													
		Water	1																																																																																																																																																													
0		Grey silty sand, loose to dense					N=Refusal																																																																																																																																																									
							-N=10																																																																																																																																																									
							-N=22																																																																																																																																																									
							-N=23																																																																																																																																																									
							-N=25																																																																																																																																																									
							-N=20																																																																																																																																																									
							-N=9																																																																																																																																																									
							-N=28																																																																																																																																																									
							-N=32																																																																																																																																																									
							-N=35																																																																																																																																																									
20		Grey silty sand and gravel, dense																																																																																																																																																														

PROJECT 68				SHEET 2 OF 2			
BOREHOLE RECORD							
PROFILE				SAMPLES		TESTS	
DEPTH (FT)	DESCRIPTION	STRAT	GROUND WATER	COND	SP & TYPE	WCC (%)	
35	Grey silty sand and gravel, continued						-N-42
40							-N-39
45							N-Refusal
50	Grey silty sand, gravel and cobbles						N-Refusal
55							N-Refusal
60							N-Refusal
65							N-Refusal
70	End of Borehole						
75							
80							
85							
90							
95							
100							
105							
110							
115							

## APPENDIX D

### Metric Conversions

#### Basic Conversion Factors

1 mm	= 0.03937 in	1 in	= 25.4 mm
1 m	= 3.281 ft	1 ft	= 0.3048 m
	= 1.094 yd	1 yd	= 0.9144 m
1 km	= 0.6214 mile	1 mile	= 1.609 km
1 sq mm	= 0.00155 sq in	1 sq in	= 645.2 sq mm
1 sq m	= 10.76 sq ft	1 sq ft	= 0.0929 sq m

#### Force

1 N	= 0.2248 lbf	= 0.1020 kgf
4.448 N	= 1 lbf	= 0.4536 kgf
9.807 N	= 2.205 lbf	= 1 kgf
1 kN	= 0.1004 tonf	= 102.0 kgf = 0.1020 tonne f
9.964 kN	= 1 tonf	= 1016 kgf = 1.016 tonne f
9.807 kN	= 0.9842 tonf	= 1000 kgf = 1 tonne f
4.448 kN	= 1 kips	= 453.6 kgf = 0.4536 tonne f
4.448 kN	= 0.5 ton(us)	= 453.6 kgf = 0.4536 tonne f

ton	--	British unit
tonne	--	Metric unit
ton(us)	--	U.S. unit

#### Force Per Unit Length

1 N/m	= 0.06852 lbf/ft	= 0.1020 kgf/m
14.59 N/m	= 1 lbf/ft	= 1.488 kgf/m
9.807 N/m	= 0.672 lbf/ft	= 1 kgf/m
1 kN/m	= 0.0306 tonf/ft	= 0.1020 tonne f/m
32.69 kN/m	= 1 tonf/ft	= 3.333 tonne f/m
9.807 kN/m	= 0.300 tonf/ft	= 1 tonne f/m

#### Force Per Unit Area

1 N/sq mm	= 145.0 lbf/sq in	= 10.20 kgf/sq cm
0.006895 N/sq mm	= 1 lbf/sq in	= 0.0703 kgf/sq cm
0.09807 N/sq mm	= 14.22 lbf/sq in	= 1 kgf/sq cm
1 N/sq m	= 0.02089 lbf/sq ft	= 0.102 kgf/sq m
47.88 N/sq m	= 1 lbf/sq ft	= 4.882 kgf/sq m
9.807 N/sq m	= 0.2048 lbf/sq ft	= 1 kgf/sq m
1 N/sq mm	= 0.06475 tonf/sq in	= 10.20 kgf/sq cm
15.44 N/sq mm	= 1 tonf/sq in	= 157.5 kgf/sq cm

continued

0.09807 N/sq mm	= 0.006350 tonf/sq in	= 1 kgf/sq cm
1 N/sq mm	= 9.324 tonf/sq ft	= 10.20 kgf/sq cm
0.1073 N/sq mm	= 1 tonf/sq ft	= 1.094 kgf/sq cm
0.09807 N/sq mm	= 0.9144 tonf/sq ft	= 1 kgf/sq cm

**Force Per Unit Volume**

1 N/cu m	= 0.006366 lbf/cu ft	= 0.102 kgf/cu m
157.1 N/cu m	= 1 lbf/cu ft	= 16.02 kgf/cu m
9.807 N/cu m	= 0.0624 lbf/cu ft	= 1 kgf/cu m
1 kN/cu m	= 0.003684 lbf/cu in	= 0.1020 tonne f/cu m
271.4 kN/cu m	= 1 lbf/cu in	= 27.68 tonne f/cu m
9.807 kN/cu m	= 0.03613 lbf/cu in	= 1 tonne f/cu m
1 kN/cu m	= 0.002842 tonf/cu ft	= 0.1020 tonne f/cu m
351.9 kN/cu m	= 1 tonf/cu ft	= 35.88 tonne f/cu m
9.807 kN/cu m	= 0.02787 tonf/cu ft	= 1 tonne f/cu m

**Velocity**

1 ft/sec	= 30.48 cm/sec	= 0.3048 m/sec
----------	----------------	----------------